Synthesis, Structural Evaluation and Studies of Reactivity of Heteroperoxovanadates (V) And Development of Solid acid Catalysts for Organic Transformations

Saitanya Kumar Bharadwaj
Department of Chemistry

A Thesis

Submitted in Fulfillment of the Degree of

Doctor of Philosophy

To

Indian Institute of Technology Guwahati
Guwahati-781039, ASSAM, INDIA

June, 2009

Dedicated to my Father

INDIAN INSTITUTE OF TECHNOLOGY GUWAHATI
Guwahati 781 039, India
Department of Chemistry

STATEMENT

I do hereby declare that the matter embodied in this thesis is the result of investigations carried out by me in the Department of Chemistry, Indian Institute of Technology Guwahati, India under the guidance of Professor Mihir K, Chaudhuri, FASc., FNA and co-guidance of Dr. Gopal Das, Associate Professor.

In keeping with the general practice of reporting scientific observations, due acknowledgements have been made wherever the work described is based on the findings of other investigators.

June, 2009
IIT Guwahati

Saitanya K Bharadwaj

INDIAN INSTITUTE OF TECHNOLOGY GUWAHATI
Guwahati 781 039, India
Department of Chemistry

CERTIFICATE

It is certified that the work contained in the thesis entitled "**Synthesis, Structural Evaluation and Studies of Reactivity of Heteroperoxovanadates (V) And Development of Solid acid Catalysts for Organic Transformations**" by Saitanya K Bharadwaj, a student in the Department of Chemistry, Indian Institute of Technology, Guwahati for the award of degree of Doctor of Philosophy has been carried out under my supervision/ co-supervision and that this work has not been submitted elsewhere for a degree.

Dr. Gopal Das
Co- Supervisor

Associate Professor, Department of Chemistry
IITGuwahati, Guwahati-781039, India
Phone: +91-361-2582314
Fax: +91-361-2582349
E-mail: gdas@iitg.ernet.in

Mihir K. Chaudhuri, FASc., FNA
Supervisor

Professor, Department of Chemistry
IITGuwahati, Guwahati-781039, India
Phone: +91-361-2582302
E-mail: mkc@iitg.ernet.in
Or
Vice Chancellor, Tezpur University
Tezpur-784 028, India
Phone: +91-3712-267003,
Fax: +91-3712-267006
E-mail: mkc@tezu.ernet.in

June 2009

INDIAN INSTITUTE OF TECHNOLOGY GUWAHATI
Guwahati 781 039, India
Department of Chemistry

CERTIFICATE OF COURSE WORK

This is to certify that Saitanya K Bharadwaj has satisfactorily completed all the courses required for the Ph. D degree program. These courses include

1) CH 605 : Applied crystallography
2) CH 627 : New Reagents in Organic Chemistry
3) CH 611 : Bioinorganic Chemistry
4) CH 630 : A Fundamental Approach to Physical Chemistry

Professor A. Chattopadhyay
Head
Department of Chemistry
IIT Guwahati

Professor T. Punniyamurthy
Secretary
Departmental Post Graduate Committee
IIT Guwahati

INDIAN INSTITUTE OF TECHNOLOGY GUWAHATI
Guwahati 781 039, India

Ph.D. GRADE CARD

Roll No.: 05612207 Department: Chemistry

Name: Saitanya K Bharadwaj Semester: July 2005-June 2006

Course	Course Name	Credit	Grade
CH 605	Applied crystallography	6	AB
CH 627	New Reagents in Organic Synthesis	6	AB
CH 611	Bioinorganic Chemistry	6	AA
CH 630	A Fundamental Approach to Physical Chemistry	6	BB

Semester Performance Index: (S. P. I): 9.00

Cumulative Performance Index: (C. P. I): 9.00

June, 2009

Assistant Registrar
(Academic)

ACKNOWLEDGMENT

It is my immense pleasure to express my sincere gratitude to my guide, Professor Mihir K. Chaudhuri, FASc., FNA for his precious suggestion, incisive guidance and decisive insights during the entire course of Ph.D. research. I would like to thank my co-guide Dr. Gopal Das for his help and support. I remain obliged to Dr. R. C. Deka of Tezpur University, who has introduced me to a new field of Chemistry. I am also thankful to Professor Samir Bhatacharya, FASc., FNA of Visva Bharati, Shantineketan, West Bengal for his kind advice and help. I would like to thank all faculty members of Department of Chemistry of IIT Guwahati for their invaluable suggestions.

I wish to acknowledge my sincere gratitude to the Council of Scientific and Industrial Research (CSIR), India for financial support and IIT Guwahati for all the facilities that were made available to me.

I am thankful to Dr. Mamoranjan Kar of Center for Nanotechnology, Mr. Babulal Das of Department of Chemistry, Mr. Chandan Borgohain and Mr. Kulakamal Senapati of Central Instruments Facility for their help in all characterizations (Powder XRD, Single Crystal XRD, SEM, NMR etc.) required during my research work. I also thank Lipikaba, Abhilashaba, Parikshitda, Digantada, Mondolda, Nylotpalda, and Santanu for helping me selflessly.

It is my pleasant duty to acknowledge with thanks the co-operation and support extended to me by the authority of Tezpur University and its staff. I extend my sincere gratitude to Dr. Alak K. Buragohain, Registrar, Tezpur University for his constant encouragement and convey my thanks to Mr. Arun Sarma, Mr. Kumarjit Dutta, Dibakarda and Chetryda of office of the Vice-chancellor, Tezpur University for their kind support.

I thank Dr. Sahid Hussain, my senior and Dr. Papori Goswami for their invaluable suggestions. I wish to thank my friends Susanda, Nirmal, Neraaj, Ramesh, Ballav, Amardeep, Rajeeb, Jeshmini, Shahzad, Jagannath, Debajyoti, Sonit, Prasanta, Bolinda, Jayashreeba, Musaweer, Mohan, Ziyauddin, Rajen and all other research scholars for the joyful moments shared with them at IITG and their support.

My special thanks go to Siva, Subhash, Jitu, Gunin, Gopal and Rajendra, for their help and support in academic and non-academic affairs all throughout. I extend my sincerest thanks to my 'TEZU' friends - Digantada, Harekrishna, Sivaprasad, Amar, Kalyanda, Subrata, Lakshi, Dhruba, Surajit and others.

Finally, I owe heartfelt gratitude to my mother for her blessings and support, and my sisters- Dharitriba, Queenba and Maina for constantly inspiring me to carry out my research work to completion. I am thankful to all my relatives and well-wishers for their encouragement.

Unique thoughts of gratitude go to my wonderful father whom I have lost just a month ago. I wish I would had the opportunity to share all this achievements with you. I miss you and I wish you were still here with me.

(Saitanya K Bharadwaj)

CONTENTS

Abstract

The thesis of aforementioned title is based on the results of studies of a few chosen aspects of peroxovanadium chemistry and heterogeneous catalysis. The text has been distributed over five chapters. The introductory chapter of the thesis presents an overview of different aspects of peroxovanadium chemistry with special reference to haloperoxidase activity and insulin mimesis, and a brief account on the importance of heterogeneous catalysis for organic transformations. The second chapter provides experimental procedures, source of reagent and solvents, and particulars of the equipment and instruments used. Chapters 3 to 5 present the newer results gathered during the Ph.D. research.

Chapter 1: Introduction and Scope of the Work

This Chapter highlights the importance of peroxovanadium related coordination chemistry and gives an account to their reactivity, biochemical relevance and commercial importance, especially with reference to haloperoxidase activity and insulin mimetic action of peroxovanadium compounds.

Briefly speaking vanadium haloperoxidases (VHPOs) are the enzymes that catalyze the oxidation of halides by H_2O_2. VHPO possesses trigonal bipyramidal geometry around vanadium in the native site and a distorted tetragonal structure in the active form (peroxo-intermediate). Structural characterization has revealed that vanadate is covalently linked to the Nε of the imidazolyl moiety of a histidine amino acid, and further through hydrogen bonds to a variety of amino acid side chains (e.g. Arg, His, Ser, Lys) and interstitial water in the proximity of the active center. Special emphasis has been put on to the understanding of chemistry of bromoperoxidase activity because of its remifications on the synthetic applications to bromo-organic compounds having commercial importance. Quite apart from the activity highlighted above, peroxovanadium complexes are also found to be potential clinical alternatives of insulin for the treatment of diabetes. Hence, insulin-mimetic action of peroxovanadium complexes is briefly reviewed in this Chapter.

Besides bio or abiomimetic catalysis, development of abio catalytic systems is yet another domain of contemporary importance. This aspect, with reference to heterogeneous catalysis and its direct bearing with Green Chemistry and Green

Technology has been dully projected in this Chapter. The potential advantages of heterogeneous catalyst in organic reactions are (a) good dispersion of active sites, (b) constraints of the pores, (c) easier and safer to handle, d) easier to remove from the reaction mixture and (e) reusability. Among various heterogeneous catalysts, the importance of solid acid catalyst has been emphasized in this Chapter. The effects of supported material in reactivity of solid acid catalysts have been also discussed, highlighting the importance of alumina and titania. Solid acid catalysts are found to replace not only mineral acids but also catalyze the organic reactions.

After laying the foundation as indicated above, the scope of work in the present Ph. D research have been brought out very clearly.

Chapter 2: Materials and Methods

The sources of chemicals and solvents, methods for quantitative chemical estimations, determination of elements and particulars of all equipment used for physico-chemical studies are provided in this Chapter. The characterization was done using a variety of physico-chemical techniques, for example, elemental analysis, IR, UV-Visible, Raman, GC-MS, NMR, SEM, XRD.

Chapter 3: Synthesis, Characterization of newer Peroxovanadates and Study of their Reactivity

With the increased interest as (i) model for vanadium haloperoxidase, (ii) compounds with insulin mimetic or antitumor activity and (iii) stoichiometric or catalytic oxidants of organic compounds, a myriad of peroxovanadium compounds has been studied in the last two and a half decades. In continuation to our interest in the chemistry of peroxo and heteroligand peroxo compounds, the following work has been done as a part of the present Ph.D. research.

Accordingly, this chapter focuses on the synthesis and characterization of newer peroxo-vanadium complexes with heteroligands such as 3,5-dimethyl pyrazole and citric acid, at or near physiological pH. Interestingly, while synthesizing the abovementioned compounds, we have often encountered the formation of a stable μ-hydroxo peroxovanadate (V), $[VO(O_2)_2(OH)(O_2)_2OV]^{3-}$ species. This observation

and akinness of OH^- to F^-, directed us to synthesize the corresponding μ- fluoro complex.

The Chapter has been subdivided into four subsections. The first three subsections have been organized to discuss the synthesis and characterization of different heteroperoxovanadates with heteroligands like 3,5-dimethyl pyrazole, citric acid and fluoride, respectively, whereas in the fourth subsection, the reactivities of all these compounds have been illustrated.

3.1 Synthesis and Characterization of Oxodiperoxo-dmpz-vanadates (dmpz= 3,5 dimethylpyrazole)

The complexes DmpzH[$VO(O_2)_2$(dmpz)] (**1**), K[$VO(O_2)_2$(dmpz)] (**2**) and $Na_2[V_2O_2(O_2)_4$(dmpz)] (**3**), have been synthesized from aqueous solutions. Typically, V_2O_5 or AVO_3 was reacted with dimethyl pyrazole(dmpz) and hydrogen peroxide at a pH *ca.* 5 or 5.5 to afford yellow crystalline and microcrystalline compounds.

$$V_2O_5\text{(aq. soln.)} \xrightarrow{\text{dmpz, 50\% } H_2O_2} \text{DmpzH}[VO(O_2)_2\text{(dmpz)}] \quad (1)$$

$$KVO_3\text{ (aq. soln.)} \xrightarrow{\text{dmpz, 50\% } H_2O_2} K[VO(O_2)_2\text{(dmpz)}] \quad (2)$$

$$NaVO_3\text{ (aq. soln.)} \xrightarrow{\text{dmpz, 50\% } H_2O_2} Na_2[V_2O_2(O_2)_4\text{(dmpz)}] \quad (3)$$

Scheme -1

Characterization of the compounds **1-3** was made by elemental analysis, IR, Raman, UV-Vis and ^{1}H NMR spectroscopy. X-ray crystal structure determination of **1** and **3** has been carried out to delineate their structure.

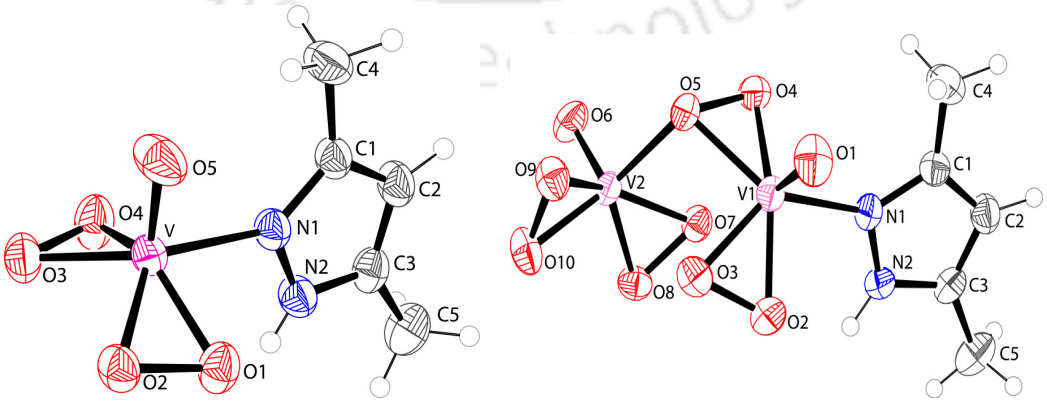

Figure 1 *Ortep diagrams of anion of compound* ***1*** *and* ***3***

While compound **1** is a diperoxo-pyrazole-vanadium anion with pyrazolium as the counter cation, compound **3** is a binuclear peroxovanadate with two coodinatively nonequivalent vanadium atoms and less commonly encountered μ-η^1: η^2-O_2 group. The binuclear unit with μ-η^1: η^2-O_2 group in compound **3** is rather uncommon in vanadium chemistry.

Compound **1** and **3** crystallize in the monoclinic P2(1)/c and monoclinic C2/c, respectively. In case of compound **1**, the basal positions are occupied by pyrazole and two peroxo groups and the distance of vanadium from the basal plane is 0.687 Å. The V=O, V-O (peroxo) and V-N bond lengths are 1.59 Å, 1.85-1.91 Å, 2.10 Å, respectively similar to those observed in some other vanadium complexes. Notably, these complexes constitute examples of rather less frequently synthesized hexa-coordinated peroxovanadates (V).

The crystal structure of compound **1** shows both intra and intermolecular H-bonding (Figure 2). As expected, the hydrogen from the protonated nitrogen in the ligated pyrazole forms H-bond with the peroxo group of neighboring peroxovanadates (N-H···O_2, 2.040 Å) and the counter pyrazolium cation forms hydrogen bonds with two peroxo groups (N-H···O_2, 1.813 and 1.837 Å) from different peroxo-vanadates.

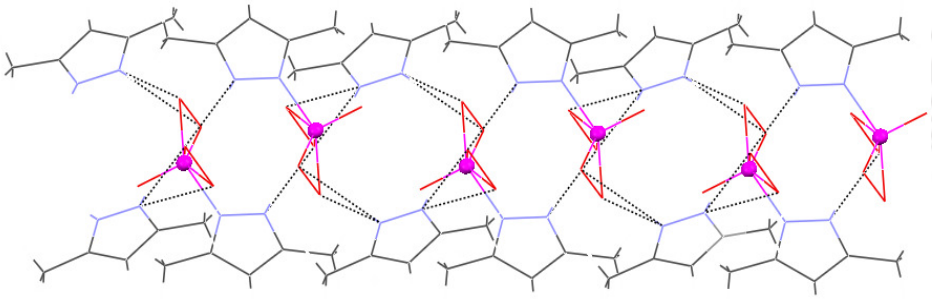

Figure 2 *Hydrogen bonding network in complex* ***1***

Density Funtional Theory (DFT) has been used to investigate structural and electronic properties, and reactivity of **1**–**3**. Structure optimizations were performed using both VWN and BLYP functionals. The bond lengths and angles matched with the experimental results. The electrophilicity of all complexes has been calculated, and found to be 6.28, 1.84 and 5.19 for compounds **1**, **2**, and **3**, respectively. These results are in line with the results of our experimental studies, as discussed in section 3.4 of this Chapter.

In VHPO, the peroxo group is activated by hydrogen bonding being formed by amino acid side chains. Compound **1** forms H-bonding with pyrazolium N-H (*c.f.* haloperoxidase structure). Further from DFT calculations, the proton of pyrazolium cation has been found to be labile between the nitrogen of pyrazole and the peroxodic oxygen thus, activating the peoxo group for nucleophilic attack. Compound **3** having the μ-η^1: η^2-O_2 is found to be more electrophilic than compound **2**. The electron density of the bridging peroxo group being pulled by V(V) (d^0-Lewis' acid) makes the peroxo group more prone to nucleophilic attack.

Like Bisperoxovanadium imidazole monoanion, reported by Crans *et.al*, (JACS, 1997, *119*, 5447) the compound **1** has been found to show highly encouraging insulin mimetic activity. Several *in vitro* as well as *in vivo* experiments confirmed glucose uptake upto 2800 µg/mL by this compound.

Section 3.2 Synthesis and Characterization of oxo-peroxo-citrato-vanadates

The synthesis of citrato(peroxo)vanadates(V) has been shown to be highly pH dependent. Reaction of aqueous solutions of metavanadate or vanadium pentoxide with citric acid (CA) at *ca.* 4°C with the molar ratio V: CA:: 1:1.5 for one hour yielded the citratovanadates $A_2[V_2O_4(C_6H_6O_7)_2].2H_2O$ [A = Na(**4**), K(**5**), NH_4(**6**)] whereas maintenance of the molar ratio of V: CA: H_2O_2 at 1: 1.2 :4 results into citrato-monoperoxovanadates, $A_2[V_2O_2(O_2)_2(C_6H_6O_7)_2].2H_2O$ [A = Na(**7**), K(**8**), NH_4(**9**)]. The pH was maintained in the range of 3-5 by adding the corresponding alkali solution, AOH (20% for A= Na or K; 2.5% for A= NH_4). A similar reaction with V: CA: H_2O_2 being maintained at 1: 1.2: 8 at pH 7.2 afforded diperoxovanadates (V), $Na_3[VO(O_2)_2(C_6H_6O_7)].4H_2O$ (**10**). The corresponding K^+ and NH_4^+ salts could not be synthesized as of now. Attempts to prepare these salts have resulted to the µ-hydroxo peroxovanadates. The pH at was fixed at 7.2 in order to go close to the physiological pH. Notably, the sodium salt of citrato(diperoxo)vanadate(V) is the first example of this kind. The crystal structures of compound (**4**) and (**8**) have revealed that the bond angles and bond lengths are similar to those reported earlier.

Section 3.3 Synthesis and Structural Evaluation of μ-hydroxo and μ-flouro peroxovanadates

The expedient synthesis of both $A_3[VO(O_2)_2(OH)(O_2)_2OV]$, [A = Na(**11**), K(**12**), NH_4(**13**)] and $A_3[VO(O_2)_2(F)(O_2)_2OV]$, [A = Na(**14**), K(**15**), NH_4(**16**)] require vanadium pentoxide or metavanadate, hydrogen peroxide, and alkali fluoride for the later. The characterizations of all compounds were made by elemental analysis, IR and UV-Vis spectroscopy. X-ray crystal structure determinations were done to delineate the structural feature.

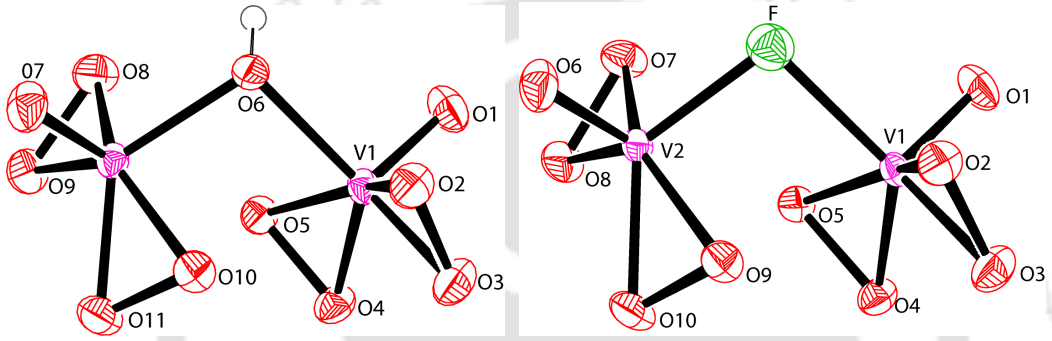

***Figure 4** ORTEP diagrams of anions of complexes **12** and **14**.*

Although the ORTEP diagrams of compound **12** and **14** show symmetric dinuclear complexes, there are differences in the bond lengths and bond angles. The compounds **12** and **14** crystallize in the monoclinic space group P2(1)/c with four molecules in the unit cell. Each vanadium atom in compound **12** and **14** are coordinated with two peroxo ligand in a C_{2v} fashion and one oxo group. However, the differences in the structure come from the presence of bridging hydroxo or fluoro group. An independent confirmation of presence of fluorine was done by ^{19}F NMR spectroscopy. A singlet peak at 77.6 ppm (with reference to C_6F_6) was observed for compound **14** as well as for **15** and **16**.

Section 3.4 Studies of Reactivity

Peroxo-metal complexes are reported to bring about a variety of oxidation/ oxygen transfer reactions such as sulfides to sufoxides and sulfones, hydrocarbons to alcohol, olefins to epoxides, alcohols to aldehydes and ketones. In this section reactivity of the newly synthesized complexes, DmpzH$[VO(O_2)_2(dmpz)]$ (**1**), $K[VO(O_2)_2(dmpz)].H_2O$(**2**), $Na_2[V_2O_2(O_2)_4(dmpz)].H_2O$ (**3**), $A_2[V_2O_4(C_6H_6O_7)_2].2H_2O$

[A = Na(**4**), K(**5**), NH_4(**6**)], $A_2[V_2O_2(O_2)_2(C_6H_6O_7)_2].2H_2O$ [A = Na(**7**), K(**8**), NH_4(**9**)], $Na_3[VO(O_2)_2(C_6H_6O_7)].4H_2O$ (**10**), finally $A_3[VO(O_2)_2(OH)(O_2)_2OV]$ [A = Na(**11**), K(**12**), NH_4(**13**)], and $A_3[VO(O_2)_2(F)(O_2)_2OV]$ [A = Na(**14**), K(**15**), NH_4(**16**)] has been carried out with respect to oxidation of bromide, sulfide, alcohol and also bromination of chalcones.

An internal comparison of the results has been made to enable us comment on their relative efficiency. The reactivity order of the catalysts is found to be as follows:

$Na_2[V_2O_2(O_2)_4(dmpz)]$ (**3**) > DmpzH$[VO(O_2)_2(dmpz)]$ (**1**) > $K[VO(O_2)_2(dmpz)]$ (**2**) > $Na_3[VO(O_2)_2(C_6H_6O_7)].4H_2O$ (**10**) > $A_2[V_2O_4(C_6H_6O_7)_2].2H_2O$ [A = Na(**4**), K(**5**), NH_4(**6**)] > $A_2[V_2O_2(O_2)_2(C_6H_6O_7)_2].2H_2O$ (A = Na(**7**), K(**8**), NH_4(**9**) > $A_3[VO(O_2)_2(OH)(O_2)_2OV]$, [A = Na(**11**), K(**12**), NH_4(**13**)] > $A_3[VO(O_2)_2(F)(O_2)_2OV]$, [A = Na(**14**), K(**15**), NH_4(**16**)].

Chapter 4: Oxidative Extraction of Bromide from 'Sea Bittern' and Bromination of phenol directly with sea bittern by bio-mimicking catalysis

It is now well established that the naturally occurring bromoorganic compounds in marine aquatics are catalyzed by VBrPO enzymes in presence of H_2O_2 followed by bromination of the organic substrates. However, synthetically bromoaromatic compounds are prepared by bromination with molecular bromine which has been a cause of great environmental concern. Taking cues from the bromoperoxidase activity and keeping environmental safety in mind in conjunction with knowledge and experience that we gained in the peroxovanadium chemistry, it was possible to develop newer and eco-friendly brominating agents i.e. tribromides, "the store house of bromine" and bromination protocols from a solution of KBr or NH_4Br. In the present Ph.D. work, like my predecessor, it has been possible to extract bromide from "bittern" (**Sea water**), the natural source of bromide and also demonstrate a catalytic protocol for bromination of phenol with sea water without external addition of Br^-.

In order to make the presentation more articulate, this Chapter has been divided into two sections. While **Section 4.1** includes the extraction of bromide from sea water as quaternary ammonium tribromides followed by their characterization, the

methodology for oxidative organic bromination of phenol without isolating the active brominating species from sea water is incorporated in **Section 4.2** of Chapter 4.

Section 4.1 Extraction of Bromide from Sea bittern: An Eco-friendly Bio-mimetic Process

The detailed experimental procedure for extraction of bromide has been laid out in this section. Tetrabutyl ammonium tribromide (**TBATB**), benzyltrimethyl ammonium tribromide (**BTMATB**), cetyltrimethylammonium tribromide (**CTMATB**), tetraethyl-ammonium tribromide (**TEATB**), and tetramethylammonium tribromide (**TMATB**) have all been prepared from sea water and characterized.

A set of catalysts has been separately used to extract bromide from sea bittern. Bromide (present as $MgBr_2$) was oxidized by H_2O_2 in presence of each catalyst and very dilute H_2SO_4. The efficacy of the catalysts was assayed by the isolation of TBATB, and then the best catalyst was identified.

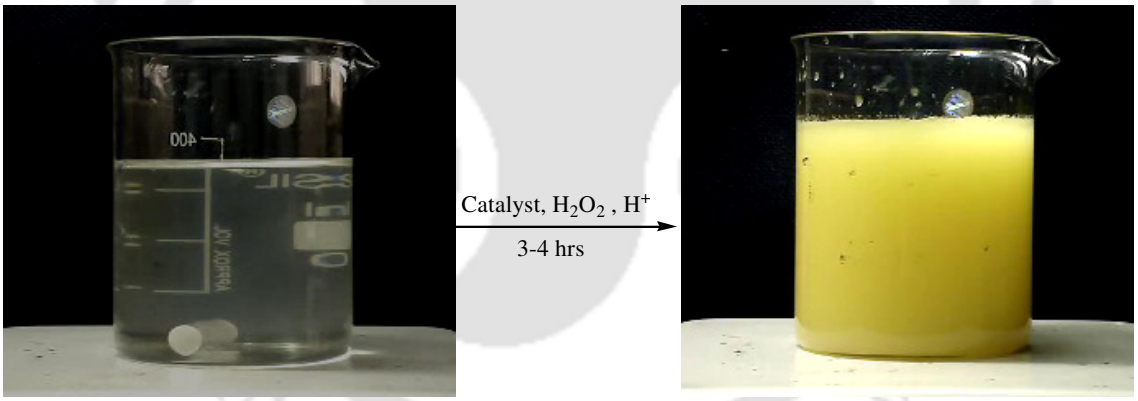

Figure 5 *Pictorial representation of extraction of bromide from sea water*

Section 4.2. Direct Bromination of Phenol with Sea bittern

This section is to demonstrate the bromination of phenol directly by sea bittern as a representative example. Several test runs have been carried out and the reactions were monitored by GC to calculate the yield of the reaction. Generally, bromination of phenol results in mono-, di- as well as tri- bromo phenol. However, controlling the experimental conditions, we have been able to obtain *p*-bromophenol selectively with 70% conversion. This appears to be a useful observation.

Chapter 5 Development of Solid acid Catalysts for Organic Transformations

Heterogeneous catalysis is a rapidly growing area as it assists in controlling the environmental pollution. It has many advantages like easy operation, separation, reusability and hence widely used in petrochemical industries. Among heterogeneous catalysts, solid acids have been the subject of most detailed and extensive studies. They have been introduced mainly to replace highly corrosive mineral acids in reaction medium. Hence, they are the beginners to play a significant role in the greening of fine and pharmaceutical chemical manufacturing processes. In this regard, several solid acid catalysts have been developed for some organic transformations. While discussing industrially important organic reactions catalyzed by solid acids, nitration and sufoxidation cannot be ignored.

Nitration of organic compounds occupies an important position in the chemical industries because nitroaromatic compounds are extensively utilized as chemical feedstocks for a wide range of useful materials. Likewise, sulfoxides are synthetically useful intermediates for the construction of various chemically and biologically active molecules including therapeutic agents such as anti-ulcer, antibacterial, antifungal, anti-athrosclertic and antihypertensive, for instance. Hence selective oxidation of organic sulfides to sulfoxides is a pivotal reaction in the sphere of organic synthesis.

This Chapter describes preparation and characterization of two newer solid acid catalysts followed by their application in selected organic transformations, viz. nitration of organic compounds and oxidation of thioethers.

(a) Preparation and Characterization of Newer Solid Acid Catalysts

Two solid acid catalysts have been developed by control heating and kneading of alumina or titania with phosphoric acid at a range of temperature 200-220^{0}C. With the specified molar ratio, this process resulted in the formation of $Al(H_2PO_4)_3$, (**A-cat**) and $(TiO_2)_{5.45}[Ti_4H_{11}(PO_4)_9].4\ H_2O$, (**T-cat**) with alumina and titania, respectively. The catalysts were characterized by chemical analysis as well as IR, powder XRD, SEM/EDAX, TG/DTG analysis.

(b) Nitration of Organic Compounds with Nitric Acid

Both A-cat and T-cat serve as efficient solid acid catalysts for nitration of a variety of organic substrates with nitric acid (70%) alone. The protocols are applicable to various substituted aromatic and polyaromatic compounds. Substrates possessing groups prone to oxidation preferably get oxidized rather than being nitrated.

(c) Chemoselective Sulfoxidation with H_2O_2 or HNO_3

A variety of organosulfur compounds have been oxidized chemoselectively in presence of phosphate impregnated titania, i.e. T-cat. Terminal oxidant viz. HNO_3 or H_2O_2, has been used. An internal comparison of the results points to the fact that T-cat/nitric acid system oxidizes simple alkyl or aryl sulfides more efficiently and selectively than the T-cat/hydrogen peroxide system. These systems chemoselectively oxidize sulfur in presence of double bond, nitrile, alcohol, aldehyde, benzylic methylene and nitrogen or sulphur atoms in a heterocyclic position. Also oxidized refractory sulfurs (DBT, 4-mehyl DBT etc), these are very important as they are found in transportation fuels. Glycosyl sulfide was easily oxidized to the corresponding sulfoxide, which are important in chemical glycosylation.

Introduction and Scope of work

Involvement of metaloenzymes in biochemical reactions has rendered the investigations of their synthetic mimics mainly addressing to structural and reactivity studies not only intriguing but also relevant to the understanding of their biochemical activities. Hence, synthesis and structural delineation of inorganic complexes aiming at mimicking enzymes constitute an active area of current research. In nature, enzymes involve as catalysts in the biochemical reactions with high turn over numbers without any structural and chemical change of its own. Being inspired by this, synthetic catalysts have been developed to replace stoichiometric reagent in chemical reactions, which can and do play an important role in secondary pollution prevention (waste clean up) as well as in primary pollution avoidance by eliminating toxic reagents, intermediates, waste stream, emissions etc. Hence, catalysis is an important tenet of "*Green Chemistry*" defined by Anastas and Warner [1]. In addition, catalysis is one of the main topics selected by James Clark for the Clean Technology Pool [2].

Vanadium, element number 23 of atomic weight 50.94, is present in plant and animal cells at concentrations as low as 10-20 nM. Vanadium is relatively abundant (~ 0.02%) in nature, occurs in a variety of oxidation states ranging from V^{II} to V^{V} [3]. The upsurge in interest in the chemistry of vanadium is because of its flexible co-ordination geometries ranging from tetrahedral and octahedral to trigonal pyramidal and pentagonal bipyramidal which are thermodynamically plausible. The versatility of vanadium in the biological field is also increased due to its potential for redox interplay within V(V)/V(IV) or V(IV)/V(III) [4]. Vanadium in the lower oxidation state has been found especially in vacuolated cell of ascidians. Again vanadium in +4 oxidation state has been isolated as vanadium-dependent nitrogenases from *Azobacter* [5] and as amavadin from mushroom *Amanita muscaria* [6]. In vanadium-dependent haloperoxidases found in marine algae, vanadium has been found in its high oxidation state, *i.e.* +5 [7, 8]. Under physiological conditions it exists predominantly in the +5 oxidation state as $H_2VO_4^-$, or in the +4 oxidation state as vanadyl cation (VO^{2+}). The anionic form resembles phosphate to some extent, while the vanadyl cation resembles Mg^{2+}. Many vanadium compounds are found to have a potential as insulin-mimetic agents in the treatment of human diabetes [9] (which will be discussed later in this chapter). Other important potentials of vanadium complexes are antitumorigenicity, metogenicity and anticancer activity [10]. Vanadium is usually found in higher

concentration in mitochondria, where some related reactions proceed, and vanadium deficiency has been found to disturb lipid metabolism among other activities [11].

Therefore, study on coordination chemistry of vanadium has emerged as one of the active areas of research. The group, where the present Ph.D. research has been carried out, has been working on synthesis and structural assessment of vanadium compounds followed by experimenting into their reaction profiles along with other metal [12]. Besides the study of reactivity of the synthesized complexes, development of newer catalysts and catalytic formulations takes an important share from this group.

One of the most interesting aspects of vanadium chemistry, which has also drawn attention of several groups of contemporary researchers [13] including us [12, 14], is its peroxo chemistry. It has received continuous attention because of its roles in biological processes as well as catalytic oxidations [15]. It may be mentioned, while discussing the peroxo chemistry, that addition of two extra electrons to $2P\pi^*$ orbital of molecular oxygen results in peroxide (O_2^{2-}) formation and decreases the O-O bond order. As a result, reactivity of peroxo compound differs from unreduced dioxygen complex. The modes of bonding of peroxide to metals are quite varied and interesting from the structural viewpoint. It can range from a symmetrical bidentate to a terminal monodentate position including all the possible angles in between. The bridging μ-peroxo could vary from cis-planar and trans-planar to trans-nonplanar configurations. Based on the mode of binding Vaska [16] classified the complexes as depicted in Table 1.1.

Simple peroxo compounds are not stable, some of them undergo spontaneous explosion, decomposition above 0^0C, and some are sensitive to shock, while several do not even exist as stoichiometric compounds. On the other hand, selective heteroligand combinations generally enhance the stability of peroxometal systems. The enhanced stability can be explained on the basis of electrostatic interaction, steric effect and back donation. Ligands can potentially tailor redox potential, electron transfer rate and magnetic moment of bound vanadium ion [24]. A significant feature of these complexes is that the O-O bond is relatively weak (120-190 $kJmol^{-1}$) [-25] and can be easily cleaved. Depending on their mode of cleavage, peroxo complexes can involve in either polar or radical oxidations. While heterolytic cleavage of peroxo bond gives polar oxidations, homolytic cleavage results in radical oxidations [26]. It is rather

interesting that often the nature of the heteroligands can dramatically change the reactivity of peroxo complexes. Owing to this ability, different sets of donor ligands with vanadium oxo and peroxo- compounds have drawn special attention.

Table 1.1 Vaska's classification of peroxo complexes

Structural type	Structural Designation	Example	Ref.
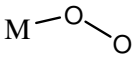	η^2 (superoxo)	$[Co(CN)_5(O_2)]^{3-}$	16
	η^2 (peroxo)	$[Mo(O_2)_4]^{3-}$,$[V(O_2)_4]^{3-}$	17
	η^2 (superoxo)	$[Cu(O_2)(HB(3\text{-}^tBu\text{-}5\text{-}^iPrpz)_3)]$	18
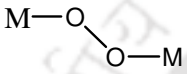	$\eta^1 : \eta^1$ (peroxo and superoxo)	$\{[Cu(TMPA)]_2(O_2)\}^{2+}$	19
		TMPA=tris[(2-pyridyl)methyl]amine	20
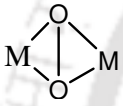	$\eta^2 : \eta^2$ (peroxo)	$[Cu(O_2)(HB(3, 5\text{-}^iPr_2pz)_3)]_2(O_2)$	21
		$[Cu(\alpha\text{-isosparteine})]_2(\mu\text{-}\eta_2\text{:}\eta_2\text{-}O_2)(coo^-)$	
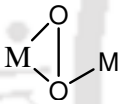	$\eta^1 : \eta^2$ (peroxo)	$[(PO_4)W_4O_4(O_2)_8]^{3-}$	22
		$Cs_3[V_2O_2(O_2)_4F]$	
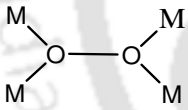		$[Mo_4O_{12}(O_2)_2]^{4-}$	22
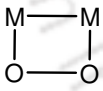		$[Ir_2I_2(CO)_2(\mu\text{-}O_2)(Ph_2PCH_2PPh_2)]$	23

As far as the reactivity is concerned, vanadium peroxides or peroxovanadates (V), in particular are capable of carrying out a variety of oxidation/oxygen transfer reactions [27] such as sulfides to sufoxides and sulfones, [28], hydrocarbons to alcohol [29], olefins to epoxides [30], alcohols to aldehydes and ketones [31], alcohols to ester [32]. Hydrocarbons can also be halogenated [33] by oxidation of halogen.

The interest in peroxo vanadium chemistry has been further bolstered by the isolation of vanadium haloperoxidase (VHPO) from marine algae in the mid eighties. These enzymes catalyze the oxidation of halides by H_2O_2. Kinetic studies reveal that V^V ions binds H_2O_2 to produce peroxo complex that reacts with halide ions to generate

an oxidized "Halogen equivalent" species, which either halogenate organic substrate or react again with H_2O_2 to form singlet oxygen (Scheme 1.1) [34-36]. However, the nature of the intermediate (e.g. HOBr, Br_3^-, Br_2, V_{enz}-Br, V_{enz}-OBr) is still a matter of uncertainty [37]. Many of halo-organic compounds produced from haloperoxidase activity have pharmaceutical significance like antifungal, antibacterial, antiviral (e.g. HIV), antiflamatory and other properties, hence, providing chemical defense to the marine organisms.

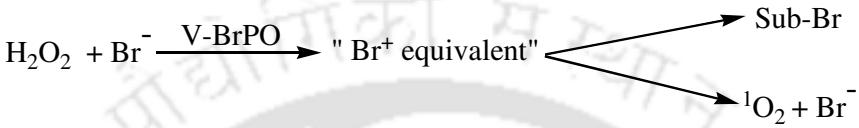

Scheme 1.1 *General reactivity for vanadium haloperoxidases*

Presently, two classes of enzymes are known which can efficiently catalyze the oxidation of halide by hydrogen peroxide. They are vanadium haloperoxidases and hemeperoxidases [38]. The hemeperoxidases have significant disadvantages of rapid inactivation during turnover because of an oxidative reaction of the heme group with the peroxide and followed by formation of hypohalous acids. Vanadium haloperoxidases (VHPO's) which contain vanadate (VO_4^{4-}) as a prosthetic group do not suffer from this disadvantage [39]. In addition, they are much more resistant toward heat, detergent and solvent denaturation [40]. The major disadvantage of VHPO's is that they are mainly active at mildly acidic pH values.

Crystal structure of VHPO's shows peculiar vanadium chemistry. In the native state, the vanadium ion is characterized by a trigonal bipyramidal geometry, where three oxygen atoms belong to the equatorial plane and another oxygen occupies an axial position. The other apical ligand is His496, which links the metal ion to the protein. In the peroxo form (*i.e.* intermediate) it shows strongly distorted trigonal bypyramidal structure (Figure1.1) [38].

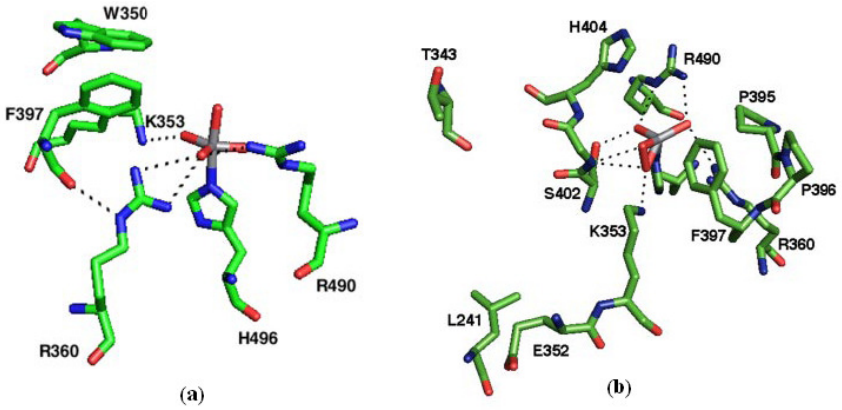

Figure 1.1 *Crystal structure of the (a) active site of native, (b) peroxo-intermediate of the VClPO. Adopted from reference 38.*

Even though the crystal structure of the VHPO's is known to date, the factors governing the halide specificity and pH optima are not fully understood. The difference of VClPO and VBrPO can be observed from the Figure 1.2. The catalytic efficiency of enzymes arises because enzyme active sites have ability to suitably polarize the reactant species and to stabilize reaction intermediates, transition states etc. Generally, it is achieved by appropriate alignments of amino acid residues to provide hydrogen-bonding interaction.

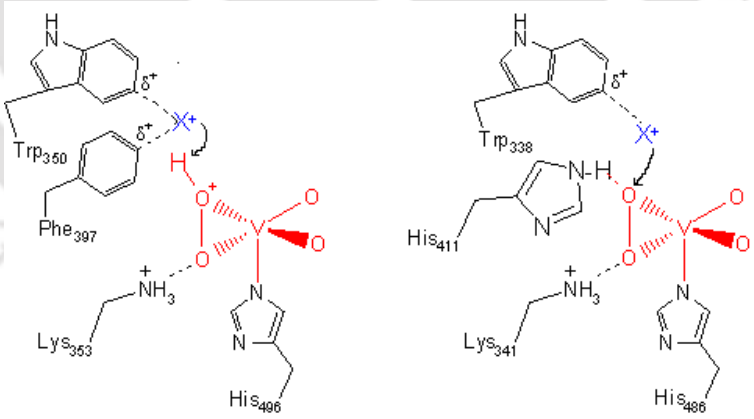

VClPO (*C. inaequalis*) **VBrPO**(*A. nodosum*)

Figure 1.2 *Line draw structures of the peroxo-intermediate of VClPO and VBrPO, demonstrating the origin of hydrogen bonding which tunes the activity in oxidation of chloride and bromide, respectively. Adopted from reference 38.*

Often nature combines both biocatalysis and metal-catalysis in single enzyme architecture, like vanadium haloperoxidases, where active site is actually an extensive

network of hydrogen bonds of vanadate cofactor with surrounding amino acid residues as shown in the Figures 1.1 and 1.2 [41]. It is clear that halide binding in VClPO is assisted by residues Phe-397 and Trp-350 via their ring edge, whereas VBrPOs have a histidine in the position corresponding to Phe-397. The VBrPOs from *C. officinalis* and *C. pilulifera* have an arginine in the position of Trp-350 [42]. In VBrPO from *A. nodosum* the bound peroxide may be deprotonated by His-411, thereby reducing the oxidative strength of these enzymes and their affinity for the halide [43]. His-411 of VBrPO from *A. nodosum* also forms a hydrogen bond with the catalytically important Lys-341. Hence, **it is relevant to note that H-bonding seems to be very important in the regulation of metal ion reactivity in biology**. Indeed, the result of mechanistic studies of VHPO's and their model complexes suggest that peroxide activation may be best achieved by protonation of the V(V) bound peroxo group to generate a side-on bound hydroperoxide complex [44]. It is believed that an increase in positive charge on a peroxo-oxygen (O_{peroxo}), by protonation, makes the attack of halide more favorable [45]. Hence, understanding of hydrogen bonding orientation is necessary to reveal the haloperoxidase activity. Interestingly, the same active site amino acid sequence is also conserved in three classes of acid phosphatases including mammalian glucose-6-phosphatase and can mimic haloperoxidase activity when it is bound to vanadate [46].

In order to shade light on the effects of H-bonding (from Lys residue) on peroxide activation, Butler and her co-workers [47] have designed the ligand N-(2-pyridylmethyl-6-amino) iminodiacetic acid, $H_2{}^{NH_2}pyg_2$, synthesized the complex, $K[VO(O_2)(^{NH_2}pyg_2)]$ and $K[VO(O_2)(^{BrNH_2}pyg_2)]$, and made structural characterization of these complexes. They have shown direct intra-molecular H-bonding between amine functionality and peroxide. The distance between NH_2 proton and bound peroxo moiety {(d(N(1)—H···O): 2.637(4) Å in $K[VO(O_2)(^{NH_2}pyg_2)]$, and 2.640(8)Å and 2.6919(8) Å in $K[VO(O_2)(^{BrNH_2}pyg_2)]$} are indicative of intra-molecular H-bonding. Their results of ^1H NMR studies also revealed that H-bond interaction is significant in solution as well as with the estimated intra-molecular H-bond strength in $[VO(O_2)(^{BrNH_2}pyg_2)]^-$ being 6 kcal/mol [48].

As far as the mechanism of the catalytic activity of V-HPOs is concerned, **the requirement of acidic pH for synthetic peroxovanadium compounds suggest protonation of peroxo group is the crucial step for its activity**, however, the exact source of proton is in haloperoxidase activity is still not certain. It may be from the

amino acid residue present in the active site. Based on chemical, biochemical and crystallographic data the mechanism can be depicted as in Figure 1.3(a) [48a]. The mechanism may as well be represented as in Figure 1.3(b) as proposed by Rehder [48b].

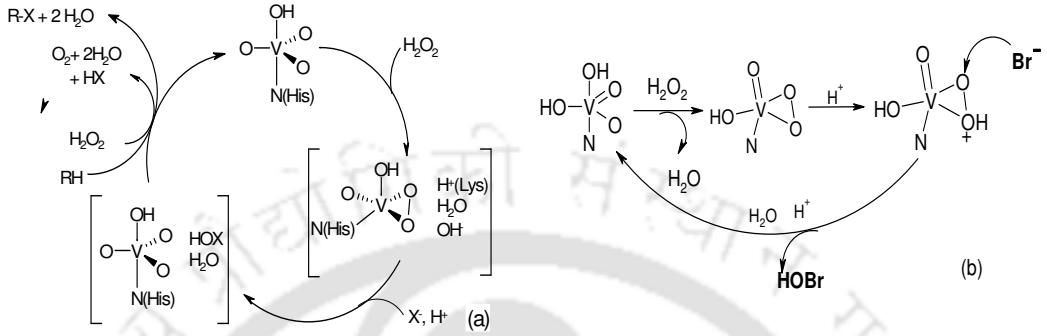

Figure 1.3 *Schematic representation of the catalytic activity of V-HPOs [48], where the enzyme activates peroxide by forming peroxo-intermediate with hydrogen peroxide subsequently oxidized halide. The oxidized halide undergoes halogenation in presence of organic substrates or disproportionates another hydorgen peroxide to oxygen.*

To understand the basis of specificity, enzyme kinetics, reactivity of the vanadium haloperoxidase and others, Density Functional Theory (DFT) is found to be a useful tool. In recent studies, Zampella *et al.* applied the DFT to inspect the structural, electronic and reactivity properties of complexes related to the peroxo form of VHPO as function of environment and protonation state [44, 49, 50]. It has been found that protonation plays the crucial role in activation of peroxo group. In addition, the role of Lysine residue in polarizing the peroxo cofactor has been explored.

In line with the natural VBrPO, which is most efficient at pH 5.5-7, most of the synthetic peroxovanadium compounds were found to be catalytically active in acidic medium. However, a series of peroxovanadates having μ-peroxo (bridging) group have been shown as efficient catalysts experimentally and theoretically at or near physiological pH [8, 51]. Although it has been proved that the reactivity of μ-peroxovanadates relates the VBrPO activity, the exact mechanism of action is not completely clear due to problem in resolving its crystal structure. It has been postulated that the VOOV moiety appears to be amenable for reductive cleavage by bromide to form –BrOVO(O_2), and then transfer the bromine to the substrate. The DFT studies on the peroxo vanadium complex [$V_2O_2(O_2)_3$(glycine)$_2$] demonstrates that the higher

electrophilicity of the O-atom from VOOV moiety makes more susceptible to nucleophilic attack by the Br^- [52]. Necessary, therefore is to study the bridging peroxovanadates to unravel the VBrPO activity.

Yet another manifestation of vanadium and its peroxo compound is that they are found to be potential clinical alternative of insulin for the treatment of diabetes [53]. Diabetes is one of the major health concerns in industrialized countries. It is of two types *viz*. type1 (IDDM, insulin-dependent diabetes mellitus), in which the minimum sufficient insulin is not produced, or type2 (NIDDM, non-insulin-dependent diabetes mellitus), in which there is insensitivity to insulin. Insulin, a pancreatic signaling hormone, regulates metabolism of fats and carbohydrates. Insulin is generally not orally active and must be administered *via* intramuscular injection. The most common form of diabetes in adult human is the non-insulin-dependent diabetes mellitus (NIDDM), which is due to the hypo- and hyperglycemic syndrome [54].

Although Lyonnet and Martin used sodium vanadate in 1899 for the treatment of diabetes mellitus [55], the insulin-enhancing activity of vanadium compounds has received growing interest only over the past two decades [56]. Vanadium makes various interactions with biological molecules because of (a) structural resemblance between phosphate and vanadate and (b) capability of formation of cationic and anionic compounds [57]. Vanadium compounds stimulate glucose metabolism without affecting the concentration of insulin. This makes them promising candidates for the treatment of the type 2 diabetes.

Based on the utility as insulin mimetic agents, vanadium-containing compounds are divided in to three general classes *viz*. (a) inorganic vanadium salts, both anionic (vanadates $[VO_4]^{3-}$) and cationic (vanadyl VO^{2+}), (b) complexes resulting from combination of vanadium(V) and hydrogen peroxide (mono- and diperoxovanadates, $[VO(O_2)(H_2O)_2(L\text{-}L')]^{n-}$ (n 0,1) and $[VO(O_2)_2(L\text{-}L')]^{n-}$ (n 1, 2, 3) where L-L´ stands for heteroligand with different donor atom, and (c) chelated vanadium(IV) complexes [58].

Nevertheless, toxicity as observed by weight loss, vomiting, diarrhea and poor appetite has been associated with ingestion of vanadium complexes, makes its therapeutic index narrower. However, **recent advances with organic transition metal chemistry suggest that modifications of the metal chemistries by the organic ligands not only increased efficacy but also decreased toxicity**. Therefore,

researchers have been involved in **synthesizing metal complexes that are reasonably soluble in both organic and aqueous environments and which are compatible to human metabolism.** Hence, a number of vanadium complexes has been prepared to achieve better results. The coordinating ligands have specially been chosen or designed to improve substantially the absorption, tissue uptake and intracellular mobility of vanadium, thereby reducing the dose required for optimal insulin enhancement [59].

Coordination complexes of vanadium (mostly vanadyl) are current candidates of insulin enhancing compounds; they can be tailored to optimize the desired properties for a drug. Therefore, particular interest has been paid to the synthesis of newer vanadium compounds with different organic ligands. Accordingly, a myriad of vanadium compounds has been synthesized which include bis(pyrolidine-N-carbodithioato)oxovanadium(IV), [60] bis(cysteine methyl ester)oxovanadium(IV), [61] N,N'-ethylenediaminediacetate and N,N'-ethylenediaminedi-(S)-methionineoxovanadium (IV), [62] bis(acetylacetonato) oxovanadium(IV) [63], bis(picolinato)oxovanadium(IV) and bis(maltolato) oxovanadium(IV) [64], to mention a few. Recently a huge number of acetamidrazone–VO^{2+} complexes have been synthesized and shown to have insulin mimetic activity [65]. The insulin-enhancing ability of bis(maltolato)oxovanadium(IV) and its analogue have completed phase I clinical trials in humans in late 2000 [64, 66]. In a very recent report BEOV has completed Phase I and has also advanced to Phase II clinical trials [66e].

Importantly, the potent activity of diperoxovanadium compounds as antidiabetic agent was first reported by Posner and his co-workers (1987) [67]. Since then, a wide range of peroxovanadium complexes has been synthesized and characterized. The chemistry and biochemistry of such compounds is currently of great interest, although, the aqueous preparations of peroxovanadium complexes appeared to be unstable and losing their insulin-mimetic activity with time. Nevertheless, this observation raised the possibility that further research (i) might lead to clinically useful agents for the treatment of diabetes, (ii) provide some insight into the mode of insulin action, and (iii) extend the bioinorganic chemistry of vanadium [4, 68].

Although these peroxovanadates are stable indefinitely in the solid state, they are prone to decomposition in aqueous solutions, however, it has been shown to be

effective in stimulating insulin receptor kinase (IRK) activity in hepatoma cells and inhibiting phosphotyrosinephosphatase (PTPase) activity in rat liver embosoms [69].

The exact mechanism of action of vanadium complex is not fully understood, till date. However, evidences suggest that vanadate and vanadium complexes presumably bypass the receptor and activate glucose metabolism within the cell, through inhibition of protein tyrosine phosphatases, [46, 70] where vanadate substitutes phosphate in the transition state analogs of phosphotyrosine phosphatase (Figure 1.4) [71].

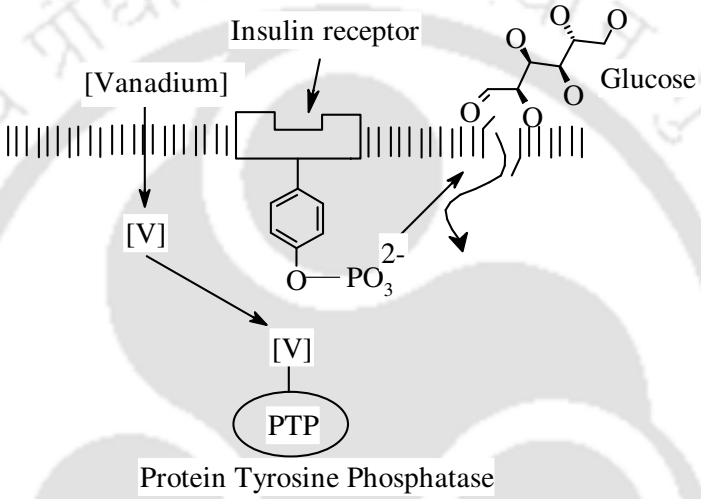

Figure 1.4 *Proposed mechanism of insulin mimetic action of Vanadium. Phosphorylation of tyrosine on the insulin receptor signals cellular glucose uptake by glucose transporters, lowering blood glucose levels. Vanadium inhibits the protein tyrosine phosphatase. This inhibition keeps the tyrosine residue of insulin receptor phosphorylated, allowing glucose transport into the cell. Adopted from reference 71.*

Two of the earliest discrete diperoxovanadate(V) compounds, potassium oxodiperoxo (pyridine-2-carboxylato) vanadate(V) and potassium oxodiperoxo(3-hydroxypyridine-2-carboxylato)vanadate(V), had been shown to improve membrane fluidity and increase the rate of glucose uptake [68]. Other peroxovanadates like potassium oxodiperoxo(1,10-phenanthroline)vanadate(V)trihydrate [72], oxoperoxopicolinatovanadate (V) dihydrate [73], pyridine-2,6-dicarboxylatooxoperoxovanadate (V) monohydrate, Bis(oxalato)oxoperoxo vanadate [74], oxodiperoxoimidazolium vanadium(V) [75], have also been shown to have potent insulin mimesis behavior. Notably, Crans *et al.* [75] has shown diperoxovanadate(V)

complex, $[VO(O_2)_2imz]^-$ as a very high insulin mimicking activity. Incidentally, Crans's complex is synthesized only at very low temperature (-20^0C) and is apparently not stable at ambient temperature thereby limiting the scope of further studies involving this complex. Lack of stability is yet another limitation of this species. Which is why there is an urgent need to develop a compound containing all the necessary attributes yet reasonably stable allowing further investigation involving it, especially in relation to insulin mimesis.

It is notable that vanadium can exert a wide spectrum of physiological effects as result of interactions with biologically relevant ligands of variable molecular mass. Understanding these interactions has been one of the foremost challenging goals of research in the past, with the specific target addressing bioavailability and solubility of vanadium species bound to organic ligands in biological fluids. Needless to mention that synthesis of the right type of complexes with desired ligand(s) environment requires strong scientific back up to decide upon and work out the appropriate experimental conditions. The *in vitro* experiment of metal with biologically related ligand(s) or model of those ligand(s) gave an idea about behavior of the active site of enzyme. With this aim, a number of ligands have been employed in the exploration of the chemistry of vanadium. Among those histidine like ligands *viz*. imidazole [76], pyrazole [77,78], and hydroxyl-polycarboxylic acid such as citric acid [79], malic acid [80], lactic acid [81], and tartaric acid [82] have drawn special attention.

Histidine, being a bio-available amino acid, not only coordinates to the metal but also plays an important role in catalytic properties of the enzymes. Especially, in vanadium haloperoxidase, it is present in the coordination sphere and regulates the redox chemistry of vanadium. In addition, imidazolic proton from the distal histidine from the protein residue plays a role in the acid-base catalysis of the substrate [83].

Interestingly pyrazole resemble imidazole except for the position of nitrogens, which is 1, 2- in case of pyrazole whereas 1, 3- for imidazole. Therefore, it is anticipated that binding pyrazole with vanadium can mimic the haloperoxidase enzymes in terms of their active site environment as well as H-bonding skeleton. In addition, this might provide better efficiency in reactivity. Further elaboration of pyrazolate coordination chemistry and different reactivity can be achieved by attaching

chelating side arms and different groups to the 3- and 5-positions of the heterocycle [84].

The pyrazole ligands, with protonated and unprotonated nitrogens as ring neighbors, possess an intriguing potential for structural modification through secondary bonding interactions. Here the unprotonated nitrogen can coordinate with the metal while leaving the **hydrogen atom of the protonated nitrogen free to form hydrogen bond with appropriate ligands in its vicinity.** Although pyrazole complexes of vanadium (II) and (III) have been known for some time [77, 85], very little work appears to have been done with vanadium (IV) and (V). Interestingly, to the best of our knowledge no peroxovanadium compound containing 3,5-dimethylpyrazole as the heteroligand has been fully characterized till now.

Apart from this, the role of citric acid [$HOOCCH_2C(OH)(COOH)CH_2COOH$], a bio-available small molecular weight hydroxyl-tricarboxylic acid, in biochemical processes can not be ignored. Citrates appear at about 0.1 mM in blood plasma and occur at 0.3% by weight in teeth and bone [86]. They regulate fundamental physiological processes and are intermediates in carbohydrate metabolism, e.g. in the Kreb's cycle and nitrogen fixation [87]. Due to more than one donor groups, coordination of citrate to vanadium is complicated but offers interesting stereochemical alternatives. It has been found to act as monodentate or polydentate ligands involving generally the central hydroxyl and carboxylic groups [88]. Despite the intense biological work carried out so far [78, 79, 89], suggesting the possible mode of action of vanadium at different oxidation states (V^{IV} and V^{V}) in biological media, synthesis characterization of complex involving vanadium-citric acid- hydrogen peroxide, at the physiological pH (i.e. 7.2) is limited. The paucity of such studies in delineating the role of vanadium in biofluids deserved attention.

It is understood from molecular orbital theory that the extra electrons of peroxide accommodated in anti-bonding orbital of peroxide decreases the bond order, resulting high reactivity. Thus, any electron-withdrawing ligand while attaching with vanadium, having peroxo group in the other side, may pull the electron density towards itself, thereby decreasing the reactivity of the peroxide. Hence, specificity and selectivity could be observed with the peroxide. Fluorine, being a strong electro-negative atom does this job. Further, capacity for formation of hydrogen bonding offers extra stability, which is observed in biochemical processes too, as a result inhibits

enzyme activity, e.g., the activity of OEC of PS II [90] and cytochrome c peroxidase [91]. Coordination of fluoride to the iron center of cytochrome C peroxidase inhibited the enzymes. The coordinated fluoride form hydrogen bonding with N-H hydrogen of the neighboring histidine or arginine group, thereby disabling the enzyme. Therefore, it is quite relevant to investigate the effect of fluoride of simple peroxo compounds. Also important is the synthesis and spectroscopic evaluation of the structural motifs of heteroligand peroxocompounds containing fluoride and/or biologically relevant ligands such as amino acids. Equally important is the studies of their reaction profiles.

The aforementioned discussions are convincing enough to believe that the **synthesis of mimics of the naturally occurring vanadium peroxidase enzymes is a very important area of research in itself**. Importantly, an understanding of their reactivity profiles provides important cues in the development of bromoperoxidase mimics as greener alternatives to the environmentally noxious brominating agents.

It is relevant to mention that naturally occurring bromo-organic compounds are the result of bromoperoxidase activity [92-94]. A wide range of bromo-organic compound is produced by marine and terrestrial plants, marine animals, bacteria, fungi, some higher animals, and a few mammals including humans [15, 27]. In the domain of synthetic chemistry, bromination of organic compounds has received significant interest in recent years owing to the increasing commercial importance of bromo-organics in the preparation of a large number of natural products as well as in the manufacture of pharmaceuticals, intermediates for agrochemicals and numerous industrially viable products like pesticides, herbicides, and fire retardants. They are also key intermediates in the preparation of organometallic reagents [95] and play vital roles in transition metal mediated coupling reactions such as Stille-Suzuki [96], Heck [97], Sonogashira reactions [98].

For over 100 years, brominations using molecular bromine as the reagent has been practiced for accessing a class of widely used synthetic bromo-organic products because molecular bromine is cheap, readily available and possess favorably low E-factor (the amount of substance produced per unit reactor volume per unit time). However, the classical bromination methods suffer from some inherent problems like 50% atom economy and the production of one equivalent of HBr. It is certain that such bromination processes do not advance the goal of non-toxic and waste free

chemistry. In large-scale operations, this is not only an economic problem but also an environmental one. In order to overcome these problems improved procedures involving the *in situ* preparation of "bromonium species" by oxidation of bromide ion with suitable oxidants under various homogeneous and heterogeneous reaction conditions have been reported in the literature [99]. The "active bromine" can effect bromination of organic substrates under soft reaction conditions. This concept has been inspired by the discovery of enzymes, vanadium dependent bromoperoxidases (VBrPOs), found in marine algae which catalyze oxidation of bromide ions by hydrogen peroxide in the biosynthesis of brominated compounds [92]. Taking cues from this, researchers [100] including us [101] have designed and developed catalysts based on nature's model VBrPOs to catalyze the oxidation of bromide with hydrogen peroxide for bromination reactions.

While the reaction mechanism of catalytic action of vanadium bromoperoxidase is not fully understood, it has been proposed that an active 'brominating species' *viz.* 'Br^+', 'OBr^-' or 'Br_3^-' is formed *in situ*. Subsequently, Br_3^- was isolated in the solid state as quaternary ammonium salts earlier in our labs [101,102]. This experience has now guided us to develop an eco-friendly general route to the synthesis of quaternary ammonium tribromides (**QATBs**) with QA being tetramethylammonium (**TMA**), tetraethylammonium (**TEA**), tetrabutylammonium (**TBA**) or cetyltrimethylammonium (**CTMA).** The organic ammonium tribromides (**OATB**s) such as tetramethylammonium tribromide (**TMATB**), benzyltrimethylammonium tribromide (**BTATB**), cetyltrimethylammonium tribromide (**CTMATB**) and tetrabutylammonium tribromide (**TBATB**) have received increasing applications as a substitute for toxic and hazardous molecular bromine in various organic reactions in recent years due to their ease of handling and ability to maintain the desired stoichiometry [103].

As far as the source of bromine or more precisely bromide is concerned, sea water is the answer. Sea covers 82,045,000 square miles of the total 139,295,000 (approximately two third) of earth. Sea water contains maximum concentration of bromide ions than anywhere else. The most authoritative work on the composition of sea water was that done by Dittmar nearly fifty years ago with samples obtained on the four-year cruise of the *Chalenger*, 1872-6, Table1.2 [104]. According to Dittmar, if not diluted by fresh coastal waters, sea water is remarkably constant in composition, however, salinity varying from 3.301 percent to 3.737 percent.

Table 1.2 Dittmar report on composition of sea water

Ions	Concentration (ppm)	Percent of total salt	Ions	Concentration (ppm)	Percent of total salt
Sodium	10,722	30.64	Chloride	19,324	55.21
Magnesium	1,316	3.76	Sulfates	2696	7.70
Calcium	420	1.20	Carbonates	74	0.21
Potassium	382	1.09	**Bromide**	**66**	**0.19**

Conventionally bromine is produced by treating bromide-containing salt solutions, sols or sea water with chlorine. Here the 'bittern' (concentrated sea water in sun light) is acidified with sulfuric acid to a pH less than four and preheated to 80-90 ^{0}C. The hot bittern is run through a tall granite tower packed where low-pressure stress and 10% excess of the theoretical chlorine are introduced. This chlorinating acidified brine liberates bromine, further the bromine is removed by blowing air through the brine solution. However, use of chlorine has several disadvantages. One major disadvantage is the contamination of bromine with chlorine, therefore necessitating use of purification step [105]. Another drawback involves the need to dispose the by-product, hydrogen chloride. Owing to the disadvantages of this blowing out method, several modification thereof and processes have been developed to achieve better and efficient process. A brief overview is presented here.

While D. Callihan and E. O. Salant have showed that alkali chlorate salts can be used to oxidize bromide ions [106], P. Schubert *et al*. [107] showed that bromine could be prepared from alkali/alkaline earth metal bromides by acidifying them and then reacting with oxygen over a metal oxide catalyst. Manganese dioxide in sulfuric acid at 60 ^{0}C was reported as good oxidant for bromide [108]. Nitrosyl tribromide was obtained by treating the bitterns with aqua regia, which on heating produces bromine [109]. However, all methods are limited due to different reason, alkali chlorates are very costly and explosive, requirement of strong acidification and additional heating and again clogging problem due to calcium and magnesium sulfates, for instance.

The traditional processes yield bromine considerably contaminated with chlorine [110]. Further bromine has to be separated from chlorine for which several methods have been developed, some of which are discussed below.

I. F. Halow concentrated the bromine vapor by condensing the water vapor while bromine vapor remains in gaseous form. The disadvantages of this method are that contamination due to chlorine cannot be controlled. Apart from this, contamination of the spent liquor by mineral acids and chlorine cannot be ruled out [111]. Sheldon B. Heath, [112] claimed that bromine liberated by blowing out methods could be concentrated by dissolving it in aqueous sulfur dioxide and then again liberating bromine by using chlorine. This process uses hazardous gases like chlorine and sulfur dioxide. Moreover, more than 80% of estimated chlorine is to be used in this process. Another method described the use of hetero-azeotropic distillation to obtain bromine with 99.9% purity. The limitations of this method are requirement of high temperature and pressure. In addition, the hetero-azetropic process is very expensive because it is highly energy intensive [113].

The above processes do not adhere to the green chemistry and clean technology principles; therefore, there is a need to develop environmentally acceptable alternative. The electrochemical methods have shown some prospects in this regime [114], however, industrial application of this process is not known till date. Also, the problem of clogging on the electrode can not be ruled out.

In view of the wide use of brominated organic compounds, **it is of interest to develop environmentally benign and economically attractive alternatives to these processes**. In this context, reactivity of bromoperoxidase appears relevant because it generates the entire naturally occurring bromo-organic products in the marine organism through oxidative bromination.

Apart from the synthesis, characterization of inorganic complexes and study of their reactivity, development of newer catalysts and catalytic processes for manufacturing fine chemicals also has a global demand for greener technologies. In addition, increasing public awareness and local authority regulations made companies to introduce a crucial factor “enviro-economics” as a driving force for new processes and products and here the development of new catalysts and catalytic processes get the paramount importance [115].

Among the three types of catalysis *viz*. homogeneous, biocatalysis and heterogeneous; the latter has been widely practiced due to its advantages over the others. The principal advantages of heterogeneously catalytic reactions are (a) good dispersion of active sites, (b) constraints of the pores, (c) easier and safer to handle, (d) easier to remove from the reaction mixture and (e) reusability. However, there are disadvantages like addition of cost for the extra component, difficulty in ensuring good mixing etc. In contrast, the catalytic system is usually more efficient under homogeneous conditions. However, the catalyst reuse becomes generally more difficult [115].

Catalysis using supported reagent and related materials is rapidly emerging as a new "enviro-technology", which is designed to improve process efficiency, to replace environmentally unacceptable reagents and catalysts. They are either solid or liquid supported on solid having a variety of applications. This can be further classified based on organic or inorganic supports. In the former organic polymer like polystyrene is used, whereas inorganic supports are numerous which include silica, alumina, zeolites, celite, montmorilonite and clay. The most important factors in determining the best support for particular application are likely to include surface areas, pore size, and acidity-basicity [115].

As far as large scale manufacturing of fine chemicals that require large quantities of mineral acid is concerned, solid acid catalysts have been enjoying spectacular success. It is a subject of the most detailed and extensive studies of all heterogeneous catalysts. They have been introduced to replace highly corrosive hydrogen fluoride in olefin alkylation, fuming sulphuric acid and molten sodium hydroxide in the production of resorcinol. In addition, they have been used in important large-scale industrial processes as alkylation (zeolites, SiO_2-H_3PO_4), paraffin isomerization (chlorinated Pt- Al_2O_3), reforming (silica-alumina, noble metal support), and many others [115,116].

Several types of solid acids has been developed which include (a) solid Brönsted acids (b) solid Lewis acids, (c) solid Superacids, (d) zeolites and (e) clays. Solid Brönsted acids are simple oxides possessing surface hydroxyls (silica, alumina etc.), mixed oxides (aluminosilicates), solid containing activated H_2O molecules (hydrated sulphates), and solids with protonic acids adsorbed on supports (SiO_2-

H_3PO_4). The acidity of Lewis solid acids rise due to unsaturation in coordination of surface cations and the strength depends on the surrounding, which gives rise to a range of catalysts by change in the environment of their active sites. Niobium pentoxide, for example, when supported on silica and alumina shows both Lewis and Brönsted acid sites, whereas on magnesia, titania shows Lewis acidity. Solid Superacids are the modified Lewis acids on supports. Treatment of alumina with P_2O_5, and $AlCl_3$ results into solid superacids, of which catalytic activity is consistent with very high acidity. Zeolites are widely used as selective catalysts, especially in petrochemical industries. Further zeolites have been modified to enable a change in catalytic properties by increasing Brönsted acidity, changing Brönsted to Lewis acids centers, and changing Si-Al ratio. Like zeolites, clays are also widely used in petrochemical industries. Ironically, clays have made much more impact than zeolites as acid catalysts in organic synthesis and are ready for a major breakthrough in the fine-chemical manufacturing industries [115].

Some representative examples of solid catalyzed organic reactions have been shown below:

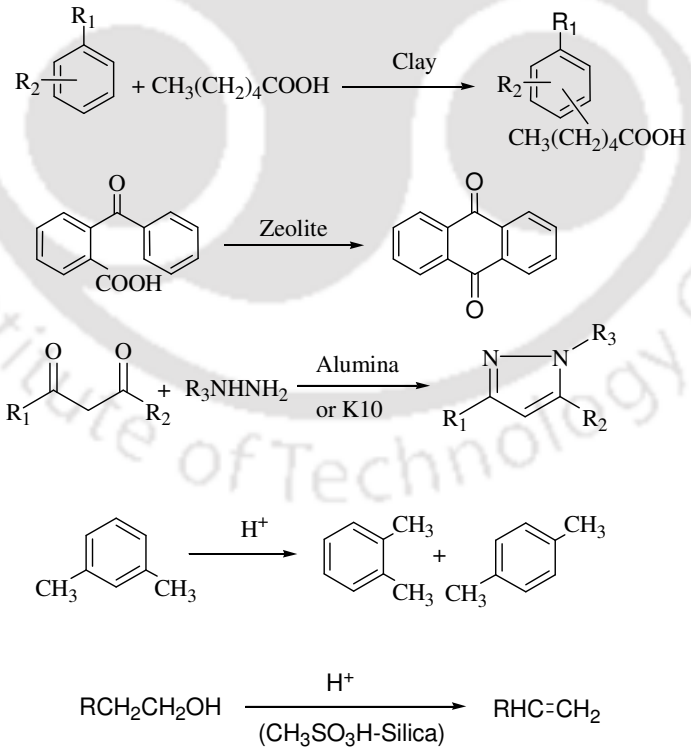

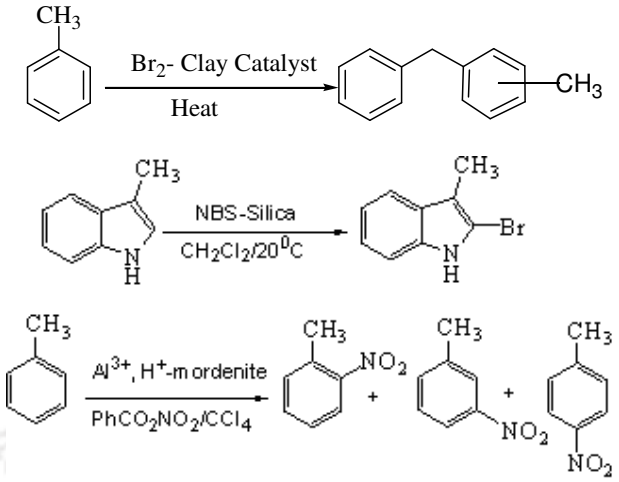

Scheme1.2 solid acid catalyzed organic reactions.

Alumina and titania have been widely studied due to their use as catalysts or catalyst supports in various organic reactions especially in petrochemistry, since they add a dual functionality to the catalyst [117]. The surface properties of these catalysts are mainly responsible for the functionality; many strategies have been proposed to modify the surface properties. Additionally they have some unique properties such as acidity, basicity, redox activitiy, thermal shock resistance capacity, ionic conductivity, chemical inertness, and promoting metal support interaction [118].

Recently, much attention has been paid to prepare super-acid titania and alumina for many industrially important acid demanding reactions [118]. So-called "solid phosphoric acid" containing phosphoric acid together with oxide phase, is a typical acidic heterogeneous catalyst widely used in industry for many years for propylene oligomerisation, alkylation and double–bond isomerisation etc. The use of phosphates as promoting additives for alumina has been reported in some instances and their effects have been suggested to be two-fold. Phosphates have been claimed to play the role to support stabilizer [120], and to suitably modify the acid-base properties of the active carriers [121]. K. M. Parida *et al*. have been involved in the study of phosphate impregnated titania, alumina and zirconia and have shown that incorporation of phosphate ion in TiO_2 and Al_2O_3 enhances important catalytic properties, like stabilization of surface area, crystal phase, improvement in surface acidity and making the material porous [122]. Direct phosphation resulted in the incorporation of phosphorus into the inorganic framework of aluminium oxides by the Al-O-P bonds and form a uniform macroporus structures.

While considering industrially important organic reactions catalyzed by solid acids, nitration, sufoxidation, bromination and oxidation of organic substrates come to fore and several solid acid catalysts have been developed for such organic transformations.

As a case in point, for example, nitro aromatic compounds are extensively utilized as chemical feedstock for a wide range of useful materials such as dyes, pharmaceuticals, perfumes, and plastics. The traditional method for nitration of aromatic compounds employs large quantities of concentrated protic acid, such as sulfuric acid, or stoichiometric quantities of Lewis acid, such as boron trifluoride, mixed with fuming nitric acid. Obviously, such materials will lead to excessive acid waste streams and heavy corrosion of equipment. In view of this as well as some unsolved problems pertaining to regioselectivity and over nitration of substrates [123], the selective and regioselective nitration of aromatic rings has received considerable attention of late with reasonable success. Yet, there is need for highly efficient, versatile and eco-friendly catalytic process for nitration under mild conditions especially without using H_2SO_4.

Besides nitration, selective oxidation of organic sulfides is a pivotal reaction in many organic syntheses because sulfoxides are very useful synthetic intermediates for the construction of various chemically and biologically active molecules including therapeutic agents such as anti-ulcer, antibacterial, antifungal, anti-athrosclertic, and antihypertensive [124]. The chemoselective oxidation of sulfides is also another point of interest. The advent of micro and mesoporous Ti-containing zeolite catalysts such as TS-1 [125], TS-2 [126], Ti-β [127], Ti-MCM-41 [128], Ti-HMS [129], Ti-MMM [130] etc. have given an impetus to the heterogeneous catalytic oxidation of organic molecules, although they may have some limitations like TS-1, TS-2 cannot oxidize the bulky sulfides and Ti-MCM-41 gives less selective products.

It is evident therefore that the development of new and efficacious catalytic systems that would allow high regio-, enantioselectivities with high efficiency (high TON and TOF) is extremely important and greatly rewarding. It is necessary to remember in this context that the ideal application in process chemistry generally requires the possibility to extend the process in order to reuse and recycle the catalyst or the catalytic system without affecting the main features of the catalyst.

Scope of Work

On the basis of brief review presented above, the following problems appear to require serious attention:

(a) Synthesis of peroxovanadium (V) complexes containing 3,5-dimethylpyrazole (dmpz), citric acid or fluoride as the heteroligand. Investigation of their structural motifs and reactivities with reference to bromoperoxidase activity, and probing onto their insulin mimicking properties. Dmpz complexes may be preferred for the later activity.

(b) Sea water is the source of bromide, and bromine is produced from seawater. Bromoperoxidase enzyme catalyses the oxidation of bromide and brominates the organic substrates in marine organism. Therefore, taking cues from this it is worthwhile to extract bromide from sea water by using a catalyst which mimicking bromoperoxidase activity. Equally important is the bromination of organic compounds by the direct use of sea water.

(c) Apart from the bio-mimetic catalysis, solid acid catalysis is also an important area of research. Development of newer solid acid catalysts and their use for specific organic transformations are the order of the day. A solid acid not only replaces mineral acids in fine chemical manufacturing process but also catalyze the reaction heterogeneously.

Research addressing the problems highlighted above is not only of topical importance but also expected to be rewarding. Accordingly, attempts have been made to address the problems defined above for the present Ph.D. research.

The work described in the thesis encompasses the synthesis, characterization and studies of reactivity of newer heteroperoxovanadates (V), and development of newer solid acid catalysts for some important organic reactions, namely nitration and sulfoxidation. The issues related to the extraction of bromide from "Sea-Bittern" and bromination of organic substrates directly using sea-bittern have also addressed. The subject matter of the thesis has been divided into five chapters. While the present chapter (i.e. **Chapter 1**) highlights background of the relevant aspects of studies, **Chapter 2** describes the sources of chemicals and solvents that were used in the work, methods of preparation of a few starting materials, details of the methods of chemical

analyses, and particulars of various instruments and equipment used for physico-chemical studies and characterization of the reported compounds. Each chapter (i.e. Chapter 3 to Chapter 5) has also been so design as to render it self contained. Thus a chapter begins with a brief introduction and sections on experimental, results and discussion, and conclusion followed by references.

The main themes of **Chapter 3** are synthesis, characterization and studies of reactivities of different heteroperoxovanadium (V) complexes. The heteroligands include 3,5- dimethylpyrazole, citric acid and fluoride. The reactivities of all compounds have been studied with respect to oxidation of bromide, alcohol, sulfide and bromination of organic substrates. In addition, Density Functional Theory (DFT) has been used to investigate and compare the electronic properties and reactivities of vanadium-peroxo-dimethylpyzole complexes. Insulin enhancing results obtained from the insulin mimicking *in vivo* experiments have also been incorporated in this chapter.

The **Chapter 4** demonstrates a catalytic protocol for oxidative extraction of bromide from "sea bittern". It also includes the results of bromination of phenol by the direct use of sea bittern.

The **Chapter 5** reports the preparation and characterization of two newer solid acid catalysts, and describes the results of catalytic reaction in nitration of organic substrates and oxidation of sulfides.

Some of the new results have been published and manuscripts of the rest are under preparation.

References

1. Anastas, P.; Warner, J. *Green Chemistry: Theory and Practice*, Oxford University Press, 2000.
2. Clark, J. H. *Green Separation Processes: Fundamentals and Applications*, Afonso C. A. M.; Crespo, J. P. S. G. Ed., Wiley-VCH, Weinheim, 2005.
3. Cotton, F. A.; Wilkinson, G. *Advanced Inorganic Chemistry*, Wiely Interscience, 6th Ed., 2005.
4. Thompson, K. H.; McNeill, J. H.; Orvig, C. *Chem. Rev*. **1999**, *99*, 2561.
5. Liang, J.; Madden, M.; Shah, V. K.; Burris, R. H. *Biochemistry* **1990**, *29*, 8577.
6. Bayer, E.; Kneifel, H. *Z. Naturforsch. B* **1972**, *27*, 207.
7. (a) Weyand, M.; Hecht, H.; Kiess, M.; Liaud, M.; Vilter, H.; Schomburg, D. *J. Mol. Biol*. **1999**, *293*, 595; (b) Sigel, H.; Sigel, A. *Met. Ions Biol. Syst.* **1995**, 31.
8. Crans, D. C.; Smee, J. J.; Gaidamauskas, E.; Yang, L. *Chem. Rev*. **2004**, *104*, 849.
9. Tracey, A. S.; Crans, D. C. Eds., *Vanadium Compounds– Chemistry, Biochemistry and Therapeutic Application,* ACS Symposium Series 711, 1998.
10. (a) Posner, B. I.; Burges, J. W.; Faure, R.; Bevan, A. P.; Lachance, D.; Zhang-Shn, G.; Fantus, I. G.; Ng, J. B.; Hall, D. A.; Soo-Lum, B.; Shaver, A. *J. Biol. Chem*. **1994**, *269*, 4596; (b) Djordjevic, C. *Metal Ions in Biological Systems: Antitumorgenic Activity of Vanadium Compounds,* Sigel, H.; Sigel, A. Eds., Marcel Dekker: New York, 1995; (c) Klarlund, J. K. *Cell* **1985**, *41*, 707.
11. Tracey, A. S.; Willsky, G. R.; Takeuchi, E. S. *Vanadium: Chemistry, Biochemistry, Pharmacology and Practical Applications*, Taylor and Francis Group, NW, 2007.
12. (a) Chaudhuri, M. K.; Ghosh, S. K. *Inorg. Chem.* **1982**, *21*, 4020; (b) Chaudhuri, M. K.; Ghosh, S. K.; Islam, N. S. *Inorg. Chem.* **1985**, *24*, 2706; (c) Basumatary, J. K.; Chaudhuri, M. K.; Purkayastha, R. N. D.; Hiese, Z. *J. Chem. Soc., Dalton Trans.* **1986**, 709; (d) Bhattacharjee, M.; Chaudhuri, M. K.; Islam, N. S.; Paul, P. C. *Inorg. Chim. Acta* **1990**, *169*, 97; (e) Bhattacharjee, M.; Chaudhuri, M. K.; Paul, P. C. *Can. J. Chem.* **1991**, *70*, 2245; (f) Chaudhuri, M. K.; Paul, P. C. *Ind. J. Chem.* **1992**, *31A*, 466.
13. (a) Jones, R. D.; Summerville, D. A.; Basolo, F. *Chem. Rev*. **1979**, *79*, 139; (b) Vuletic, N.; Djordjevic, C. *J. Chem. Soc. A* **1973**, 1137; (c) Yamada, S.; Ukei, Y.; Tanaka, M. *Inorg. Chem*. **1976**, *15*, 964; (d) Wieghardt, K. *Inorg. Chem.* **1978**, *37*, 57; (e) Funahashi, S.; Ishihara, K.; Tanaka, M. *Inorg. Chem.* **1981**, *20*, 51.

14. (a) Bhattacharjee, M. N.; Chaudhuri, M. K.; Islam, N. S. *Inorg. Chem.* **1989**, *28*, 2420; (b) Bhattacharjee, M. N.; Chaudhuri, M. K.; Islam, N. S. *Proc. Indian Acad. Sci.* **1990**, *102*, 365.

15. (a) Bortolini, O.; Conte, V. *J. Inorg. Biochem*. **2005**, *99*, 1549; (b) Bolm, C. *Coord. Chem. Rev.* **2003**, *237*, 245.

16. Vaska, L. *Acc. Chem. Res*. **1976**, *9*, 175.

17. (a) McLendon, G.; Pickens, S. R.; Martell, A. E. *Inorg. Chem*. **1977**, *16*, 1551; (b) Won, T. J.; Barnes, C. L.; Schlemper, E. O.; Thompson, R. C. *Inorg. Chem.* **1995**, *34,* 4499; (c) Grzywa, M.; Nitek, W.; Łasocha, W. *J. Mol. Struct.* **2007**, *828,* 111.

18. Won, T. J.; Barens, C. L.; Schlemper, E. O.; Thompson, R. C. *Inog. Chem*. **1995**, *34*, 4499.

19. Fujisawa, K.; Tanaka, M.; Moro-oka, Y.; Kitajima, N. *J. Am. Chem. Soc*. **1994**, *116*, 12079.

20. Tyeklar, Z.; Jacobson, R. R.; Wie, N.; Murthy, N. N.; Zubieta, J.; Karlin, K. D. *J. Am. Chem. Soc*. **1993**, *115,* 2677.

21. (a) Jacobson, R. R.; Tyeklar, Z.; Farooq, A.; Karlin, K. D.; Liu, S.; Zubieta, J. *J. Am. Chem. Soc.* **1988**, *110,* 3690; (b) Funahashi, Y.; Nishikawa, T.; Wasada-Tsutsui, Y.; Kajita, Y.; Yamaguchi, S.; Arii, H.; Ozawa, T.; Jitsukawa, K.; Tosha, T. Hirota, S.; Kitagawa, T.; Masuda, H. *J. Am. Chem. Soc.* **2008**, *130*, 16444

22. (a) Kitajima, N.; Fujisawa, K.; Fujimoto, C.; Moro-oka, Y.; Hashimoto, S.; Kitagawa, T.; Toriumi, K.; Tatsumi, K.; Nakamura, A. *J. Am. Chem. Soc.* **1992**, *114*, 1277; (b) Chrappova, J.; Schwendt, P.; Sivak, M.; Repisky, M.; Malkin, V.G.; Marek, J. *Dalton Trans.* **2009,** 465; (c) Gabriel, C.; Kaliva, M.; Venetis, J.; Baran, P.; Rodriguez-Escudero, I.; Voyiatzis, G.; Zervou, M.; Salifoglou, A. *Inorg. Chem.* **2009**, *48*, 476.

23. Dickman, M. H.; Pope, M. T. *Chem. Rev.* **1994**, *94*, 569.

24. Bygott, T.; Sargeson, A. M. *Inorg. Chem*. **1998**, *37*, 4750.

25. Curci, R.; Edwards, J. O. *Catalytic Oxidations with Hydrogen Peroxide as Oxidant*, Strukul, G.; Dordrecht, K. Ed., 1992, *Chapt. 3*, p. 46.

26. Curci, R.; Edwards, J. O. *Organic Peroxides*, Swern, D. Ed., Wiley-Interscience, New York, 1970, *Chapt. 4.*

27. (a) Butler, A.; Clague, M. J.; Meister, G. E. *Chem. Rev.* **1994**, *94*, 625; (b) Adao, P.; Pessoa, J. C.; Henriques, R. T.; Kuznetsov, M. L.; Avecilla, F.; Maurya, M. R.; Kumar, U.; Correia, I. *Inorg. Chem.* **2009**, doi: 10.1021/ic8017985.

28. (a) Smith, T. S.; Pecoraro, V. L. *Inorg. Chem.* **2002**, *41*, 6754; (b) Kantam, M. L.; Neelima, B.; Reddy, V. C.; Chaudhuri, M. K.; Dehury, S. K. *Cat. Lett.* **2004**, *95*, 19; (c) Sun, J.; Zhu, C.; Dai, Z.; Yang, M.; Pan, Y.; Hu, H. *J. Org. Chem*. **2004**, *69,* 8500; (d) Drago, C.; Caggiano, L.; Jackson, R. F. W. *Angew. Chem. Int. Ed*. **2005**, *44,* 7221; (e) Kelly, P.; Lawrence, S. E. M.; Anita, R. *Euro. J. Org. Chem*. **2006**, *19*, 4500; (f) Khedher, I.; Ghorbel, A.; Fraile, J. M.; Mayoral, J. A. *J. Mol. Cat. A: Chem.* **2006**, *255*, 92.

29. (a) Adam, W.; Korb, M. N.; Roschmann, K. J.; Moeller, S.; Chantu, R. *J. Org. Chem.* **1998**, *63,* 103423; (b) Pombeiro, A. J. L. *ACS Symposium Series*, **2007**, *974,* 51.

30. (a) Wahl, G.; Kleinhenz, D.; Schorm, A.; Sundermeyer, J.; Stowasser, R.; Rummey, C.; Bringmann, G.; Fichert, C.; Kifer, W. *Chem. Eur. J.* **1999**, *5,* 3237; (b) Cross, R. J.; Newman, P. D.; Peacock, R. D.; Stirling, D. *J. Mol. Catal. A: Chem.* **1999**, *144*, 273; (c) Csányi, L. J.; Jáky, K. *J. Catal.* **1999**, *127*, 42; (d) Deubel, D. V.; Sundermeyer, J.; Frenking, G. *Inorg. Chem.* **2000**, *39*, 2314; (e) Valentin, C. D.; Gisdakis, P.; Yudanov, I. V.; Rösch, N. *J. Org. Chem.* **2000**, *65,* 2996; (f) Deubel, D. V.; Sundermeyer, J.; Frenking, G. *J. Am. Chem. Soc.* **2000**, *122*, 10101; (g) Wang, X. Y.; Shi, H. C.; Xu, S. Y. *J. Mol. Catal. A: Chem.* **2003**, *206*, 213; (h) Zhang, W.; Yamamoto, H. *J. Am. Chem. Soc.* **2007**, *129*, 286.

31. Rout, L.; Nath, P.; Punniyamurthy, T. *Adv. Syn. Catal.* **2007**, *349*, 846.

32. Gopinath, R.; Barkakaty, B.; Talukdar, B.; Patel, B. K. *J. Org. Chem*. **2003**, *68*, 2944.

33. (a) Mimoun, H.; Saussine, L.; Daire, E.; Postel, M.; Fischer, J.; Weiss, R. *J. Am. Chem. Soc.* **1983**, *105*, 3101; (b) Conte, V.; Furia, F. D.; Moro, S. *Tetrahedron Lett.* **1994**, *35*, 7429; (c) Bora, U.; Bose, G.; Chaudhuri, M. K.; Dhar, S. S.; Gopinath, R.; Khan, A. T.; Patel, B. K. *Org. Lett.* **2000**, *2*, 247; (d) Bora, U.; Chaudhuri, M. K.; Dey, D.; Dhar, S. S. *Pure Appl. Chem.* **2001**, *73,* 93; (e) Carter-Franklin, J. N.; Butler, A. *J. A. Chem. Soc*. **2004**, *126,* 15060; (f) Maurya, M. R.; Kumar, U.; Manikandan, P. *Dalton Trans*. **2006**, *29*, 3561; (g) Moriuchi, T.; Yamaguchi, M.; Kikushima, K.; Hirao, T. *Tetrahedron Lett.* **2007**, *48*, 2667.

34. Butler, A.; Baldwin, A. H. *Structure and Bonding-Metal sites in Proteins and Models, Vol. 89*, Springer Verlag, Berlin-Heidelberg, Dordrecht, 1997, p.109.

35. Pecoraro, V.; Slebodnick, C.; Hamstra, B. *Vanadium Compounds: Chemistry Biochemistry and Therapeuthic Applications,* Crans, D. C.; Tracey, A. Eds., ACS Symposium Series 711, 1998, *Chapt. 12*.

36. (a) Butler, A. *Coord. Chem. Rev*. **1999**, *187*, 1735; (b) Conte, V.; Bortolini, O.; Carraro, M.; Moro, S. *J. Inorg. Biochem.* **2000**, *80*, 41.

37. (a) Rosa, R. I.; Clague, M. J.; Butler, A. *J. Am. Chem. Soc.* **1992**, *114,* 760; (b) Martinez, V. M. ; Cremer, G. ; Roeffaers, M. B. J. ; Sliwa, M.; Baruah, M.; Vos, D. E. D.; Hofkens, J.; Sels, B. F. *J. Am. Chem. Soc.* **2008**, *130*, 13192.

38. Hasan, Z.; Renirie, R.; Kerkman, R.; Ruijssenaars, H. J.; Hartog, A. F.; Wever, R. *J. Biol. Chem.* **2006**, *281*, 9738.

39. Renirie, R.; Pierlot, C.; Aubry, J. M.; Hartog, A. F.; Schoemaker, H. E.; Alsters, P. L.; Wever, R. ~~2003,~~ *Adv. Synth. Cat.* **2003**, ~~.~~ *345*, 849.

40. Boer, E. D.; Plat, H.; Tromp, M. G. M.; Franssen, M. C. R.; Van der Plas, H. C.; Meijer, E. M.; Schoemaker, H. E.; Wever, R. *Biotechnol. Bioeng. Symp.* **1987**, 30, 607.

41. Messerschimdt, A.; Wever, R. *Proc. Natl. Acad. Sci. USA* **1996**, *93*, 392.

42. Littlechild, J.; Garcia-Rodriguez, E.; Dalby, A.; Isupov, M. *J. Mol. Recognit.* **2002**, *15,* 291.

43. Renirie, R.; Hemrika, W.; Wever, R. *J. Biol. Chem.* **2000**, *275,* 11650.

44. (a) Zampella, G.; Fantucci, P.; Pecoraro, V. L.; Gioia, L. D. *J. Am. Chem. Soc.* **2005**, *127*, 953; (b) Schneider, C. J.; Penner-Hahn, J. E.; Pecoraro, V. L. *J. Am. Chem. Soc.* **2008**, *130*, 2712.

45. (a) Messerschmidt, A.; Prade, L.; Wever, R. *Biol. Chem.* **1997**, *378,* 309; (b) Butler, A.; Baldwin, A. H. *Struct. Bonding* **1997**, *89*, 109; (c) Colpas, G. J.; Hamstra, B. J.; Kampf, J. W.; Pecoraro, V. L. *J. Am. Chem. Soc.* **1996,** *118*, 3469.

46. Macedo-Ribeiro, S.; Renirie, R.; Wever, R.; Messerschmidt, A. *Biochemistry* **2008**, *47,* 929.

47. Kimblin, C.; Bu, X.; Butler, A. *Inorg. Chem.* **2002**, *41*, 161.

48. (a) Butler, A. *Bioinorganic Catalysis*, 2nd Ed. New York, 1998; (b) Rehder, D *Bioinorganic Vanadium Chemistry,* Wiley, Chichester, 2008.

49. Zampella, G.; Fantucci, P.; Pecoraro, V. L.; Gioia, L. D. *Inorg. Chem*. **2006**, *45*, 7133.

50. Niu, S.; Hall, M. B. *Chem. Rev*. **2000**, *100*, 353.

51. (a) Ravishankar, H. N.; Chaudhuri, M. K.; Ramasarma, T. *Inorg. Chem.* **1994**, *33*, 3788; (b) Ravishankar, H. N.; Ramasarma, T. *Arch. Biochem. Biophys*. **1995**, *316*, 319; (c) Tanaka, N.; Dumay, V.; Liao, Q.; Lange, A. J.; Wever, R. *Eur. J. Biochem.* **2002**, *269*, 2162.

52. Kalita, D.; Deka, R. C.; Islam, N. S. *Inorg. Chem. Commun.* **2007**, *10*, 45.

53. Thompson, K. H.; McNeill, J. H.; Orvig, C. *Chem. Rev.* **1999**, *99,* 2561.

54. (a) Watanabe, H.; Nakai, M.; Komazawa, K.; Sakurai, H. *J. Med. Chem*. **1994,** *37,* 876; (b) Srivastava, A. K.; Mehdi, M. Z. *Diabetic Medicine* **2004**, *22*, 2; (c) Saatchi, K.; Thompson, K. H.; Patrick, B. O.; Pink, M.; Yuen, V. G.; McNeill, J. H.; Orvig, C. *Inorg. Chem.* **2005**, *44,* 2689.

55. Lyonnet, B. M.; Martin, E. *Presse Med.* **1899**, *7*, 191.

56. Thompson, K. H.; Orvig, C. *Met. Ions Biol. Syst.* **2004**, *41*, 221.

57. (a) Gresser, M. J.; Tracey, A. S. *Vanadium in Biological Systems: Physiology and Biochemistry*; Kluwer Academic Publishers: Dordrecht, Netherlands, 1990, p. 63; (b) Plass, W. *Angew. Chem. Int. Ed.* **1999**, *38*, 909; (c) Song, B.; Aebischer, N.; Orvig, C. *Inorg. Chem.* **2002**, *41*, 1341; (d) Rehder, D. *Bio Metals* **1992**, *5*, 3; (e) Rehder, D.; Priebsch, W.; Holst, H.; Hillerns, F.; Richter, J. *J. Inorg. Biochem.* **1991**, *43*, 409.

58. Thompson, K. H.; McNeill, J. H.; Orvig, C. *Topics in Biological Inorganic Chemistry*; Clarke, M. J.; Sadler, P. J. Eds., Springer-Verlag: Heidelberg, 1999, *Vol. 2*, p 139.

59. Crans, D. C.; Yang, L.; Jakusch, T.; Kiss, T. *Inorg Chem.* **2000**, *39*, 4409.

60. Watanabe, H.; Nakai, M.; Komazawa, K.; Sakurai, H. *J. Med. Chem.* **1994**, *37*, 876.

61. Sakurai, H.; Tsuchiya, K.; Nukatsuka, M.; Kawada, J.; Ishikawa, S.; Yoshida, H.; Komatsu, M. *J. Clin. Biochem. Nutr.* **1990**, *8*, 193.

62. Kawabe, K.; Tadokoro, M.; Kojima, Y.; Fujisawa, Y.; Sakurai, H. *Chem. Lett.* **1998**, 9.

63. Li, J.; Elberg, G.; Crans, D. C.; Shechter, Y. *Biochemistry* **1996**, *35*, 8314.

64. Sakurai, H.; Fujii, K.; Watanabe, H.; Tamura, H. *Biochem. Biophys. Res. Commun.* **1995**, *214*, 1095.

65. McNeil, J. H.; Yuen, V. G.; Hoveyda, H. R.; Orvig, C. *J. Med. Chem.* **1992**, *35*, 1489.

66. (a) Dai, S.; Yuen, V. G.; Orvig, C.; McNeill, J. H. *Pharmacol. Commun.* **1993**, *3*, 311; (b) Caravan, P.; Gelmini, L.; Glover, N.; Li, F. G.; Herring, H.; McNeill, J. H.; Rettig, S. J.; Setyawati, I. A.; Shuter, E.; Sun, Y.; Tracey, A. S.; Yuen, V. G.; Orvig, C. *J. Am. Chem. Soc.* **1995**, *117*, 12759; (c) Thompson, K. H.; Liboiron, B. D.; Sun, Y.; Bellman, K.; Setyawati, I. A.; Patrick, B. O.; Karunaratne, V.; Rawji, G.; Wheeler, J. Sutton, K.; Bhanot, S.; Cassidy, C.; McNeill, J. H.; Yuen, V. G.; Orvig, C. *J. Biol. Inorg. Chem.* **2003**, *8*, 66; (d) Cocco, M. T.; Onnis, V.; Ponticelli, G.; Meier, B.; Rehder, D.; Garribba, E.; Micera, G. *J. Inorg. Biochem.* **2007**, *101*, 19; (e) Thompson, K. H.; Lichter, J.; LeBel, C.; Scaife, C.; McNeill, J. H.; Orvig, C. *J. Inorg. Biochem.***2009**, *103*, 554.

67. (a) Kadota, S.; Fantus, I. G.; Deragon, G.; Guyda, H. J.; Posner, B. I. *J. Biol. Chem*. **1987**, *262,* 8252; (b) Kadota, S.; Fantus, I. G.; Fantus, G.; Deragon, H.; Guyda, J.; Hersh, B.; Posner, B. I. *Biochem. Biophys, Res. Comm*. **1987**, *147*, 259.

68. Shaver, A.; Ng, J. B.; Hall, D. A.; Lum, B. S.; Posner, B. I. *Inorg. Chem*. **1993**, *32*, 3109.

69. Posner, B. I.; Faure, R.; Burgess, J. W.; Bevan, A. P.; Lachance, D.; Zhang-Sun, G.; Fantus, I. G.; Ng, J. B.; Hall, D. A.; Lum, B. S.; Shaver, A. *J. Biol. Chem.* **1994**, *269*, 4596.

70. Shechter, Y.; Elberg, G.; Shisheva, A.; Gefel, D.; Sekar, N.; Qian, S.; Bruck, R.; Gershonov, E.; Crans, D. C.; Goldwasser, Y.; Fridkin, M.; Li, J. *ACS Symposium. Series* **1998**, *No. 711*, 308.

71. Rehder, D. *Inorg. Chem. Commun.* **2003**, *6*, 604.

72. Evans, G. W.; Bowman, T. D. *J. Inorg. Biochem.* **1992**, *46*, 243.

73. Yale, J. F.; Lachance, D.; Bevan, A. P.; Vigeant, C.; Shaver, A.; Posner, B. I. *Diabetes* **1995**, *44*, 1274.

74. Bevan, A. P.; Burgess, J. W.; Yale, J. F.; Drake, P. G.; LaChance, D.; Baquiran, G.; Shaver, A.; Posner, B. I. *Am. J. Physiol.* **1995**, *268*, E60.

75. Crans, D. C.; Keramidas, A. D.; Hoover-Litty, H.; Anderson, O. P.; Miller, M. M.; Lemoine, L. M.; Pleasic-Williams, S.; Vandenberg, M.; Rossomoando, A. J.; Sweet, L. J. *J. Am. Chem. Soc.* **1997**, *119*, 5447.

76. Bortolini, O.; Carraro, M.; Conte, V.; Moro, S. *Eur. J. Inorg. Chem*. **1999**, 1489.

77. Mohan, M.; Bond, M. R.; Otieno, T.; Carrano, C. J. *Inorg. Chem.* **1995**, *34*, 1233.

78. (a) Prokofieva, A.; Prikhod'ko, A. I.; Enyedy, E. A.; Farkas, E.; Maringgele, W.; Demeshko, S. Dechert, S.; Meyer, F. *Inorg. Chem*. **2007**, *46,* 4298; (b) Müller, H.; Bauer-Siebenlist, B.; Csapo, E.; Dechert, S.; Farkas, E.; Meyer, F. *Inorg. Chem.* **2008**, *47*, 5278.

79. (a) Kaliva, M.; Raptopoulou, C. P.; Terzis, A.; Salifoglou, A. *Inorg. Chem*. **2004**, *43,* 2895; (b) Kaliva, M.; Kyriakakis, E.; Gabriel, C.; Raptopoulou, C. P.; Terzis, A.; Tuchagues, J. P.; Salifoglou, A. *Inorg. Chim. Acta* **2006**, *359,* 4535.

80. Kaliva, M.; Giannadaki, T.; Raptopoulou, C. P.; Tangoulis, V.; Terzis, A.; Salifoglou, A. *Inorg. Chem.* **2001**, *40,* 3711 and refferences therein.

81. Gorzsás, A.; Andersson, I.; Pettersson, L. *Dalton Trans*. **2003**, 2503.

82. Schwendt, P.; Tracey, A. S.; Tatiersky, J.; Galikova, J.; Zak, Z. *Inorg. Chem*. **2007**, *46*, 3971.

83. (a) Mukai, M.; Nagano, S.; Tanaka, M.; Ishimori, K.; Morishima, I.; Ogura, T.; Watanabe, Y.; Kitagawa, T. *J. Am. Chem. Soc.* **1997**, *119*, 758; (b) Poulos, T. L. *J. Biol. Inorg. Chem*. **1996**, *1,* 356; (c) Goodin, D. B. *J. Biol. Inorg. Chem.* **1996**, *1*, 360.

84. Mukherjee, R. N. *Coord. Chem. Re*v. **2000**, *203*, 151.

85. (a) Kawecka, Z. *J. Coord. Chem.* **1979**, *9,* 37; (b) Larkworthy, L. F.; O'Donoghue, M. W. *Inorg. Chim. Acta* **1983**, *71*, 81.

86. Crans, D. C. *Metal Ions in Biological Systems: Vanadium and its Role in Life*, Sigel H.; Sigel, A. Eds., Marcel Dekker, New York, 1995, Vol. 31, *Chapt.5*, p. 147.

87. Etcheverry, S. B.; Apella, M. C.; Baran, E. J. *J. Inorg. Biochem.* **1984**, *20*, 269.

88. Glusker, J. P. *Acc. Chem. Res.* **1980**, *13,* 345.

89. (a) Crans, D. C.; Bunch, R. L.; Theisen, L. A. *J. Am. Chem. Soc.* **1989**, *111*, 7597; (b) Djordjevic, C.; Lee, M.; Sinn, E. *Inorg. Chem.* **1989**, *28*, 719; (b) Tracey, A. L.; Li, H.; Gresser, M. J. *Inorg. Chem.* **1990**, *29*, 2267; (c) Crans, D. C.; Felty, R. A.; Miller, M. M. *J. Am. Chem. Soc.* **1991**, *113*, 265; (d) Crans, D. C.; Ehde, P. M.; Shin, P. K.; Pettersson, L. *J. Am. Chem. Soc.* **1991**, *113*, 3728; (e) Kiss, T.; Buglyo, P.; Sanna, D.; Micera, G.; Decock, P.; Dewaele, D. *Inorg. Chim. Acta* **1995**, *239*, 145; (f) Djordjevic, C.; Lee, M.; Sinn, E. *Inorg. Chem. Acta.* **1995**, *238*, 97; (g) Biagioli, M.; Strinna-Erre, L.; Micera, G.; Panzanelli, A.; Zema, M. *Inorg. Chim. Acta* **2000**, *310*, 1; (h) Tsaramyrsi, M.; Kavousanki, D.; Raptopoulou, C. P.; Terzis, A.; Salifoglou, A. *Inorg. Chim. Acta* **2001**, *320*, 47.

90. Ewards, S. L.; Poulos, T. L.; Krant, J. *J. Biol. Chem*. **1984**, *259,* 12984.

91. Weighardt, K. *Angew. Chem. Int. Ed*. **1989**, *28*, 1153.

92. Butler, A.; Walker, J. V. *Chem. Rev*. **1993**, *93*, 1937.

93. Gribble, G. W. *Chem. Soc. Rev*. **1999**, *28*, 335.

94. Sels, B.; Vos, D. D.; Buntinx, M.; Pierard, F.; Mesmaeker, A. K.; Jacobs, P. *Nature* **1999**, *400*, 855.

95. Davis, S. G. *Organotransition Metal Chemistry: Application to Organic Synthesis*, Pergamon Press, Oxford, 1982.

96. Stille, J. K. *Pure Appl. Chem.* **1985**, *57*, 1771; (b) Miyura, N.; Suzuki, A. *Chem. Rev.* **1995**, *95*, 2457.

97. (a) Beletskaya, I. P.; Cheprakov, A. V. *Chem. Rev.* **2000**, *100*, 3009; (b) Eberhard, M. R. *Org. Lett.* **2004**, *6,* 2125.

98. Sonogashira, K. *Metal-Catalysed Cross-Coupling Reactions*, Wiley-VCH, Germany, 1998, 203.

99. Eissen, M.; Lenoir, D. *Chem. Eur. J.* **2008**, *14*, 9830.

100. (a) Conte, V.; Furia, F. D.; Moro, S. *Tetrahedron Lett.* **1994**, *35*, 7429; (b) Andersson, M.; Conte, V.; Furia, F. D.; Moro, S. *Tetrahedron Lett.* **1995**, *36,* 2675; (c) Bhattacharjee, M.; Ganguli, S.; Mukherjee, J. *J. Chem. Res.***1995**, 80; (d) Sels, B. F.; Vos, D. E. D; Jacobs, P. A. *J. Am. Chem. Soc.* **2001**, *123*, 8350.

101. Chaudhuri, M. K.; Khan, A. T.; Patel, B. K.; Dey, D.; Kharmawophlang, W.; Lakshmiprabha T. R.; Mandal, G. C. *Tetrahedron Lett.* **1998**, *39*, 8163.

102. Chaudhuri, M. K.; Bora, U.; Dehury, S. K.; Dey, D.; Dhar, S. S.; Kharmawphlang, W.; Choudary, B. M.; Kantam, M. L. *US Pat*. **2006**, 7005548.

103. Kar, G.; Saikia, A. K.; Bora, U.; Dehury, S. K.; Chaudhuri, M. K. *Tetrahedron Lett.* **2003**, *44,* 4503.

104. Dittmar, W. (1884) Report on researches into the composition of ocean water collected by H. M. S. Challenger during the years 1873-1876, Murray, J. Ed., Voyage of H. M. S. Challenger. H. M. Stationery Office, London.

105. Naude, S. M.; Verleger, H. *Proc. Phys. Soc.* **1950**, *63A*, 470.

106. Callihan, D.; Salant, E. O. *J. Chem. Phys.* **1934**, *2*, 317.

107. Schubert, P. F.; Smith, A. R.; Taube, H.; Schubert, D. W. *US Pat.* **1993**, 9306038

108. Frank, A.; Jolles, Z. E. *Bromine and its Compounds*, Ernest Benn Limited, London, **1966**.

109. Kenat, J. *US Pat.* **1966**, 3437444.

110. Diprose, G.; Hesketh, B. *US Pat.* **1973**, 1326357.

111. Halow, F.; Kenaga, I. A.; Dressel, G. F. *US Pat.* **1930**, 1902801.

112. Sheldon, B. H. *US Pat.* **1939**, 2143223.

113. Mulet, J.; Leonard, C.; Albert, A.; Kirrmann, C.; Cervantes, V. *PCT Int. Application* WO 9600696, **1996**.

114. (a) Homing, D. F.; Osberg, W. E. *J. Chem. Phys.* **1955**, 23, 662; (b) Ramachandraiah, G.; Ghosh, P. K.; Susarla, V. R. K. S. *US Pat*. **2004**, 6811697 B2.

115. Clark, J. H. *Catalysis of organic reactions by supported inorganic reagents*, VCH, 1994;

116. Clark, J. H. *Acc. Chem. Res.* **2002**, *35*, 791.

117. Richardson, T. J. *Principles of Catalyst Development. Fundamental and Applied Catalysis;* Twigg, M. V.; Spencer, M. S. Eds., Plenum Press: New York, 1989, 23.

118. Samantaray, S. K.; Parida, K. M. *J. Mol. Catal. A: Chem.* **2001**, *176,* 151.

119. Samantaray, S. K.; Mishra, T.; Parida, K. M. *J. Mol. Catal. A: Chem.* **2000**, *156*, 267.

120. Basca, G. ; Ramis, G.; Lorenzelli, V.; Rossi, P. F.; Ginestra A. L.; Petrone, P. *Langmuir* **1989**, *5,* 917.

121. Lewis, J. M.; Kydd, A. R. *J. Catal.* **1991**, *132*, 465.

122. (a) Parida, K. M.; Acharya, M.; Samantaray, S. K.; Mishra, T. *J. Colloid Interf. Sci.* **1999**, *217*, 388; (b) Samantaray, S. K.; Parida, K. M. *J. Mat. Sci.* **2003**, *38*, 1835.

123. (a) Olah, G. A.; Malhotra, R.; Narang, S. C. *Nitration: Method and Mechanism*, VCH, New York, 1989; (b) Schofield, K. *Aromatic Nitration*, Cambridge University Press, Cambridge, 1980; (c) Esakkidurai, T.; Pitchumani, K. *J. Mol. Catal. A: Chem*. **2002**, *185* 305; (d) Clark, J. H. *Chemistry of Waste Minimization*, Chapman and Hall, London, 1995.

124. Drabowski, J.; Kielbasinski, P.; Mikolajcyk, M. *Synthesis of Sulfoxides*, Wiley, New York, 1994.

125. Raghavan, P. S.; Ramaswamy, V.; Upadhya, T. T.; Sudalai, A.; Ramaswamy, A. V.; Sivasanker, S. *J. Mol. Catal. A: Chem.* **1997**, *122*, 75.

126. Raju, S. V. N.; Upadhya, T. T.; Ponatnam, S.; Daniel, T.; Sudalai, A. *Chem. Commun.* **1996**, 1969.

127. Moreau, P.; Hulea, V.; Gomez, S.; Brunel, D.; Renzo, F. D. *Appl. Catal. A: Gen.* **1997**, *155,* 253.

128. Corma, A.; Iglesias, M.; Sanchez, F. *Catal. Lett.* **1996**, *39,* 153.

129. Iwamoto, M.; Tanaka, Y.; Hirosumi, J.; Kita, N.; Triwahyono, S. *Microporous Mesoporous Mater.* **2001**, *48,* 271.

130. Kholdeeva, O. A.; Derevyankin, A. Y.; Shmakov, A. N.; Trukhan, N. N.; Paukshtis, E. A.; Tuel, A.; Romannikov, V. N. *J. Mol. Catal. A: Chem*. **2000**, *158*, 417.

Materials and Methods

A comprehensive account of the procedures adopted for preparation of some of the starting materials, the details of the methods used for quantitative determination of various constituents and the relevant particulars of the instruments/equipment used for the characterization and structural assessment of the newly synthesized compounds are described in this chapter.

All the chemicals and solvents used for the present work were of analytical grade quality. Following are the sources of the chemicals and solvents: Sigma Aldrich India, s.d.fine-chem ltd, Qualigens Fine Chemicals, E. Merck (India) Limited, Loba Chemie Industries, and Spectrochem (India). All tissue culture materials were obtained from Gibco-BRL, Life Technologies Inc., Gaithersburg, USA. Porcine insulin was purchased from Sigma Chemical Company, St. Louis, MO, USA. [^{3}H] 2-deoxyglucose (Specific activity: 12.0 Ci/mmol) and γ-^{32}P ATP (Specific activity: 6000 ci/mmol) were from GE Healthcare, Asia Pacific Region, Singapore.

Preparation of starting materials

3,5-dimethylpyrazole (dmpz)[1]

A methanolic solution of 25 mL of hydrazine hydrate, $N_2H_4.H_2O$, (25.0 g, 499.4 mmol) was added slowly with stirring to a methanolic solution of 25 mL of acetylacetone (25.0 g, 249.7 mmol) in an ice-cold condition. A light yellow solution was obtained. The solution was concentrated to *ca.* 20 mL on a steam-bath and left overnight in a refrigerator. A white crystalline compound was obtained and this was isolated by filtration, washed 4 or 5 times with water and dried in air. The yield of pure 3,5-dimethylpyrazole was 23.5 g (98 %). M.p. was found 107 ^{0}C (lit. m.p.107 –109 ^{0}C).

Benzylideneacetophenone (Chalcone or 1,3- diphenylprop-2-en-1-one)[2]

A solution of 22 g of sodium hydroxide was prepared in 200 mL of water and 122.5 mL of ethanol in a 500 mL bolt-head flask. The flask was immersed in an ice bath, and poured in 52 g (430 mmol) of freshly distilled acetophenone. To the solution 46 g (430 mmol) of pure benzaldehyde was added under continuous stirring. The temperature of the mixture was maintained at *ca.* 25 ^{0}C and stirred vigorously for 2-3 h.

Then the reaction mixture was left in refrigerator overnight. The product was filtered under suction on a Buchner funnel and washed with cold water until the washings were neutral to litmus, and then with 20 mL of ice-cold ethanol. The air-dried crude chalcone weighed 88 g. This was then recrystallized from warm ethanol. The yield of pure benzylideneacetophenone (a pale yellow solid) was 77 g (85 %). M.P. was recorded at 57 ^{0}C (lit. m.p. 55 – 57 ^{0}C.)

Potassium metavanadate (KVO_3)[3]

An amount of 69.11 g (500 mmol) of potassium carbonate was dissolved with stirring in 400 mL of water contained in an 800 mL beaker. The solution was maintained at 85 – 90 ^{0}C by heating on a hot water-bath or a well-adjusted hot plate. To the clear solution 90.95g (500 mmol) of V_2O_5 was added, in small portions, under heating and constant stirring. When the effervescence subsided, 10 mL of 3% H_2O_2 was added to assist complete dissolution of the vanadium oxide. The reaction mixture was maintained at 85-90 ^{0}C with constant stirring for *ca.* 2.5 h during which time the volume was reduced to 150-200 mL by evaporation. The mixture was heated to just below boiling and then filtered immediately by suction through a 9 cm coarse-porosity fritted glass funnel into a 500 mL filter flask. A boiling chip was added to the filter-flask containing the clear light yellow and slightly viscous filtrate. The exact color of the solution depended upon the pH (*A deep yellow color would indicate that too little K_2CO_3 had been used while colorless solution would indicate that too much K_2CO_3 has been used*). The flask was stoppered and evaporated with aspirator suction on a hot (85-90 ^{0}C) water bath. The solution became increasingly viscous and suddenly a nearly white precipitate began to form. The volume of the mixture was reduced to *ca.* 75 mL and the powdery pale-yellow precipitate was collected on a 9 cm fritted-glass funnel, washed first with 20 mL of 95% ethanol, and finally air-dried. The yield of the powdery pale-yellow product was 40 g (29%). When the reaction mixture was evaporated to a volume of *ca.* 25 mL, a second crop of the product (*ca.* 30 g, *ca.* 20%) was also obtained.

Elemental analysis

Vanadium[4]

Vanadium was estimated iodometrically.

An accurately weighed amount (*ca.* 0.1 g) of vanadium compound was dissolved in 100 mL of water. To the solution 5 mL of 5M H_2SO_4 was added. The solution was boiled for 20 min to remove peroxide. To this solution 5 g of potassium persulphate was added followed by the addition of one drop of silver nitrate, $AgNO_3$, solution. The resultant mixture was boiled for 1 h. Again 15 mL of 5M H_2SO_4 was added and the solution boiled for a further period of 30 min. The solution was allowed to cool to room temperature and *ca.* 5 g of KI was added with stirring. This was then kept in the dark for 15 min. The liberated iodine was then titrated with standard $Na_2S_2O_3$ solution using starch as an indicator. The end point was detected by the appearance of a light-blue color.

$$1 \text{ mL of } 0.1 \text{ M } Na_2S_2O_3 = 0.00519 \text{ g of vanadium}$$

Fluoride[5]

An accurately weighed amount (*ca.* 0.1 g) of fluoride containing compound was dissolved in 150 mL of water. The solution was digested on a steam bath for *ca.* 30 min. To this, two or three drops of bromophenol blue indicator and 3 mL of a 10% sodium chloride solution were added and diluted to *ca.* 250 mL. 6 M nitric acid was added to it until the color just changed to yellow, followed by the addition of 0.1 M NaOH solution until the color changed to blue. The mixture was then treated with 1 mL of conc. HCl and 5 g of $Pb(NO_3)_2$ and heated on a steam-bath. After all the lead nitrate had dissolved, 5 g of crystallised sodium acetate was added to the solution and the solution digested on a steam-bath for *ca.* 30 min. with occasional stirring and then allowed to stand overnight.

The precipitate was filtered through a Whatman 42 filter paper, washed five or six times with water to make it free from chloride. The precipitate was dissolved in 1% HNO_3 by slight warming. A known excess of standard $AgNO_3$ (0.1 M) solution was added and the suspension of AgCl heated almost to boiling and stirred vigorously. The beaker and its contents were kept in the dark for 1 h, the precipitated AgCl was filtered

out and washed with water. The unreacted $AgNO_3$ was finally titrated with standard KSCN solution using $Fe(NO_3)_3$ as indicator. The end point was marked with the appearance of a faint-red brown color. The volume of $AgNO_3$ in the filtrate thus found was subtracted from the amount that originally added. The fluoride content was calculated from the volume of $AgNO_3$ solution consumed.

1 mL of 1 M $AgNO_3$ = 0.019 g of fluoride

Bromide[6]

Bromide was estimated volumetrically following Volhard's method.

An accurately weighed amount (*ca.* 0.1 g) of organicammonium tribromide was dissolved in 20 mL of acetonitrile. The solution was treated with 20 mL of a 20% NaOH solution, followed by the addition of 100 mL of water. The solution was boiled for 1 h and acidified with dilute (1:1) HNO_3. The acidified bromide solution was then treated with an excess of 0.1 M silver nitrate solution. The suspension was heated upto boiling and stirred vigorously. The beaker along with the suspension was kept in the dark for 30 min. The precipitated AgBr was separated out by filtration and washed several times with water. The filtrate and the washings were collected and the unreacted $AgNO_3$ was titrated with standard KSCN solution using $Fe(NO_3)_3$ as indicator. The end point was marked by the appearance of a faint red – brown color. From the equivalence of standard $AgNO_3$ and standard KSCN solutions, the volume of excess $AgNO_3$ was calculated and this was subtracted from the volume of $AgNO_3$ initially added. The difference is the volume of $AgNO_3$ solution consumed.

1 mL of 1 M $AgNO_3$ = 0.0799 g of bromide

Peroxide

(a) Permanganometry[7]

Nearly 1 g of boric acid was dissolved in 100 mL of water taken in a conical flask. To this was added an accurately weighed amount (*ca.* 0.1 g) of peroxo compound followed by the addition of 7 mL of 5M H_2SO_4. The solution was shaken well to dissolve

the compound. The peroxide was then estimated by redox titration with standard $KMnO_4$ solution. The end point was marked by the appearance of a permanent faint pink color.

$$1 \text{ mL of } 0.2 \text{ M } KMnO_4 = 0.016 \text{ of peroxide}$$

(b) Iodometry[8]

To a freshly prepared 2 M sulphuric acid solution, containing an appropriate amount of potassium iodide (~2 g in 100 mL) was added an accurately weighed amount (*ca.* 0.1 g) of a peroxo compound with stirring. The mixture was allowed to stand for *ca.* 15 min in carbon dioxide atmosphere in dark. The amount of iodine liberated was then titrated with a standard sodium thiosulphate solution, adding 2 mL of freshly prepared starch solution.

$$1 \text{ mL of } 1N \ Na_2S_2O_3 = 0.01701 \text{ g of peroxide } (O_2^{2-})$$

[In case of a peroxovanadate(V) complex, this method gives the total amount of peroxide plus vanadium present in the compound. On deduction of the contribution of vanadium (V) from the total amount of iodine liberated, the net peroxide content of the compound is evaluated.]

Aluminium[9]

An accurately weighed amount (0.1g) of aluminium compound, $[Al(H_2PO_4)_3]$ was added to water (10 mL). The solution was treated with dilute NaOH to increase the pH to *ca.* 5. The precipitate obtained was then filtered with Whatman 42 filter paper. Later, the precipitate was again dissolved in dilute NaOH (0.1N). A freshly prepared oxime solution* was added until the color of supernatant liquid just changed yellow. The solution warmed at temperature *ca.* 70^0C. At this stage the precipitate coagulated. The precipitate thus obtained filtered through glass crucible. The precipitate with crucible was dried in oven at temperature not exceeding 120-130^0C and weighed.

* [2 g of 8-hydroxyquinoline was dissolved in 100 mL of acetic acid. To this solution NH_3 was added dropwise till turbidity begins. Then the turbidity was cleared by addition of little ethanolic solution of acetic acid].

Titanium[10]

An accurately weighed amount (0.5g) of titanium compound, $(TiO_2)_{5.45}[Ti_4H_{11}(PO_4)_9].4\ H_2O$, was added to water (50mL). The solution was treated with dilute NaOH (0.1N) to increase the pH to *ca.* 5. The precipitate obtained was separated by filtration, washed several times water to make it free from alkali and then dissolved in 3N hydrochloric acid. To the clear solution thus obtained was added a slight excess of a freshly prepared 6% aqueous solution of cupferron (ammonium salt of N-nitroso-N-phenylhydroxylamine) with stirring until the curdy precipitate ceased to appear. The precipitate was then filtered off on a filter paper. The precipitated along with the filter paper was transferred in a large crucible and was cautiously ignited with a gradual increase in temperature to constant weight. Finally the titanium was weighed as TiO_2.

Phosphate[11]

To a neutral or weakly acidic solution (50-100 mL) of the phosphate containing compound, 3 mL of conc. HCl and few drops of methyl red indicator was added. A magnesia mixture** was introduced, followed by addition of conc. NH_3 solution slowly. The solution was then vigorously stirred until the color of indicator turns yellow. At that point precipitate appeared, and allowed the solution to stand for few hours. Then the precipitate was filtered off through sintered glass crucible and washed with 0.8 M aqueous solution of NH_3. The washing continues until a few mL of filtrate, when acidified with dil HNO_3 and tested with $AgNO_3$ gave no test for Cl^-. Further it was washed with small portions of alcohol or ether and drained well. The outside of crucible is then wiped with cloth, kept in desiccator for about 20 minutes and weighed.

** [25g of magnesium chloride, $MgCl_2.6H_2O$ and 50 g of NH_4Cl was dissolved in 250 mL water. Slight excess of NH_3 solution was added to that and allowed to stand overnight. Acidified with dil. HCl, further 1 mL of conc. HCl was added and diluted to 500 mL].

Carbon, Hydrogen and Nitrogen

The carbon, hydrogen and nitrogen contents were estimated by micro-analytical methods. The results of the analyses were obtained using a 2400 Perkin Elmer Series II CHNS/O Analyzer.

Particulars of Instruments/Equipment Used for the Following Physico-chemical Studies

pH Measurement

pH values of the reaction solutions were recorded with a Systronics Type 335 digital pH meter and also by using Merck pH indicator paper.

Solution Electrical Conductance Measurement

Solution electrical conductance measurements were measured on a Systronics Type 304 direct digital reading conductivity meter. Solution strength was maintained at 10^{-3} M in appropriate solvents.

Recording of Melting Point

Melting points of the compounds were recorded using a Type B-540 Buchi melting point apparatus. The heating rate was maintained at either 5 °C or 10 °C.

Infrared Spectroscopy

Infrared spectra of the compounds were recorded as KBr pellets or as thin films using a Nicolet Impact–410 Fourier Transform Infra Red Spectrophotometer, or on a Perkin-Elmer Spectrophotometer (spectrum one).

Raman Spectroscopy

Raman spectra were recorded in the back-scattering geometry using vertically polarized 800 nm argon-ion laser beams, double grating monochromator and cooled photomultipler tube.

Electronic Absorption Spectroscopy

UV-visible spectra were recorded, by dissolving a calculated amount of the sample in appropriate solvents, on a Hitachi UV-visible U–2001 Spectrophotometer or on a Perkin Elmer Lambda 25 UV–visible Spectrophotometer.

^{1}H Nuclear Magnetic Resonance Spectroscopy

^{1}H and ^{13}C NMR spectra were recorded on a Varian 400MHz spectrometers using tetramethylsilane (TMS) as internal standard

Thermal Studies

Thermogravimetry (TG) and Differential Scanning Calorimetry (DSC) experiments were conducted on a Mettler-Toledo TGA/SDTA 851^{e} and DSC 821^{e} instruments. Experiments were done using either aluminium or platinum crucibles. Pure N_2 gas was used as the flow gas.

Mass Spectrometry

GC-MS was recorded on Perkin-Elmer Precisely Clarus 500 instrument using a capillary column (30×0.25×0.25 mμ) in EI mode.

LC-MS was recorded on Waters Q-Tof Premier & Aquity UPLC instrument using a capillary column (35×0.25×0.25 mμ) in EI mode.

Gas Chromatography

Gas chromatographic analysis was done on a Hewlett Packard HP 6890 GC system with the aid of an FID detector by using a SE-30 capillary column. In all cases, nitrogen gas was used as a carrier gas. The results were recorded on an HP 3395 integrator.

Surface area measurement

Surface area (BET), pore volume, average pore size and pore size distribution were determined by the nitrogen adsorption-desorption method at liquid N_2 temperature on a BECKMAN COULTER(SA3100 serial no.AJ15007). The samples were degassed at 220 ^{0}C for 3 hours.

Powder X-ray diffraction

The powder XRD was recorded on BRUKER-D8ADVANCE with CuK_α source (λ = 1.54 Å) on glass surface of air-dried sample.

X-ray Crystallography

The X-ray data were collected at 293 K with MoK_α radiation (λ= 0.71073Å) on a Bruker Nonious SMART CCD difractometer equipped with graphite monochromater. The SMART software was used for data collection, indexing the reflection and determination of the unit cell parameters. Integration of the collected data was made using SAINT XPREP software.[12] Multi-scan empirical absorption corrections were applied to the data using the program SADABS.[13] The structures were solved by direct methods and refined by full-matrix least-square calculations by using SHELXTL software.[14] All non-hydrogen atoms were refined in the anisotropic approximation against F^2 of all reflections. The hydrogen atoms attached were located in difference Fourier maps and refined with isotropic displacement coefficients. The hydrogen atoms were placed in their geometrically generated positions. Crystal parameters for the compounds are presented in the experimental section of the respective chapters.

Computational details

In order to investigate the reactivity of the complexes we performed density functional theory (DFT) calculations. All calculations were performed with the DMol3 program using BLYP functional and DNP basis set. The size of the DNP basis sets is comparable to that of the Gaussian 6-31G** basis sets, but this numerical basis set is more accurate than a Gaussian basis set of the same size.[15] The integration grid referred to as FINE in the software program has been used for optimization of the complexes.

References

1. Weley R. H.; Hexner, P. E. *Organic Synthesis,* McGraw-Hill, New York, 1962, p. 351.
2. Furniss, B. S.; Hannaford, A. J.; Smith P. W. G.; Tatchell, A. R. *Vogel's Textbook of Practical Organic Chemistry*, 5th ed., Longman Group UK Ltd, 1989, p.1034.
3. Kauffman, G. B.; Fuller, R.; Felser, J.; Flynn C. M.; Pope, M. T. *Inorg. Synth.* Vol. XV, McGraw Hill Book Company, 1974, p.103.
4. P. C. Paul, *Ph. D thesis*, North Eastern Hill University, Shillong, **1992**.
5. S. K. Chettri, *Ph. D thesis*, North Eastern Hill University, Shillong, **1995**.
6. Vogel, A. I. *A Textbook of Quantitative Inorganic Analysis*, 3rd ed., Longman and Green, London, **1962**, p.267.
7. Jeffery, G. H.; Bassett, J.; Mendham J.; Denney, R. C. *Vogel's Textbook of Quantitative Chemical Analysis*, 5th ed., Addison Wesley Longman Limited, 1989, p. 812.
8. Ref. 7, p.356.
9. Ref. 6, p.516.
10. Ref. 6, p.574.
11. Ref.6, p. 544.
12. *SMART, SAINT and XPREP*, Siemens Analytical X-ray Instruments Inc., Madison, Wisconsin, USA, **1995**.
13. Sheldrick, G. M. *SADABS*: *Empirical Absorption and Correction Software*, University of Göttingen, Institut für Anorganische Chemie der Universität, Tammanstrasse 4, D-3400 Göttingen, Germany, **1999–2003**.
14. G. M. Sheldrick, *SHELXS-97*, University of Göttingen, Germany, **1997.**
15. Delley, B. *Int. J. Quant. Chem.* **1998**, *69,* 423.

Newer Heteroperoxovanadates (V) : Synthesis, Structure and Reactivity

Participation of vanadium in biological systems as well as in diverse abiotic processes spurred considerable research activities. Apart from the direct involvement in the active site of enymes like haloperoxidases [1,2] and nitrogenase [3], vanadium also possess some unique properties like inhibition of metabolic enzyme [4], mitogenicity [5], antitumorigenicity [6] and others [7]. Importantly, vanadium enhances the glucose uptake by the cell. To this end, a number of vanadium and peroxovanadium compounds have been proposed as prospective antidiabetic agent. While simple vanadate solution results in toxicity along with minimization of diabetic symptoms, vanadium complexes of organic ligands are found to minimize the adverse effects without sacrificing the important benefits [8]. Crans *et al.* [9] reported a new bisperoxovanadate (V) imidazole compound claiming equal or greater insulinomimetic potency than other reported compounds.

The thermal stability of the peroxo complexes in terms of release of active oxygen [10], stability in aqueous solution [11] and reactivity towards organic or inorganic substrates [12] depend on the nature of the heteroligand coordinated to the vanadium. Moreover, nature of cations which are use to neutralize the vanadate species has also significant influence on the stability and hence the reactivity [13]. In this regard pyrazole (pz) and its derivative have drawn attention as pz resembles imidazole. This resemblance allows some light to be shed on the nature of histidine-containing binding sites in vanadoproteins and other metallobiomolecules. Although pz complexes of vanadium(II) and (III) have been known for quite some time, very little work appears to have been done with vanadium(IV) or (V) except probably those reported by C. J. Carrano *et al.* [14]. The pyrazole ligand with protonated and deprotonated nitrogens as ring neighbors possesses an intriguing potential for structural modifications through secondary bond interactions. Here the deprotonated nitrogen can coordinate with the metal while leaving the hydrogen atom of the protonated nitrogen free for hydrogen bonding with appropriate ligands in its vicinity.

Apart from this, vanadium in the two physiologically relevant oxidation states, *viz.* V(IV), and V(V), elicits interactions with high and low molecular mass substrates in biofluid. Among the low molecular mass, outstanding example is citric acid, a α-hydroxytricarboxylic acid [15] which regulates fundamental physiological processes

and is an intermediate in carbohydrate metabolism, *e.g.* in the Kreb's cycle and nitrogen fixation [16]. Synthetic efforts revealed a number of dinuclear vanadium species of variable structural and spectroscopic properties with citric acid [17]. However, interaction of vanadium-peroxide-citrate at physiological pH (*i.e.* ~7.2) has been a matter of concern deserving attention.

Apart from pyrazole and citric acid, fluoride is an important ligand for vanadium (V) and (IV) playing at times, some antagonistic biochemical role. Fluorine being a strong electronegative atom, its presence in an active site of enzyme may pull the electron density along with the formation of hydrogen bond, thereby inhibiting the enzyme catalysis. But, fluoride and oxide ligands are known to stabilize higher valent, *i.e.* +4 and +5, states of vanadium [18] and also peroxovanadium complexes [19]. Moreover, fluoro-oxoperoxovanadates can be used as precursors for the vanadium oxide fluoride compounds, which are interesting in solid-state chemistry.[19h]

Perusal of some results of experimental and theoretical studies reveals that the μ-peroxo groups are more reactive than the terminal ones. Thus, a series of peroxovanadate compounds having μ-peroxo (bridging) group were found to be efficient catalysts at or near physiological pH [20-22]. However, the exact mechanism of action is not completely clear due to problem in resolving the crystal structure of many μ-peroxovanadates. In this regard, Density Funtional Theory (DFT) based calculations have been found to be an important tool [23]. Indeed, DFT is a useful tool to investigate structural, electronic and reactivity profiles of transition metal complexes [24].

Vanadium dependent haloperoxidase has fascinated researchers for some time now and drawn their attention highly towards the synthesis of model complexes and study of their reactivity. Vanadium haloperoxidases (VHPO), found in marine algae, lichens, and certain terrestrial fungi, catalyze the halogenation (Cl, Br, I) of organic substrates or the halide assisted disproportionation of hydrogen peroxide [1, 2]. Vanadium with peroxide or peroxovanadate serves as active intermediates in oxidation reactions [25]. Additionally, these complexes have been studied as functional models [26] for the haloperoxidase enzymes and oxidants for a variety of substrates, including benzene and other aromatics, alkenes, allylic alcohols, sulfides, halides, primary and secondary alcohols [26-31].

With an objective to synthesize some newer heteroperoxovanadium compounds, as a sequel to our continuous efforts in perxovanadium chemistry, we have now synthesized several heteroligated peroxovanadates (V) with 3,5-dimethylpyrazole (dmpz), citric acid and fluoride, at or near physiological pH and studied their reactivity with reference to haloperoxidase activity. The results obtained are described in four subsections of this chapter. The first three subsections discuss the synthesis and characterization of peroxovanadates with heteroligands like 3,5-dimethyl pyrazole (dmpz), citric acid and fluoride, whereas in the fourth subsection the reactivities of all these compounds have been illustrated.

The compounds thus reported herein are DmpzH[$VO(O_2)_2$(dmpz)](**1**), K[$VO(O_2)_2$(dmpz)].H_2O(**2**), $Na_2[V_2O_2(O_2)_4$(dmpz)].H_2O(**3**), $A_2[V_2O_4(C_6H_6O_7)_2].2H_2O$ [A = Na(**4**), K(**5**), NH_4(**6**)], $A_2[V_2O_2(O_2)_2(C_6H_6O_7)_2].2H_2O$ [A = Na(**7**), K(**8**), NH_4(**9**)], $Na_3[VO(O_2)_2(C_6H_6O_7)].4H_2O$(**10**), $A_3[VO(O_2)_2(OH)(O_2)_2OV]$. H_2O [A = Na(**11**), K(**12**), NH_4(**13**)], and $A_3[VO(O_2)_2(F)(O_2)_2OV].H_2O$ [A = Na(**14**), K(**15**), NH_4(**16**)]. Characterization of the complexes has been made on the basis of elemental analyses and a variety of spectroscopic studies.

The chemicals used were of reagent grade. The sources of the chemicals and solvents have all been already recorded in Chapter 2. Quantitative determination of elements and details of all the equipment used for physico-chemical studies have been summerized in Chapter 2.

Section 3.1

Synthesis, structural delineation and DFT investigation of Oxo-peroxo-dimethylpyrazole-vanadate (V)

3.1.1 Experimental

*(a) Synthesis of DmpzH[VO(O$_2$)$_2$(dmpz)] (**1**)*

To an aqueous solution of 0.5 g (2.76 mmol) of vanadium pentoxide, V_2O_5, in 5 mL of water, 2 mL (27 mmol) of 46 % hydrogen peroxide was taken in a pre-cooled (*ca.* 0 °C) 100 mL beaker. The reaction mixture being maintained at *ca.* 0 °C was stirred till all the V_2O_5 dissolved and the solution became reddish-brown. To the clear solution dmpz was added maintaining the ratio V: dmpz as 1: 2.4. The pH of the solution at this stage was recorded to be *ca.* 5.5. It was stirred for 3 hours at ice cold condition and ethanol was added to initiate the precipitation.

The product was obtained as bright yellow crystals. Well formed rod-shaped yellow crystal suitable for XRD analysis was obtained after two months from very dilute mother liquor. Yield of the product was 1.45 g (81%).

*(b) Synthesis of K[VO(O$_2$)$_2$(dmpz)].H$_2$O (**2**)*

An amount of 0.5 g (3.6 mmol) of potassium metavanadate, KVO_3, was added to 5 mL of water, taken in a 100 mL beaker. To the mixture an amount of 0.4 g (4.2 mmol) of dmpz was added in small portions with stirring. The solution was then cooled at an ice-water bath temperature. To the cooled solution 2 mL (27 mmol) of 46 % hydrogen peroxide was added in portion. The reaction solution was stirred for 3 h under ice-cold conditions. The reaction solution registered a pH value of *ca.* 6. Few drops of ethanol were added to bring about just haziness, and the beaker was then placed in a refrigerator. After a period of 3 or 4 days, shiny yellow crystals started precipitating out. The yield of the product was 0.66 g (85%).

*(c) Synthesis of $Na_2[V_2O_2(O_2)_4(dmpz)]$ $6H_2O$ (**3**)*

An amount of 0.5 g (4.1 mmol) of sodium metavanadate, $NaVO_3$ was added to 5 mL water and dmpz was added to the solution in the ratio V: dmpz as 1: 1.2 with stirring in ice cold condition. To the cooled solution 2 mL of 46% H_2O_2 (27 mmol) was added with stirring. The pH of the solution at this stage was recorded to be *ca.* 5.5. The whole was stirred for 3 hours at ice cold condition and ethanol was added to initiate the precipitation. The solution was kept in deep freezer; a shiny microcrystalline product came out within 14 days. The crystals were isolated in lots and after the isolation of a crop of crystals, the mother liquor, containing a crystal as seed, was returned to the refrigerator for further precipitation of crystals. Yield of the product was 0.54 g (51%).

(d) General procedure for cell culture and treatments

L6 skeletal muscle cell line was procured from the National Centre for Cell Science, Pune, India and was cultured in a manner as described. Briefly, L6 skeletal muscle cells were cultivated in DMEM (Dulbecco's Modified Eagle's Medium) medium supplemented with 10% fetal calf serum, 25 mM glucose, penicillin (100 U/mL) and streptomycin (100 µg/mL) in a humidified 95% O_2 / 5% CO_2 atmosphere at 37ºC. Cells were treated with insulin (100 nM) or insulin mimetic (100nM) or without any of them (control). On termination of incubations, cells were washed twice with ice-cold PBS (Phosphate Buffered Saline) and harvested with trypsin (0.25%)–EDTA (0.5 mM). Cell pellets were resuspended in lysis buffer [1% NP-40, 20 mM HEPES (pH 7.4), 2 mM EDTA, 100 mM NaF, 10 mM sodium pyrophosphate, 1 mM sodium orthovanadate, 1 µg/mL leupeptin, 1 µg/mL aprotinin, 1 µg/mL pepstatin and 1 mM PMSF] and sonicated on ice for 10 min (with 20 s pulse, 2 min between each pulse). Lysates were centrifuged for 10 min at 10,000 g.

(e) General procedure for [3H] 2-deoxyglucose uptake

[^{3}H] 2-deoxyglucose uptake in L6 myocytes was conducted according to the following method. L6 myocytes were serum starved overnight in Kreb's Ringer Phosphate (KRP) buffer (12.5 mM HEPES, pH 7.4, 120 mM NaCl, 6 mM KCl, 1.2 mM $MgSO_4$, 1 mM $CaCl_2$, 0.4 mM NaH_2PO_4, 0.6 mM Na_2HPO_4) supplemented with 0.2% bovine serum albumin. Cells were incubated separately for 30 min with porcine

insulin (100 nM) or insulin mimetic (100nM). Incubations in the absence of any of these chemicals were taken as the control. After 25 min, [^{3}H] 2-deoxyglucose (0.4 nmoles/mL) was added to each of the incubations 5 min before the termination of experiment. Cells were washed thrice with ice-cold KRP buffer in the presence of 0.3 mM phloretin to correct the glucose uptake data from simple diffusion and non-specific trapping of radioactivity. Cells were harvested with trypsin (0.25%)-EDTA (0.5 mM), solubilized with 1% NP-40 and [^{3}H] 2-deoxyglucose (2-DOG) was measured in a Liquid Scintillation counter (Perkin Elmer, Tri-Carb 2800TR).

3.1.2 Results and Discussion

The importance of pH in the reactions of vanadium (V) with hydrogen peroxide is well acknowledged. The pH value of 5.5 or 6 was found to be conducive to the successful synthesis of the targeted complexes. Incidentally the conducive pH was attained spontaneously during the reaction.

The complexes DmpzH[$VO(O_2)_2$(dmpz)] (**1**), K[$VO(O_2)_2$(dmpz)] (**2**), $Na_2[V_2O_2(O_2)_4$(dmpz)] (**3**), were synthesized in aqueous solution. Typically, V_2O_5 or AVO_3 reacted with dmpz and hydrogen peroxide at pH *ca* 5.5-6. In case of complex (**1**), dmpz acts both as a ligand as well as the counter cation ($dmpzH^+$) to stabilize peroxovanadate anion. As a ligand, dmpz behaves as a monodentate ligand, coordinating through the pyrazole N of the azole ring. It is believed that the heteroligand dmpz being a weak base (Lewis base) neutralizes the weak acidity arising from the H_2O_2 solution thereby rendering the reaction medium nearly neutral, as observed in the present cases. Needless to mention that the counter cation ($dmpzH^+$) not only balances the negative charges but stabilizes the peroxo group also.

Characterization of the compounds (**1**)-(**3**) was made by elemental analysis, IR, Raman and UV-Vis spectroscopy. X-ray crystal structures of (**1**) and (**3**) have been determined to delineate their structural motifs. The compounds are highly soluble in water. Interestingly, compound (**1**) is soluble in organic solvents like methanol, ethanol, acetonitrile, DMF, acetone and chloroform; however, it gives a red colored solution indicating the formation of mono-peroxo species. This was confirmed by determination

of V and O_2^{2-} contents. It is insoluble in hexane and toluene. Compounds (**2**) and (**3**) are insoluble in organic solvents. The results of chemical analysis have shown the presence of two peroxide groups per vanadium (V) in compounds (**1**)-(**3**) and the results are summarized in Table 3.1.1. The peroxide content was determined by redox titrations involving potassium permanganate in an acidic medium, and that of vanadium by iodometry. The consistent occurrence V(V) : O_2^{2-} as 1 : 2 supports the contention that the complexes are all di-peroxo species.

Table 3.1.1 Elemental analysis of compounds (**1**)-(**3**)

Compound	Found % (calcd. %)				
	V	O_2^{2-}	C	H	N
(**1**)	15.8 (15.7)	19.5 (19.7)	36.92 (37.03)	5.15 (5.24)	17.20 (17.28)
(**2**)	20.3 (19.7)	23.3 (24.0)	26.53 (27.06)	3.03 (3.00)	10.56 (10.53)
(**3**)	20.8 (20.0)	24.5 (25.0)	28.85 (11.73)	3.23 (1.56)	11.26 (5.47)

Molar conductance of the compounds (**1**) and (**2**) were found to be in the range of 110-130 $\Omega^{-1}cm^2mol^{-1}$ suggesting their 1: 1 electrolytic nature, whereas (**3**) gave 223 $\Omega^{-1}cm^2mol^{-1}$ indicating it to be an 1: 2 type electrolyte. The conductance values have been set out in Table 3.1.2. The solution electronic spectra of the complexes exhibited two bands around 328-330 nm and 210-212 nm for $\pi_v \rightarrow d_\sigma^*$ and $\pi_h \rightarrow d_\sigma^*$ transition respectively [32] (Table 3.1.2).

Table 3.1.2 Molar conductance values and UV-visible data of compounds (**1**)-(**3**)

Compound	Solution electrical conductance (10^{-3} M) ($\Omega^{-1}cm^2mol^{-1}$)	UV-Vis λ (nm) (ε, $M^{-1}cm^{-1}$)
(1)	122	330 (691), 212 (40,700)
(2)	119	330 (700), 210.5 (49,800)
(3)	223	329 (472), 211 (38,300)

Vibrational spectroscopy is an essential technique for the characterization of complexes containing coordinated peroxo ligands. Bidentate peroxide coordination creates a local C_{2v} environment which has three IR active modes: the symmetric O-O

stretch, the symmetric metal-peroxo stretch, and the asymmetric metal-peroxo stretch [33], and occur at *ca.* 880, 600 and 500 cm^{-1}, respectively. The significant IR frequencies of the compounds are given Table 3.1.3.

Table 3.1.3 Structurally significant IR and Raman spectral data of compounds (**1**)-(**3**)

Compound	IR ν (cm^{-1})		Raman ν (cm^{-1})	Assignment
	Experimental	Theoretical		
(**1**)	535(m)	531	540	$\nu_{V\text{-}O2}(\nu_2)$
	628(s)	636	596	$\nu_{V\text{-}O2}$ (ν_3)
	876(vs)	866	885	$\nu_{O\text{-}O}$ (ν_1)
	944(vs)	937	988	$\nu_{V=O}$
	1419(s)	1435		$\delta_{N\text{-}H}$ (dmpz)
	1569(s)	1545		$\nu_{C\text{-}N}$
	2874(s), 2927(s)	3243		$\nu_{N\text{-}H}$ (free and coord. dmpz)
(**2**)	528(m)	500.9	526.90	$\nu_{V\text{-}O2}(\nu_2)$
	629(s)	620.7	630.41	$\nu_{V\text{-}O2}$ (ν_3)
	878(vs)	855.0	883.73	$\nu_{O\text{-}O}$ (ν_1)
	944(vs)	908.4	945.67	$\nu_{V=O}$
	1420(w)	1413.3		$\delta_{N\text{-}H}$ (dmpz)
	1568(s)	1531.5		$\nu_{C\text{-}N}$
	3248(bs)	3355.5		$\nu_{N\text{-}H}$ (dmpz)
(**3**)	526(m)	507	534	$\nu_{V\text{-}O2}(\nu_2)$
	616(s)	610	607	$\nu_{V\text{-}O2}$ (ν_3)
	870(vs), 886(s)	853, 872	889	$\nu_{O\text{-}O}$ (ν_1)
	949(vs)	923.3	978	$\nu_{V=O}$
	1414(w)	1412, 1434		$\delta_{N\text{-}H}$ (dmpz)
	1584(m)	1537		$\nu_{C\text{-}N}$
	3392(b)	3459		$\nu_{N\text{-}H}$ (dmpz)

While the IR spectra of compounds (**1**) and (**2**) are similar, indicating their close structural similarity, IR spectrum of (**3**) is slightly different (Figure 3.1.1) indicating that the compound is structurally somewhat different from the other two. The IR

spectra show bands at ~945, ~877, ~630 and ~530 cm^{-1} which have been assigned to $\nu_{V=O}$, ν_{O-O} (ν_1), ν_{V-O_2} (ν_3) and ν_{V-O_2} (ν_2) modes, respectively. Notable in this context is that, in addition to the strong absorption appearing at 886.1(s) cm^{-1}, an additional band has been observed for compound (**3**) at 870.2(s) cm^{-1}, which has been assigned to the ν_{O-O} of terminal and bridging peroxo group [34]. Significantly, no band appeared at *ca.* 870 cm^{-1} in the specta of compound (**1**) and (**2**). These results suggest the presence of two different types of peroxo group in the complex (**3**), whereas one type for compound (**1**) and (**2**) in line with their formulation. This asserion has been attested to by the X-ray crystal structures of compounds (**1**) and (**3**) and DFT optimized structure of compound (**2**).

The spectral pattern originating from the presence of dmpz ligand is quite representative of its monodentate coordination to the metal center [35]. Importantly, a positive shift of the ν_{C-N} (pyrazole ring) band by about 12 cm^{-1} compared to that of the free ligand suggests that the tertiary ring nitrogen possibly provides the binding site. This contention gains further support from the appearance of a band at *ca.* 3240 cm^{-1} owing its origin to ν_{N-H}. In other words, it is the non-protonated nitrogen that appears to be bonded to the V (V) center.

The stretching frequencies of compound (**1**)-(**3**) have been calculated by using DFT and the results are compared in Table 3.1.4. Further the peak values have been assigned to the corresponding bond. In case of compound (**3**), the additional peak at *ca.* 870.2(vs) cm^{-1} has been assigned to bridged peroxo group (i.e. O4-O5). The average error for the frequencies is found to be in the order of 10-20 cm^{-1} with respect to experimental result, which is quite good in terms of reproducibility.

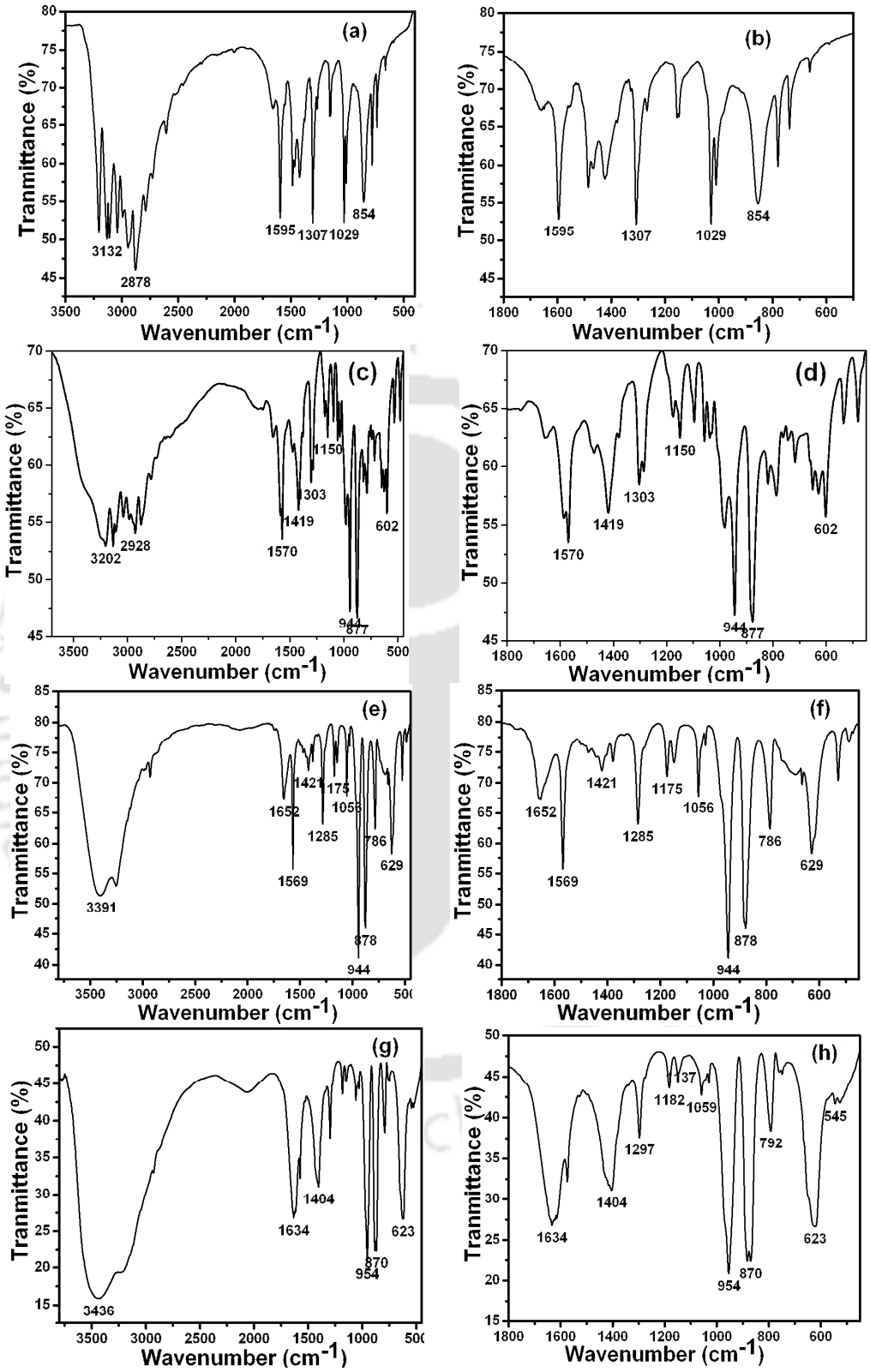

Figures 3.1.1 *FTIR spectra of (a) 3,5-dimethylpyrazole, (c) compound (**1**), (e) compound (**2**), and (g) compound (**3**) in 4000-450 cm^{-1} region. Figures (b), (d), (f) and (h) are the expanded view of the region 1800-500 cm^{-1} of (a), (c), (e) and (g), respectively.*

Like IR spectroscopy, Raman spectroscopy is also an important tool to characterize peroxo complexes of metal. The structurally significant Raman bands are assigned in Table 3.1.4 and the spectra are given in Figure 3.1.2. The spectra shows strong bands at ~988.66, ~881.00, ~599.30, ~542.43 cm^{-1} which have been assigned to $\nu_{V=O}$, ν_{O-O} (ν_1), ν_{V-O_2} (ν_3) and ν_{V-O_2} (ν_2) modes, respectively. The Raman spectrum of compound (**3**) has been also recorded in solution to check the behavior in solution. No notable changes have been observed in the spectral pattern [Figure 3.1.2 (d)], however, decrease in intensity of peak at *ca.* 985 cm^{-1} was observed.

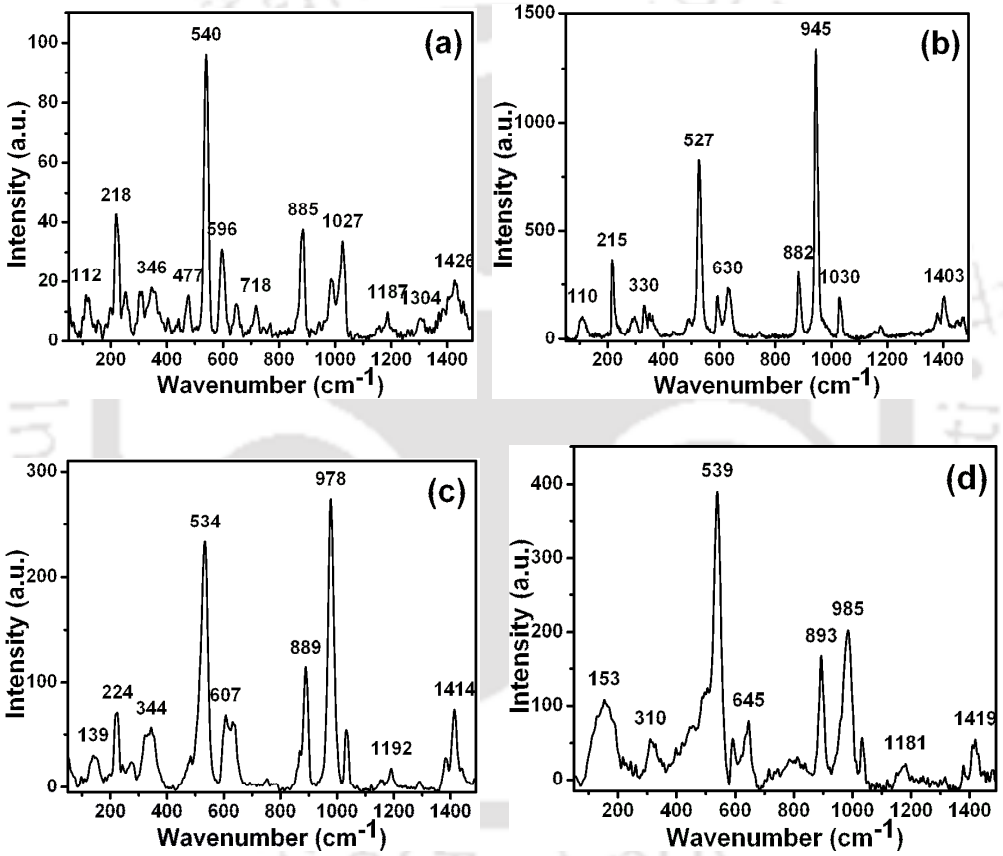

Figures 3.1.2 *(a), (b) and (c) are the Raman spectra of compound (**1**), compound (**2**), and compound (**3**), respectively. (d) is the Raman spectrum of compound (**3**) in solution.*

Isolation of crystals of diperxovanadium complexes is rather tricky, due to its low stability at room temperature and insolubility in organic solvents. However, we have been able to isolate compounds (**1**) and (**3**) in crystalline form, but have so far been unsuccessful for compound (**2**). The crystals suitable for X-ray diffraction could

be obtained from the mother liquor of the reaction mixture after a period of two months for compound (**1**), and after fourteen days for compound (**3**).

A yellow crystal of compound (**1**) with dimensions 0.45 x 0.28 x 0.16 mm^3, was mounted on capillary for data collection. A summary of crystal parameters is incorporated in Table 3.1.4. The X-ray crystal structure of compound (**1**) consists of discrete peroxovanadate (V) anion with one dmpz ligand and another $dmpzH^+$ as a cation. Compound (**1**) crystallizes in the monoclinic system P2(1)/c with four molecules in the unit cell. The ORTEP diagram of the anion in (**1**) with numbering scheme is shown in Figure 3.1.3. A selected list of interatomic distances and bond angles for (**1**) is provided in Table 3.1.5. The coordination environment of the vanadium atom approximates a pentagonal pyramid, with the oxo group occupying the axial position. The basal positions are occupied by the pyrazole and the two peroxo groups, and the distance of the vanadium from the basal plane is 0.687 Å. The V=O, V-O (peroxo) and V-N bond lengths (*ca.* 1.59, 1.85-1.91, and 2.10 Å) are similar to those found in other vanadium complexes [9, 36]. In general peroxovanadium complexes are seven-coordinate species with respect to vanadium, however, the present complex is a six coordinate ion. Incidently, only a few peroxovanadium complexes with similar coordination environment such as $NH_4[VO(O_2)_2NH_3]$ [36b] and $ImzH[VO(O_2)_2Imz]$ [9] have been observed. A comparison of different bond lengths of the compound (**1**) with those of $ImzH[VO(O_2)_2Imz]$ is presented in Table 3.1.6.

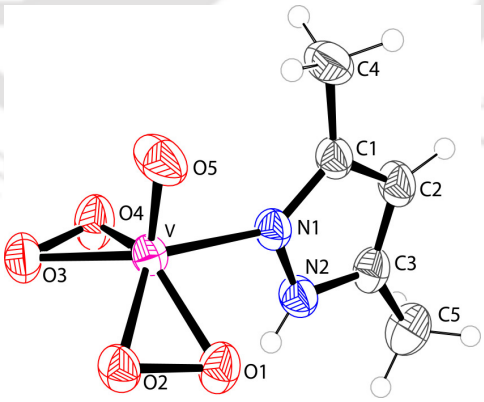

Figure 3.1.3 *ORTEP plot of the anion of compound (**1**), $[VO(O_2)_2dmpz]^-$.*

Table 3.1.4 Crystal data and structure refinement for compound (**1**) and (**3**)

Parameter	Compound (**1**)	Compound (**3**)
Empirical formula	C10 H17 N4 O5 V	C5 H8 N2 Na2 O16 V2
Formula weight	324.22	499.99
Temperature K	296(2)	296(2)
Wavelength Å	0.71073	0.71073
Crystal system	Monoclinic	Monoclinic
Space group	P2(1)/c	C2/c
Unit cell dimensions, Å and ^{0}	a = 8.726(5) α= 90 b = 8.294(4) β= 99 c= 20.100 (11) γ = 90	a = 32.644(9) α= 90 b = 8.502(3) β= 93.23(3) c = 13.630(4) γ = 90
Volume Å^3	1436.95(13)	3777(2)
Z	4	8
Density (calculated)Mg/m^3	1.499	1.759
Absorption coefficient, mm^{-1}	0.714	1.113
F(000)	672	1984
Crystal size mm^3	0.45 x 0.28 x 0.16	0.45 x 0.32 x 0.24
Index ranges	-11<=h<=11, -10<=k<=11, -26<=l<=26	-39<=h<=44, -11<=k<=11, -18<=l<=18
Reflections collected	16280	17669
Independent reflections	3565 [R(int) = 0.0314]	5003 [R(int) = 0.0795]
Completeness to theta =28.42°	98.7 %	94.5 %
Absorption correction	None	None
Data / restraints / parameters	3565 / 0 / 197	5003 / 0 / 251
Goodness-of-fit on F^2	1.013	1.077
Final R indices [I>2sigma(I)]	R1 = 0.0370, wR2 = 0.1010	R1 = 0.0691, wR2 = 0.1790
R indices (all data)	R1 = 0.0444, wR2 = 0.1061	R1 = 0.1263, wR2 = 0.2303
Largest diff. peak and hole,	0.744 and -0.200 e.Å^{-3}	0.849 and -0.777 e.Å^{-3}

Table 3.1.5 Selected bond lengths [Å] and angles [°] for compound (**1**)

Parameter	Experimental	Theoretical	Parameter	Experimental	Theoretical
V-O(1)	1.8515(14)	1.816	O(5)-V-O(2)	108.14(8)	112.63
V-O(2)	1.8929(13)	1.820	O(1)-V-O(2)	46.03(6)	45.68
V-O(3)	1.8586(14)	1.847	O(3)-V-O(2)	124.67(6)	122.40
V-O(4)	1.9176(13)	1.987	O(5)-V-O(4)	104.14(7)	103.99
V-O(5)	1.5898(15)	1.642	O(1)-V-O(4)	128.76(7)	130.40
V-N(1)	2.1072(14)	2.065	O(3)-V-O(4)	46.00(6)	43.50
N(1)-N(2)	1.3575(12)	1.336	O(2)-V-O(4)	89.55(6)	91.06
O(2)-O(1)	1.4645(19)	1.412	O(5)-V-N(1)	96.48(7)	96.84
O(3)-O(4)	1.4765(18)	1.427	O(1)-V-N(1)	82.36(6)	82.95
N(3)-N(4)	1.3343(12)	1.335	O(3)-V-N(1)	82.41(6)	80.52
N(3)-H(3N)	0.8656(13)	1.256	O(2)-V-N(1)	127.89(6)	127.21
N(4)-H(4N)	0.7832(12)	1.078	O(4)-V-N(1)	128.39(6)	124.01
O(5)-V-O(1)	112.38(18)	113.77	O(2)-O(1)-V	68.48(8)	67.33
O(5)-V-O(2)	112.95(18)	111.63	O(3)-O(4)-V	64.89(7)	63.01
O(3)-V-O(1)	134.07(13)	133.06	O(4)-O(3)-V	69.11(7)	73.49

Table 3.1.6 Comparison of bond lengths of compound (**1**) and ImzH[$VO(O_2)_2$Imz]

Bond	Dmpz[$VO(O_2)_2$dmpz]	ImzH[$VO(O_2)_2$Imz]
V-O(1)	1.8515(14)	1.865(2))
V-O(2)	1.8929(13)	1.884(2)
V-O(3)	1.8586(14)	1.866(2)
V-O(4)	1.9176(13)	1.922(2
V-O(5)	1.5898(15)	1.603(2)
V-N1	2.1072(14)	2.092(2)
O(2)-O(1)	1.4645(19)	1.467(3)
O(3)-O(4)	1.4765(18)	1.475(2)

The importance of hydrogen bonding in the catalytic activity of vanadium haloperoxidases is now well understood. Mechanistic studies of VHPO and VHPO-model complexes suggest that peroxide activation may be achieved by protonation of the V(V)-bound peroxo group to generate a side-on bound

hydroperoxide complex [37]. It has been proposed that an increase in positive charge on O_{peroxo}, by protonation, makes attack by halide more favorable [38]. In accord with that, Butler and her co-workers [39] had synthesized $K[VO(O_2)(^{NH_2}pyg_2)]$ and showed the intramolecular H-bonding (d(N(1)—H···O) : 2.637(4) Å). Incidentally, for no diperoxovanadium complex the possibility of H-bonding was studied. Notably, the compounds (1) has intra as well as inter molecular H-bonding, as shown in Figures 3.1.4 (a) and (b). As expected, the hydrogen from the protonated nitrogen in the ligated pyrazole forms H-bond with the peroxo group of neighboring peroxovanadates (N-H···O_2, 2.040 Å) and the counter pyrazolium cation forms hydrogen bonds with two peroxo groups (N-H···O_2, 1.813 and 1.837 Å) from different peroxo-vanadates thus stabilizing the peroxo groups. The presence of strong N3–H···O and N4–H···O hydrogen bonding network results in the formation of 3D coordination polymer (Figure 3.5). The bond lengths of donor and acceptor, which involve in the H-bonding, are given in Table 3.1.7. These H-bonding provide important clues to the haloperoxidase activity.

Table 3.1.7 Hydrogen bond distances (Å) and angles (°) in compound (**1**)

D–H…A[a]	D–H (Å)	H...A(Å)	D...A(Å)	∠D–H….A (°)
N2-H…O4	0.774	2.040	2.804	169.03
N3-H…O4	0.860	1.816	2.665	164.86
N3-H…O3	0.860	2.353	2.992	131.41
N4-H…O2	0.781	1.841	2.610	168.02
N4-H…O1	0.781	2.448	3.053	135.43

[a]*D = donor, A = acceptor*

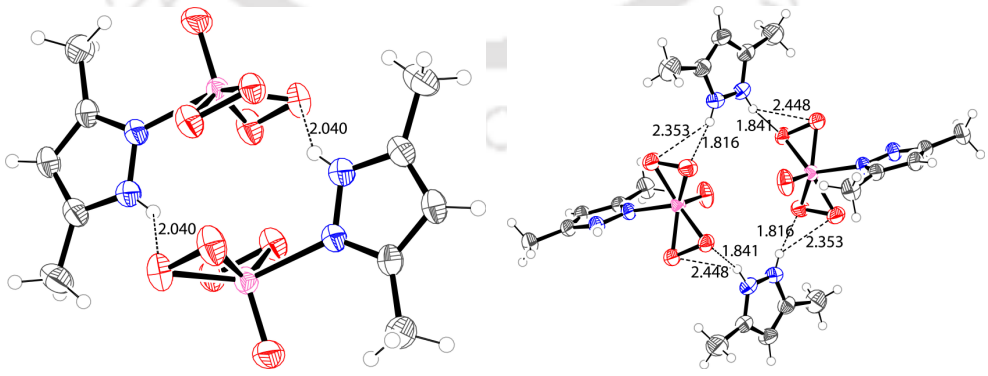

)

(b)

Figure 3.1.4 *(a) and (b) N-H ···O hydrogen bonding in compound (**1**); the hydrogen bonds are represented by dashed line.*

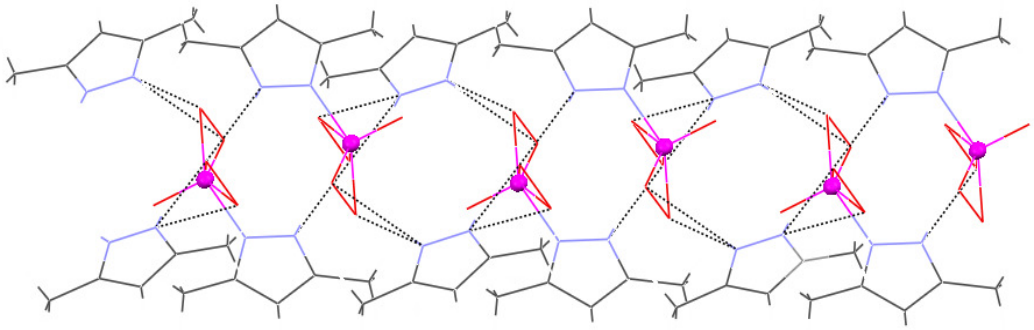

***Figure 3.1.5** Hydrogen bonding network in compound (**1**)*

While compound (**1**) consists of a bisperoxovanadate (V) pyrazole anion with pyrazolium as the counter cation, compound (**3**) is binuclear bisperoxovanadate (V) having sodium as the counter cation. Compound (**3**) is stable at 4^0C for a long period, but remains unchanged only for a few hours at ambient temperature. A suitable crystal was collected from the reaction mixture and mounted for X-ray analysis. The ORTEP diagram of the anion in compound (**3**) with numbering scheme is shown in Figures 3.6 (a) and (b). Compound (**3**) crystallizes in the monoclinic system C2/c with eight molecules in the unit cell. The crystal data and refinement results are set out in Table 3.1.4 and the selected list of interatomic distances and bond angles for (1) is provided in Table 3.1.8. The anion has a dinuclear structure with coordinatively nonequivalent vanadium atoms with pentagonal pyramidal arrangement. The pentagonal planes of V1 and V2, are defined by O2, O3, O4, O5, N1 and O5, O7, O8, O9, O10 atoms, respectively, and they are connected by the O5 peroxo atom. The dihedral angle between these two planes is 57.57°. The V1 and V2 atoms are displaced from the pentagonal planes by 0.455 and 0.509 Å, respectively. As a consequence, the shortest distances between the vanadium atoms and the non-cordinated oxygen atoms in the seventh position of the two pentagonal bipyramids are 2.543 (for V1-O7) and 2.664 Å (for V2-O3), which might be due to the tendency of the vanadium atoms to attain the coordination number seven. The four O_p-O_p distances are comparable, *i.e.* the bridging has no significant effect; however, it causes an elongation of the V1-O_p distances to 1.892 (for O4) and 1.940 Å (for O5). Oxygen from peroxo groups and water saturate the coordination environment of sodium. It has been found that one sodium is hexa-

coordinated whereas the other one is hepta-coordinated. Interestingly sodium ions from another unit making a bridge between two consequetive dinuclear units.

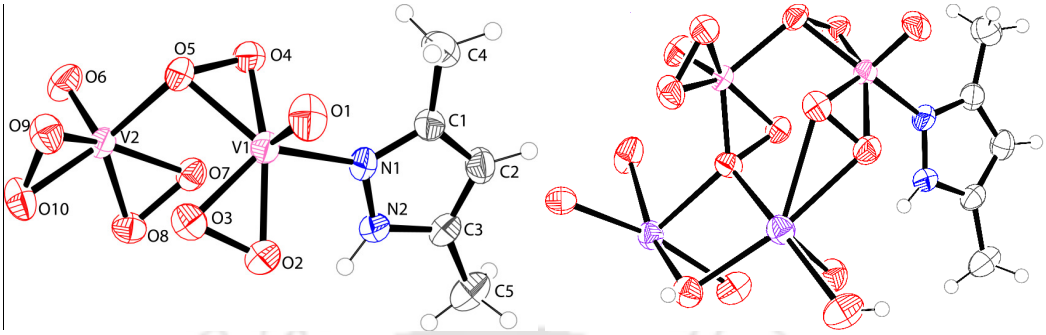

Figure 3.1.6 *Ortep diagrams of the (a) anion and (b) total unit of compound (**3**).*

Table 3.1.8 Selected bond lengths [Å] and angles [°] for compound (**3**)

Parameter	Experimental	Theoretical	Parameter	Experimental	Theoretical
V(1)-O(1)	1.597(3)	1.614	O(4)-V(1)-O(5)	45.02(12)	43.92
V(1)-O(2)	1.867(3)	1.921	O(1)-V(1)-N(1)	98.38(15)	96.38
V(1)-O(3)	1.869(3)	1.924	O(2)-V(1)-N(1)	83.98(14)	81.78
V(1)-O(4)	1.893(3)	1.904	O(3)-V(1)-N(1)	129.10(15)	126.40
V(1)-O(5)	1.939(3)	2.013	O(4)-V(1)-N(1)	86.41(14)	82.77
V(2)-O(6)	1.600(3)	1.653	O(5)-V(1)-N(1)	130.48(14)	126.14
V(2)-O(7)	1.890(3)	1.954	O(6)-V(2)-O(7)	105.05(16)	103.62
V(2)-O(8)	1.878(3)	1.991	O(6)-V(2)-O(8)	108.22(16)	101.63
V(2)-O(9)	1.877(3)	1.882	O(6)-V(2)-O(9)	107.01(15)	113.15
V(2)-O(10)	1.888(3)	1.900	O(6)-V(2)-O(10)	106.12(15)	114.07
V(2)-O(5)	2.043(3)	2.070	O(7)-V(2)-O(10)	130.62(14)	141.72
V(1)-N(1)	2.080(3)	2.170	O(7)-V(2)-O(8)	45.98(14)	44.92
O(1)-V(1)-O(2)	107.46(17)	112.13	O(7)-V(2)-O(9)	131.85(14)	123.32
O(1)-V(1)-O(3)	105.46(15)	109.34	O(7)-V(2)-O(10)	146.79(13)	141.72
O(2)-V(1)-O(3)	46.21(13)	45.28	O(8)-V(2)-O(9)	90.04(15)	85.66
O(1)-V(1)-O(4)	105.20(17)	110.00	O(8)-V(2)-O(10)	130.59(14)	127.61
O(2)-V(1)-O(4)	146.92(15)	136.35	O(10)-V(2)-(9)	45.97(13)	45.81
O(3)-V(1)-O(4)	127.49(13)	126.61	O(5)-V(2)-(6)	101.24(13)	106.27
O(1)-V(1)-O(5)	102.95(16)	107.27	O(5)-V(2)-(7)	82.14(12)	83.49
O(2)-V(1)-O(5)	129.21(13)	127.98	O(5)-V(2)-O(8)	124.68(14)	125.90
O(3)-V(1)-O(5)	86.99(13)	90.45	O(5)-V(2)-O(9)	124.48(12)	121.64

Interestingly only a few peroxovanadium compounds with the dinuclear unit being bridged in μ-η^1: η^2-O_2 fashion are known, for instance, $[V_2O_2(O_2)_4(PO_4)]^{5-}$, [40] $K_7[V_4O_4(O_2)_8(PO_4)]$ [41] and $CymH_2[V_2O_2(O_2)_4(H_2O)]$ [42]. The V-O (bridging peroxo) (V_2-O_5) distances in $[V_2O_2(O_2)_4(PO_4)]^{5-}$ and $[V_4O_4(O_2)_8(PO_4)]^{7-}$ are higher (2.45(±5) Å) than those of $[V_2O_2(O_2)_4(H_2O)]^{2-}$ (2.035 Å) as well as compound (**1**) (2.041 Å). Very recently, $Cs_3[V_2\ O_2(O_2)_4F].\ H_2O$ has been reported with a μ-η^1: η^2-O_2 group where the corresponding distance is found to be 2.041 Å [43]. In addition, a dinuclear peroxovanadaium compound with two μ-η^1: η^2-O_2 groups and one bridging glycinato group has been reported having the bridging bond distances 2.328 and 2.354 Å [44].

Density Functional Theory based study

DFT calculations have been carried out to investigate the structural and electronic properties of the complexes (**1**)-(**3**). The structures have been optimized with VWN and BLYP functionals. The experimental solid-state geometries of compound (**1**) and (**3**) are well reproduced by DFT calculations. Also an optimized structure has been obtained for compound (**2**). The optimized geometry of compound (**2**) has been shown in Figure 3.1.7. In general, a reasonable agreement is seen between the results obtained from DFT calculation and X-ray crystallographic studies. The differences between the theoretical and experimental bond lengths are within the order of a few angstroms, and the bond angles agree within a few degrees. It can also be noted that the computations predict an almost similar structure with the experimental one. We next calculated Fukui function and the relative electrophilicity values using Mulliken and Hirshfeld population schemes in order to understand the reactivity of O-O moieties at the optimized geometries of the compounds (**1**) - (**3**). The total electophility values are found to be 6.28, 1.84 and 5.19 for the compounds (**1**), (**2**) and (**3**), respectively.

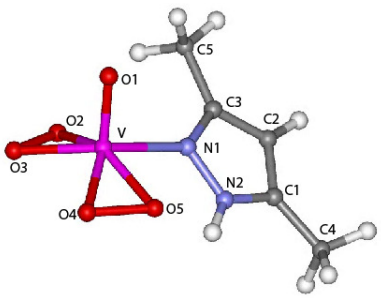

Figure 3.1.7 *Optimized geometry of compound (**2**) derived from DFT calculation at BLYP/DNP level. The significant bond distances are V-O1 1.657, V-O2 1.919, V-O3 1.948, V-O4 1.901, V-O5 1.878, V-N1 2.221.*

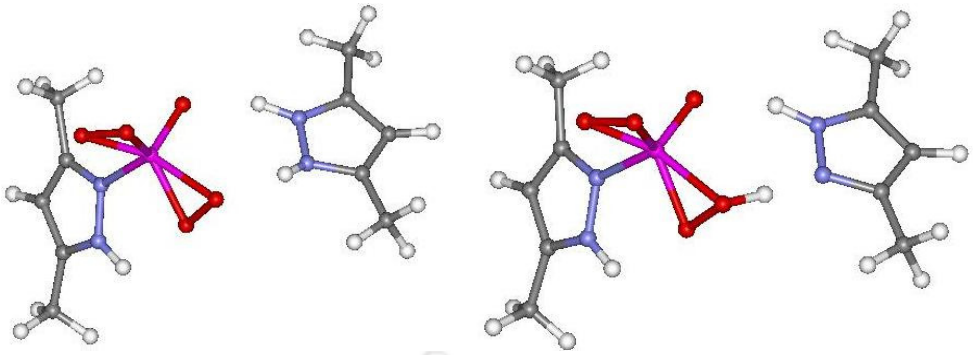

(a) (b)

Figure 3.1.8 *Optimized geometry of compound (**1**) derived by using (a) VWN and (b) BLYP functionals. Strong H-bonding has been observed between N-H (pyrazolium) and peroxo-oxygen, as a result proton shifts to oxygen.*

Interestingly, when we optimized the structure of compound (**1**) with BLYP functionals, it has been observed that the proton shifts from the pyrazole ring to the peroxidic oxygen due to strong hydrogen bond between N-H (from pyrazolium cation) and peroxidic oxygen. As a result the electrophilicity of the compound (**1**) becomes higher than the other compounds. HOMO and LUMO of the complexes have also been calculated. The HOMO's obtained from the calculations are shown in Figures 3.1.9 (a)-(c). From the HOMO it is clear that the electron density near the peroxidic oxygen is less in case of compound (**1**) and (**3**), however, this is very high for compound (**2**). Hence compound (**1**) and (**3**) are more reactive toward the nucleophilic attack of a nucleophile, like Br^-. The higher reactivity might be due to protonation of the peroxidic oxygen by the pyrazolium proton. A similar observation was made in the case of vanadium haloperoxidase enzymes [37], where the proton from Lysine residue regulates the activity. In this respect, compound (**1**) is the first example of diperoxovanadium complex to have shown this activity. The higher reactivity of compound (**3**) compared to compound (**2**) is attributed to the presence of bridging peroxo group. Vanadium with d^0 configuration, possessing Lewis acid character pulls the electron density towards itself thereby making the bridging peroxo group more electrophilic.

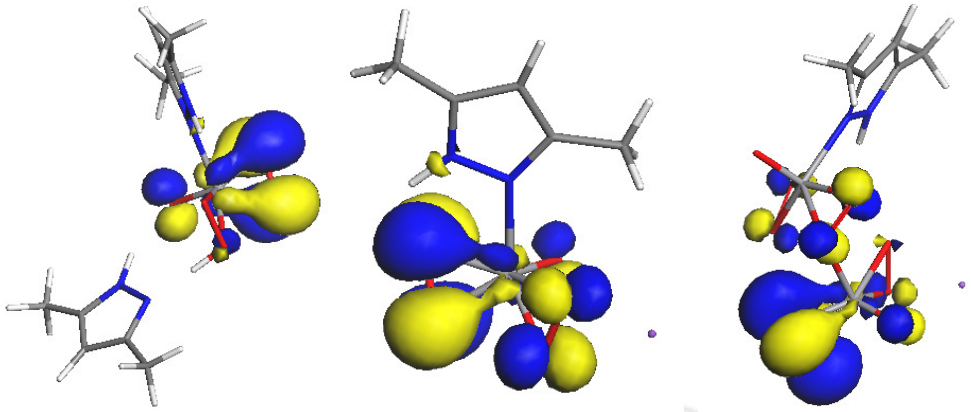

(a) (b) (c)

Figure 3.1.9 *HOMO of (a) compound (**1**), (b) compound (**2**) and (c) compound (**3**).*

Insulinomimetic Study of Compound (1), DmpzH[VO(O$_2$)$_2$dmpz]

Vanadium compounds have been shown to mimic the effects of insulin, resulting in enhanced glucose uptake of cells. Moreover, peroxovanadim compounds have been found to be more efficient than oxovanadium compounds. Bisperoxovanadium imidazole monoanion has been reported to enhance glucose uptake as good as or better than earlier reported compounds [9]. Thus, to evaluate the insulinomimetic activities of compound (**1**), DmpzH[VO(O$_2$)$_2$dmpz], we assayed its effects on uptake of [^{3}H] 2-deoxyglucose in cultured L6 skeletal muscle cells and also compared the results with insulin.

Comparison of [^{3}H] 2-deoxyglucose uptake augmentation by human insulin and insulin mimetic DmpzH[VO(O$_2$)$_2$dmpz] augmentation in L6 skeletal muscle cells

L6 is a human skeletal muscle cell line and suitable to examine insulin activity since majority of the excess glucose in the blood circulation is uptaken by skeletal muscle cells by the action of insulin. Skeletal muscle has robust expression of insulin receptor in the cell membrane. It could be seen from Figure 3.1.10 that both human insulin and insulin mimetic increased the glucose uptake more than 2.5 fold over the control and this increase was statistically highly significant. Since both human insulin

and insulin mimetic were used at same concentration, the effect of insulin mimetic here indicates meaningful physiological relevance. Another experiment was performed to examine the stability of insulin mimetic through the evaluation of bioactivity which is uptake of [^{3}H]- deoxyglucose by L6 skeletal muscle cells. Figure 3.1.11 shows that insulin mimetic compound was as active as human insulin but its activity decreased considerably on 20th day. In contrast if insulin mimetic compound remains in buffer solution its activity remains almost intact till 60 days.

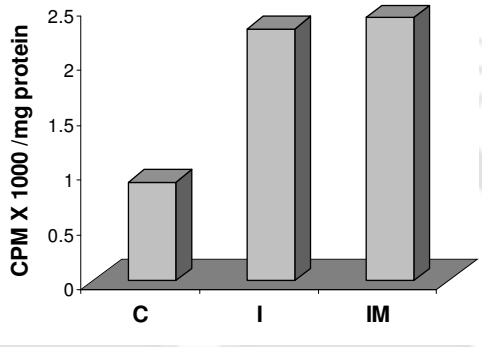

Figure 3.1.10 Effect of insulin and insulin mimetic on stimulation of radio labelled glucose uptake in L6 myocytes. The unit of glucose uptake in Y axis is (CPM x 10^3)/mg protein

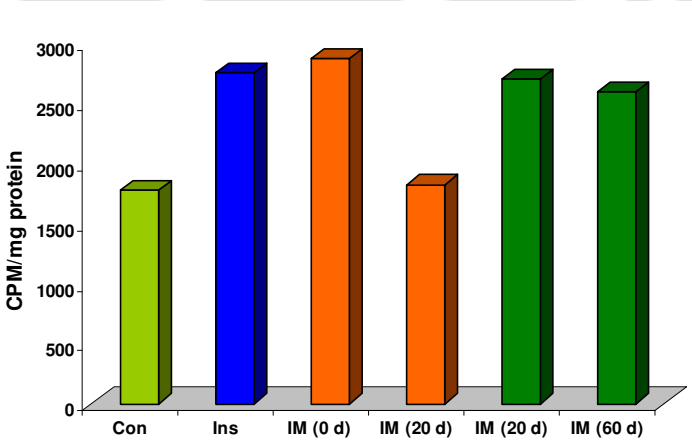

Figure 3.1.11 Stability study of insulin-mimetic compound where Con= Control, Ins= Insulin, IM= Insulino-mimetic, d= day, Columns 3 and 4 (marun colored) are the results from the crystals whereas columns 5 and 6 (green colored) are results obtained from the solution in PBS= 50 mM, pH 7.5, NaCl 0.15 M (phosphate buffered saline of the insulinomimetic complex.

Interestingly, DmpzH[$VO(O_2)_2$dmpz] dose that was used in this study was remarkably less as compared to other insulin mimetic compounds used for *in vitro* and *in vivo* studies (Table 3.1.9).

Table. 3.1.9 *Comparative study of different insulin mimetic compounds.*

In vitro		In vivo	
Name of the compound	Dose	Name of the compound	Dose/Kg body weight
L-Glit(γ)HXM	30 µM	Vanadyl sulfate	100 mg
Vanadate	1 µM- 100 µM	BFOV	0.2 mM
pervanadate	5 µM-20 µM	BMOV	0.1 mM
BMOV	0.12 mM	Present compound	**60 µg**
bpV	100 µM		
Present compound	**100 nM**		

3.1.3 Conclusion

Targated synthesis to mimic haloperoxidase enzyme as well as insulin activity led us to isolate and characterize DmpzH[$VO(O_2)_2$(dmpz)] (**1**), K[$VO(O_2)_2$(dmpz)].H_2O (**2**) and $Na_2[V_2O_2(O_2)_4$(dmpz)].H_2O (**3**). While compound (**1**) and (**2**) are mononuclear bisperoxovannadates, compound (**3**) is dinuclear bisperoxovanadate with a less commonly encountered bridged µ-η^1: η^2-peroxo group. The pyrazole is bonded with vanadium in monodentate fashion. Hence pyrazole mimics the binding of imidazole in haloperoxidase enzyme. The structural, electronic and reactivity properties of the complexes have been successfully investigated by DFT based calculations. The higher reactivity of compound (**1**) and (**3**) than compound (**2**) is due to the presence of inter and intra molecular H-bonding in compound (**1**) and µ-peroxo group in compound (**3**). Preliminary investigations with compound (**1**) for insulin activity showed enhance glucose uptake by cells (L6 muscle cell). Compound (**1**) is as good as or better than previously reported compounds. Further studies on the insulinomimetic properties and toxicity of compound (**1**) are in progress.

Section 3.2

Synthesis and Structural Delineation of Oxo-peroxo-citrato-vanadates (V)

3.2.1 Experimental

(a) Synthesis of $A_2[V_2O_4(C_6H_6O_7)_2].2H_2O$ *[A = Na(**4**), K(**5**),* NH_4*(**6**)]*

To an aqueous suspension of AVO_3 (A= K, Na or NH_4) or V_2O_5 (5 mmol) in 10 mL of water was taken in a 100 mL beaker and a few drops of the corresponding hydroxide solution was added to get a clear solution. While 20% NaOH and KOH solutions were used in these reactions, the concentration of aqueous ammonia was maintained at 2.5%. Citric acid (7 mmol) dissolved in 2 mL of water was added drop wise with constant stirring to the ice-cooled solution which turned orange. The solutions were stirred for another 30 min. Cold ethanol was then added until light haziness appeared and kept in a refrigerator. After 10—12 days, orange red crystals were isolated and washed with cold 95% ethanol, finally dried *in vacuo* over fused $CaCl_2$. The yields of $Na_2[V_2O_4(C_6H_6O_7)_2].2H_2O$(**4**), $K_2[V_2O_4(C_6H_6O_7)_2].2H_2O$(**5**) and $(NH_4)_2[V_2O_4\ (C_6H_6O_7)_2].2H_2O$ (**6**) were 1.1 g (75%), 1.2g (77%) and 0.9g (67%), respectively.

(b) Synthesis of $A_2[V_2O_2(O_2)_2(C_6H_6O_7)_2].2H_2O$ *[A=Na(**7**),K(**8**),* NH_4*(**9**)]*

To an aqueous suspension of AVO_3(A= Na, K or NH_4) or V_2O_5 (5 mmol) in 5 mL of water, taken in a 100 mL beaker that was cooled in an ice-water bath, a few drops of the respective hydroxide solution was added to get a clear solution. While 20% NaOH and KOH solutions were used in these reactions, the concentration of aqueous ammonia was maintained at 2.5%. Citric acid (7 mmol) dissolved in 2 mL of water was added drop wise with constant stirring to the ice-cooled solution which turned orange. The mixture was stirred for 30 min. 46% H_2O_2 (20 mmol) was added slowly in portions followed by addition of the hydroxide solution to adjust the pH at 4 or 5. The whole was stirred for another 30 min. Cold ethanol was then added until light haziness appeared and kept in a refrigerator. After 10—12 days, orange red crystals were isolated and washed with cold 95% ethanol, finally dried in *vacuo* over fused $CaCl_2$. The yields

of $Na_2[V_2O_2(O_2)_2(C_6H_6O_7)_2].2H_2O$(**7**), $K_2[V_2O_2(O_2)_2(C_6H_6O_7)_2].2H_2O$(**8**) and $(NH_4)_2[V_2O_2(O_2)_2(C_6H_6O_7)_2].2H_2O$ (**9**) were 1.2g (73%), 1.4g (82%) and 1.1g (68%) respectively.

*(c) Synthesis of $Na_2[V_2O_2(O_2)_4(C_6H_5O_7)].H_2O$ (**10**)*

To 5mL aqueous suspension of $NaVO_3$ (5 mmol) or V_2O_5, citric acid (5 mmol) dissolved in 2mL of water was added drop wise with constant stirring at an ice-water bath temperature and stirred for 30 min. 46% H_2O_2 (40 mmol) was added slowly with constant stirring and 20% NaOH solution was added to adjust the pH at ~7.2. The reaction mixture was stirred for additional 15 min. Cold ethanol was then added untill haziness appeared and the whole was kept in a refrigerator. After one hour, an oily mass appeared which on scratching gave a yellow solid product. The solid was filtered, washed three or four times with cold ethanol and finally dried in *vacuo* over fused $CaCl_2$. The yield of $Na_2[V_2O_2(O_2)_4(C_6H_5O_7)].H_2O$ (**10**) was 1.97g(85%).

Our attempts to synthesize the corresponding K^+ and NH_4^+ salts were unsuccesfull. The compounds obtained were $K_3[VO(O_2)_2(OH)(O_2)_2OV]$ (**12**), and $(NH_4)_3[VO(O_2)_2(OH)(O_2)_2OV]$ (**13**) in stead.

*(d) Synthesis of $Na_2[V_2O_2(O_2)_4(C_6H_5O_7)].H_2O$ (**10**) from $Na_2[V_2O_4(C_6H_6O_7)_2].2H_2O$ (**4**) via $Na_2[V_2O_2(O_2)_2(C_6H_6O_7)_2].2H_2O$ (**7**)*

A quantity of $Na_2[V_2O_4(C_6H_6O_7)_2].2H_2O$ (**4**) (2 mmol, 1.2 g) was placed in a beaker and dissolved in 5 mL water. The pH of the resulting solution was ~4.0. The solution was placed in ice bath and 46% hydrogen peroxide (4 mmol, 0.3 mL) was added slowly under continuous stirring. Subsequently, the reaction mixture was stirred at ice bath temperature for an additional 20 min. During the period, the color of the solution turned orange-red and stayed as such, pH was found to be *ca* 3.5 or 4. One portion (**A**) of the solution was taken out from the reaction mixture, and to that solution cold ethanol was added to bring about haziness and finally kept in refrigerator. To the another portion (**B**) excess amount of hydrogen peroxide (4 mmol, 0.3 mL) was added and the pH was maintained at 7 or 7.2 by adding dilute NaOH. Further, the solution was stirred at ice bath temperature for an additional half an hour. In the mean time the

solution color became yellow. Cold ethanol was added drop-wise upto the point of haziness, then the solution was kept in refrigerator. One week later, red crystals appeared from the portion (**A**), whereas second portion (**B**) gave yellow oily mass which on scratching gave solid. Elemental analyses, FT-IR, UV-visible spectra revealed the compounds to be $Na_2[V_2O_2(O_2)_2(C_6H_6O_7)_2].2H_2O$ (**7**) and $Na_2[V_2O_2(O_2)_4(C_6H_5O_7)].H_2O$ (**10**), respectively.

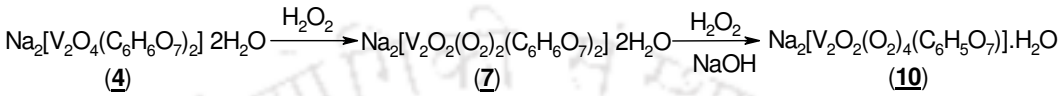

3.2.2 Results and Discussion

In addition to the pH dependence of peroxovanadates, citric acid, in the present study, being a monohydroxy tricarboxylic acid, its deprotonation followed by coordination is also pH dependent. Therefore, only appropriate experimental conditions will lead to the successful synthesis of the targeted compounds. Accordingly, a number of test runs were conducted to work out the optimum reaction conditions for the synthesis of mono- and di-peroxo-citrato-vanadates (V). In addition, simple citrato-vanadates are also prepared without involving hydrogen peroxide.

Reaction of aqueous solutions of metavanadate or vanadium pentoxide with citric acid (CA) at *ca.* 4 ^{0}C, with the molar ratio being maintained at V: CA:: 1:1.5, yielded the citratovanadates $A_2[V_2O_4(C_6H_6O_7)_2].2H_2O$ [A = Na(**4**), K(**5**), NH_4(**6**)]. The pH was maintained by adding the corresponding alkali solution, AOH (20% for A= Na or K; 2.5% for A= NH_4). Ethanol was added to one part of solution until haziness appeared. The whole was then kept in a freezer for slow precipitation. The addition of an excess alkali to the other portion of the solution afforded a oily product which finally turned to solid product, $A_2[V_2O_4(C_6H_6O_7)_2].2H_2O$ [A = Na(**4**), K(**5**), NH_4(**6**)]..

Again, maintaining the pH at 3-5, the synthesis of monoperoxo(citrato)vanadates(V), $A_2[V_2O_2(O_2)_2(C_6H_6O_7)_2].2H_2O$ [A = Na(**7**), K(**8**), NH_4(**9**)] has been achieved by carring out the reaction of V: CA: H_2O_2 at 1: 1.2: 4 at *ca.* 4^{o}C. The source of vanadium can be either AVO_3 or V_2O_5. The pH of the reaction was adjusted with corresponding alkali solution, AOH (20% for A= Na or K; 2.5% for

A= NH_4). For quick precipitation of the compounds, an excess of cold ethanol was added. However, for crystallization the reaction solution was turned to just haziness by the addition of cold ethanol and left in a refrigerator for 10-12 days.

A similar reaction with V: CA: H_2O_2 being maintained at 1: 1.2: 8 at pH 7.2 produced sodium salt of diperoxovanadate (V), $Na_2[V_2O_2(O_2)_4(C_6H_5O_7)].H_2O$ (**10**). Our attempts to synthesize the corresponding K^+ and NH_4^+ salts gave hydroxo-bridged bisoxodiperoxovanadates (V), instead. The reason for fixing the pH at 7.2 was to go as close to the physiological pH as possible. Most importantly the sodium salt of citrate-diperoxo-vanadate (V) is the first example of to be reported. The synthesis of compound (**10**) has been achieved from compound (**4**) *via* compound (**7**). Typically, 1 equivalent of compound (**4**) reacted with 2.5 equivalents of H_2O_2 at ice cold condition leading to the formation of compound (**7**). Further with the addition of an excess of H_2O_2 and maintenance of pH at 7 or 7.2 by adding dil. NaOH, the compound (**10**) could as well be obtained (**4**).

Citratovanadates (V) (**4**)-(**6**) are dark yellow, monoperoxo-citrato-vanadates (V) (**7**)-(**8**) are all orange-red in color, whereas the diperoxo compound (**10**) is yellow in color. The compounds are all stable at low temperature *ca*. 4^{o}C for a long period but unstable at room temperature. However, nonperoxo-citrato-vanadates are stable at ambient temperature in a closed vial for several days.

The characterization of compounds have been made by elemental analysis, FTIR, UV-Vis and Raman spectroscopy. X-ray crystal structure determination of $Na_2[V_2O_4(C_6\ H_6O_7)_2].2H_2O$ (**4**) and $K_2[V_2O_2(O_2)_2(C_6H_6O_7)_2].2H_2O$ (**8**) have been carried to delineate their structure. The results of elemental analysis have shown the occurrence of one peroxide group per vanadium (V) in compounds (**7**)-(**9**) and two peroxides per vanadium (V) in compound (**10**). The compounds (**4**)-(**6**) did not contain any active oxygen (O_2^{2-}). Notably, the chemical determination of active oxygen content (i.e., O_2^{2-}) is extremely important for peroxovanadates (V), as stated earlier. This has been accomplished by iodometry. The results are summarized in Table 3.2.1.

Table 3.2.1 Elemental analysis of the compounds (**4**)-(**10**)

Compound	Found %(Calcd.%)			
	V	O_2^{2-}	C	H
(**4**)	15.75 (16.24)	00.00 (00.00)	22.38 (22.93)	2.35 (2.55)
(**5**)	15.30 (15.45)	00.00 (00.00)	21.55 (21.81)	2.25 (2.42)
(**6**)	16.20 (16.50)	00.00 (00.00)	23.13 (23.30)	2.98 (3.88)
(**7**)	15.20 (15.45)	09.10 (09.69)	21.75 (21.82)	2.23 (2.42)
(**8**)	14.20 (14.47)	08.50 (09.25)	20.65 (20.81)	2.05 (2.31)
(**9**)	16.30 (16.66)	10.45 (10.45)	21.95 (22.15)	2.95 (3.69)
(**10**)	12.60 (12.98)	15.90 (16.28)	18.25 (18.32)	2.85 (3.56)

The vibrational spectra of these compounds are interesting and informative; however, they are somewhat complicated. The FTIR spectra of compounds (**4**)-(**6**) are relatively less complicated owing to the absence of peroxo ligand. Structurally significant FTIR features have been summarized in Table 3.2.2. The terminally bonded oxo group gives very distinct and strong absorption in the FTIR spectra of oxovanadates. Accordingly, the ν(V=O) bands were found to occur in the region 945-990 cm^{-1} for all compounds**.** The ν(V=O) for (**4**)-(**6**) is split into two bands each (980 and 965 cm^{-1}) suggesting the presence of cis-VO_2. This is further supported by the X-crystallographically ascertained molecular structure of the compound (**4**). The compounds (**7**)-(**9**) and (**10**) showed three characteristic absorptions, for ν(O-O), $\nu_{as}(VO_2)$ and $\nu_s(VO_2)$. The ν(O-O) band for each of the citrato(monoperoxo)vanadates(V) [(**7**)-(**9**)] occurs at *ca.* 932 cm^{-1}, whereas for the citrato(diperoxo)vanadate(V) (**10**) this appears at 870 cm^{-1}. The observed lowering of ν(O-O) bands is due to decrease in bond order of the peroxo group, which is attributed to comparatively higher degree of removal of π_{2P} density of O_2^{2-} to the vanadium(V) centre in case of the compound (**10**) as compared to the compounds (**7**)-(**9**) [34]. The coordination of peroxide leads to the occurrence of the corresponding $\nu_{as}(VO_2)$ and $\nu_s(VO_2)$ at *ca.* 550m and *ca.* 616m, respectively. The typical FTIR signatures of the coordinated peroxide ligand clearly indicate that the peroxide ligand in each case is coordinated to the vanadium (V) centre in a triangular bidentate (C_{2V}) fashion [45]. This has been further supported by the X-ray crystal structure of

$K_2[V_2O_2(O_2)_2(C_6H_6O_7)_2].2H_2O$ (**8**) (discussed later). The mode of bonding of citrato group to the metal centre can be confirmed by comparing the FTIR spectrum with that of free citric acid. Thus antisymmetric stretching vibrations $\nu_{as}(COO^-)$ were found to be present for the carboxylate carbonyl in the range 1725-1600 cm^{-1}. The corresponding symmetric vibrations $\nu_s(COO^-)$ for the same group were found to occur at *ca.* 1405 cm^{-1}. The observed carbonyl vibrations are shifted to lower frequencies compared to the corresponding vibrations in the free citric acid. This change has been ascribed to the coordination of the acid ligand to the vanadium (V) centers [46]. Also, difference between the antisymmetric and symmetric stretches, $\Delta(\nu_{as}(COO^-)- \nu_s(COO^-))$ is found to be more than 200 cm^{-1}, which suggest that citrate carboxylate groups were coordinated to the vanadium(V) centers in a monodentate fashion. This was further confirmed from the results of X-ray crystal structures of (**4**) and (**8**).

Table 3.2.2 Structurally significant FTIR bands in cm^{-1} of the compounds (**4**)- (**10**)

Compound	ν (O-H)	ν (N-H)	ν_{as} (COO^-)	$\nu_s(COO^-)$	ν(V=O)	ν (O-O)	$\nu(V(O_2)$
(**4**)	3564s, 3469s	-	1724vs, 1652vs	1391vs	980vs, 906vs	-	-
(**5**)	2929b	-	1730vs, 1707vs	1399s	957s, 895s	-	-
(**6**)	3245b	3098b, 2934b	1734vs, 1699sb	1398vs	934vs, 867vs	-	-
(**7**)	3552s, 3496s	-	1710vs, 1679vs, 1603vs	1414vs	989s	931s	549m, 612m
(**8**)	3592s, 3485s	-	1719vs, 1673vs, 1614vs	1418vs	988s	933s	557m, 616m
(**9**)	3576s, 3415s	3281s, 3031s	1725vs, 1674vs, 1610vs	1415vs	988s	930s	554m, 606m
(**10**)	3434b	-	1609vs	1402vs	947s	870s	547m, 619m

UV-Vis spectra of the compounds recorded in water show typical absorptions with high molar extinction coefficient at 275, 270, 278, 295, 288, 291 nm and 318 nm

for (**4**)-(**10**), as listed in Table 3.2.3. These bands are assigned to the ligand (peroxide) to metal (vanadium) charge transfer (LMCT) transitions ($\pi_h \rightarrow d_\sigma^*$). These are very characteristic for peroxovanadates (V). The solution electrical conductances (10^{-3}M) of the compounds (**4**)-(**10**), were recorded in water at ambient temperature (Table 3.2.3). The conductance values for (**7**)-(**9**) have been found to be around 220 $\Omega^{-1}cm^2mol^{-1}$ whereas that for (**10**) was 299 $\Omega^{-1}cm^2mol^{-1}$, indicating thereby that the compounds (**7**)-(**9**) are 2:1 type of electrolytes whereas the compound (**10**) is a 3:1 species. The results not only support their formulae but also suggest that both the non-peroxo and heteroligated peroxo vanadates (V) studied herein are all stable in water, at least under the present experimental conditions.

Table 3.2.3 Electronic spectral data and molar conductance values of compounds (**4**)-(**10**)

Compound	UV-Vis λ (nm) (ε, $M^{-1}cm^{-1}$)	Solution electrical conductance (10^{-3} M) ($\Omega^{-1}cm^2mol^{-1}$)
(**4**)	275 (3245)	230
(**5**)	270 (3473)	212
(**6**)	278 (2976)	215
(**7**)	295 (3945)	214
(**8**)	288 (4123)	221
(**9**)	291 (3856)	219
(**10**)	318 (2950)	254

The X–ray crystal structure of compound (**4**) and (**8**) consist of dimeric discrete anions. The ORTEP diagrams of the anions are shown in Figures 3.2.1 (a) and (b). Compound (**4**) crystallizes in the orthorhombic space group Pbca with two molecules in the unit cell. Summary of crystal, intensity collection and refinement data for the complex are given in Table 3.2.5 and a selected list of interatomic distances and bond angle are given in Table 3.2.6. The terminal V=O bond distances are 1.639 Å and 1.613 Å and V···V distance is 3.231 Å. The values obtained for the compound (**4**) are similar to the corresponding distances in other dinuclear citrato-vanadates (V) reported earlier [17]. Importantly the O(1)-V(1)-O(2) angle is found to be 106.59° revealing the cis

arrangement of the two oxo groups as indicated by the FTIR spectrum of the compound.

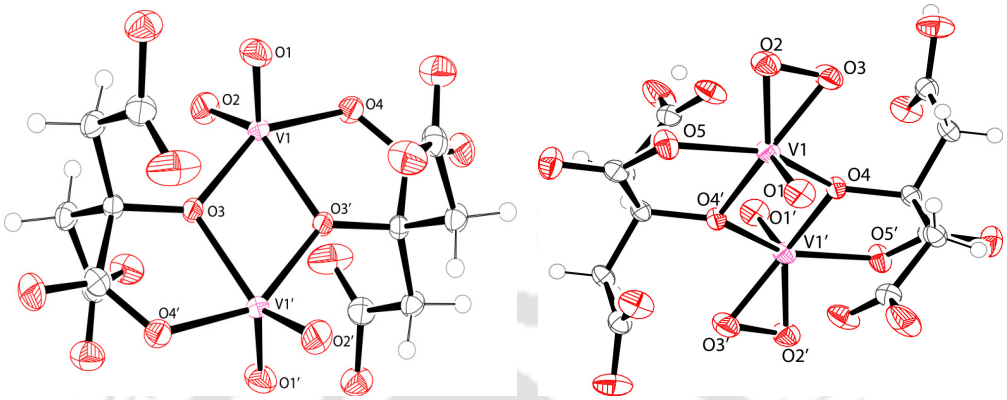

(a) (b)

Figure 3.2.1 *ORTEP diagrams of the anions of (a) compound (**4**) and (b) (**8**)*

Table 3.2.5 Crystal data and structure refinement for compound (**4**) and (**8**)

Empirical formula	C12 H12 Na2 O18 V2	C12 H16 K2 O22 V2
Formula weight	592.14	692.24
Temperature(K)	296(2)	296(2)
Wavelength	0.71073	0.71073
Crystal system	Orthorhombic	Monoclinic
Space group	Pbca	P2(1)/n
Unit cell dimensions, Å and ^{0}	a = 11.492(6) α= 90	a = 9.320(5) α= 90
	b = 10.622(6) β= 90	b = 12.098(7) β= 110.54(4)
	c= 16.908(9) γ = 90	c = 10.699(7) γ = 90
V(Å^3)	2064.10(19)	1129.75(12)
Z	8	4
Density (mg/m^3) Mg/m^3	1.603	0.991
Absorption coeff., μ mm^{-1}	0.799	0.649
F(000)	1008	338
Goodness-of-fit on F^2	1.036	0.921
Final R indices R1,wR2	0.0394, 0.1270	0.0419, 0.0910
R indices (all data) R1, wR2	0.0425, 0.1299	0.0598, 0.0995

Table 3.2.6 Selected bond length [Å] and bond angle [^{0}] for (**4**) and (**8**)

Compound (**4**)		Compound (**8**)	
V(1)-O(1)	1.639(19)	V(1)-O(1)	1.588(2)
V(1)-O(2)	1.613(2)	V(1)-O(2)	1.870(2)
V(1)-O(3)	1.962(18)	V(1)-O(3)	1.880(2)
V(1)-O(4)	2.005(16)	V(1)-O(4)	1.992(2)
V(1)-O(8)	1.976(16)	V(1)-O(5)	2.012(2)
V(1)-V(1′)	3.231(12)	V(1)-O(9	2.032(19)
O(1)-V(1)-O(2)	106.59(12)	O(2)-O(3)	1.420(2)
O(1)-V(1)-O(3)	95.99(9)	V(1)-V(1′)	3.231(12)
O(1)-V(1)-O(4)	98.98(8)	O(1)-V(1)-O(2)	100.91(11)
O(1)-V(1)-O(8)	137.62(9)	O(1)-V(1)-O(3)	102.98 (12)
O(4)-V(1)-O(8)	71.47(7)	O(1)-V(1)-O(4)	103.63(10)
O(2)-V(1)-O(3)	101.51(9)	O(1)-V(1)-O(5)	94.81(8)
O(2)-V(1)-O(8)	101.49(9)	O(1)-V(1)-O(9)	96.14(12)

Compound (**8**) crystallizes in the monoclinic space group P2(1)/n with two molecules in the unit cell. Summary of crystal, intensity collection and refinement data for the complex (**8**) are given in the Table 3.2.5 and a selected list of interatomic distances and bond angles are given in Table 3.2.7. The complex consists of a V_2O_2 core with two vanadium ions in the oxidation state +5. The rhombic core unit is planar due to the presence of a centre of inversion. The two oxygen bridges derived from the alkoxide moieties of two citrate ligands are attached to the core. Each vanadium ion is bound to doubly bonded oxygen, with the remaining sites being occupied by oxygens from the citrate ligands and a peroxo group (O_2^{2-}). The citrate participating in the coordination sphere around each vanadium ion are doubly deprotonated. They coordinate through the central alkoxide and one carboxylate groups only. The two terminal carboxylate groups are not bound to the vanadium ions. The coordination environment around each vanadium ion is pentagonal pyramidal, with the peroxo group, the two bridging alkoxide oxygens and the central carboxylate lying in the equatorial plane, and the doubly bonded oxygen of the V_2O_2 core occupying apical position. The V=O (1.588 Å) and V$\cdots$V (3.252 Å) distances of the complex (**8**) are similar to the corresponding distances in other dinuclear citrato-peroxovanadates (V) reported earlier [16]. Inter molecular strong hydrogen bonding O-H$\cdots$O, 2.065 Å) is

observed in the compound (**8**) between the free carboxylic end of one and bonded caboxylate end of the other. Most interestingly, a $K_2(H_2O)_2$ rhombic core unit (edge 3.015 and 2.802 Å) was observed between two dinuclear units.

The ESI mass spectrum of compound (**10**) has been recorded in aqueous solution. The spectrum is shown in Figure 3.2.2. In negative mode only, the peak corresponding to $[Na[V_2O_2(O_2)_4(C_6H_5O_7)].H_2O]^-$ (found 492.47, calculated 492.93) was observed.

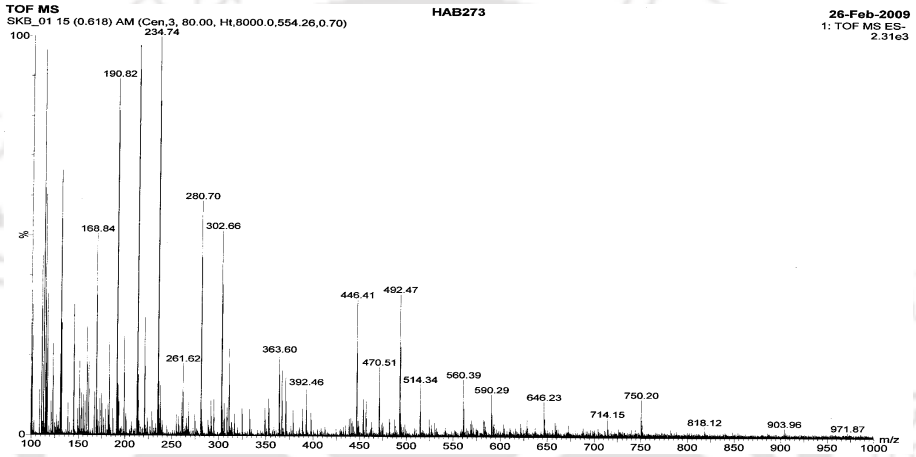

*Figure 3.2.2 ESI mass spectrum of Compound (**10**) in aqueous solution*

3.2.3 Conclusion

While pH *ca.* ~4 favors the formation of 1:1:1 complex containing oxovanadate (V), a bidentate citrate and a C_{2V} type peroxoligand, the physiologically akin pH, *i.e.* 7.2, supports the formation of a 1:1:2 species containing oxovanadate (V) : a bidentate citrate : two C_{2V} type peroxoligands affording the heretofore unreported complex $Na_2[V_2O_2(O_2)_4(C_6H_5O_7)].H_2O$ (**10**). The observed chemical reactivity of vanadium with citric acid in presence of hydrogen peroxide revealed the presence of intermediate dinuclear complexes, which on increasing the pH give diperoxovanadate. Moreover, since interactions of biologically connected species namely, vanadium, hydrogen peroxide and citric acid at the physiological pH generated the compound (**10**), it is quite rational to expect that the complex may have a crucial biochemical relevance, and this is going to be a subject of future investigations.

Section 3.3

Synthesis and structural investigation of oxo-peroxo- μ-hydroxo and μ-fluoro-vanadates (V)

3.3.1 Experimental

*(a) Synthesis of $A_3[VO(O_2)_2(OH)(O_2)_2OV]$, [A = Na(**11**), K(**12**), NH_4(**13**)]*

To the 15 mL of aqueous solution of alkali metal or ammonium metavanadate (5 mmol) or V_2O_5 (5 mmol) an excess of 46% H_2O_2 (5 mL) was added with stirring in the molar ratio V: H_2O_2 as 1: 6. The pH was recorded to be 4.0 or 4.5. A dilute solution (0.01M) of alkali metal hydroxide or 2.5% ammonia solution were added to adjust the pH at 6 or 7 and stirred for one hour. It was stirred for one hour. While stirring, yellow precipitate appeared in case of potassium salt which was filtered off. The reaction solution was warmed at 50^0-55^0C for one hour and then cooled to room temperature. Shiny deep yellow crystals for the sodium salt whereas yellow crystals for potassium and ammonium salts precipitated out. The yields of $A_3[VO(O_2)_2(OH)(O_2)_2OV]$, [A= Na(**11**), K(**12**), NH_4(**13**)] were 0.78g (85%), 0.9g (87%) and 0.7g (80%), respectively.

*(b) Synthesis of $A_3[VO(O_2)_2(F)(O_2)_2OV]$, [A = Na(**14**), K(**15**), NH_4(**16**)]*

To a stirred aqueous solution (10 mL) of alkali metal or ammonium metavanadate or V_2O_5 (5 mmol), solid AF (7mmol) (A= Na, K or NH_4) was added followed by addition of 46% H_2O_2 (40 mmol). A dilute solution (0.01M) of alkali metal hydroxide or 2.5% ammonia solution were added to adjust the pH at 6 or 7 and stirred for one hour. The solution was warmed at 50^0-55^0C for one hour. It was then cooled to room temperature to afford lemon yellow crystals. The yields of $A_3[VO(O_2)_2(F)(O_2)_2OV]$, [A = Na(**14**), K(**15**), NH_4(**16**)] were 0.55g (62%), 0.74g (72%) and 0.6g (70%), respectively.

(c) Synthesis of $A_3[VO(O_2)_2(F)(O_2)_2OV]$, from $A_3[VO(O_2)_2(OH)(O_2)_2OV]$, [A = Na, K, NH_4]

A quantity of $A_3[VO(O_2)_2(OH)(O_2)_2OV]$ (2 mmol) was taken in a round bottomed flask equipped with a condenser and dissolved in 5 mL water. To this solution corresponding AF (3 mmol) [A = Na, K, or NH_4] was added and the whole was stirred in an oil-bath maintaining the temperature 55^0C for three hours. Then the solution was allowed to cool to room temperature overnight. On the following day, lemon yellow crystals that formed overnight were filtered off and dried *in vacuo*. The yield of $A_3[VO(O_2)_2(F)(O_2)_2OV]$, [A = Na(**14**), K(**15**), NH_4(**16**)] were 0.44g (60%), 0.53g (63%), 0.2g (56%), respectively.

3.3.2 Results and Discussion

While synthesizing the complex $[V_2O_2(O_2)_4(C_6H_5O_7)]^{2-}$ (described in section 3.2) at or near physiological pH with potassium and ammonium counter cation, we frequently observed the formation of a stable dinuclear diperoxovanadate anion, $[VO(O_2)_2(OH)(O_2)_2OV]^{3-}$. This complex was also observed as intermediate in benzylic oxidation and benzylic bromination by using triperoxovanadate (V) catalyst [47] where triperoxovanadate (V) was the precursor of the diperoxovanadate anion. In quest of understanding the structural motif and electronic properties, as well as to develop a dedicated synthetic procedure for the same, we have now succeded in synthesizing compounds (**11**)–(**13**). Following this work and considering the akinness of OH^- to F^- as well as its ability to stabilize higher valent vanadium encouraged us to synthesize the corresponding fluoro derivatives.

The expedient synthesis of both $A_3[VO(O_2)_2(OH)(O_2)_2OV]$, [A = Na**(11),** K**(12),** NH_4**(13)**] and $A_3[VO(O_2)_2(F)(O_2)_2OV]$, [A = Na(**14**), K(**15**), NH_4(**16**)] involve either vanadium pentoxide or metavanadates and hydrogen peroxide, and alkali fluoride for the latter. The reaction of aqueous alkaline solution of V_2O_5 or AVO_3 with

hydrogen peroxide at a mol ratio of V: H_2O_2:: 1: 8 results in the formation of a yellow solution. Warming this solution in the temperature range 55-60 ^{0}C and then slow cooling to room temperature yielded a yellow crystalline product. Similarly, the mixture of V_2O_5 or AVO_3, AF and hydrogen peroxide gave the flouro bridged dinuclear diperoxovanadates. The pH of the reaction mixture was maintained at 6 or 7. Ethanol was employed for precipitation.

While the hydroxo bridged dinuclear diperoxovanadates are light yellow, flouro bridges complexes are found to be lemon yellow in color. All the complexes are stable at room temperature for months in the solid form as well as in solution. They are soluble in water, but not in organic solvents. Characterization of the compounds was made by elemental analysis, IR and UV-Vis spectroscopy. X-ray crystal structure determinations were done to delineate the structural feature. The results of elemental analysis confirmed the presence of two peroxide per vanadium (V) in all compounds, and single fluoride for two vanadium (V) centers in the fluoro derived compounds. The results are provided in Table 3.3.1.

Table 3.3.1 Elemental analysis of compounds (**11**)-(**16**)

Compound	Found %(Calcd.%)		
	V	O_2^{2-}	F
(11)	27.80 (27.86)	34.53 (34.97)	-
(12)	24.65 (24.63)	30.80 (30.90)	-
(13)	28.82 (29.00)	36.15 (36.47)	-
(14)	27.55 (27.72)	34.60 (34.78)	4.85 (5.16)
(15)	24.60 (24.52)	30.75 (30.76)	4.24 (4.56)
(16)	28.55 (28.89)	36.94 (36.26)	5.90 (5.38)

The molar conductance of the compounds was recorded in water and found in the range of 330-345 $\Omega^{-1}cm^2mol^{-1}$ which indicates a 1:3 electrolytic nature. The results of conductance measurements have been set out in Table 3.3.2. The UV-visible spectra of the compounds showed two transitions one each for $\pi_v \rightarrow d_\sigma^*$ and $\pi_h \rightarrow d_\sigma^*$, and the results are set out in Table 3.3.2.

Table 3.3.2 Conductance values and electronic spectral data of compounds (**11**)-(**16**)

Compound	Solution electrical conductance (10^{-3} M) ($\Omega^{-1}cm^2mol^{-1}$)	UV-Vis λ (nm) (ε, $M^{-1}cm^{-1}$)
(11)	345	327 (682), 211 (40,200)
(12)	338	329(724), 210 (49,400)
(13)	332	328 (496), 211 (38,200)
(14)	340	329 (721), 212 (40,600)
(15)	336	328 (784), 211 (49,500)
(16)	330	329 (603), 210 (38,200)

The FTIR spectra of these compounds are simple and clean. The significant FTIR frequencies of the compounds are given Table 3.3.3. The spectra exhibit bands at ~945, ~877, ~630 and ~530 cm^{-1} which have been assigned to $\nu_{V=O}$, ν_{O-O} (ν_1), ν_{V-O_2} (ν_3) and ν_{V-O_2} (ν_2) modes, respectively. Further, an additional band at ~1045cm^{-1} is ascribed to the bridging hydroxo or fluoro ligand. The peak of ν(V=O) is split into two bands (~980 and ~965 cm^{-1}) suggesting the presence of cis-VO_2. This is further supported by the single crystal X-ray crystallography for compound (**12**) and (**14**). The peaks observed *ca.* 616(s) is due to coordinated peroxo group corresponding to $\nu_{as}(VO_2)$. The typical FTIR signatures arising out of the coordinated peroxide ligand clearly indicate that the peroxide ligand in each case is coordinated to the vanadium (V) centre in a triangular bidentate (C_{2V}) fashion.

Table 3.3.3 Structurally significant IR bands in cm^{-1} of the compounds (**11**)-(**16**)

Compound	ν (O-H)	ν (N-H)	ν(V=O)	ν (O-O)	ν($V(O_2)$
(11)	3201s	-	942s, 970s	866s	615s
(12)	3179s	-	945s, 971s	868s	617s
(13)	3189s,	3067s	943s, 966s	869s	615s
(14)	3196s	-	940s, 974s	860s	608s
(15)	3146s	-	947s, 978s	855s	607s
(16)	3165s,	3077s	940s, 961s	858s	611s

The compound (**12**) and (**14**) were mounted for the single crystal XRD data to characterize crystallographically, as representative. The ORTEP diagrams of them are presented in Figures 3.3.1 (a) and (b) and the summary of crystal, intensity collection and refinement data for the complexes are given in Table 3.3.4. Comparisons in bond lengths and bond angles have been provided in Table 3.3.5 and Table 3.3.6.

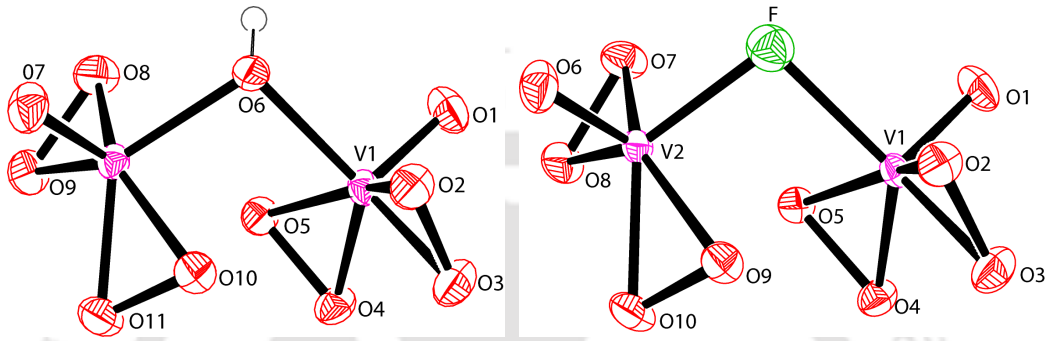

(a) (b)

Figure 3.3.1 *ORTEP diagrams of the anions of compounds (a) (**12**) and (b) compound (**14**).*

Table 3.3.4 Crystal data and structure refinement for compound (**12**) and (**14**)

Empirical formula	$H_3 K_3 O_{12} V_2$	H2 F K3 O11 V2
Formula weight	414.00	416.20
Temperature(K)	296(2)	296(2)
Wavelength	0.71073	0.71073
Crystal system	Monoclinic	Monoclinic
Space group	P2(1)/c	P2(1)/c
Unit cell dimensions, Å and ^{0}	a = 6.708(3) α= 90	a = 6.706(5) α= 90
	b = 9.955(5) β= 93.72(3)	b = 9.953(9) β= 93.74(4)
	c= 15.809(6) γ = 90	c = 15.826(14) γ = 90
V(Å^3)	1053.58(8)	1054.20(15)
Z	4	4
Density (mg/m^3) Mg/m^3	2.118	1.967
Absorption coeff., μ mm^{-1}	2.218	2.265
F(000)	656	606
Goodness-of-fit on F^2	1.095	1.050
Final R indices R1, wR2	0.0427, 0.1229	0.0298, 0.0790
R indices (all data)R1, wR2	0.0504, 0.1308	0.0351, 0.0821

The compounds (**12**) and (**14**) both crystallize in the monoclinic space group P2(1)/c with four molecules in the unit cells. Each vanadium atom in both of the compounds is coordinated to one oxo and two peroxo groups. The sixth position is occupied by either a μ-fluoro or a μ-hydroxo group. The peroxo groups are bonded in a C_{2v} fashion. The terminal V=O distances for compound (**12**) are 1.617 and 1.605 Å, whereas those for compound (**14**) are 1.613 and 1.604 Å. The values obtained for the compound (**12**) are similar to the corresponding distances in other compounds of vanadium reported earlier [48]. Although there is structural similarity between the compounds (**12**) and (**14**), the compound (**14**) is heretofore unreported, and so are, of course, (**15**), and (**16**).

Table 3.3.5 Comparison of selected bond lengths [Å] of compound (**12**) and (**14**)

Parameter	Compound (**12**)	Compound (**14**)
V(1)-O(1)	1.604(2)	1.613(2)
V(1)-O(2)	1.903(2)	1.887(2)
V(1)-O(3)	1.878(2)	1.873(2)
V(1)-O(4)	1.880(2)	1.909(2)
V(1)-O(5)	1.916(2)	1.876(2)
O(2)-O(3)	1.468(4)	1.471(4)
O(4)-O(5)	1.466(4)	1.469(4)
V(1)-O(6)/F	2.006(19)	2.000(19)
V(1)-V(2)	3.047(12)	3.048(12)
V(2)-O(6)/ F	1.997(2)	2.010(2)
V(2)-O(7)/ O(6)	1.617(2)	1.604(2)
V(2)-O(8)/ O(7)	1.885(2)	1.881(2)
V(2)-O(9)/ O(8)	1.871(2)	1.904(2)
V(2)-O(10)/ O(9)	1.908(2)	1.882(2)
V(2)-O(11)/ O(10)	1.874(2)	1.915(2)
O(8)-O(9) / O(7)-O(8)	1.464(4)	1.470(4)
O(10)-O(11)/ O(9)-O(10)	1.470(4)	1.474(4)

Table 3.3.6 Comparison of selected bond angle [^{0}] of compound (**12**) and (**14**)

Parameter (**12/14**)	Compound (**12**)	Compound (**14**)
O(1)-V(1)-O(2)	105.19(11)	105.08(11)
O(1)-V(1)-O(3)	103.99(12)	104.33(12)
O(1)-V(1)-O(4)	103.16(10)	101.97(10)
O(1)-V(1)-O(5)	104. 97(8)	107. 12(8)
O(1)-V(2)-O(6) / F	99.60(12)	99.60(12)
O(7)-V(2)-O(6) / O(6)-V(2)-O(F)	99.55(10)	99.32(10)
O(7)-V(2)-O8) / O(6)-V(2)-O(7)	105.34(8)	105.09(8)
O(7)-V(2)-O(9) / O(6)-V(2)-O(8)	104.66(12)	104.01(12)
O(7)-V(2)-O(10) / O(6)-V(2)-O(9)	101.62(11)	103.20(11)
O(7)-V(2)-O(11) / O(6)-V(2)-O(10)	106.89(12)	105.15(12)

Importantly, from the XRD data, it is very difficult to discern the Q-peak whether is for oxygen or fluorine, since the electron density of both seems to be equal. Therefore, an independent confirmation for the presence of fluorine was in order which was accomplished by ^{19}F NMR spectroscopy. A singlet peak at -122.59 ppm (or 40.46 ppm with reference to C_6F_6) was observed for compound **14** as well as for **15** and **16** (Figure 3.3.2), thereby confirming the identity of the compound.

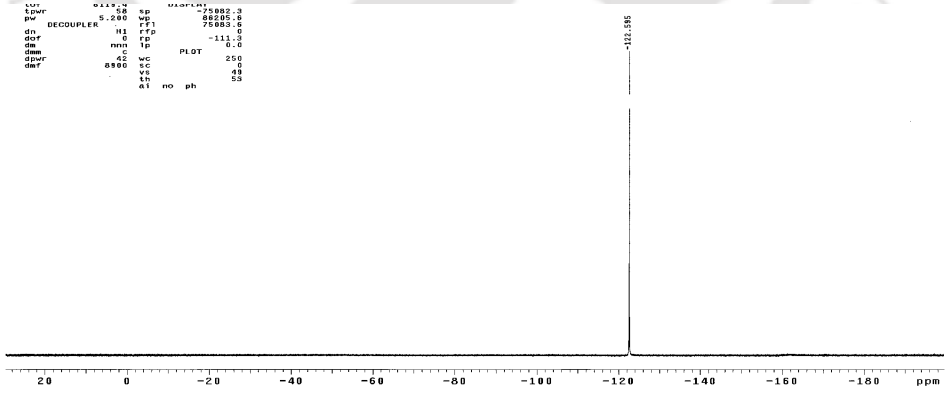

Figure 3.3.2 *^{19}F NMR spectrum of compound (**14**) without any reference*

It is well established that fluoride stabilizes the higher oxidation states of vanadium (V) as well as also peroxovanadium complexes [18]. In a very recent report, a few fluoro peroxovanadium (V) complexes have been reported to reveal the effect of fluoride on the stability of peroxovanadates (V) [19h]. It has been shown that the fluorine stabilized the reactive μ-η^1: η^2 and μ-η^2: η^2 peroxo groups. The present compounds, i.e. compounds (**14**)-(**16**) are also found to be more stable than the corresponding hydroxo bridged compounds (**11**)-(**13**). The reactivity of these compounds will be discussed in the next section. It has been observed that the distances between the vanadium and non-coordinated peroxo oxygen in the seventh position of pentagonal bipyramids are 2.48 Å and 2.52 Å in the present fluoro-peroxovanadates whereas the bond distances reported so far are 2.50 Å and 2.59 Å [19h]. This observation suggests that the fluoride stabilizes the compounds (**14**)-(**16**) as much as or or relatively more than what was observed earlier.

3.3.3 Conclusion

A set of dinuclear diperoxovanadates (V) having μ- hydroxo and μ-flouro groups as bridging ligands has been synthesized and characterized. These compounds exhibit interesting structural features in the solid state as well in solution. The compounds (**14**)**–**(**16**) represents a new class of fluoroperoxovanadates (V). They may serve as precursors for newer oxofluorovanadates (V).

Section 3.4

Studies of Reactivity of Newer Peroxovanadates (V)

3.4.1 Experimental

(a) Oxidation of bromide

To a stirred mixture of 3.7 g (31.1 mmol) of potassium bromide (KBr) and 5 g (15.5 mmol) of tetrabutylammonium bromide (TBAB) in 10 mL of water at ice bath temperature, the catalyst (peroxo-vanadate) (0.1 mmol, 0.3 mol %) in 15 mL (132.4 mmol) of 30% hydrogen peroxide (H_2O_2) was added. To this, 5 mL of 1M sulphuric acid (H_2SO_4) was added in small portions. The reaction mixture was stirred at 0–5 °C temperature in an ice-water bath for 4 hours. The yellow solid product thus formed was filtered. The compound was then dried in a vacuum desiccator using anhydrous calcium chloride ($CaCl_2$) as desiccant. Recrystalization of the product from acetonitrile gave orange red crystals. M.p. 72-75 °C (lit. m. p. 76 °C). The chemical analysis, IR, and conductance of the compound matched very well with those reported in literature [49].

Analysis: Tetrabutylammoniumtribromide (TBATB), $C_{16}H_{36}NBr_3$: Calculated (Found) (%): C, 39.86 (39.41); H, 7.52 (8.28); N, 2.90 (2.78); Br, 49.71 (49.53). IR (KBr, cm^{-1}): ν_{sym} (ν_1) 171(s), ν_{asym} (ν_3) 191(s). UV-Visible (nm, $M^{-1}cm^{-1}$): 267 (49000), 400 (150). Conductance (10^{-3} M) ($\Omega^{-1}cm^2mol^{-1}$): 155.

(b) General procedure for sulfide oxidation

Phenylmethyl sulfide (2 mmol) in methanol (5 mL) as solvent was reacted with H_2O_2 (4 mmol) in presence of the catalyst (peroxo-vanadate) (0.02 mmol) with stirring at ice bath temperature. The reaction was monitored by TLC (n-hexane/ethyl acetate: 8/2). On completion of the reaction, methanol was removed under reduced pressure followed by addition of water (5 mL). The product was extracted with ethyl acetate and dried over $MgSO_4$. Evaporation of solvent followed by column chromatography on silica gel using n-hexane and ethyl acetate (95:5) as eluent afforded the pure sulfoxide and sulfone.

Analysis: (a) Methanesulfinyl-benzene, C_7H_8SO. Calculated (Found) (%): C, 59.56 (59.67); H, 5.71 (5.95); O, 11.34 (11.38); S, 23.38 (23.29). IR(Neat, cm^{-1}):

692(s), 750(s), 1032(s), 1090(s), 1444(s). ^{1}H NMR (400MHz, $CDCl_3$, ppm): δ 2.74(s, 3H), 7.51-7.53(m, 3H), 7.64-7.66(m, 2H). ^{13}C NMR(100MHz, $CDCl_3$, ppm): δ 38.1, 123.7(2C), 128.5(2C), 130.2, 145.8. MS: m/z 141(M^+). (b) Methanesulfonyl-benzene, $C_7H_8SO_2$. Calculated (Found) (%): C, 53.52 (53.60); H, 5.13 (5.05); O, 20.37 (20.40); S, 14.88 (14.85). IR (Neat, cm^{-1}): 1148(s), 1286(s). ^{1}H NMR (400 MHz, $CDCl_3$, ppm): δ 3.06 (s, 3H), 7.58(t, *J* = 7.2Hz, , 2H), 7.66(t, *J* = 8Hz, 1H), 7.95(d, *J* = 7.6Hz, 2H). ^{13}C NMR (400 MHz, $CDCl_3$, ppm): δ 41.6, 126.8(2C), 129.4(2C), 133.5, 137.3. MS: m/z 157(M^+).

(c) General procedure for oxidation of benzylic alcohols

To a 25 mL round-bottomed flask 0.1 mmol of the catalyst, 2.2 mmol of H_2O_2 (50%), 2 mmol of the alcohol, and 0.002 mmol of CTAB were added and mixed with 10 mL of water followed by the addition of 0.2M H_2SO_4 (two drops). The mixture was heated to 60°C under stirring. The reaction was monitored by TLC. After completion of the reaction, the mixture was extracted with ethyl acetate (3x5 mL). The combined extracts was dried over Na_2SO_4, concentrated and purified by column (silica) chromatography (hexane/ethyl acetate: 90/10), after which the isolated yield was calculated.

Analysis: Benzaldehyde, C_7H_6O. Calculated Found (%): C, 77.79 (77.82); H, 7.44 (7.42); O, 14.81 (14.72). IR(Neat, cm^{-1}): 1706(s). ^{1}H NMR (400 MHz, $CDCl_3$, ppm): δ 7.47(t, *J* = 7.6 Hz, 2H), 7.54(t, *J* = 7.8 Hz, 2H), 7.89(d, *J* = 7.6 Hz, 1H), 10.02 (s, 1H). ^{13}C NMR (100MHz, $CDCl_3$, ppm): δ 129.0(2C), 129.9(2C), 134.5, 136.8, 295.7. MS : m/z 106(M^+).

(d) *Bromination of chalcone*

Chalcone (0.5 mmol, 0.104g) was dissolved in acetone and water mixture (2:1) followed by addition of potassium bromide (1.2 mmol. 0.141g). To the stirred solution, the catalyst (peroxo-vanadate) (0.012 mmol) and 30% H_2O_2 (15 mmol, 1.7 mL) were added with stirring. Further 0.1 mL of 0.2M H_2SO_4 (0.2 mmol) was added to the reaction mixture. The reaction mixture was allowed to stir at room temperature. Interestingly, dibromochalcone precipitated out from the reaction mixture. The consumption of starting material was monitored by TLC. After completion of reactant

as indicated by TLC, the reaction mixture was filtered off and the product was further purified by recrystalization from acetone to get the pure product.

Analysis: Dibromochalcone, $C_{15}H_{12}OBr_2$. Calculated (Found) (%): C, 48.92 (48.94); H, 3.28 (3.26); O, 4.35 (4.28); Br, 43.45 (43.42). IR (KBr, cm^{-1}): 1380(s), 1460(s), 1600(m), 1680(s), 2865(m). ^{1}H NMR (400 MHz, $CDCl_3$, ppm): δ 5.48(d, *J* = 8.6 Hz, 1H), 5.63(d, *J* = 8.6 Hz, 2H), 7.02-7.89(m, 10H). ^{13}C NMR (100MHz, $CDCl_3$, ppm): δ 123.5, 126.9(2C), 127.5, 128.5(2C), 129.4(2C), 129.8(2C), 134.5(2C), 136.8, 143.6, 190.4. M.p. 159 or160 ^{0}C.

3.4.2 Results and Discussion

In order to study reactivity of the complexes presented in previous sections of this chapter, they were applied in the (i) oxidation of bromide to tribromide, (ii) oxidation of phenylmethyl sulfide, (iii) oxidation of benzyl alcohol to aldehyde, and (iv) bromination of chalcone, as representative cases (Scheme 3.4.1). Each of the compounds has been used for the reactions and repeated reactions have been carried out to achieve the optimum conditions. The optimal results with some representative compounds are shown in Table 3.4.1.

For ready reference, the synthesized compounds being used as catalysts are: $DmpzH[VO(O_2)_2(dmpz)]$ (**1**), $K[VO(O_2)_2(dmpz)].H_2O$(**2**), $Na_2[V_2O_2(O_2)_4(dmpz)].H_2O$ (**3**), $A_2[V_2O_4(C_6H_6O_7)_2].2H_2O$ [A = Na(**4**), K(**5**), NH_4(**6**)], $A_2[V_2O_2(O_2)_2(C_6H_6O_7)_2].2H_2O$ [A = Na(**7**), K(**8**), NH_4(**9**)], $Na_3[VO(O_2)_2(C_6H_6O_7)].4H_2O$(**10**), $A_3[VO(O_2)_2(OH)(O_2)_2OV]$ [A = Na(**11**), K(**12**), NH_4(**13**)], and $A_3[VO(O_2)_2(F)(O_2)_2OV]$ [A = Na(**14**), K(**15**), NH_4(**16**)].

The reactions were optimized with $DmpzH[VO(O_2)_2(dmpz)]$ (**1**). The reactivity of other compounds has been checked with the optimized reaction conditions.

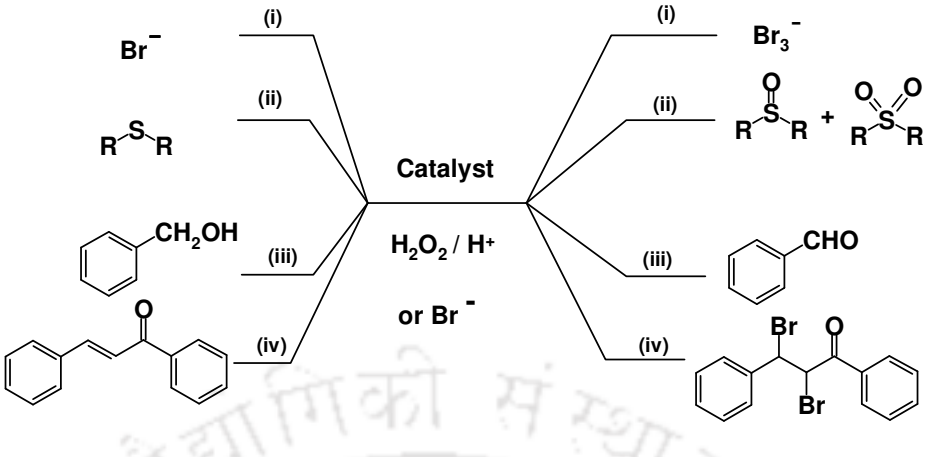

Scheme 3.4.1 Catalytic oxidation of (i) bromide, (ii) sulfide, (iii) benzyl alcohol and (iv) bromination of chalcone. Solvent systems (i) water, (ii) methanol/water (1:1), (iii) methano/water (1:1) and (iv) acetone/water (2:1) were used.

(i) Oxidation of bromide

The vanadadium dependent bromoperoxidase enzyme is known to oxidize bromide and brominate organic substrates in the marine organism through the formation of active species $OBr^- \leftrightarrows Br_2 \leftrightarrows Br_3^-$ *in situ* [31d]. The tribromide (Br_3^-) has been isolated in the solid state as quaternary ammonium salts. Therefore, the oxidation of bromide to tribromide is one of the important reactions to check the reactivity of a newly synthesized peroxovanadium compound with reference to bromoperoxidase activity. Accordingly, the reactivity of the synthesized compounds has been studied for oxidation of bromide and the results are reported in Table 3.4.1.

The reactions were carried out in water at ice-bath temperature (*ca.* 4^0C). The formation of yellow precipitate indicates the progress of reaction. After completion of the reaction, the product was isolated quantitatively by filtering through Whatman paper. All the catalysts gave very good yields, however, compound (**1**) and (**3**) showed better efficiency compared to other compounds. The compound (**16**) has been found to be least reactive of all.

(ii) Oxidation of sulfide

The potential of peroxovanadium compounds in oxidation of sulfide is well documented [31c]. In the present study, the reactions were carried out in

methanol/water solvent system. Methanol is believed to activate the peroxo group by formation of hydrogen bonding, thereby increasing the rate of the reaction than other solvent, as observed from the control reactions. Selectivity of the catalyst can be controlled by varying the amount of hydrogen peroxide, however, 1 equivalent of H_2O_2 with respect to substrate slowed down the rate of reaction. Therefore, a little excess of H_2O_2 was added and found to be conducive to the oxidation with formation of only 20% sulfone. The reactivity order has been found to be similar to that of bromide oxidation.

Table 3.4.1 Oxidation and bromination reactions using peroxovanadate as catalyst

Reaction	Catalyst (Compd.)	Time (h)	Yield (%)	Reaction	Catalyst (Compd.)	Time (h)	Yield (%)
(i)	(**1**)	3	99	(ii)	(**1**)	0.7	97
	(**2**)	4	92		(**2**)	1.5	80
	(**3**)	2	98		(**3**)	0.5	95
	(**6**)	3	95		(**6**)	1	90
	(**9**)	3	95		(**9**)	1	92
	(**10**)	4	92		(**10**)	2	87
	(**13**)	5	88		(**13**)	3	80
	(**16**)	6	80		(**16**)	4	78
(iii)	(**1**)	4	92	(iv)	(**1**)	2	95
	(**2**)	6	85		(**2**)	3	90
	(**3**)	3	92		(**3**)	2	96
	(**6**)	5	80		(**6**)	3	85
	(**9**)	5	85		(**9**)	3	88
	(**10**)	3	75		(**10**)	3	65
	(**13**)	8	67		(**13**)	5	53
	(**16**)	10	60		(**16**)	6	48

(iii) Oxidation of benzyl alcohol

Peroxovandaium compounds are also reported to be capable of bringing about oxidation of benzyl alcohol. Reactivity of the newly synthesized compounds has been investigated in terms of selective oxidation of benzyl alcohols to benzaldehyde with H_2O_2 as the terminal oxidant. Under the optimized reaction condition, benzyl alcohol

was converted to the corresponding benzaldehyde selectively and efficiently in good yields.

(iv) Bromination of chalcone

Chalcone has been brominated in the present study with the synthesized complexes as catalysts. The reaction was carried out in acetone water mixture at ambient temperature. In this solvent system, the product *i.e.* dibromochalcone precipitated out as the reaction proceeded forward. Interestingly, the double bond was brominated selectively in presence of the aromatic ring. The product is an important precursor for the synthesis of flavonoids. Here again, the order of reactivity was found to be similar to the previous reactions.

3.4.3 Conclusion

The reactivity of the newly synthesized compounds has been studied. An internal comparison of the results has been made to enable us comment on their relative efficiency. The reactivity order of the catalysts is found to be as follows:

DmpzH[$VO(O_2)_2$(dmpz)] (**1**) > $Na_2[V_2O_2(O_2)_4$(dmpz)] (**3**) > K[$VO(O_2)_2$(dmpz)] (**2**) > $Na_3[VO(O_2)_2(C_6H_6O_7)].4H_2O$ (**10**) > $A_2[V_2O_4(C_6H_6O_7)_2].2H_2O$ [A = Na(**4**), K(**5**), NH_4(**6**)] > $A_2[V_2O_2(O_2)_2(C_6H_6O_7)_2].2H_2O$ (A = Na(**7**), K(**8**), NH_4(**9**) > $A_3[VO(O_2)_2(OH)(O_2)_2OV]$, [A = Na**(11),** K**(12),** NH_4**(13)**] > $A_3[VO(O_2)_2(F)(O_2)_2OV]$, [A = Na(**14**), K(**15**), NH_4(**16**)].

It has also been observed that a complex anion with different counter cation show similar reactivity, however, the ammonium salts have been found to be slightly more reactive than the corresponding sodium and potassium salts.

The results obtained with compounds (**1**)-(**3**) are in line with the results derived from the DFT calculations (discussed in section 3.2). The presence of hydrogen bonding in compound (**1**) and bridging peroxo group in compound (**3**) make them more reactive than the others. Citrato group has no effect on the reactivity, monoperoxo vanadate (V) compounds are found to be more reactive than non- and di-peroxocitratovanadate(V), as expected. In case of μ-fluoro diperoxovanadate (V), the fluoride stabilizes the peroxovanadate as well as makes less reactive towards the nucleophilic attack.

References

[1] (a) Boer, E.; Wever, R. *J. Biol. Chem.* **1988**, *263*, 12326; (b) Schijndel, J. W. P. M. V.; Barnet, P.; Roelse, J.; Vollenbroek, E. G. M.; Wever, R. *Eur. J. Biochem.* **1994**, *225*, 151; (c) Everett, R. R.; Soedjak, H. S.; Butler, A. *J. Biol. Chem.* **1990**, *265*, 15671.

[2] (a) Butler, A.; Carter, J.; Simpson, M. *Handbook on Metalloproteins*, Bertini, I.; Sigel, A.; Sigel, H. Eds.; Marcel Dekker Inc.: New York, Basel, 2001; p 153. (b) Butler, A. *Coord. Chem. Rev.* **1999**, *187*, 17.

[3] Liang, J.; Madden, M.; Shah, V. K.; Burris, R. H. *Biochem.* **1990,** *29,* 8577.

[4] (a) Lau, K. H. W.; Farley, J. R.; Baylink, D. J. *J. Biol. Chem.* **1989**, *257*, 23; (b) Walton, K. M. ; Dixon, J. E. *Annu. Rev. Biochem.* **1993**, *62*, 101.

[5] (a) Smith, J. B. *Proc. Natl. Acad. Sci. USA.* **1983**, *80*, 6162; (b) Klarlund, J. K. *Cell* **1985**, *41*, 707.

[6] Djordjevic, C. *Metal Ions in Biological Systems: Antitumorigenic Activity of Vanadium Compounds*, Sigel, H.; Sigel, A. Eds.; Marcel Dekker: New York, 1995; Vol. 31, *Chapt. 18*, p 595.

[7] Aureliano,M.; Henao, F.; Tiago, T.; Duarte, R. O.; Moura, J. J. G.; Baruah, B.; Crans, D. C. *Inorg. Chem.* **2008**, *47*, 5677.

[8] (a) Kadota, S.; Fantus, I. G.; Deragon, G.; Guyda H. J.; Posner, B. I. *J. Biol. Chem.,* **1987**, *262*, 8252; (b) Posner, B. I.; Shaver A.; Fantus, I. G. *New Antidiabetic Drugs,* Bailey; C. Flatt P. R. Eds.; Smith-Gordon: London, **1990**, *Chapt. 8*, p 107; (c) Thompson, K. H.; Yuen, V. G.; McNeill J.; Orvig C. *Vanadium Compounds*: *Chemistry*, *Biochemistry*, *and Therapeutic Applications*, Tracey A. S.; Crans, D. C. Eds.; Oxford University Press, New York, 1998, p 329; (d) Thompson, K. H.; Orvig, C. *J. Chem. Soc*., *Dalton Trans*. **2000**, 2885.

[9] Crans, D. C.; Keramidas, A. D.; Litty, H. H.; Anderson, O. P.; Miller, M. M.; Lemoine, L. M.; Williams, S. P.; Vandenberg, M.; Rossomando A. J.; Sweet, L. J. *J. Am. Chem. Soc*. **1997**, *119*, 5447.

[10] Sivak, M.; Tyrselova, J.; Pavelcik, F.; Marek, J. *Polyhedron,* **1996**, *15*, 1507.

[11] Sivak, M.; Schwendt, P. *Trans. Met. Chem.* **1989**, *14*, 273.

[12] (a) Conte, V.; Furia, F. D.; Moro, S. *J. Mol. Catal.* **1995**, *104,* 159; (b) Conte, V. Furia, F. D. ; Moro, S. ; *J. Phys. Org. Chem.* **1996**, *9,* 329.

[13] Sucha, V.; Sivak, M.; Tyrselova, J.; Marek, J. *Polyhedron,* **1997,** *16*, 2837.

[14] Mohan, M.; Bond, M. R.; Otieno, T.; Carrano, C. J. *Inorg. Chem.* **1995**, *34*, 1233.

[15] Crans, D. C. *Metal Ions in Biological Systems: Vanadium and its Role in Life*, Sigel H.; Sigel, A. Eds,; Marcel Dekker, New York, 1995, Vol. 31, *Chapt. 5*, p 147.

[16] Kaliva, M.; Gabriel, C.; Raptopoulou, C. P.; Terzis, A.; Salifoglou, A. *Inorg. Chim. Acta* **2008**, *361*, 2631.

[17] (a) Djordjevic, C.; Lee, M.; Sinn, E. *Inorg. Chem.* **1989**, *28*, 719;(b) Wright, D. W.; Humiston, P. A.; Orme-Johnson, W. H.; Davis, W. M. *Inorg. Chem.* **1995,** *34*, 4194; (c) Crans, D. C.; Jiang, F.; Chen, J.; Anderson, O. P.; Miller, S. M. *Inorg. Chem.* **1997**, *36*, 1038; (d) Crans, D. C. Jiang, F.; Anderson, O. P.; Miller, S. M. *Inorg. Chem.* **1998**, *37*, 6645; (e) Velayutham, M.; Varghese, B.; Subramanian, S. *Inorg. Chem.* **1998**, *37*, 1336; (f) Kaliva, M.; Giannadaki, T.; Raptopoulou, C. P.; Tangoulis, V.; Terzis, A.; Salifoglou, A. *Inorg. Chem.* **2001**, *40*, 3711; (g) Tsaramyrsi, M.; Kaliva, M.; Giannadaki, T.; Raptopoulou, C. P.; Tangoulis, V.; Terzis, A.; Giapintzakis, J.; Salifoglou, A. *Inorg. Chem.* **2001**, *40*, 5772; (h) Kaliva, M.; Giannadaki, T.; Raptopoulou, C. P.; Terzis, A.; Salifoglou, A. *Inorg. Chem.* **2002**, *41*, 3850; (k) Kaliva, M.; Kyriakakis, E.; Gabriel, C. Raptopoulou, C. P.; Terzis, A.; Tuchagues, J. P.; Salifoglou, A. *Inorg. Chim. Acta* **2006**, *359*, 4535.

[18] (a) Clark, H. C.; Emeleus, H. J. *J. Chem. Soc.* **1957**, 2119; (b) Dodge, R. P.; Templeton, D. H.; Zalkin, A. *J. Chem. Phys.* **1962**, *35*, 55; (c) Chaudhuri, M. K.; Dasgupta, H. S.; Ghosh, S. K.; Khating, D. T. *Synth. React. Inorg. Met. Org. Chem.* **1982**, *12*, 63.

[19] (a) Stomberg, R. *Acta Chem. Scand. Ser. A* **1984**, *38*, 223; (b) Stomberg R.; Olson, S. *Acta Chem. Scand. A* **1984**, *38*, 821; (c) Stomberg R.; Olson, S. *Acta Chem. Scand. Ser. A* **1984**, ***38***, 801; (d) Stomberg, R. *Acta Chem. Scand. Ser. A* **1984,** *38*, 541; (e) Schwendt, P.; Joniakov´a D.; Ezr, V. *Chem. Pap. 1985*, *39*, 353; (f) Lapshin, A. E.; Smolin, Y. I.; Shepelev, Y. F.; Schwendt P.; Gyepesova, D. *Acta Crystallogr. Sect. C: Cryst. Struct. Commun.* **1990**, *46,* 1753; (g) Chrappova, J.; Schwendt P.; Marek, J. *J. Fluorine Chem.* **2005**, *126*, 1297; (h) Kirsch, J. E.; Izumi, H. K.; Stern Ch. L.; Poeppelmeier, K. R. *Inorg.Chem.* **2005**, *44*, 4586; (i) Chrappova, J.; Schwendt P.; Sivak, M. Repisky, M. Malkin, V. G. Marek J. *Dalton Trans.* **2009**, 465.

[20] (a) Ravishankar, H. N.; Chaudhuri, M. K.; Ramasarma, T. *Inorg. Chem.* **1994**, *33*, 3788; (b) Ravishankar, H. N.; Ramasarma, T. *Arch. Biochem. Biophys.* **1995**, *316,* 319.

[21] (a) Crans, D. C.; Smee, J. J.; Gaidamauskas, E.; Yang, L. *Chem. Rev.* **2004**, *104*, 849; (b) Tanaka, N.; Dumay, V.; Liao, Q.; Lange, A. J.; Wever, R. *Eur. J. Biochem.* **2002**, *269*, 2162.

[22] Kalita, D.; Deka, R. C.; Islam, N. S. *Inorg. Chem. Commun*. **2007**, *10,* 45.

[23] (a) Zampella, G.; Fantucci, P.; Pecoraro, V. L.; Gioia, L. D. *J. Am. Chem. Soc.* **2005**, *127*, 953; (b) Zampella, G.; Fantucci, P.; Picoraro, V. L.; Gioia, L. D. *Inorg. Chem.* **2006**, *45*, 7133.

[24] (a) Buhl, M. *J. Comput. Chem*. **1999**, *20*, 1254; (b) Niu, S.; Hall, M. B. *Chem. Rev*. **2000**, *100*, 353; (c) Conte, V.; Bartolini, O.; Carraro, M.; Moro, S. *J. Inorg. Biochem.* **2000**, *80*, 41.

[25] Butler, A.; Clague, M. J.; Meister, G. E. *Chem. Rev*. **1994**, *94*, 625.

[26] (a) Colpas, G. J.; Hamstra, B. J.; Kampf, J. W.; Pecoraro, V. L. *J. Am. Chem. Soc.* **1994**, *116*, 3627; (b) Colpas, G. J.; Hamstra, B. J.; Kampf, J. W.; Pecoraro, V. L. *J. Am. Chem. Soc.* **1996**, *118*, 3469; (c) Kanamori, K.; Nishida, K.; Miyata, N.; Okamoto, K. *Chem. Lett.* **1998,** 1267.

[27] (a) Hirao, T. *Chem. Rev.* **1997**, *97*, 2707; (b) Kelly, P.; Lawrence, S. E. M.; Anita, R. *Euro. J. Org. Chem.* **2006,** 19, 4500.

[28] (a) Tsuchida, E.; Oyaizu, K. *Coord. Chem. Rev.* **2003**, *237*, 213; (b) Pombeiro, A. J. L. *ACS Symposium Series* **2007,** *974*, 51 and references therein.

[29] (a) Deubel, D. V.; Sundermeyer J.; Frenking, G. *J. Am. Chem. Soc.* **2000**, *122*, 10101; (b) Wang, X. Y.; Shi H. C.; Xu, S. Y. *J. Mol. Catal. A: Chem.* **2003**, *206*, 213.

[30] (a) Bolm, C. *Coord. Chem. Rev.* **2003***, 237,* 245; (b) Gopinath, R.; Barkakaty, B.; Talukdar, B.; Patel, B. K. *J. Org. Chem.* **2003**, *68*, 2944.

[31] (a) Bora, U.; Bose, G.; Chaudhuri, M. K.; Dhar, S. S.; Gopinath, R.; Khan, A. T.; Patel, B. K. *Org. Lett.* **2000**, *2*, 247; (b) Carter-Franklin, J. N.; Butler, A. *J. A. Chem. Soc.* **2004**, *126,* 15060; (c) Khedher, I.; Ghorbel, A.; Fraile, J. M.; Mayoral, J. A. *J. Mol. Cat. A: Chem.*, **2006**, *255*, 92; (d) Chaudhuri, M. K.; Bora, U.; Dehury, S. K.; Dey, D.; Dhar, S. S.; Kharmawphlang W.; Choudary, B. M.; Kantam, M. L. *US Pat*. **2006**, 7005548; (f) Moriuchi, T.; Yamaguchi, M.; Kikushima, K.; Hirao, T. *Tetrahedron Lett.* **2007**, *48,* 2667.

[32] Lever, A. B. P. *Inorganic Electronic Spectroscopy,* 2nd edn., Elsevier, Amsterdam, **1984**, p. 287, 294.

[33] (a) Griffith W. P.; Wickens, T. D. *J. Chem. Soc.* **1967**, *590*; (b) Chaudhuri M. K.; Das, B. *Inorg. Chem.* **1986**, *25*, 168-170; (c) Bhattacharjee, C. R.; Bhattacharjee, M.; Chaudhuri M. K. *Polyhedron,* **1990**, *9*, 1653.

[34] Nakamoto, K. *Infrared and Raman spectra of Inorganic and Coordination Compounds, Part B,* 5th Ed., John-Wiley and Sons, New York, 1997, p 71.

[35] (a) Singh, C. B.; Satpathy S.; Sahoo, B. *J. Inorg. Nucl. Chem.,* **1973**, *35*, 3947; (b) Turner, H. W.; Anderson, R. A.; Zalkin A.; Templeton, D. H. *Inorg. Chem.* **1979**, *18*, 1221.

[36] (a) Szentivanyi, H.; Stomberg, R. *Acta Chem. Scand. A* **1983**, *37*, 553; (b) Shaver, A.; Hall, D. A.; Ng, J. B.; Lebuis, A. M.; Hynes, R. C.; Posner, B. I. *Inorg. Chim. Acta* **1995**, *229*, 253.

[37] Messerschmidt, A.; Prade, L.; Wever, R. *Biol. Chem.* **1997,** *378*, 309.

[38] (a) Colpas, G. J.; Hamstra, B. J.; Kampf, J. W.; Pecoraro, V. L. *J. Am.Chem. Soc.* **1996**, *118*, 3469; (b) Butler, A.; Baldwin, A. H. *Struct. Bonding* **1997**, *89*, 109.

[39] Kimblin, C.; Bu X.; Butler, A. *Inorg. Chem.,* 2002, *41*, 161.

[40] Schwendt, P.; Tyrselova, J.; Pavelcik, F. *Inorg. Chem.* **1995**, *34*, 1964-1966.

[41] Schwendt, P.; Oravcova, A.; Tyrselova, J.; Pavelcik, F.; Marek, J. *Polyhedron,* **1996**, *15*, 4507-4511.

[42] Sucha, V.; Sivak, M. ; Tyrselova, J.; Marek, J. *Polyhedron*, **1997,** *16,* 2837-2842.

[43] Chrappova, J.; Schwendt, P.; Sivak, M.; Repisky, M.; Malkin, V.G.; Marek, J. *Dalton Trans.* **2009,** 465-473.

[44] Gabriel, C.; Kaliva, M.; Venetis, J.; Baran, P.; Rodriguez-Escudero, I.; Voyiatzis, G.; Zervou, M.; Salifoglou, A. *Inorg. Chem.* **2009**, *48*, 476–487.

[45] Bonchio, M.; Bartolini, O.; Conte, V.; Moro, S. *Eur. J. Inorg. Chem*. **2001**, 2913.

[46] Deacon, G. B.; Philips, R. *J. Coord. Chem. Rev*. **1980**, *33*, 227.

[47] Hussain, S.; Bharadwaj, S. K.; Pandey, R.; Chaudhuri, M. K. *Under Review.*

[48] Campbell, N. J.; Flanagan, J.; Griffith, W. P.; Skapski, A. C. *Transition Met. Chem.* **1985**, *10*, 353.

Spectra of some selected compounds

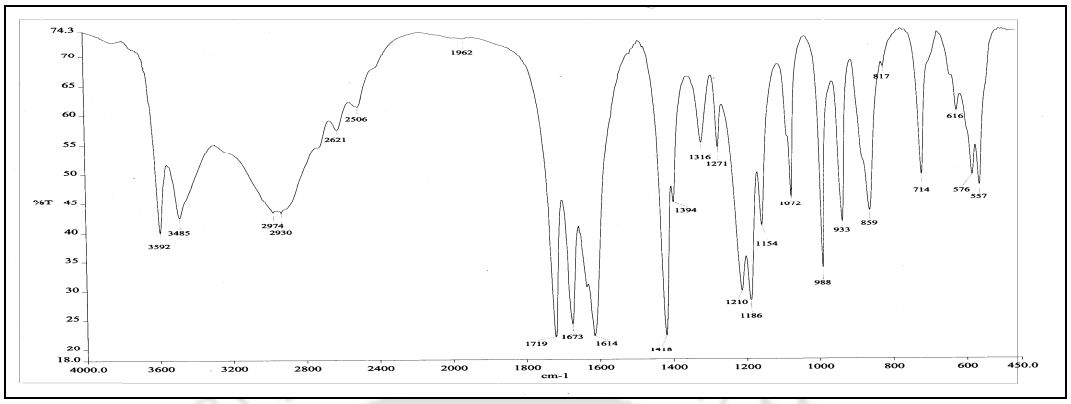

Figure 3.S1 FTIR spectrum of $K_2[V_2O_2(O_2)_2(C_6H_6O_7)_2].2H_2O$ **(2)**

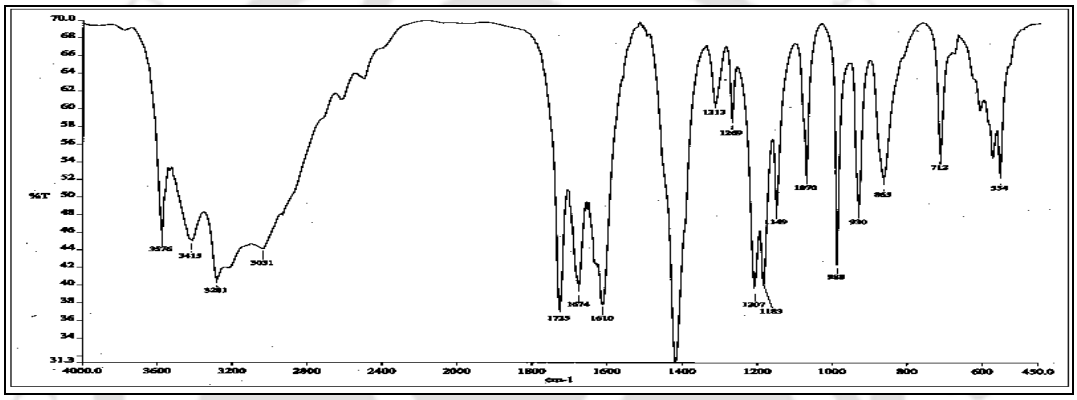

Figure 3.S2 FTIR spectrum of $(NH_4)_2[V_2O_2(O_2)_2(C_6H_6O_7)_2].2H_2O$**(3)**

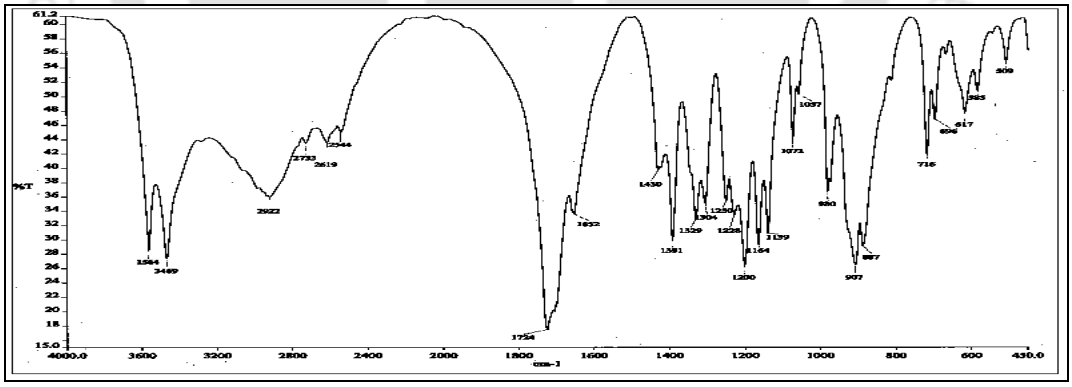

Figure 3.S3 FTIR spectrum of $Na_2[V_2O_4(C_6H_6O_7)_2].2H_2O$ **(4)**

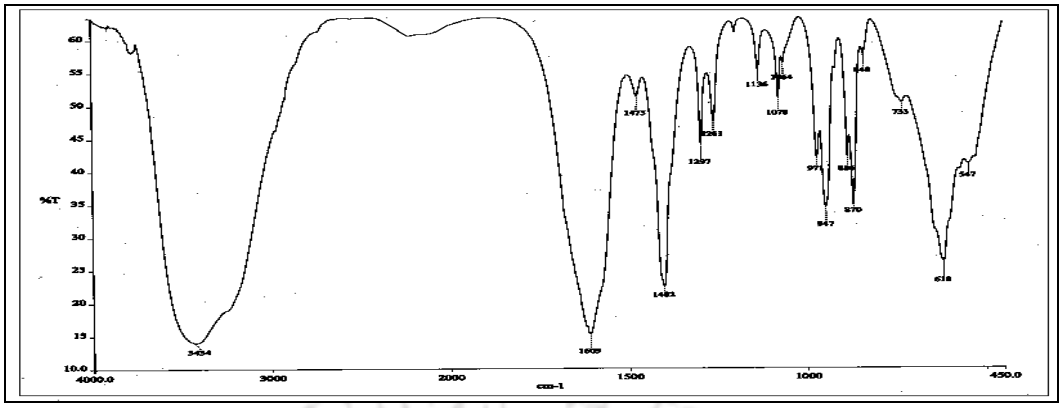

Figure 3.S4 FTIR spectrum of of $Na_2[V_2O_2(O_2)_4(C_6H_5O_7)].H_2O$ (**10**)

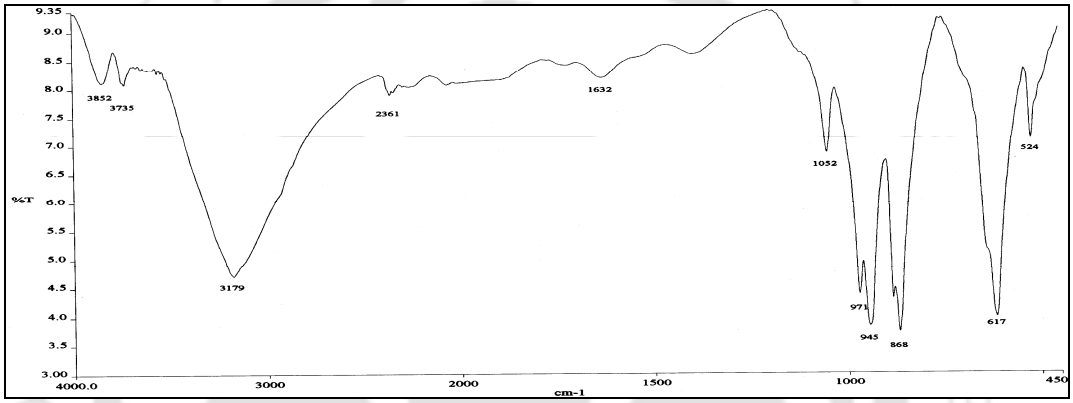

Figure 3.S5 FTIR spectrum of of $Na_3[V_2O_2(O_2)_4(OH)].H_2O$ (**11**)

Oxidative Extraction of Bromide from "Sea Bittern" and Bromination of phenol directly with Sea bittern by bio-mimicking catalysis

In view of wider use of bromo-organic compounds in the synthesis of a large number of natural products as well as the manufacture of pharmaceuticals, agrochemicals and numerous industrially valuable products [1], bromination of organic compounds has received significant attention in recent years. For over a century, molecular bromine has been the most commonly and widely used brominating reagent because of its being inexpensive and easily available. Therefore development of reagents and process for bromination of organic compounds without using molecular bromine are in order.

In the nature, vanadium-dependent bomoperoxidase enzyme catalyses the oxidation of bromide by hydrogen peroxide followed by bromination of the organic substrates. The prosthetic group of bromperoxidase contains vanadium (V) which forms peroxovanadate by reacting with hydrogen peroxide. The peroxovanadate thus formed served as the active catalyst for bromination reaction. The reaction mechanism of catalytic action of vanadium is not fully understood, however, it has been proposed that an active 'brominating species' *viz*. 'Br^{+}', 'OBr^{-}' or 'Br_3^{-}' is formed *in situ*. Taking cues from the bromoperoxidase activity and keeping environmental safety in mind, in conjunction with knowledge and experience that we gained in the peroxovanadium chemistry [2], it was possible to develop newer and eco-friendly brominating agents i.e. tribromides, "the store house of bromine" and bromination protocols from a solution of KBr or NH_4Br [3].

Industrially bromine is produced from sea water by oxidation with chlorine which is known as blowing out process. Requirement of large amount of mineral acid, high pressure and temperature make this environmentally unfriendly [4]. Several other methods have been developed for extraction of bromine from sea water, however, they have certain disadvantages as discussed in Chapter 1.

In the present Ph. D. work, it has been possible to extract bromide from "bittern" (sea water concentrated under the sun), the natural source of bromide, by bio-mimcking catalysis, and this has been thus discussed in this Chapter.

Involvement of VBrPO in bromination and the need for an eco-friendly bromide extraction process led us to develop VBrPO mimicking catalyst for extraction of bromide

from sea water in a very soft way. Accordingly, several catalysts have been developed in our laboratories and screened for extraction of bromide from sea water. In addition, while studying the reactivity of compounds synthesized in Chapter 3, Section 3.4, it was observed that the compounds efficiently catalyzed the oxidation of bromide with hydrogen peroxide. The compound, DmpzH[$VO(O_2)_2$dmpz] was found to be one of the most efficient catalysts for this purpose. This investigation also suggested that the catalyst, DmpzH[$VO(O_2)_2$dmpz] might as well be efficient for direct bromination of phenol with 'bittern' without any additional bromide. Hence, demonstrated herein is a catalytic protocol for bromination of phenol with sea bittern without extraneous addition of Br^-.

In order to make the presentation more articulate, this chapter has been divided into two sections. While **Section 4.1** includes the extraction of bromide from sea water as quaternary ammonium tribromides followed by their characterization, the methodology for oxidative organic bromination of phenol without isolating the active brominating species from sea bittern is incorporated in **Section 4.2**.

Section 4.1

Extraction of Bromide from Sea bittern: An Eco-friendly Bio-mimetic Process

4.1.1 Experimental

Bittern (concentrated sea bittern) containing 2.26 g/L magnesium bromide, 68.59 g/L magnesium sulfate, 125.23 g/L magnesium chloride, 163.36 g/L sodium chloride, [54.73 g/L sulfate, 191.48 g/L chloride and 1.96 g/L bromide] was employed for the reaction. The pre-analyzed sea bittern was obtained from the bromine producing industry, Tata Chemicals Ltd., Mithapur, Gujarat, India.

(a) General procedure for extraction of bromide as TBATB from bittern

To 100 mL of bittern, 1 mol% of catalyst, 1.5 mL of 45% H_2O_2 ,0.6g of tetrabutylammonium chloride, TBAC and 1.2 mL of 5M H_2SO_4 were added. The mixture was stirred constantly at ambient temperature for 4 hours and was then left overnight for settling. The solution was then filtered through suction pump and then the precipitate was dried in desiccator. The product was recrystallized using acetonitrile to obtain 0.392g of tetrabutylammonium tribromide, TBATB. The yield was noted to be 98.5%. The melting point of the product was found to be 72 or 73 ^oC. The compound was analyzed as $C_{16}H_{36}NBr_3$ .Calculated (Found) (%): C, 39.86 (39.41); H, 7.52 (8.28); N, 2.90 (2.78); Br, 49.71 (49.53).

(b) General procedure for extraction of bromide from bittern

The bittern was concentrated to 80 mL from 100 mL. To this 80 mL solution, 1 mol % of catalyst, 1.2 mL of 55% H_2O_2 , 0.4g tetrabutylammonium chloride (TBAC) and 0.7 mL of 5M H_2SO_4 were added. The solution was stirred for 3 h. The solution was left overnight for settling. The product obtained after filtration and recrystallization was 0.39g of tetrabutylammonium tribromide (TBATB). Yield 99% .

4.1.2 Results and Discussion

Determination of crystal structures and studies of mechanistic aspects of vanadium haloperoxidase enzymes revealed that the ability of vanadium in oxidation of halides depends on the protein environment of active site [4]. Accordingly they are classified as chloroperoxidase, bromoperoxidase and iodoperoxidase. While chloroperoxidase can oxidize all halides, bromoperoxidase oxidizes bromide and iodide. Our sustained involvement in peroxovanadium chemistry and studies of reactivity, particularly with reference to bromoperoxidase activity, has led us to develop a process for oxidation of bromide to tribromide with hydrogen peroxide in presence of vanadium as catalyst [2]. Further, it has been observed that vanadium can oxidize bromide at very low concentration. This observation led us to think it worthwhile to carry out an oxidation reaction for bromide in bittern, where concentration of bromide is very less when compared to other ions. The sea water was collected from Arabian Sea and concentrated under sun to obtain "bittern" containing only 1.96g/L of bromide compared to 191.48 g/L chloride. Importantly, the catalyst ($NaVO_3$) worked well and oxidized only bromide from bittern. Tetrabutylammonium chloride (TBAC) has been taken as the source of counter ion. In order to optimize the reaction conditions several reactions have been carried out (Table 4.1.1, entries 1-5). The amount of catalyst, H_2O_2, TBAC, and acid have been taken with reference to concentration of bromide in bittern. Finally, 0.003g of catalyst ($NaVO_3$), 1.2 mL of H_2O_2 (45%), 0.4g of TBAC and 0.7 mL of 5M H_2SO_4 gave the best result with isolation of 0.39g tetrabutylammonium tribromide, TBATB (99% yield) from 100 mL sea water, which was reduced to 80 mL before reaction. This reaction conditions also performed well with 500 mL bittern (400 mL after reduction) (Table 4.1.1, entry 6). Recrystallization of the product obtained from 500 mL bittern gave 96% of pure TBATB. Similarly, tribromides such as benzyltriethylammonium tribromide (BTEATB), cetyltrimethylammonium tribromide (CTATB), tetraethylammonium tribromide (TEATB), tetramethylammonium tribromide (TMATB) also been synthesized from sea water. The results of optimization reactions are shown in Table 4.1.1.

Table 4.1.1 Optimization of reaction conditions with $NaVO_3$ as the catalyst

Exp. no.	Bittern[a] (original Vol[m]) (mL)	$NaVO_3$ (mg)	H_2O_2 (45%) (mL)	Ammonium salt (g)	H_2SO_4 (mL)	Yield in g (% wrt $MgBr_2$)
1	100 (100)	3	1.0	TBAC (0.5)	0.5	0.33 (83%)
2	100 (100)	3	1.0	TBAC (0.6)	1.2	0.37 (98%)
3	50 (100)	3	1.0	TBAC (4.0)	1.0	0.27 (69%)
4	70 (100)	3	1.5	TBAC (0.6)	0.5	0.34 (88%)
5	**80 (100)**	**3**	**1.2**	**TBAC (0.4)**	**0.7**	**0.39 (99%)**
6	**400 (500)**	**15**	**5.5**	**TBAC (1.4)**	**3.5**	**1.9 (96%)[b]**
7	500 (500)	15	9.0	TBAB (3.0)	5.5	2.41 (83%)
8	250 (250)	9	10.5	BTEAC (0.8)	4.5	0.147 (25%)
9	200 (250)	9	4.0	BTEAC (2.5)	5.0	0.56 (79%)
10	160 (200)	7	3.0	BTEAC (0.4)	1.5	0.52 (81%)
11	**160 (200)**	**7**	**2.2**	**BTEAC (0.6)**	**1.2**	**0.65 (85%)**
12	**500 - 400**	**16**	**6.0**	**BTEAC (1.5)**	**4.0**	**1.2 (80%)[b]**
13	100 (100)	3	7.0	CTMATB (0.5)	0.8	0.40(61%)
14	80 (100)	3	7.0	CTMATB (0.5)	0.5	0.35(53%)
15	80 (100)	3	4.0	CTMATB (0.6)	1.5	0.43(65%)
16	**80 (100)**	**3**	**5.0**	**CTMATB (0.6)**	**1.0**	**0.45(70%)**
17	**160 (200)**	**7**	**1.2**	**CTMATB (1.0)**	**0.8**	**0.85(68%)[b]**
18	80 (100)	3	3.0	TEAB (0.3)	0.5	0.20(46%)
19	80 (100)	3	2.0	TEAB (0.4)	0.7	0.25 (55%)
20	80 (100)	3	1.0	TEAB (0.5)	0.8	0.25 (55%)
21	**80 (100)**	**3**	**1.5**	**TEAB (0.5)**	**0.8**	**0.28 (61%)**
22	**160 (200)**	**7**	**3**	**TEAB (1.1)**	**1.5**	**0.60 (63%)**
23	100 (100)	3	4.0	TMAB (0.3)	0.8	0.20 (50%)
24	80 (100)	3	2.0	TMAB (0.4)	0.6	0.18 (45%)
25	80 (100)	3	2.5	TMAB (0.4)	0.6	0.19 (48%)
26	**80 (100)**	**3**	**3.0**	**TMAB (0.5)**	**0.5**	**0.45 (50%)**
27	**160 (200)**	**7**	**6.0**	**TMAB (1.2)**	**1.0**	**0.39 (52%)**

[a] the volume of bittern was reduced by warming and filtered to remove the NaCl, [b] yields after recrystalization.

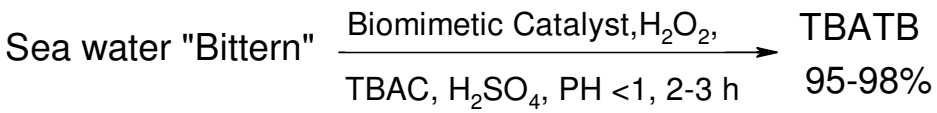

Scheme 4.1 Schematic representation of Extraction of Br^- as TBATB

After obtaining encouraging result with sodium metavanadate ($NaVO_3$), several other catalysts have been used for oxidation of bromide (Br_3^-) by hydrogen peroxide in the presence of a very small amount of acid to compare their efficacy. The results are included in Table 4.1.2.

Table 4.1.2 Extraction of bromide with different catalyst from 100 mL of bittern (the bittern was reduced to 80 mL before reaction)

Exp. no.	Catalyst (mg)	H_2O_2 (45%) (mL)	Ammonium salt (g)	H_2SO_4 (mL)	Yield in g (% wrt $MgBr_2$)
1	C_{Mo}=4	1.1	TBAC (1.0)	4	0.32 (83.7)
2	C_{25}=3	1.1	TBAC (4.0)	1	0.38 (96%)
3	C_w=4	1.1	TBAC (0.4)	0.7	0.28 (70%)
4	C_1= 3	1.1	TBAC (0.4)	0.7	0.25 (63%)
5	C_{Ti}=3	1.1	TBAC (0.4)	0.7	0.20 (50%)
6	C_{Fe}=9	2	TBAB (0.6)	2.5	0.532 (90%)
7	C_2=3	1.0	TBAC (0.4)	0.5	0.38 (96%)
8	C_3=3	1.0	TBAC (0.4)	0.5	0.38 (99%)

C_{Mo}=$H_2Mo_4H_2O$, C_{25}=V_2O_5, C_w=$NaWO_4$, C_1=$Na_3[V_2O_2(O_2)_4(OH)$, C_{Ti}=TiO_2, C_{Fe}=$Fe(acac)_3$, C_2= $Na_2[V_2O_2(O_2)_4$dmpz], C_3= DmpzH[$VO(O_2)_2$dmpz].

It has been observed that the catalysts were capable of oxidizing bromide from sea bittern. However, most of them gave either comparatively less yield or required higher amount of acid than that with $NaVO_3$. Interestingly, the catalysts $Na_2[V_2O_2(O_2)_4$dmpz] and DmpzH[$VO(O_2)_2$dmpz] gave very good yields with relatively less amount of acid. It is pertinent to mention here that these two compounds have been found to be efficient catalysts for oxidation of bromide, sulfide and alcohols as well (discussed in Chapter 3, section 3.1). The compound, DmpzH[$VO(O_2)_2$dmpz], was also used as the catalyst for extraction of bromide from sea water with different quaternary ammonium salts. The

reactions were performed with one litre of bittern. The results have been incorporated in Table 4.1.3.

Table 4.1.3 Extraction of bromide from sea bittern with DmpzH[$VO(O_2)_2$dmpz] as the catalyst

Serial No.	QAB/QAC used	QAB/QAC used (g/L)	QATB (g/L)	% yield
1	TBAB	4.2	5.9	93.8
2	TBAC	2.5	4	91.9
3	BTEAC	1.8	3.1	81.8
4	CTMAB	4.9	5.0	75.3
5	TEAB	3.7	4.3	63.4
6	TMAB	4.3	4.5	55.5

QAB= Quaternary ammonium bromide, QAC= Quaternary ammonium chloride,
QATB= Quaternary ammonium tribromide

The isolated tribromides (TBs) are well crystalline and stable species. These solids are actually the store house of bromine and are popularly known as solid bromine. These can brominate a variety of organic substrates under clean conditions and also be used for solid-phase brominations. The quarternary ammonium bromide can be recycled after brominations for the regeneration of the corresponding tribromides thereby rendering the process to be cost effective.

The tribromides **TBATB, BTEATB, CTMATB, TEATB**, and **TMATB** are all bright yellow or orange in color. Recrystallization from acetonitrile gives deep orange crystals. All the tribromides were characterized by IR, UV-visible, and ^{1}HNMR spectroscopy and matched well with earlier reported results [5]. Indeed, matching melting point with the literature enables us to know the purity of tribromides. Each of them has a sharp melting point (Table 4.1.4) and all of them have moderate to high solubility in the common organic solvents. The tribromides synthesized by the present protocol have a very long shelf life too. Stored in sample vials, they remain stable for months. Their stability can be ascertained by the determination of bromine contents periodically and recording melting points from time to time.

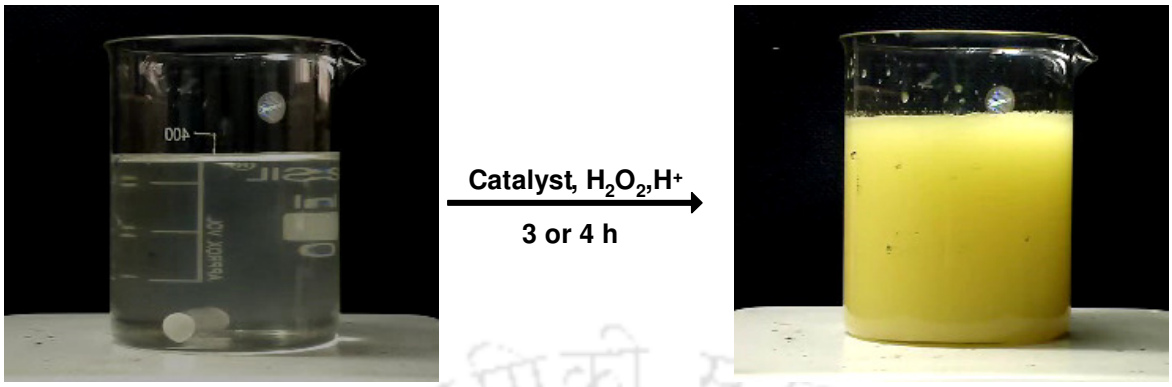

(a) (b)

Figure 4.1.1 *Pictorial representation of a bittern sample (a) before and (b) after tribromide formation.*

Table 4.1.4 Melting points, analytical Data and molar conductance values of tribromides

Compound (QATB)	M.P. (°C)	% found (% calcd.)				Conductance (10^{-3} M) ($\Omega^{-1}cm^2\,mol^{-1}$)
		C	H	N	Br	
TBATB ($C_{16}H_{36}NBr_3$)	75	39.41 (39.86)	8.28 (7.52)	2.78 (2.90)	49.53 (49.71)	155
BTEATB ($C_{13}H_{22}NBr_3$)	97-98	36.68 (36.16)	5.02 (5.15)	3.38 (3.24)	54.24 (54.34)	136
CTMATB ($C_{19}H_{42}NBr_3$)	87-88	40.99 (43.53)	7.91 (8.07)	2.74 (2.67)	48.36 (45.72)	162
TEATB ($C_8H_{20}NBr_3$)	85-86	25.99 (5.97)	5.82 5.45)	3.67 3.79)	64.52 64.79)	115
TMATB ($C_4H_{12}NBr_3$)	90-92	15.29 15.31)	3.86 (3.85)	4.45 (4.46)	76.4 76.38)	165

Solution electronic spectroscopy is an extremely important technique for characterization of tribromides in solutions which bear characteristic signature at *ca.* 265 nm with a shoulder at *ca.* 385 nm due to the transitions σ - σ^* and π - π^*, respectively [6]. The tribromides gave values in the range 267 – 269 nm and 380 – 400 nm, [Figures 4.1.2 (a) and (b)].

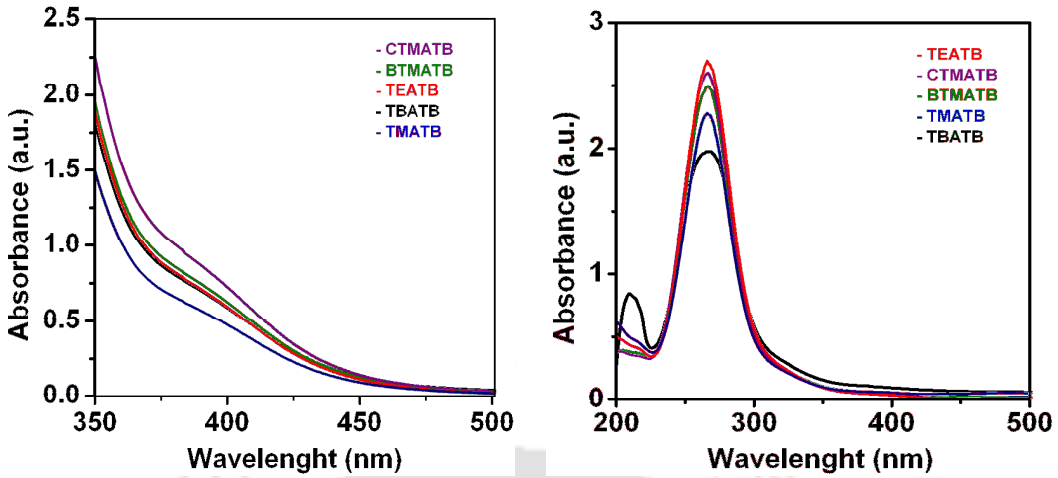

Figures 4.1.2 *UV-visible spectra of QATBs at (a) ~ 380 nm (b) ~ 267 nm*

The vibrational spectroscopy is also a very important technique for characterization of tribromides. For a linear tribromide (Br_3^-), three vibrational modes, ν_{sym} (ν_1), ν_{asym} (ν_3) and bending (ν_2) are expected in the far-IR region [8]. Of the three modes ν_1 and ν_3 occur at *ca.* 165 cm^{-1} and *ca.* 195 cm^{-1}, respectively, while the bending mode ν_2 generally appears at a far low value of *ca.* 50 cm^{-1}. In the present vibrational spectroscopic experiments ν_1 and ν_3 have been observed in the range 145 – 172 cm^{-1} and 185 – 192 cm^{-1} in complete agreement with those expected for a linear Br_3^- species. Unfortunately, owing to the instrumental limitations the region of the peak corresponding to ν_2 mode (at *ca.* 50 cm^{-1}) could not be covered. The symmetric stretch for Br_3^- is IR-active as symmetry is lowered owing to packing effect (for TBATB). In addition, the Br-Br-Br angle in other QATBs is not linear, hence IR-active.

Table 4.1.5 Structurally significant IR and electronic spectral bands of tribromides

Compound (QATB)	IR bands (cm^{-1})	UV-visible (λ , nm) (ε, $M^{-1}cm^{-1}$)
TBATB ($C_{16}H_{36}NBr_3$)	171(s), 191(s)	267 (49000), 400 (150)
BTEATB ($C_9H_{16}NBr_3$)	156(s), 195(s)	268 (51000), 385(152)
CTMATB ($C_{19}H_{42}NBr_3$)	152(s), 203(s)	269 (51500), 385 (155)
TEATB ($C_8H_{20}NBr_3$)	162(s), 192(s)	269 (52000), 390 (150)
TMATB ($C_4H_{12}NBr_3$)	146(s), 188(s)	269 (50500), 380 (149)

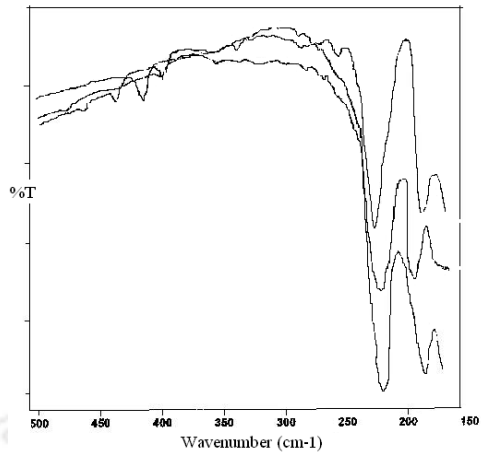

Figure 4.1.3 *Representative Far-IR spectra of* ***TBATB, CTMATB****, and* ***TMATB***

Single crystal X-ray structures have been determined for TBATB, BTEATB, and CTMATB. The ORTEP diagrams of these tribromides are shown in Figure 4.1.4. The crystal data and structure refinement results are incorporated in Table 4.1.6. While TBATB and CTMAB were crystallizing in monoclinic system, the BTEATB crystallized in orthorhombic system. The number of molecules per unit cell has been found to be 4, 5, and 2 for TBATB, BTEATB and CTMATB, respectively.

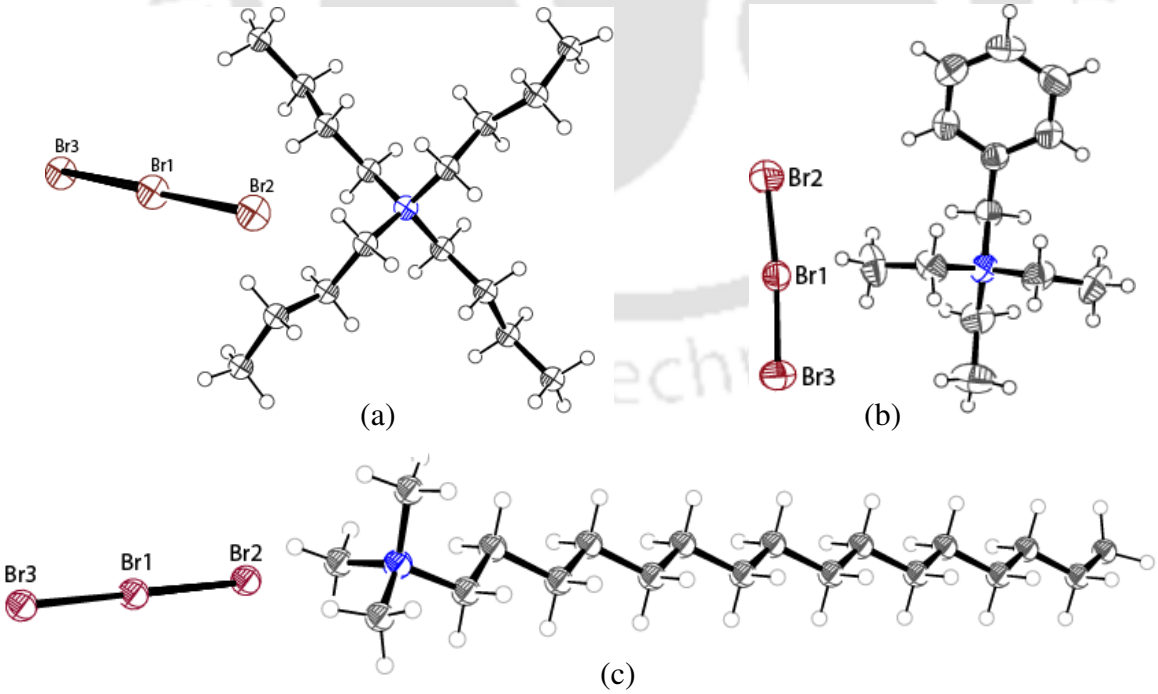

Figures 4.2.4 ORTEP diagrams of (a) TBATB, (b) BTEATB, and (c) CTMATB

Table 4.1.6 Crystal data and structure refinement for TBATB, BTEATB and CTMATB

Empirical formula	C16 H36 Br3 N	C13 H22 Br3 N	C19 H42 N1 Br3
Formula weight	482.19	432.05	524.27
Temperature, K	296(2)	296(2)	273(2)
Wavelength, Å	0.71073	0.71073	0.71073
Crystal system	Monoclinic	Orthorhombic	Monoclinic
Space group	C2/c	P2(1)2(1)2(1)	P2(1)/m
Unit cell dimensions	a= 12.981(7), α=90.	a= 8.422(4), α= 90.	a= 7.177(4), α = 90.
(Å and ^{0})	b= 10.382(6), β= 93.9	b= 10.132(4), β= 90.	b= 7.495(4), β= 96.7
	c= 16.242(8), γ= 90.	c=19.475(9), γ = 90.	c= 23.152(5), γ= 90.
Volume, Å^3	2184.0(2)	1661.9(13)	1236.77(12)
Z	4	4	2
Density (calc.) Mg/m^3	1.466	2.158	1.408
Absorption coefficient	5.536 mm^{-1}	9.081 mm^{-1}	4.894 mm^{-1}
F(000)	976	1060	536
Theta range for data collection	2.51 to 28.28°.	2.09 to 28.11°.	2.66to 23.91°.
Index ranges	-17<=h<=16, -13<=k<=13, -21<=l<=21	-11<=h<=10, -13<=k<=13, -25<=l<=24	-6<=h<=9, -10<=k<=9, -26<=l<=26
Reflections collected	13946	16234	2842
Completeness to theta = 28.28°	99.0 %	97.9 %	98.9%
Final R indices [I>2sigma(I)]	R1 = 0.0317,	R1 = 0.0318,	R1 = 0.0393,
	wR2 = 0.0688	wR2 = 0.0436	wR2 = 0.1020
R indices (all data)	R1 = 0.0664,	R1 = 0.0878,	R1 = 0.1150,
	wR2 = 0.0793	wR2 = 0.0497	wR2 = 0.0666.

Tribromides are known to be capable of bromination of organic substrates and do most of the job what molecular bromine does. It is expected that the counter cation of tribromide anion might change its reactivity, due to which number of tribromides have been synthesized with different cations (organic as well as inorganic). The variation in reactivity might have some relation with the bond angle (∟Br-Br-Br) and bond length (Br-Br) among the three bromine atoms. Moreover, cation like cetylammonium acts as a phase transfer agent in the reaction medium. The bond angles and lengths of these tribromides

are summarized in Table 4.2.7. Notably, TBATB shows equal bonds length of two Br-Br bond and a linear structure with ∟Br-Br-Br = 180 ^{0}. Although the two Br-Br bond distance are almost similar, the bond angle of BTEATB is 174.75 ^{0}, as observed. In case of CTMATB the bond angle is found to be 179.07^0 which is close to linearity, however, the bond distances differ by 0.161 Å as compared to the other two. The structural details of these compounds along with a couple of more of this class will be a part of the subject matter of another thesis to follow.

Table 4.1.6 Selected bond angles and bond lengths of tribromides

Parameter	TBATB	BTEATB	CTMATB
Br1-Br2 (Å)	2.539	2.531	2.623
Br1-Br3 (Å)	2.539	2.539	2.462
Br2-Br1-Br3 (^{0})	180.00	174.75	179.07

4.1.3 Conclusion

A novel, environmentally benign process for oxidative extraction of bromide with hydrogen peroxide in presence of bio-mimetic catalyst from sea bittern has been developed. The bromide is oxidized to tribromide (Br_3^-) and stabilized by quaternary ammonium salt. Finally, the Br_3^- has been isolated quantitatively as stable solid, viz. TBATB, BTEATB, CTMATB, TEATB and TMATB.

Section 4.2

Direct Bromination of Phenol with Sea bittern

4.2.1 Experimental

General procedure for bromination of phenol with sea bittern

To the 40 mL of sea water (concentrated from 50 mL of bittern) in a round bottomed flask, 0.01 g of catalyst (1 mol %), 2.5 mL of H_2O_2 (46%), 0.09g of phenol and 0.2 mL of 5M H_2SO_4 were added. The reaction mixture was stirred at ambient temperature. The progress of reaction was monitored by GC from time to time by taking out an amount of the reaction mixture (5 mL) and extracting with distilled dichloromethane. Then the solvent was treated with dry Na_2SO_4 and injected in the GC instrument. The percentage of conversion was calculated from the GC chromatogram.

4.2.2 Results and discussion

Driven by the (i) role of vanadium haloperoxidase enzyme in bromination of marine organism, (ii) efficiency of tribromides in bromination reactions, and finally (iii) encouraging results with the extraction of bromide from sea water (discussed in the previous section), herein we have used sea bittern as the bromine source for bromination of phenol, without using additional bromide. Since the compound, DmpzH[$VO(O_2)_2$dmpz] was found as one of the best catalysts for extraction of bromide from sea bittern, the same compound has been used as the catalyst for bromination reaction with sea water. The volume of sea water has been reduced by 20% for the reaction. The bromination reactions were conducted at ambient temperature.

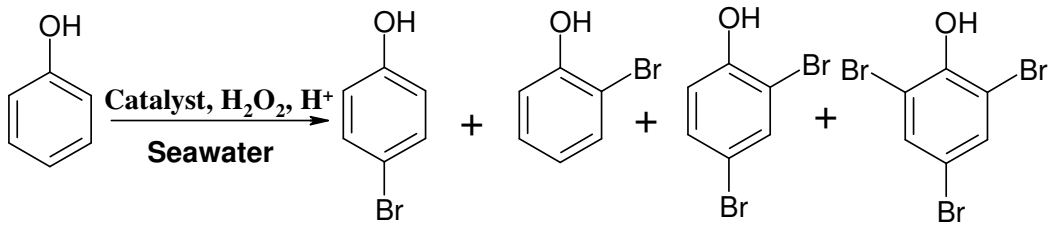

Scheme 4.2.1 *Bromination of phenol with bittern*

In order to optimize the reaction, several runs were carried out. The results appear in Table 4.2.1. It has been observed that slight variation of the reaction conditions might lead to the formation of a mixture of product such as ortho-, para-, di- and tri-bromophenol. An amount of 1 mol % of the catalyst, 2.5 mL of H_2O_2 (46%), 0.09g of phenol and 0.5 mL of 5M H_2SO_4 for 40 mL (after 20% reduction) has been found to be favorable to produce para-bromophenol selectively with 67% yield.

Table 4.2.1 Optimization of reaction conditions for bromination of phenol with bittern

Entry	Phenol	H_2O_2 (mL)	Catalyst (mol %)	Acid (mL)	Phenol: 2-bromo: 4-bromo: di-bromo	
					Time (24 h)	Time (36 h)
1	1:1	2.5	1	0.5	33:0:67:0	30:0:60:7
2				1	30:8:42:20	25:10:38:23
3			5	0.5	28:13:40:20	24:12:46:34
4				1	22:12:36:30	20:15:35:30
5		5	1	0.5	17:15:46:22	12:10:42:36
6				1	12:18:45:25	8:12:45:35
7			5	0.5	15:18:35:32	12:15:33:40
8				1	8:24:35:38	6:22:30:42
9	1:1.5	2.5	1	0.5	64:16:20:0	58:14:22:6
10				1	57:15:28:0	55:12:24:9
11			5	0.5	52:16:32:0	48:18:28:6
12				1	48:24:28:0	42:22:25:11
13		5	1	0.5	45:20:35:0	44:20:25:14
14				1	40:18:32:10	35:19:28:18
15			5	0.5	33:22:28:17	28:22:25:25
16				1	30:25:23:22	22:18:28:32

A few important observations have been made during the course of the reactions like (i) a limited amount of acid is required to push the reaction, control reaction without acid did not lead to bromophenol, (ii) slight excess of acid (*ca.* 1 mL of 5M H_2SO_4) leads

to the formation of tribromophenol, (iii) other factors like amount of the catalyst, H_2O_2 did not make any significant differences.

4.2.3 Conclusion

A possible way for bromination of organic substrates with bittern has been shown by taking phenol as the representative example. Phenol has been brominated to corresponding bromo derivative with sea bittern by a bio mimetic catalytic process where hydrogen peroxide was taken as terminal oxidant. Notably, the selective para bromination was achieved by controlling the reaction conditions.

References

[1] Katritzky, A. R.; Meth-Cohn, O.; Rees, C. W. *Comprehensive Organic Functional Group Transformations*, Pergamon, Oxford, 1995, vol. 2, p. 3.

[2] (a) Chaudhuri, M. K.; Ghosh, S. K. *Inorg. Chem.* **1982**, *21*, 4020; (b) Chaudhuri, M. K.; Ghosh, S. K.; Islam, N. S. *Inorg. Chem.* **1985**, *24*, 2706; (c) Basumatary, J. K.; Chaudhuri, M. K.; Purkayastha, R. N. D.; Hiese, Z. *J. Chem. Soc., Dalton Trans.* **1986**, 709; (d) Bhattacharjee, M. N.; Chaudhuri, M. K.; Islam, N. S. *Inorg. Chem.* **1989**, *28*, 2420; (e) Bhattacharjee, M.; Chaudhuri, M. K.; Islam, N. S.; Paul, P. C. *Inorg. Chim. Acta* **1990**, *169*, 97; (f) Bhattacharjee, M.; Chaudhuri, M. K.; Paul, P. C. *Can. J. Chem.* **1991**, *70*, 2245; (g) Chaudhuri, M. K.; Paul, P. C. *Ind. J. Chem.* **1992**, *31A*, 466.

[3] Chaudhuri, M. K.; Bora, U.; Dehury, S. K.; Dey, D.; Dhar, S. S.; Kharmawphlang, W.; Choudary, B. M.; Kantam, M. L. *US Pat*. **2006**, 7005548.

[4] Naude, S. M.; Verleger, H. *Proc. Phys. Soc.* **1950**, *63A*, 470.

[5] Hasan, Z.; Renirie, R.; Kerkman, R.; Ruijssenaars, H. J.; Hartog, A. F.; Wever, R. *J. Biol. Chem.* **2006**, *281*, 9738.

[6] Ph.D thesis, U. Bora, *Chapter 3*, p. 57.

[7] Buckles, R. E.; Popov, A. I.; Zelenzny, W. F.; Smith, R. J. *J. Am. Chem. Soc.* **1951**, *73*, 4525.

[8] Reynolds, M. S.; Morandi, S. J.; Raebiger, J. W.; Melican, S. P.; Smith, S. P. E. *Inorg. Chem.* **1994**, *33*, 4977.

[9] Nakamoto, K. Infrared and Raman Spectra of Inorganic and Coordination Compounds, 5th ed., Part A, Wiley, New York, 1997, p.169.

Spectra of some selected compounds

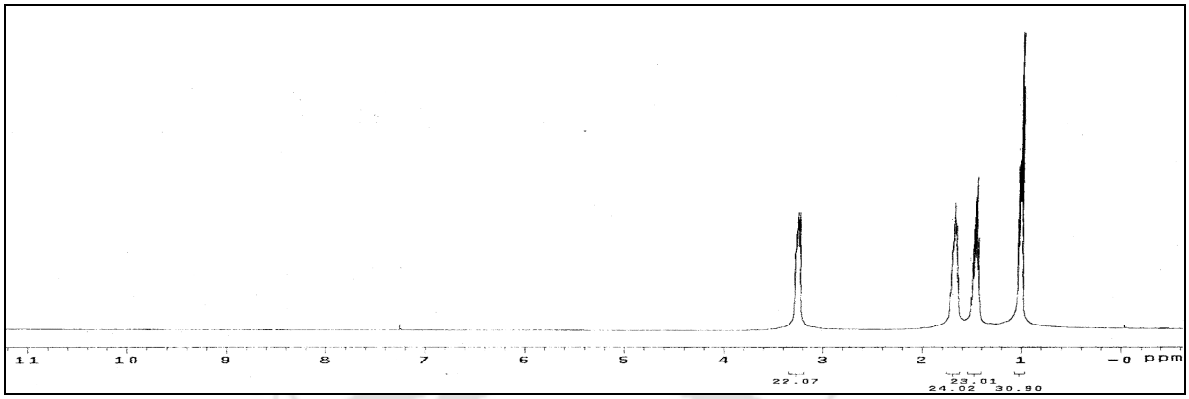

Figure 4.S1 ^{1}H NMR spectrum of TBATB

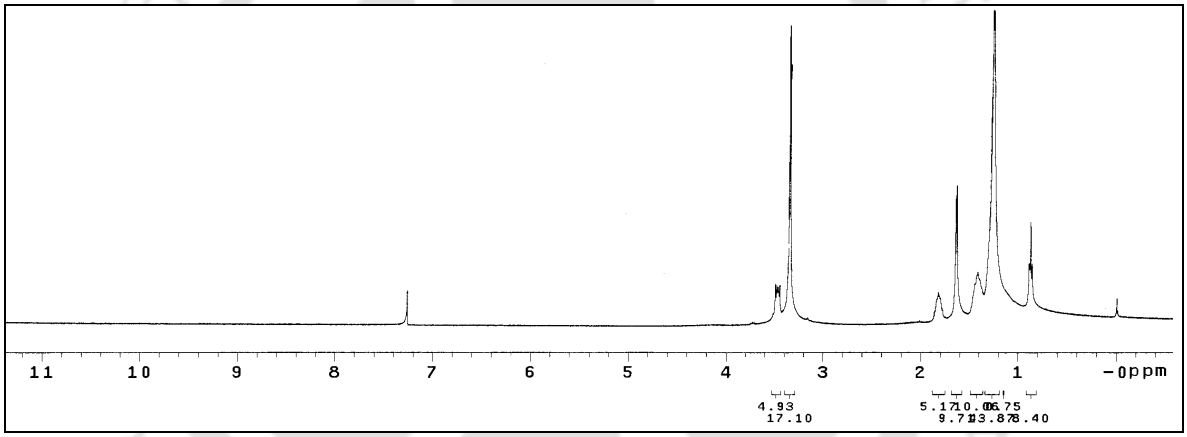

Figure 4.S2 ^{1}H NMR spectrum of CTMATB

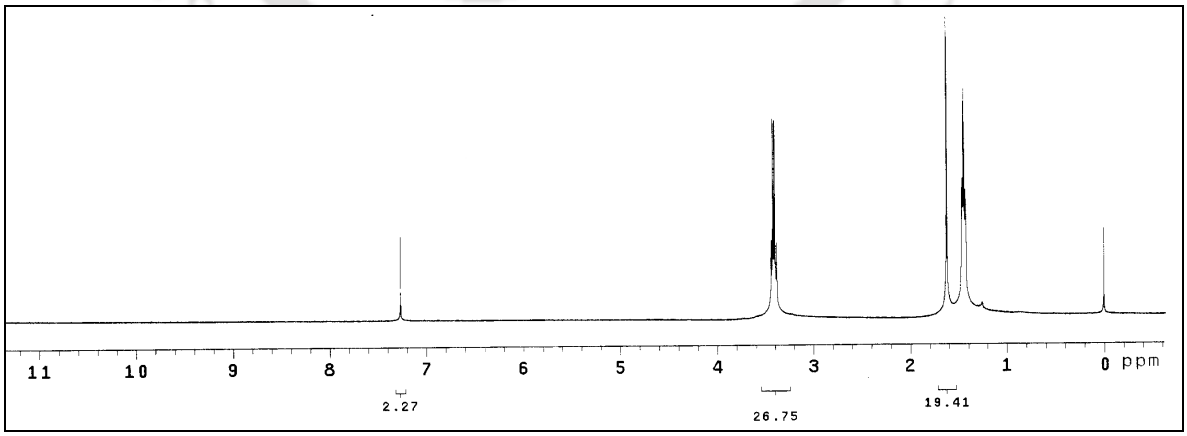

Figure 4.S3 ^{1}H NMR spectrum of TEATB

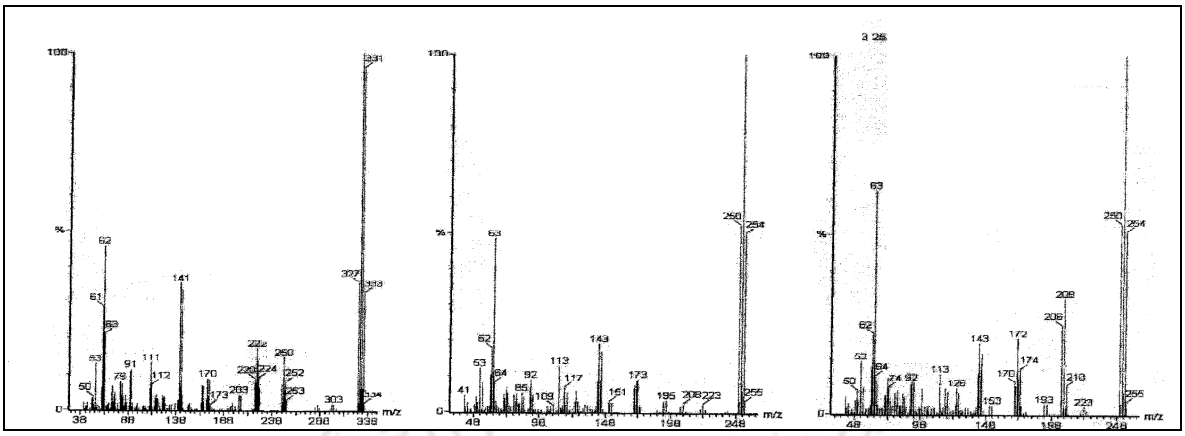

Figure 4.S4 GCMS chromatogram of the reaction mixture of bromination reaction

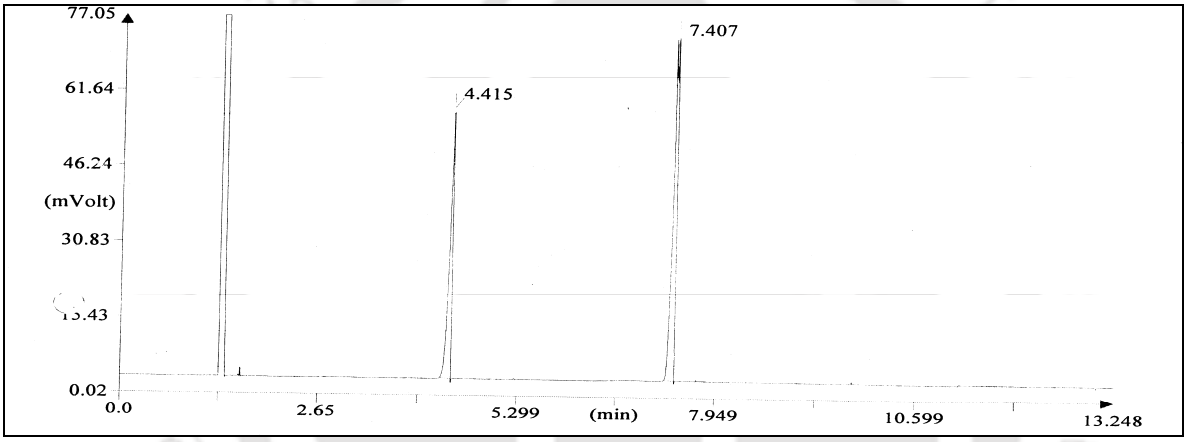

Figure 4.S4 GC chromatogram of another reaction mixture of bromination reaction

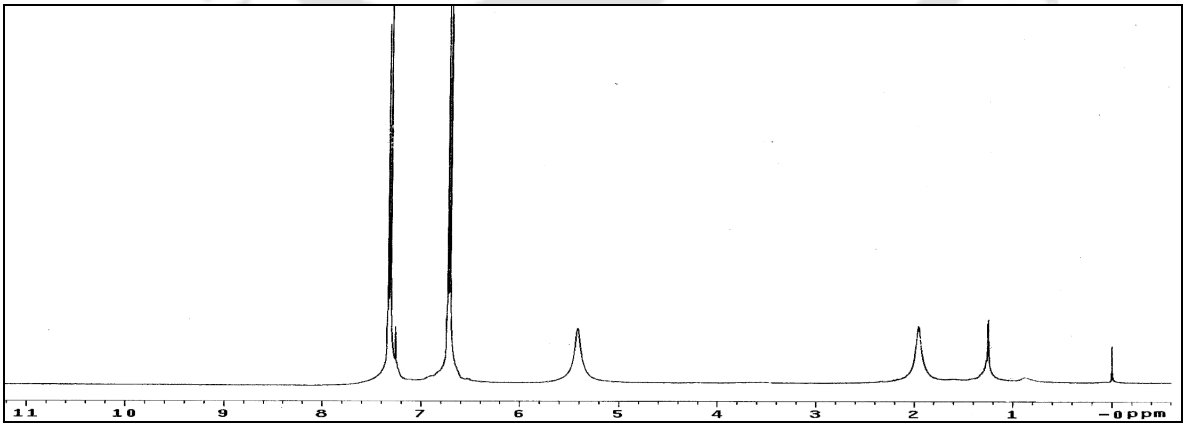

Figure 4.S1 ^{1}H NMR spectrum of p-bromophenol

Development of Newer Solid Acid Catalysts for Organic Transformations

The growing interest in heterogeneous catalysts is due to their advantages over others, such as (i) good dispersion of active sites, (ii) constraints of the pores, (iii) easier and safer to handle, (iv) easier to remove from the reaction mixture and (v) reusability [1]. However, majority of fine and pharmaceutical chemicals processes rely on homogeneous reagents and catalysts due to lack of efficient heterogeneous catalyst. Among heterogeneous catalysts, solid acids have been the subject of the most detailed and extensive studies. They have been used in important large-scale industrial processes such as alkylation, catalytic cracking, paraffin isomerization and many others [1, 2]. They have been introduced mainly to replace highly corrosive mineral acids in reaction medium and to catalyze the reaction. In this regard, solids with protonic acids adsorbed on supports are most promising example. Alumina and titania have been widely studied as catalyst's supports, also used as catalysts in various organic reactions [3]. The surface properties of these are mainly responsible for their functionality [4].

Phosphoric acid based solid acid catalysts have shown excellent performance in industrially important acid-demanding reactions [5]. Generally, metal oxide is considered as the supporting phase for "solid-phosphoric acid". Alumina and titania have been widely used as supporting phase, because phosphates stabilize their oxide phases and modify the acid-base properties [6,7]. Catalytic properties like stabilization of surface area, crystal phase, and improvement in surface acidity and porosity have been found to be enhanced by incorporation of phosphate ion in alumina or titania [8,9].

Nitration of aromatic compounds is a ubiquitous reaction [10]. Nitroaromatic compounds are widely studied because of their applications as solvents, dyes, pharmaceuticals, perfumes, agrochemicals, explosives and plastics in industries. The nitro derivatives of xylene isomers are used as intermediates for the production of vitamins, agrochemicals, fragrance and dyes. The conventional nitration process [11], employing a nitrating mixture of nitric and sulfuric acid, for the last 150 years has remained unchallenged in the commercial arena owing to uneconomical alternative options. The disadvantages of classical nitration methodology include corrosive nitrating reagents, formation of environmentally unfriendly waste that is expensive to dispose off, over nitration, poor selectivity and oxidation of by-products. In order to overcome difficulties, researchers have introduced a number of reagents and catalysts,

for instance, acetyl nitrate, benzoyl nitrate, trimethylsilyl nitrate [12], N-nitropyridinium salts, nitrogen oxide, P_2O_5/silica gel [13], mixed metal oxide [14], lanthanide reagents [15], $NaHSO_4.H_2O$, $Mg(HSO_4)_2$, Oxone®[16], $Bi(NO_3)_3.5H_2O$ [17], $VO(NO_3)_2$ [18], $Fe(NO_3)_3 9H_2O$,[19] $(Me_4N)NO_3$ [20], $Mg(NO_3)6H_2O$[21] and $NaNO_3$[22]. Each method has some advantages over the others. Contemporarily, solid acids have also been developed for nitration reactions and it has been found that they are more effective than other catalyst or reagents [23]. Solid acids effectively play the role of sulfuric acid in the reaction, assisting the formation of nitronium species.

Beside the nitroaromatic compounds, sulfoxides are also very useful synthetic intermediates for the construction of various chemically and biologically active molecules including therapeutic agents such as antiulcer, antibacterial, antifungal, anti-athrosclertic, antihypertensive [24]. Thus, selective oxidation of sulfides has received continued attention leading to the development of a number of reagents [25-27], acids [28] transition metal catalysts like titanium [29-32], vanadium[33], iron[34], molybdenum [35], tungsten [36], manganese [37], copper [38], and zeolite based catalysts [39, 40], to mention a few. While all these are important developments, there are several difficulties associated with the protocols being used in practice, *viz.*, non selectivity, over oxidation, cost effectiveness and toxicity of catalyst. In view of the above, research in this area continues in the quest of newer catalysts and protocols for selective sulfoxidation under easy operational conditions. A great variety of titanium containing catalysts was tested for sufoxidation reaction with better efficiency as well as selectivity [29]. Of particular relevance here is the titanium based zeolite catalysts. Ti-containing micro and mesoporous zeolite catalysts such as TS-1 [41], TS-2 [39b], Ti-β[42], Ti-MCM-41 [43], Ti-HMS [44], and Ti-MMM [45] have been used for oxidation of organic sulfides.

As a sequel to our sustained interest in the development of newer catalysts and catalytic protocols for organic transformations, in the present Ph.D. research, we have developed two newer solid acid catalysts. In this Chapter, indeed concluding Chapter, preparation and characterization of these catalysts have been discussed. Also reported herein are the results obtained from catalytic nitration of organic compounds and oxidation of organic sulfides to sulfoxide.

5.1 Experimental

The sources of chemicals and solvents, the methods for quantitative determination of elements and the details of all the equipment used for physico-chemical studies have been described in **Chapter 2**.

(a) Preparation of Catalyst-A, $Al(H_2PO_4)_3$

The catalyst was prepared by taking a mixture of alumina (neutral) (Loba Chemie, India) and phosphoric acid (96%) (E. Merck) in a silica boat maintaining the molar ratio of Al: H_3PO_4 as 1: 3 and heating at 200-220^{0}C on a hot sand bath. The mixture was stirred at the stipulated temperature until the swampy mass solidified and then the temperature was reduced to around 100^{0}C. The whole was then placed in a vacuum desiccator and cooled to ambient temperature. The catalyst thus prepared was finally transferred and stored in an air tight sample vial.

(b) Preparation of Catalyst-T, $(TiO_2)_{5.45}[Ti_4H_{11}(PO_4)_9].4\ H_2O$

The catalyst was prepared by first mixing titania with phosphoric acid (88%), in the molar ratio of TiO_2 : H_3PO_4 as 1 : 1, in a silica boat followed by heating at 200-220 ^{0}C on a hot sand bath under stirring until the mass solidified. Heating was then discontinued and when the temperature came down to ca. 100 ^{0}C, the catalyst was transferred to a vacuum desiccator. Finally the catalyst was stored in an airtight sample vial.

(c) General experimental procedure for nitration reaction catalyzed by catalyst-A,

In a typical experiment, to a round-bottomed flask containing a stirring mixture of the catalyst-A (0.03 mmol, 0.5 mol%) and nitric acid (70%)(9 mmol, 0.81 mL), the bromobenzene (6 mmol, 0.628 mL) was added and stirred at room temperature. The reaction was monitored by TLC. After completion of the reaction, the reaction mixture was extracted with ethyl acetate and washed with 5% aqueous solution of sodium bicarbonate (2.5 mL) followed by water (5 ml) and dried with anhydrous sodium sulphate. Evaporation of the solvent followed by column chromatography of the crude mixture on silica gel using *n*-hexane and ethyl acetate (95:5) as eluent gave pure products viz 2-nitro bromobenzene and 4-nitro bromobenzene in 25: 75 ratio with overall yield 75%. In cases of solid substrates, acetonitrile (3-5mL) was used as the solvent.

(d) General experimental procedure for nitration reaction catalyzed by catalyst-T

To a round-bottomed flask containing a stirred mixture of the catalyst (composed of 84.5% of TiO_2 and 15.5% of $[Ti_4H_{11}(PO_4)_9].n\ H_2O$(n =1-4)) (0.03 mmol, 0.01 g, 0.5 mol%) and nitric acid (70%) (9 mmol, 0.81 mL), toluene (6 mmol, 0. 0.628 mL) was added at room temperature. The reaction was monitored by TLC. On completion of reaction, the product was extracted with ethyl acetate, washed sequentially with 5% aqueous solution of sodium bicarbonate (2.5mL), and water (5mL), and then dried with anhydrous Na_2SO_4. Evaporation of the solvent followed by column chromatography of the crude mixture on silica gel using *n*-hexane and ethyl acetate (95:5) as eluent, afforded 2-nitro toluene and 4-nitro toluene in the ratio 48 : 52 in pure form. The overall yield was 87%. In cases of solid substrates, acetonitrile (3-5mL) was used as the solvent.

(e) General experimental procedure for catalytic sulfoxidation reaction

In a typical experiment, to a round-bottomed flask containing a mixture of the catalyst (0.02 mmol, 1 mol%) and hydrogen peroxide (50%) (3 mmol, 0.204 mL) or nitric acid (70%) (3 mmol, 0.27 mL) in 3 mL of solvent, benzyl phenyl sulfide (2 mmol, 0.2 g) was added and stirred at room temperature for the time period specified in Table 1. While methanol was used as the solvent for hydrogen peroxide, acetonitrile was used for nitric acid oxidations. The reaction was monitored by TLC. After completion of the reaction, the product was extracted with ethyl acetate and washed with 5% aqueous solution of sodium bicarbonate (2.5 mL) followed by water (5 mL) in the cases of nitric acid oxidations, whereas for those of the hydrogen peroxide oxidation washing with water alone was done. The ethyl acetate extract was dried with anhydrous Na_2SO_4. Evaporation of solvent followed by column chromatography on silica gel using n-hexane and ethyl acetate (95:5) as eluent afforded the corresponding sulfoxide and sulfone in the ratio 95:5 and 98:2, respectively, for hydrogen peroxide and nitric acid with the overall yields of 85% and 90%.

5.2 Results and Discussion

5.2.1 Preparation and characterization of catalysts

(a) Catalyst – A, $Al(H_2PO_4)_3$

The catalyst-A was synthesized by heating alumina and phosphoric acid in the specific molar ratio. It was stored in vacuum desiccator as it is hygroscopic. The elemental analysis of the catalyst resulted in 8.16 % of Al (calc. 8.5%) and 85.6% of PO_4^{3-} (calc. 89.6%).

The catalyst exhibited characteristic spectral patterns in the IR region showing the presence of phosphate (Figure 5.1). The strong but broad peak at ca. 1127 cm^{-1} is assigned to ν_{P-O} and another peak at 989 cm^{-1} is attributable to ν_{Al-O-P} vibration [46]. Additionally, peaks observed at 3500-3300 cm^{-1} and 1634 cm^{-1} correspond to ν_{O-H} and δ_{H-O-H} modes of vibration of water. A clear difference can be observed from the figures (a) and (b).

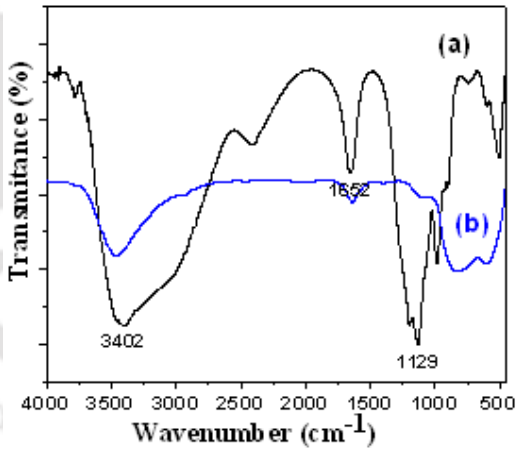

Figures 5.1 *FTIR spectrum of (a) Catalyst- A (black line) and (b) Al_2O_3 (blue line).*

The powder X-ray diffraction patters of commercial alumina and the catalyst is shown in Figure 5.2. It has been found that the pattern of the catalyst matched well with the pattern of aluminum trishydrogen phosphate [47].

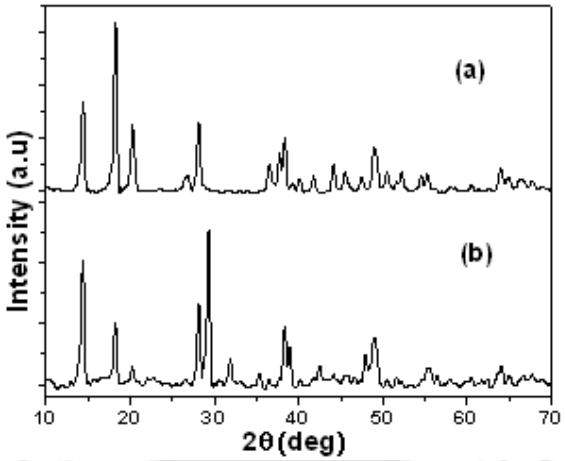

Figures 5.2 *XRD patterns of (a) commercial Al_2O_3 and (b) Catalyst- A*

The TGA curve of the catalyst is presented in Figure 5.3. The data indicated that after initial dehydration, the catalyst looses two water molecules from the molecular composition. The corresponding weight loss of 9.8 % observed between the temperatures 475-550 ^{0}C is in good agreement with the calculated value of 11.0% of the catalyst. Afterward the catalyst looses weight continuously upto 950 ^{0}C which is attributable to complete loss of water from the molecular composition leading to $Al_2O_3.P_2O_5$.

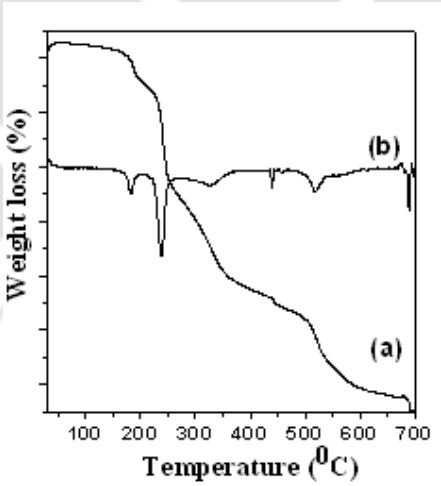

Figures 5.3 *(a) Thermo gravimetric (TG) and (b) DTG profiles of Catalyst- A.*

Scanning electron microscopy was used to investigate the morphological changes occurring in the surface. Unfortunately due to hygroscopic nature of the catalyst, we could not obtain a clear micrograph, however, macrospores were observed

throughout the catalyst due to the aggregation [Figures 5.4(a) and (b)]. The EDAX analysis gave a qualitative composition of the catalyst that was in good agreement with the elemental analysis values.

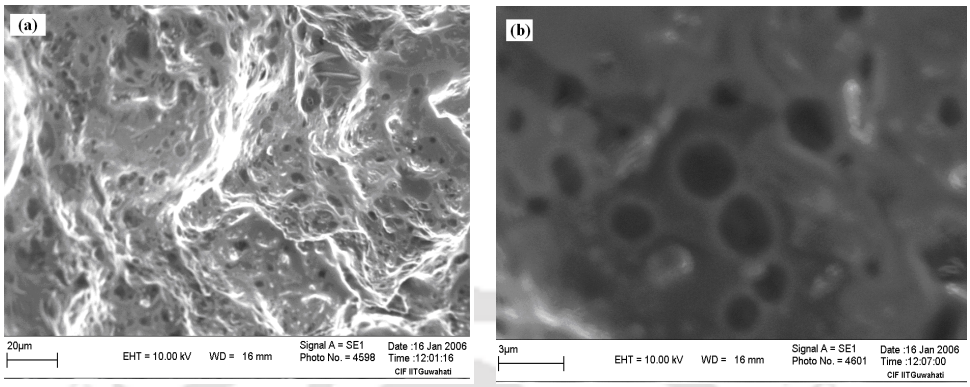

Figures 5.4 *Scanning Electron Micrographs of Catalyst- A in different magnifications viz. (a) 20 µm and (b)3 µm.*

(b) Catalyst-T, $(TiO_2)_{5.45}[Ti_4H_{11}(PO_4)_9].4\ H_2O$

The IR spectrum of the catalyst-T [Figure 5.5] shows a strong but broad peak at ca. 1230 cm^{-1} and broad weak peaks in the region 700-600 cm^{-1}, which are typical of $\nu_{P\text{-}O}$ stretching and $\delta_{O\text{-}P\text{-}O}$ bending vibrations, respectively [46]. The broad peaks at 700-600 cm^{-1} have resulted from a lowering of the symmetry of free PO_4^{3-} due to its binding [8, 9] to the titania surface. Additionally, the two peaks observed at 3375 cm^{-1} and 1635 cm^{-1} correspond respectively to $\nu_{O\text{-}H}$ and $\delta_{H\text{-}O\text{-}H}$ modes of vibration of water.

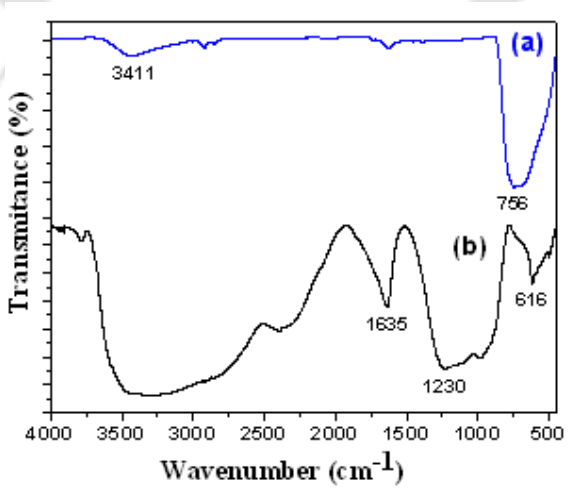

Figures 5.5 *FTIR spectra of (a) TiO_2 (blue line) and (b) Catalyst- T (black line).*

The XRD patterns of the catalyst and a fresh sample of TiO_2 are shown in Figure 5.6. The diffraction patterns reveal the presence of the anatase phase of TiO_2 [48] along with a new species, $[Ti_4H_{11}(PO_4)_9].n\ H_2O(n = 1\text{-}4)$ [49] present in the ratio of 84.5% : 15.5%, as determined by Klug's equation for semiqualitative analysis [50]. The results of chemical determination of Ti (calc. 28.96, found 28.2%) and PO_4^{3-} (calc. 54.59, found 53.1%) support the composition. The average crystallite size of a fresh sample of titania as well as that of the catalyst was calculated from the XRD patterns using Scherrer's equation [51]. The crystallite sizes of the former and TiO_2 present in the catalyst were found to be 62.15 nm and 41.54 nm, respectively. This indicates that phospahate has not only stabilized the anatase phase of TiO_2 in the catalyst but has also caused lowering of its crystallite size. The crystallite size of $[Ti_4H_{11}(PO_4)_9]xH_2O(x=1\text{-}4)$ was found to be 20.15 nm. It appears that $[Ti_4H_{11}(PO_4)_9].\ n\ H_2O(n = 1\text{-}4)$ is physically adsorbed by TiO_2 and held by van der Waal forces and hydrogen bonding.

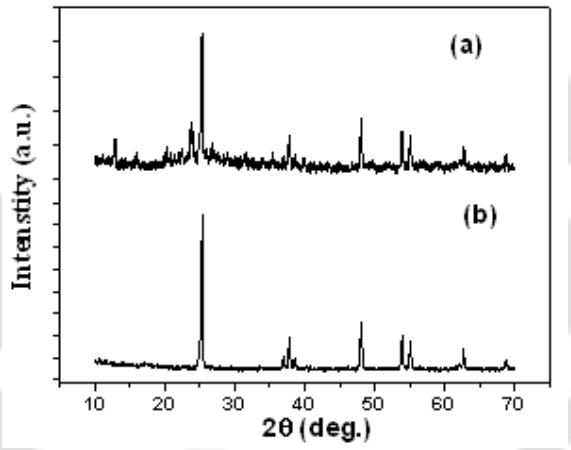

Figures 5.6 *XRD patterns of (a) Catalyst- T and (b) commercial TiO_2.*

The thermogram (TG) of the catalyst [Figure 5.7] shows weight losses in steps. The loss of weight between 40 ^{0}C and 110 ^{0}C corresponds to the loss of loosely bound water. The second weight loss occurring between 174 ^{0}C and 281 ^{0}C, and the subsequent loss at >620 ^{0}C have been assigned to the loss of water drawn from the molecular composition, finally leading to TiP_2O_7, as ascertained from XRD analysis.

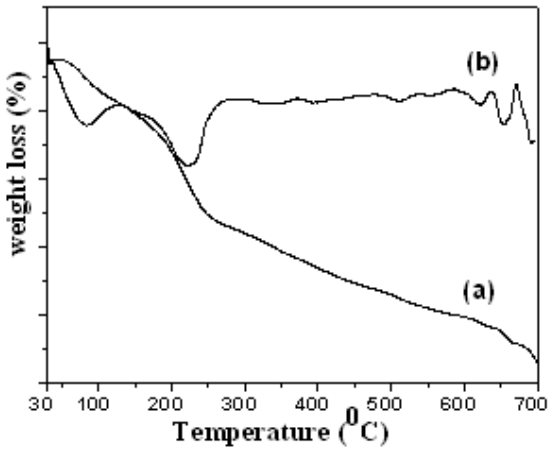

Figures 5.7 *(a) Thermo gravimetric (TG) and (b) DTG profiles of Catalyst- T.*

The BET surface areas of TiO_2 and the catalyst have been found to be 9.793 m^2/g and 5.387 m^2/g respectively and with the corresponding the pore volume being 0.0373 mL/g and 0.0410 mL/g. The calculated desorption and adsorption BJH pore size distributions [52] are set out in Table 5.1. It is evident from the result that there are no significant changes in the suface area and pore volume in going from a fresh sample of TiO_2 to the catalyst. However, desorption pore size above 80 nm appears to be reduced approximately by 10%.

Table 5.1 Desorption and adsorption of pore volume of TiO_2 and Catalyst-T

Pore Diameter Range (nm)	Desorption pore volume (%)		Adsorption Pore volume (%)	
	TiO_2	Catalyst	TiO_2	Catalyst
Below 6	5.23	7.89	6.89	6.12
6-8	3.27	3.27	3.77	3.04
8-10	2.04	1.95	2.24	1.75
10-12	2.53	2.58	2.72	2.00
12-16	3.54	3.77	3.33	2.43
16-20	4.50	5.90	4.01	3.06
20-80	49.91	58.37	38.50	40.99
Over 80	28.97	16.27	38.55	40.61
Total	100.00	100.00	100.00	100.00

The scanning electron micrograph of the catalyst-T [Figures 5.8 (a) and (b)] showed an ordered morphology, with the average particle size being 1 μm. A comparison of this with that of the fresh sample of TiO_2 reveals an enhancement of particle size in the case of the catalyst. The EDAX results agree with the composition of the catalyst. Finally we believe that the new species, $[Ti_4H_{11}(PO_4)_9]$, in conjunction with the stabilized anatase phase of TiO_2 present in the catalyst, is responsible for the observed activity.

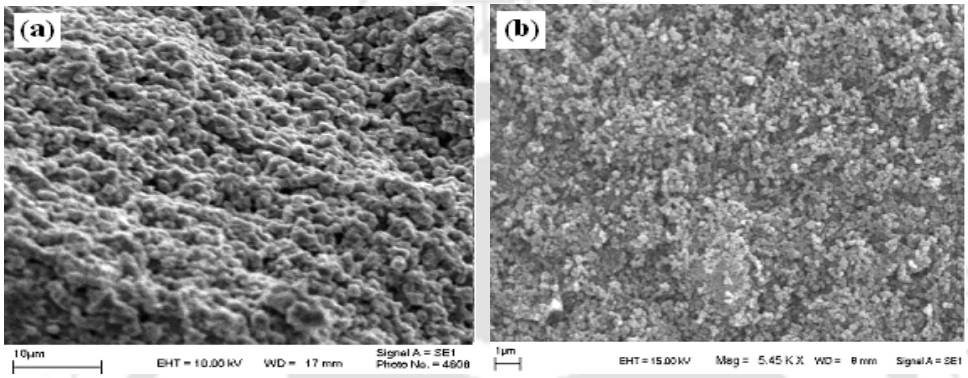

Figures 5.8 *Scanning Electron Micrographs of (a) Catalyst- T with magnification of 10 μm and (b) pure TiO_2 with 1 μm magnification.*

5.2.2 Nitration of organic compounds with nitric acid

One of our major concerns was to examine the efficacy of the catalysts for organic reactions. Here nitration of aromatic compounds has been studied. A great variety of aromatic compounds has been efficiently nitrated with nitric acid in presence of Catalyst-A and Catalyst-T separately and the results obtained are shown in Table 5.2. While the column 3 of Table 5.2 represents the isolated yield and reaction time for Catalyst-A, the same for Catalyst-T have been shown in Column 4.

In order to ascertain the optimum condition, several reaction runs were carried out on bromobenzene as a model substrate. An amount of 0.5 mol% of the catalyst-A or 0.3 mol% for the catalyst-T and 1.5 equiv. of HNO_3 were found to be conducive to the reaction.

Having established the reaction conditions, a number of reactions were carried out with a variety of aromatic compounds. As evident, aromatic compounds having electron donating group (Table 5.2, entries 2, 3, 4, 5, 13 and 14) readily underwent

nitration in excellent yields. Also, deactivated aromatic compounds underwent nitration in good yields (Table 5.2, entries 6 and 7), however, with a relatively longer time. Notably, polyaromatic hydrocarbons such as naphthalene, anthracene, phenanthrene (Table 5.2, entries 8, 9 and 10) underwent smooth and regioselective nitrations under the same experimental condition. It is pertinent to mention that nitropolyaromatic hydrocarbons are important as intermediate for the synthesis of anti-tumor agents [53] but such nitrations are rather tedious. Interestingly, with substrate amenable to facile oxidation, the protocol prefers oxidation. Thus the reaction of benzaldehyde (Table 5.2, entry 16) provided benzoic acid whereas 2-hydroxy benzaldehyde (Table 5.2, entry 17) and 2,4-dihydroxy benzaldehyde (Table 5.2, entry 18) underwent nitration. The reason for nitration of these substrates may be attributed to involvement of intra and intermolecular hydrogen bonding thereby rendering the aldehyde group relatively less responsive to oxidation. In addition, the presence of hydroxy group activates the ring further facilitating nitration, as observed. Similarly, the reaction of phenyl methyl sulfide (Table 5.2, entry 19) provided the corresponding sulfoxide quantitatively whereas dibenzothiophene (DBT) (Table 5.2, entry 20) and pyridine (Table 5.2, entry 21) afforded both nitrated and oxidized products.

In control experiments, reactions were conducted separately with catalytic amounts of (a) alumina, (b) titania and (c) phosphoric acid. The conversion in each case was comparatively far less. Therefore, it is clear that neither of them is effective to forward the desired reaction (Table 5.3).

Upon completion of reaction, recycleability of the catalysts was examined by evaporating the aqueous layer after conducting the reaction with toluene. The catalysts were heated at 200-220 ^{0}C for 30 min and then reused. The results are summarized in Table 5.4. It is evident that the catalyst worked well up to the third cycle; thereafter, the yield started decreasing because of leaching of the catalyst (Table 5.3).

Table 5.2 Catalyst- A and Catalyst-T catalyzed nitration of organic compounds

Entry	Substrate	Catalyst-A Time/Yield (min/%)	Catalyst-T Time/Yield (min/%)	Product	Product Code
1		5/85	5/86	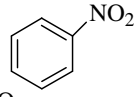	**1**
2	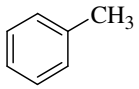	3/90	5/93	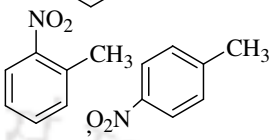	**2a, 2b**
3	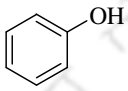	2/88	2/90	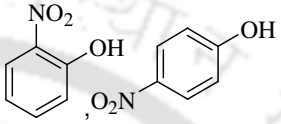	**3a, 3b**
4	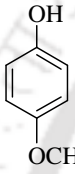	5/82	5/90	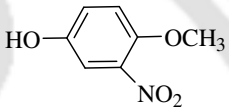	**4**
5	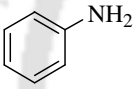	10/45	10/43	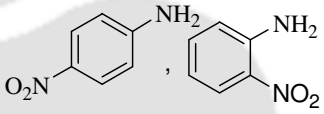	**5a, 5b**
6	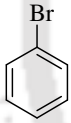	40/70	90/70	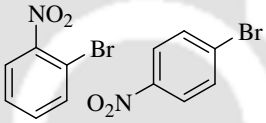	**6a, 6b**
7	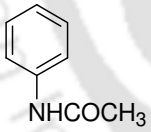	12h/80	12h/80	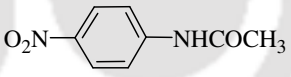	**7**
8	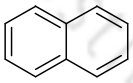	25/76	25/80	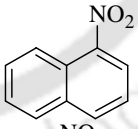	**8**
9	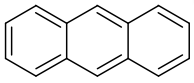	20/80	10/85	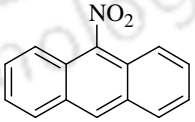	**9**
10	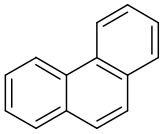	90/63	90/65	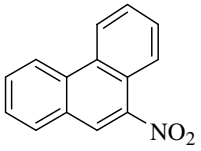	**10**

11	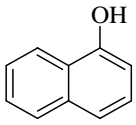	25/73	30/75	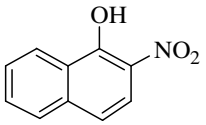	**11**
12	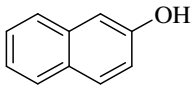	25/60	30/62	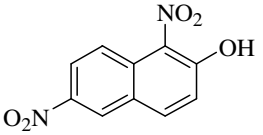	**12**
13	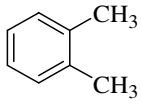	10/85	10/87	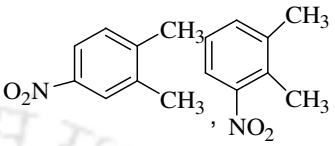	**13a, 13b**
14	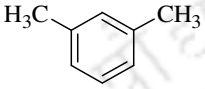	10/90	10/90	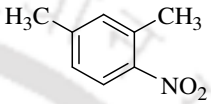	**14**
15	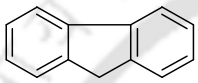	15/90	15/85	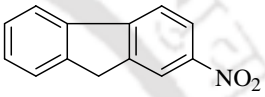	**15**
16	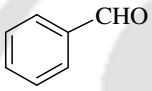	50/57	50/65	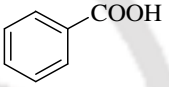	**16**
17	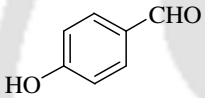	30/80	30/85	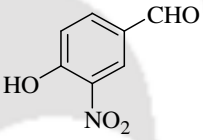	**17**
18	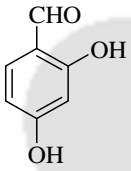	25/60	25/65	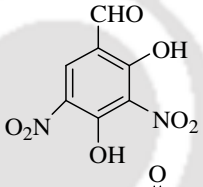	**18**
19	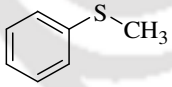	5/98	5/98	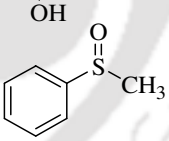	**19**
20	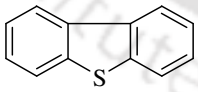	25/60	25/75	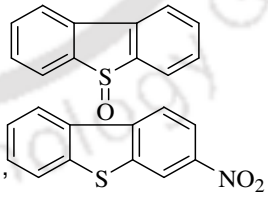	**20a, 20b**
21		12h/35	12h/40	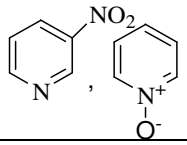	**21a, 21b**

Table 5.3 Control reactions of bromobenzene with catalytic amount of alumina, titania and phosphoric acid

Entry	Catalyst	Time (h)	Conversion (%)	Yield (%)
1	Al_2O_3	12	70	65
2	TiO_2	12	60	55
3	H_3PO_4	12	85	70

Table 5.4 Efficacy of recycled catalysts in the reaction with toluene

Run	Catalyst-A		Catalyst-T	
	Time (min)	Yield (%)	Time (min)	Yield (%)
1	3	90	5	93
2	15	80	15	85
3	35	72	35	78
4	50	60	50	62
5	80	55	80	58

It is well known that aromatic nitration is a classical electrophilic substitution involving an attack by nitronium ion (NO_2^+). Here we have presented a plausible mechanism for the nitration reaction with the catalytic cycle.

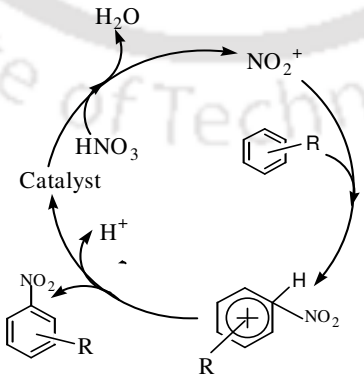

Figure 5.9 Plausible mechanism for nitration

5.2.3 Phosphate impregnated titania (catalyst-T) catalyzed chemoselective sulfoxidation of organic sulfides with hydrogen peroxide or nitric acid

Based upon the results of trial runs, the reaction conditions were optimized with 1 mol% of the catalyst and 1.5 mmol of oxidant against 1 mmol of benzyl phenyl sulfide either in acetonitrile for HNO_3 or in methanol in the case of H_2O_2. Whereas acetonitrile was found to work well for HNO_3, methanol appeared to be a better solvent for the H_2O_2 oxidations. Coordination of alcohol to the active site of titanium (*c.f.* Alkoxy-Ti) presumably increases the electrophilicity of the coordinated peroxy oxygen atom thereby favoring the nucleophilic attack of the organic substrate; ultimately facilitating the overall oxidation [54]. The inherent acidity of the catalyst might have further enhanced the reactivity.

Structurally diverse sulfides were subjected to oxidation under the optimized reaction conditions and the results are summarized in Table 5.5. Evidently, both the oxidants worked well though HNO_3 appeared to be comparatively better in terms of both selectivity as well as efficiency (Table 1). The reagent systems chemoselectively oxidize sulfides in presence of other oxidation prone functional groups such as -CN, -C=C-, -CHO, -OH (Table 1, entries 2, 4, 9 and 10). The protocol works efficiently in oxidizing 2-(benzylthio)benzothiazole to afford the exocyclic sulfoxide (Table 1, entry 11). Notably, neither sulphur or nitrogen in the heterocycle ring nor the benzylic position was affected in the process. Importantly, this product is comparatively easily biodegradable than the substrate [55]. Glycosyl sulfide was easily oxidized to the corresponding sulfoxide (Table 1, entry 14), which is used in chemical glycosylation [56].

Though the oxidation of refractory sulfides is rather difficult, the present protocol, however, oxidizes dibenzothiophene (DBT) (Table 1, entry 15) and mono and disubstituted DBT's (Table 1, entries 16 and 17) with reasonably good success. The ease of oxidation followed the expected trend, viz. DBT > 4-methyl DBT > 4, 6-dimethyl DBT. Steric crowding on the disubstituted DBT restricting the approach of the active oxidant to sulfur is attributed to the difficulty in its oxidation. The presence of a very small amount of nitrated product was detected in each of these cases when HNO_3 was the oxidant.

Table 5.5 Sulfoxidation of organic sulfides with H_2O_2 and HNO_3

Entry	Substrate	H_2O_2		HNO_3		Product code
		Time (h)	Yield (%)[a] SO:SO_2	Time (min)	Yield (%)[a] SO:SO_2	
1	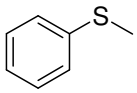	0.8	98 (95:5)	5	99 (100:0)	**19**
2	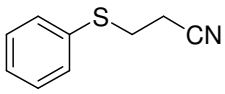	6	73 (85:15)	20	70 (90:10)	**22**
3	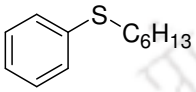	10	90 (98:2)	10	95 (100:0)	**23**
4	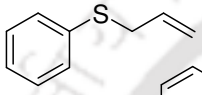	9	70 (85:15)	20	65 (95:5)	**24**
5	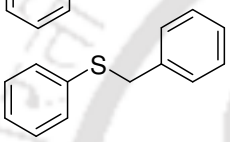	8, 12d	85, 88[d] (95:5)	45, 60d	90, 92[d] (98:2)	**25**
6	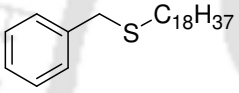	13	75 (95:5)	45	90 (100:0)	**26**
7	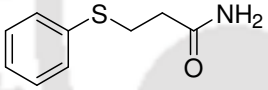	10	85 (85:15)	60	90 (98:2)	**27**
8	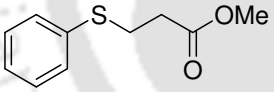	10	78 (90:10)	55	92 (98:2)	**28**
9	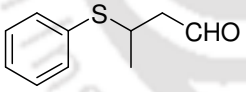	2	65 (85:15)	30	58 (95:5)	**29**
10	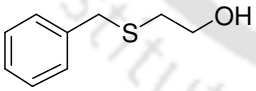	3	73 (90:10)	30	50 (95:5)	**30**
11	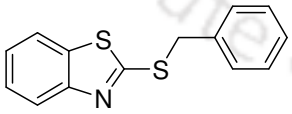	10	85 (79:21)	20	90 (100:0)	**31**
12	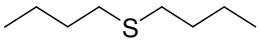	7	90 (72:28)	15	95 (100:0)	**32**
13		0.25	99 (20:80)	15	99 (95:5)	**33**

14	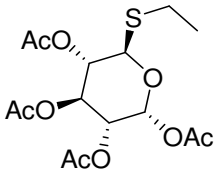	6	90 (95:5)	20	65 (95:5)	**34**
15	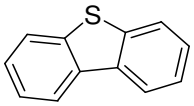	12	84 (75:25)	30	90 (100:0)c	**20a**
16	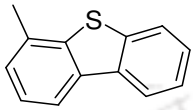	24	77 (75:25)	90	65 (100:0)c	**35**
17	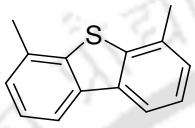	42	35 (80:20)	360	30 (100:0)c	**36**

[a] *Isolated yield,* [b] *Reaction was carried out at 0* ^{0}*C,*
[c] *nitrated product was observed along with sulfoxide,* [d] *reaction in 5 g scale*

The comparative reactivity of sulfide and the corresponding sulfoxide was also studied to ensure the selectivity of the catalyst (Table 2). The sulfides are more reactive than sulfoxides. The more reactive sulfide competes with the sulfoxide thereby resulting in a very low yield of sulfone.

Table 5.6 Comparative reactivity of benzyl phenyl sulfide and sulfoxide

Entry	Substrate	H_2O_2		HNO_3	
		Time (h)	$SO:SO_2$	Time (min)	$SO:SO_2$
1	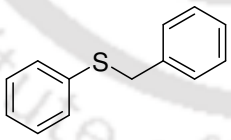	8	95:5	45	98:2
2	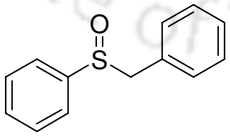	24	25:75	80	15:85
3	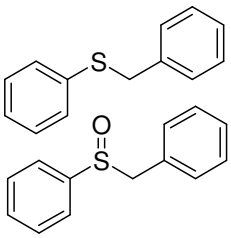	8	91:9	45	98:2

Though hydrogen peroxide and nitric acid can themselves oxidize benzyl phenyl sulfides (Table 5.7, entries 1 and 2), reactions are sluggish, thereby demanding the need of catalyst for the activation.

Table 5.7 Oxidation of benzyl phenyl sulfides with H_2O_2 and HNO_3

Entry	Reagent	Time (h)	Yield (%)
1	H_2O_2	36	25
2	HNO_3	3	65

In separate experiments, evaluation of the catalyst and its analogs were done to ensure the efficiency of the catalyst over the others and the results are presented in Table 5.8. These observations suggest that neither titania nor phosphoric acid alone is very effective to forward the desired reaction.

Table 5.8 Oxidation of benzyl phenyl sulfide with different catalyst

Entry	Catalyst	H_2O_2		HNO_3	
		Time (h)	Yield (%)	Time (min)	Yield (%)
1	TiO_2	36	65	120	75
2	H_3PO_4	17	70	90	76
3	Catalyst	8	85	45	90

From the preparative point of view, it is noteworthy that the catalyst can be efficiently recovered by evaporating the aqueous layer and then recharging by heating on silica boat at 200-220 ^{0}C for 30 min. Indeed, the catalyst was reused with benzyl phenyl sulfide for at least four reaction cycles with consistent activity and selectivity. The reaction can be scaled up (5 g) to give good yield (Table 5.5, entry 5) showing its prospect for preparative scale applications.

In order to evaluate the efficiency of the catalyst, we have compared the reaction of methyl phenyl sulfide and H_2O_2 with those of a few other titanium containing catalysts (Table 5). It is clear from the results that although the yields are similar, the reaction time in the present case is shorter and the selectivity is better than

the others. In addition, the chemoselectivity appears to be relatively higher than its companion catalysts.

Table 5.9 Comparison of the catalyst with other titanium based catalysts in terms of efficiency and selectivity of methyl phenyl sulfide oxidation with H_2O_2

Catalyst	Solvent	Temp (^{0}C)	Time [h]	Yield (%)	Ratio [SO:SO_2]	Ref.
TS-1	Acetone	Reflux	2.5	98	-	40
TS-2	Acetone	Reflux	2.5	98	78:22	32
Ti-β	Acetone	RT	2	85	-	33
Ti-MCM-41	Acetonitrile	RT	5	99	83:17	40b
Ti(IV)-glycolate	-	RT	2	71	86:14	30b
TiO_2-$VO(acac)_2$	DCM	RT	1.5	99	97:3	54
Present-catalyst	MeOH	RT	0.8	98	95:5	-

5.3 Conclusions

Two heterogeneous catalysts have been developed by control heating and kneading of alumina or titania with phosphoric acid at a range of temperature 200-220^{0}C. With the specified molar ratio, this process resulted in the formation of $Al(H_2PO_4)_3$, **Catalyst-A** and $(TiO_2)_{5.45}[Ti_4H_{11}(PO_4)_9].4\ H_2O$, **Catalyst-T** with alumina and titania, respectively. Incorporation of phosphate in alumina increases its surface acidity of both alumina and titania.

These newly developed heterogeneous catalysts have been used for nitration of various aromatic compounds with nitric acid. Both the catalysts seemed to be equally efficient for the nitration; however, they oxidize the substrates amenable to oxidation. Avoidance of sulfuric acid is one of the most significant advantages of the present processes. In addition to the efficacy and ease of handling and operation, recycleability and scaleability render these protocols attractive and useful.

In addition, an efficient method for the selective oxidation of sulfides to sulfoxides under mild condition has been developed. A variety of organosulfur compounds have been selectively oxidized to the corresponding sulfoxides by either H_2O_2 or HNO_3 using the **Catalyst-T**. The catalyst-nitric acid system oxidizes simple alkyl or aryl sulfides more efficiently and selectively than the catalyst-hydrogen peroxide system. However, latter one is preferable from the environmental point of view. These processes chemoselectively oxidize sulfur in presence of a double bond, nitrile, alcohol, aldehyde, benzylic methylene and nitrogen or sulphur atom in a heterocyclic position. Applications to the refractory sulfurs and glycosyl sulfide make the catalytic protocols more generalized. Easy work up and separability are other important attributes of the protocol.

References

[1] Clark, J. H. *Catalysis of organic reactions by supported inorganic reagents*, VCH, New York, 1994.

[2] Clark, J. H. *Acc. Chem. Res*. **2002**, *35*, 791.

[3] Richardson, T. J. *Principles of Catalyst Development: Fundamental and Applied Catalysis*; Twigg, M. V.; Spencer, M. S. Eds., Plenum Press: New York, 1989.

[4] Samantaray, S. K.; Parida, K. M. *J. Mol. Catal. A: Chem.* **2001**, *176*, 151.

[5] Samantaray, S. K.; Mishra, T.; Parida, K. M. *J. Mol. Catal. A: Chem.* **2000**, *156*, 267.

[6] Basca, G.; Ramis, G.; Lorenzelli, V.; Rossi, P. F.; Ginestra, A. L.; Petrone, P. *Langmuir* **1989**, *5*, 917.

[7] Lewis, J. M.; Kydd, A. R. *J. Catal*. **1991**, *132*, 465.

[8] Parida, K. M.; Acharya, M.; Samantaray, S. K.; Mishra, T. *J. Colloid Interf. Sci.* **1999**, *217*, 388.

[9] Samantaray, S. K.; Parida, K. M. *J. Mat. Sci.* **2003**, *38*, 1835.

[10] Olah, G. A.; Malhotra, R.; Narang, S. C. *Nitration: Methods and Mechanisms*, VCH, New York, 1989.

[11] Schofield, K. *Aromatic Nitration*, Cambridge University Press, Cambridge, 1980.

[12] Iranpoor, N.; Firouzabadi, H.; Heydari, R. *Synth. Commun*. **1999**, *29*, 3295.

[13] (a) Radoslaw, R. B.; Andrew, J. S. *Tetrahedron Lett.* **2001**, *42*, 6767; (b) Iranpoor, N.; Firouzabadi, H.; Pourali, A. R. *Synth. Commun*. **2005**, *35,* 1517; (c) Rodriues, J. A. R.; Oliveira, A. P. F.; Moran, P. J. S.; Custodio, R. *Tetrahedron* **1999**, *25,* 6733; (d) Ramana, M. M. V.; Malik, S. S.; Parihar, J. A.; *Tetrahedron Lett*. **2004**, *45,* 8681; (e) Hajipour, A. R.; Ruoho, A. E. *Tetrahedron Lett.* **2005**, *46*, 8307.

[14] Chaubal, N. S.; Sawant, M. R. *Catal. Commun*. **2006**, *7*, 443.

[15] (a) Waller, F. J.; Barrett, A. G. M.; Braddock, D. C.; Ramparsad, D. *Chem.Commun.* **1997**, 613; (b) Waller, F. J.; Barrett, A. G. M.; Braddock, D. C.; Ramparsad, D. *Tetrahedron Lett*. **1998**, *39*, 1641; (c) Waller, F. J.; Barrett, A. G. M.; Braddock, D. C.; McKinnell, R. M.; Ramparsad, D. *J. Chem. Soc. Perkin Trans.1* **1999**, 867 ; (d) Shi, M.; Cui, S. C. *Chem. Commun*. **2002**, 994; (e) Parac-Vogt, T. N.; Binnemans, K. *Tetrahedron Lett.* **2004**, *45*, 3137.

[16] (a) Zolfigol, M. A.; Bagherzadeh, M.; Madrakian, E.; Ghaemi, E.; Taqian-nasab, A. *J. Chem. Res.(S)* **2001**, 140; (b) Zolfigol, M. A.; Madrakian, E.; Ghaemi, E. *Indian J. Chem.* **2001**, *40B*, 1191.

[17] Sun, H. B.; Hua, R.; Yin, Y. *J. Org. Chem*. **2005**, *70*, 9071.

[18] Dove, M. F.; Manz, B.; Montgomery, J.; Pattenden, G.; Wood, S. A. *J. Chem. Soc. Perkin Trans. 1* **1998**, 1589.

[19] Rajagopal, R.; Srinivasan, K. V. *Synth. Commun*. **2003**, *33*, 961.

[20] Shackelford, S. A.; Anderson, M. B.; Christie, L. C.; Goetzen, T.; Guzman, M. C.; Hananel, M. A.; Korneich, W. D.; Li, H.; Pathak, V. P.; Rabinovich, A. K.; Rajapakse, R. J.; Truesdale, L. K.; Tsank, S. M.; Vazir, H. N. *J. Org. Chem.* **2003**, *68*, 267.

[21] Zolfigol, M. A.; Ghaemi, E.; Madrakian, E. *Synth. Commun*. **2000**, *30*, 1689.

[22] Zolfigol, M. A.; Ghaemi, E.; Madrakian, E. *Molecules* **2001**, *6*, 614.

[23] (a) Riego, J. M.; Sadin, Z.; Zaldivar, J. M.; Marziano, N. C.; Tortato, C. *Tetrahedron Lett.* **1996**, *37,* 513; (b) Choudary, B. M.; Sateesh, M.; Kantam, M. L.; Rao, K. K.; Ramprasad, K. V.; Sarma, J. A. R. P. *Chem. Commun.* **2000**, 25; (c) Peng, X.; Suzuki, H.; Lu, C. *Tetrahedron Lett.* **2001**, *42, 4357*; (d) Esakkidurai, T.; Pitchumani, K. *J. Mol. Catal. A: Chem*. **2002**, *18* 5, 305; (e) Choudary, B. M.; Kantam, M. L.; Ramprasad, K. V. *US Pat.* **2003**, 6620981; (f) Patil, P. T.; Masle, K. M.; Dagade, S. P.; Dongare, M. K. *Catal. Commun*. **2003**, *44,* 29; (g) Sunajadevi, K. R.; Sugunan, S. *Catal. Commun.* **2005**, *6,* 611; (h) Sunajadevi, K. R.; Sugunan, S. *Materials Lett.* **2006**, *60,* 3813; (i) Iranpoor, N.; Firouzabadi, H.; Nourouzia, N.; Firouzabadi, D. *Tetrahedron Lett.* **2006**, *4,* 6879; (j) Chaubal, N. S.; Sawant, M. R. *Catal. Commun.* **2006**, *7,* 443; (k) Rao, G. R.; Rajkumar, T. *J. Colloids Interface Sci.* **2008**, *324,* 134; (l) Khder, A. S.; Ahmed, A. I. *App. Catal. A: Gen.* **2009**, *354*, 153 and references cited therein.

[24] Drabowski, J.; Kielbasinski, P.; Mikolajcyk, M.; *Synthesis of Sulfoxides*, Wiley, New York, 1994.

[25] Gomez, M. V.; Caballero, R.; Vazquez, E.; Moreno, A.; Hoz, A.; Diaz-Ortiz, A. *Green Chem*. **2007**, *9,* 331.

[26] (a) Selvam, J. J. P.; Suresh, V.; Rajesh, K.; Chanti Babu, D.; Suryakiran, N.; Venkateswarlu, Y. *Tetrahedron Lett.* **2008**, *49*, 3463; (b) For review on reagents for

sulfoxidation see: Kowalski, P.; Mitka, K.; Ossowskab, K.; Kolarska, Z. *Tetrahedron* **2005**, *61*, 1933.

[27] Kar, G.; Saikia, A. K.; Bora, U.; Dehury, S. K.; Chaudhuri, M. K. *Tetrahedron Lett.* **2003**, *44,* 4503.

[28] (a) Firouzabadi, H.; Iranpoor, N.; Jafari, A. A.; Riazymontazer, E. *Adv. Synth. Catal.* **2006**, *348*, 434; (b) Shukla, V. G.; Salgaonkar, P. D.; Akamanchi, K. G. *J. Org. Chem.* **2003**, *68*, 5422; (c) Kasai, J.; Nakagawa, Y.; Uchida, S.; Yamaguchi, K.; Mizuno, N. *Chem. Eur. J.* **2006**, *12*, 4176.

[29] For reviews on titanium based oxidation catalysts see: Corma, A. *Chem. Rev.* **1997**, *97,* 2373 and Kholdeeva, O. A.; Trukhan, T. N. *Russ. Chem. Rev*. **2006**, *75*, 411.

[30] (a) Rosa, M. D.; Lamberti, M.; Pellecchia, C.; Scettri, A.; Villano, R.; Soriente, A. *Tetrahedron Lett.* **2006**, *47*, 7233 ; (b) Massa, A.; Lorenzo, E. M. D.; Scettri, A. *J. Mol. Cat. A: Chem.* **2006**, *250*, 27; (c) Cimpeanu, V.; Hardacre, C.; Parvulescu, V. I.; Thompson, I. M. *Green Chem.* **2005**, *7*, 326; (d) Mba, M.; Prins, L. J.; Licini, G. *Org. Lett*. **2007**, *9*, 21; (e) Maksoud, W. A.; Daniele, S.; Sorokin, A. B. *Green Chem.* **2008**, *10*, 447.

[31] Reddy, R. S.; Reddy, J. S.; Kumar, R.; Kumar, P. *J. Chem. Soc. Chem. Commun.* **1992**, 84.

[32] Reddy, T. I.; Varma, R. S. *Chem. Commun*. **1997**, 471.

[33] (a) Moussa, N.; Fraile, J. M.; Ghorbel, A.; Mayoral, J. A. *J. Mol. Cat. A: Chem*. **2006**, *255*, 62; (b) Hashimi, M. A.; Fisset, E.; Sullivan, A. C.; Wilson, J. R. H. *Tetrahedron Lett.* **2006**, *47*, 8017; (c) Maurya, M. R.; Chandrakar, A. K.; Chand, S. *J. Mol. Catal. A: Chem*. **2007**, *263*, 227; (d) Ballistreri, F. P.; Fortuna, C. G.; Pappalardo, A.; Tomaselli, G. A.; Toscano R. M. *J. Mol. Cat. A: Chem*, **2009**, *in press*, doi.org/doi:10.1016/j.molcata.2009.03.034

[34] (a) Legros, J.; Bolm, C. *Chem. Eur. J.* **2005**, *11*, 1086; (b) Legros, J.; Bolm, C. *Angew. Chem. Int. Ed.* **2004**, *43*, 4225; (c) Baciocchi, E.; Gerini, M. F.; Lapi, A. *J. Org. Chem.* **2004**, *69*, 3586.

[35] (a) Costa, A. P. D.; Reis, P. M.; Gamelas, C.; Roma, C. C.; Royo, B. *Inorg. Chim. Acta* **2008**, *361,* 1915; (b) Bertinchamps, F.; Cimpeanu, V.; Gaigneaux, E. M.; Parvulescu V. I. *Appl. Catal. A: Gen.* **2007**, *325*, 283.

[36] Karimi, B.; Nezhad, M.G.; Clark, J. H. *Org. Lett.* **2005**, *7*, 625.

[37] (a) Hosseinpoor, F.; Golchoubian, H. *Tetrahedron Lett.* **2006**, *47*, 5719; (b) Gao, A.; Wang, M.; Shi, J.; Wang, D.; Tian, W.; Sun, L. *Appl. Organomet. Chem.* **2006**, *20*, 830; (c) Mirkhani, V.; Tangestaninejad, S.; Moghadam, P.; Mohammapoor- Baltork, I.; Kargar, H. *J. Mol. Catal. A: Chem.* **2005**, *242,* 251.

[38] (a) Velusamy, S.; Kumar, A. V.; Saini, R.; Punniyamuthy, T. *Tetrahedron Lett.* **2005**, *46*, 3819; (b) Liu, R.; Wu, L.; Feng, X.; Zhang, Z.; Li, Y.; Wang, Z. *Inorg. Chim. Acta* **2007**, *360*, 656.

[39] (a) Fraile, J. M.; García, J. I.; Lázaro, B.; Mayoral, J. A. *Chem. Commun.* **1998**, 1807; (b) Raju, S. V. N.; Upadhya, T. T.; Ponatnam, S.; Daniel, T.; Sudalai, A. *Chem. Commun.* **1996**, 1969; (c) Moreau, P.; Hulea, V.; Gomez, S.; Brunel, D.; Renzo, F. D. *Appl. Catal. A: Gen.* **1997**, *155*, 253.

[40] (a) Corma, A.; Iglesias, M.; Sanchez, F. *Catal. Lett.* **1996**, *39*, 153; (b) Iwamoto, M.; Tanaka, Y.; Hirosumi, J.; Kita, N.; Triwahyono, S. *Microporous Mesoporous Mater.* **2001**, *48*, 271; (c) Kholdeeva, O. A.; Derevyankin, A. Y.; Shmakov, A. N.; Trukhan, N. N.; Paukshtis, E. A.; Tuel, A.; Romannikov, V. N. *J. Mol. Catal. A: Chem.* **2000**, *158*, 417.

[41] Raghavan, P. S.; Ramaswamy, V.; Upadhya, T. T.; Sudalai, A.; Ramaswamy, A. V.; Sivasanker, S. *J. Mol. Catal. A: Chem*. **1997**, *122*, 75.

[42] Moreau, P.; Hulea, V.; Gomez, S.; Brunel, D.; Renzo, F. D. *Appl. Catal. A: Gen.* **1997**, *155*, 253.

[43] Corma, A.; Iglesias, M.; Sanchez, F. *Catal. Lett*. **1996**, *39*, 153.

[44] Iwamoto, M.; Tanaka, Y.; Hirosumi, J.; Kita, N.; Triwahyono, S. *Microporous Mesoporous Mater.* **2001**, *48*, 271.

[45] Kholdeeva, O. A.; Derevyankin, A. Y.; Shmakov, A. N.; Trukhan, N. N.; Paukshtis, E. A.; Tuel, A.; Romannikov,V. N. *J. Mol. Catal. A: Chem*. **2000**, *158*, 417.

[46] Nakamoto, K. *Infrared and Raman Spectra of Inorganic and Coordination Compounds, Part A: Theory and Applications in Inorganic Chemistry.* 5th Ed., John Wiley and Sons, 1997, p. 265.

[47] d'Yvoire., *Bull. Soc. Chim. Fr.,* **1961**, 2277, pdf file no.00-014-0546.

[48] Cromer, D. T.; Herrington, K. *J. Am. Chem. Soc*. **1955**, *77,* 4708, pdf file no.03-065-5714.

[49] Tegehall, P. E. *Acta Chem. Scand. Ser. A*, **1986**, 40507, pdf file no. 00-039-0168.

[50] Klug's equation for semiquantitative analysis from XRD pattern

$$f_1 = \frac{(I^{mix} / I^{pure})A_2}{A_1 - (I^{mix} / I^{pure})(A_1 - A_2)}$$

A_1= X ray atomic absorption co-efficient of Ti_2O,191.7
A_2= X ray atomic absorption co-efficient of $Ti_4H_{11}(PO_4)_9(x.H_2O)(0<x<4)$,183.6
I^{mix}=850, I^{pure}=999 } Assuming by taking the reference of pure TiO_2

[51] Scherer's equation for average crystallite size

$$S_C = \frac{K\lambda}{\beta Cos\theta}$$

Where K = constant (assuming circular grain ≈ 0.9)

λ = Wavelength of the X- ray (≈ 1.5420Å)

θ = Bragg's diffraction angle

β = Full Width Half Maximum (FWHM) in 2θ profile

[52] Barrett, E. P.; Joyner, L. G.; Halonga, P. P. *J. Am. Chem. Soc.* **1951**, *73*, 373.

[53] Samajdar, S.; Becker, F. F.; Banik, B. K. *Tetrahedron Lett.* **2000**, *41,* 8017.

[54] Hulea, V.; Fajula, F.; Bousquet, J. *J. Catal.* **2001**, *198*, 179.

[55] Buffin, B. P.; Clarkson, J. P.; Belitz, N. L.; Kundu, A. *J. Mol. Catal. A: Chem.* **2005**, *225*, 111.

[56] (a) Kahne, D.; Walker, S.; Cheng, Y.; Engan, V. D. *J. Am. Chem. Soc.* **1989**, *111,* 6881; (b) Agnihotri, G.; Misra, A. K. *Tetrahedron Lett.* **2005**, *46*, 8113.

Characterization of products

The compounds were characterized by m.p., elemental analysis, IR, ^{1}H and ^{13}C NMR and Mass spectrometry. The ^{1}H NMR and ^{13}C NMR spectra were recorded on 400 MHz and 100 MHz magnetic field, respectively. All compounds were soluble in $CDCl_3$. The data of the products are summarized as follows:

Nitrobenzene (1)

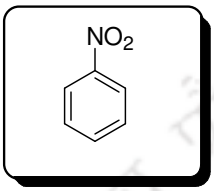

Yellow liquid;

IR(neat): 702(s), 1107(m), **1347(vs)**, **1532(s)**, 1619(m) cm^{-1}; ^{1}H NMR: δ 7.53(t, *J*=7.6 Hz, 2H), 7.68(t, *J*=8 Hz, 1H), 8.21(d, *J*=8.4 Hz, 2H) ppm; ^{13}C NMR: δ 123.8(2C), 129.4(2C),134.6, 148.46 ppm; MS : m/z 123(M^+).

2-nitro toluene (2a)

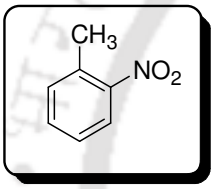

Yellow viscous liquid;

IR(neat): 732(m), 848(w), **1348(s)**, **1522(s)**, 2928(m) cm^{-1}; ^{1}H NMR: δ 2.60(s, 3H), 7.30(t, *J*=8.4 Hz, 2H), 7.94(d, *J*=7.6 Hz, 2H) ppm; ^{13}C NMR: δ 12.1, 126.4, 123.5, 130.1, 132.8, 134.5, 149.1 ppm; MS : m/z 137(M^+).

4-nitro toluene (2b)

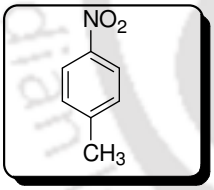

Yellow Solid;

IR(neat): 693(m), 909(w), **1348(m)**, **1540(s)**, 2924(m) cm^{-1}; ^{1}H NMR: δ 2.46(s, 3H), 7.94(d, *J*=8.4 Hz, 2H) 8.09(d, *J*=8.4 Hz, 2H) ppm; ^{13}C NMR: δ 20.9, 123.5(2C), 130.1(2C), 143.8, 145.4 ppm; MS : m/z 137(M^+).

2-nitro phenol (3a)

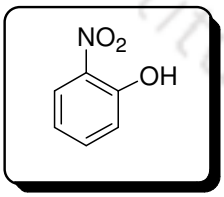

Yellow liquid;

IR(neat): 661(s), 1122(m), **1450(s)**, **1525(s)**, 1614(s) cm^{-1}; ^{1}H NMR: δ 6.98(t, *J*=7.2 Hz, 1H), 7.14(d, *J*=8.4 Hz, 1H), 7.57(t, *J*=7.2 Hz, 1H), 8.09(d, *J*=8.4 Hz, 1H), 10.56(s, 1H) ppm; ^{13}C NMR: δ 116.6, 122.0, 125.0, 135.6, 136.0, 152.4 ppm; MS : m/z 139 (M^+).

4-nitro phenol (3b)

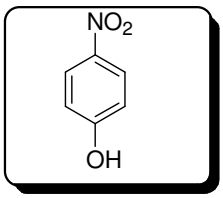

Yellow liquid;

IR(neat): 661(s), 1122(m), **1450(s)**, **1525(s)**, 1614(s) cm^{-1}; ^{1}H NMR: δ 5.81(s, 1H), 6.90(d, *J*=9.2 Hz, 2H), 8.15(d, *J*=8.8 Hz, 2H) ppm; ^{13}C NMR: δ 116.6(2C), 125.0(2C), 141.0, 163.4 ppm; MS: m/z 139(M^+).

4-Methyl-3-nitro-phenol(4) 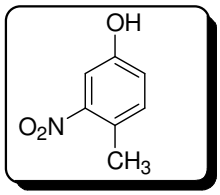	**Yellow Liquid;** IR(neat): 1178(s), 1245(s),**1322(s), 1537(s)**, 2356(m) cm^{-1}; ^1H NMR: δ 2.33(s, 3H), 7.02(d, *J*=8.4 Hz, 1H), 7.36(d, *J*=8.8 Hz, 1H), 7.86(s,1H), 10.40(s, 1H) ppm; ^{13}C NMR: δ 55.0, 111.8, 116.4, 122.8, 135.4, 149.7, 150.5 ppm; MS: m/z 153(M^+).
2-Nitro-aniline (5a) 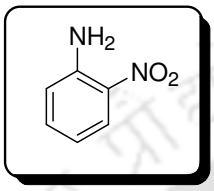	**Yellow liquid;** IR(neat): 846(w) 1264(m) **1343(s)**, **1531(s)**, 1603(m) cm^{-1}; ^1H NMR: δ 5.1(s, 2H), 6.72-6.89(m, 2H), 7.43(t, *J*=7.2 Hz, 1H), 7.89(d, *J*=8.2 Hz, 1H) ppm; ^{13}C NMR: δ 116.0, 119.4, 124.4, 135.0, 135.4, 141.8 ppm.
4-Nitro-aniline (5b) 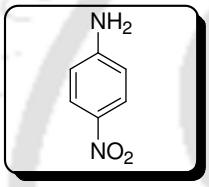	**Brownish solid;** IR(neat): 845(w) 1111(m), 1286(m), **1340(s)**, **1511(s)** cm^{-1}; ^1H NMR: δ 5.4(s, 2H), 6.88(d, *J*=8.4 Hz, 2H), 8.13(d, *J*=8.4 Hz, 2H) ppm; ^{13}C NMR: δ 115.8 (2C), 126.3 (2C), 143.23, 148.43 ppm.
2-nitro-bromobenzene (6a) 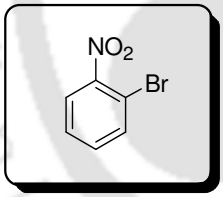	**Yellow liquid;** IR(neat): 461(m), 820(s), 1041(w), **1350(s)**, **1532(vs)** cm^{-1}; ^1H NMR: δ 7.53(m, 2H), 7.64(d, *J*=8.4 Hz, 1H), 6.78(d, *J*=8.4 Hz, 1H) ppm; ^{13}C NMR: δ 118.2, 125.8, 128.4, 132.7, 136.8, 151.7 ppm; MS: m/z 201, 203(M^+, M^++2).
4-nitro-bromobenzene (6b) 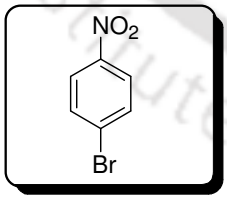	**Light Yellow Solid;** (m.p. 124 ^0C) IR(neat): 738(m), 840(s), 1061(w), **1358(s)**, **1511(vs)** cm^{-1}; ^1H NMR: δ 7.67(d, *J*=9.2 Hz, 2H), 8.08(d, *J*=9.2 Hz, 2H) ppm; ^{13}C NMR: δ 125.8(2C), 129.2, 132.7(2C), 147.4 ppm; MS: m/z 201, 203 (M^+, M^++2).
4-Nitro-acetanilide (7) 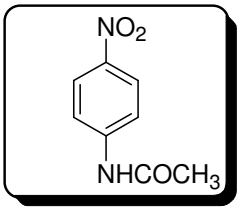	**Yellow Solid;** IR(neat): 856(s), 1061(w), **1338(s)**, **1519(vs)**, 1607(s), 1681(s) cm^{-1}; ^1H NMR: δ 2.24(s, 3H), 7.44(s, 1H), 7.67(d, *J*=9.2 Hz, 2H), 8.19(d, *J*=9.2 Hz, 2H) ppm; ^{13}C NMR: δ 17.6, 121.8(2C), 123.7(2C), 144.4, 146.4, 168.4 ppm; MS: m/z 180(M^+).

1-Nitro-naphthalene (8)

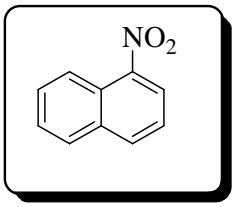

Yellow Solid;

IR(neat): 763(vs), 805(m), **1339(vs)**, **1520(vs)** cm^{-1}; ^{1}H NMR: δ 7.56-7.75(m, 3H), 7.90-8.32(m, 4H) ppm; ^{13}C NMR: δ 122.9, 123.8, 123.9, 124.9, 127.2, 128.5, 129.3, 134.2, 134.5, 146.5 ppm; MS: m/z 173(M^+).

9-Nitro-anthracene (9)

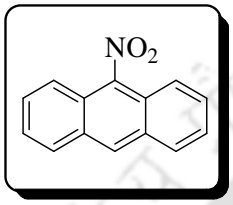

Crystalline yellow solid;

IR(neat): 687(m), **1291(s)**, **1588(s)**, 1675(s), 2919(s) cm^{-1}; ^{1}H NMR: δ 7.74-7.76(m, 1H), 7.79-7.84(m, 4H), 7.94 - 7.96(m, 1H) 8.30-8.33(m, 2H), 8.39-8.42(m, 1H) ppm; ^{13}C NMR: δ 125.5(2C), 125.9(2C), 126.4(2C), 127.0(2C), 128.3(2C), 131.1(2C), 132.7, 144.7 ppm; MS: m/z 223(M^+).

9-Nitro-phenanthrene (10)

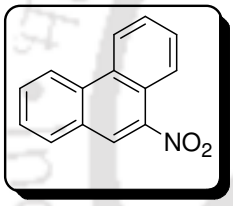

Yellow solid;

IR(KBr): 726(s), 765(s), **1336(s)**, **1519(s)** cm^{-1}; ^{1}H NMR: δ 7.74-7.76(m, 1H), 7.79-7.89(m, 4H), 7.98-8.20(m, 2H) 8.60-8.83(m, 3H) ppm; ^{13}C NMR: δ 121.7, 122.4(2C), 125.2, 126.3(4C), 128.3(2C), 131.0, 132.8, 138.0, 146.5 ppm.

2-Nitro-naphthol (11)

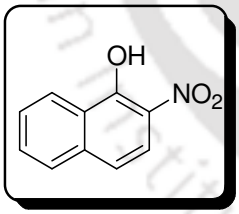

Yellow Solid;

IR(KBr): 1285(s), **1331(s)**, 1430(s), **1516(s)**, 1585(s) cm^{-1}; ^{1}H NMR: δ 7.10(d, *J*=7.2 Hz, 1H), 7.50-7.77(m, 2H), 7.95(d, *J*=7.2 Hz, 1H), 8.65(d, *J*=7.2 Hz, 1H), 8.72(d, *J*=7.2 Hz, 1H), 9.00(s, 1H) ppm; ^{13}C NMR: δ 119.1, 122.4, 123.5(2C), 127.7, 128.4(2C), 130.4, 137.0, 148.1 ppm; MS: m/z 189(M^+).

1,6-Dinitro-2-naphthol (12)

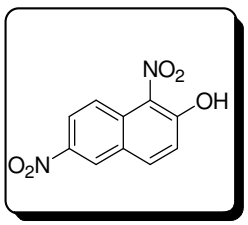

Yellow solid;

IR(KBr): 800(m), 1102(m), 1261(m), **1551(s)**, 1646(s) cm^{-1} ; ^{1}H NMR: δ 7.43(d, *J*=9.2 Hz, 1H), 8.13(d, *J*=9.2 Hz, 1H), 8.46(d, *J*=7.2 Hz, 1H), 8.72(s, 1H), 9.05(d, *J*=9.6 Hz, 1H), 12.16(s, 1H) ppm; ^{13}C NMR: δ 117.8, 122.9, 123.1, 124.8, 128.2(2C), 128.4, 138.2, 144.8, 155.1 ppm.

4-nitro-*O*-xylene (13b)

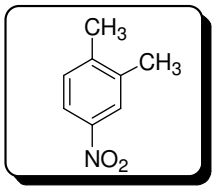

Yellow liquid;

IR(neat): 740(m), 1093(w) **1346(vs)**, **1519(vs)** cm^{-1}; ^{1}H NMR: δ 2.23(s, 3H), 2.27(s, 3H), 7.25(d, *J*=8.4 Hz, 1H), 7.93(d, 1H), 7.98(s, 1H) ppm; ^{13}C NMR: δ 13.2, 15.4, 120.6, 124.1, 130.5, 139.7, 145.1, 150.3 ppm; MS: m/z 151(M^+).

3-nitro-*O*-xylene (13b)

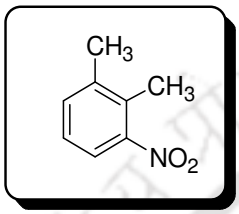

Yellow liquid;

IR(neat): 572(m), 1021(m), **1259(s), 1543(s)** 1625(m) cm^{-1}; ^{1}H NMR: δ 2.24(s, 3H), 2.76(s, 3H), 7.20(t, *J*=7.2 Hz, 1H), 7.38(d, *J*=8.8 Hz, 1H), 7.65(d, *J*=8.4 Hz, 1H) ppm; ^{13}C NMR: δ 14.9, 21.4, 122.4, 126.3, 130.4, 133.9, 139.5, 150.2 ppm; MS: m/z 151(M^+).

4-nitro-*m*-xylene (13b)

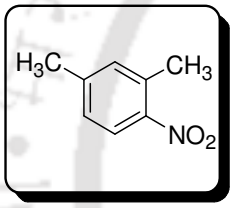

Yellow liquid;

IR(neat): 835(m), **1343(s)**, **1518(s)**, 1602(m) cm^{-1}; ^{1}H NMR: δ 2.38(s, 3H), 2.57(s, 3H), 7.09-7.10(m, 2H), 7.89(d, *J*=7.2 Hz, 1H) ppm; ^{13}C NMR: δ 5.9, 13.5, 120.5, 126.4, 133.5, 135.7, 139.1, 149.2 ppm; MS: m/z 151(M^+).

2-Nitro-9H-fluorene (15)

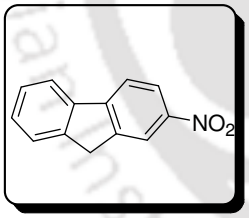

Yellow solid;

IR(KBr): 782(m), 987(m), **1345(s)**, **1567(s)**, 2987(m) cm^{-1}; ^{1}H NMR: δ 4.00(s, 2H), 7.42(t, *J*=5.6 Hz, 2H), 7.60(d, *J*=8.0 Hz, 1H), 7.85(d, *J*=8.0 Hz, 2H), 8.27(s, 1H), 8.38(s, 1H) ppm; ^{13}C NMR: δ 32.4, 121.7, 124.3, 126.3, 127.9(2C), 129.6(2C), 136.3, 141.1, 142.7, 146.3 ppm; MS: m/z 211(M^+).

Benzoic acid (16)

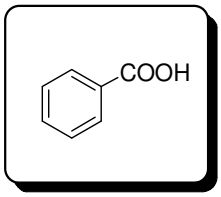

White solid; (m.p. 122 ^{0}C)

IR(KBr): 800 (m), 1010(s), 1610(s) cm^{-1}; ^{1}H NMR: δ 7.46(t, *J*=8.4 Hz, 2H), 7.60(t, *J*=8.4 Hz, 1H), 8.10(d, *J*=8.4 Hz, 2H) ppm; ^{13}C NMR: 128.3(2C), 130.4(2C), 130.5, 131.2, 169.4 ppm.

4-Hydroxy-3-nitro-benzaldehyde (17)

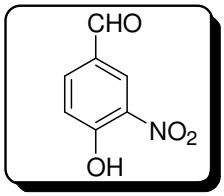

Yellow Solid;

IR(KBr): 1271(m), **1336(s)**, **1568(m)**, 1609(s) cm^{-1}; ^{1}H NMR: δ 7.30(d, *J*=8.0 Hz, 1H), 8.12(d, *J*=8.8 Hz, 1H), 8.62(s, 1H), 9.91(s, 1H), 11.00(s, 1H) ppm; ^{13}C NMR: δ 117.1, 126.2, 136.2, 130.2, 137.2, 158.2, 190.0 ppm.

2,4-Dihydroxy-3,5-dinitro-benzaldehyde (18)

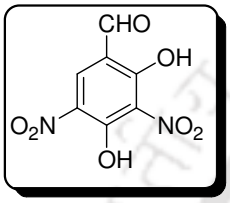

Yellow solid; (mp 147-149^{0}C);

IR (neat): 1173(m), **1301(vs)**, **1520(vs)**, 1644(s) cm^{-1}; ^{1}H NMR: δ 6.58 (s, 1H), 8.64 (s, 1H), 11.04 (s, 1H), 12.88 (s, 1H); ^{13}C NMR: 106.3, 114.3, 130.7(2C), 160.8, 169.3, 203.0; MS: m/z 228 (M^{+}).

Methylsulfinyl-benzene (19)

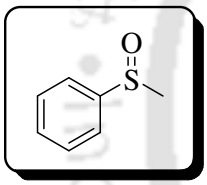

Yellow liquid;

IR(neat): 692(s), 750(s), **1032(s)**, 1090(s), 1444(s) cm^{-1};

^{1}H NMR: δ 2.74(s, 3H), 7.51-7.53(m, 3H), 7.64-7.66(m, 2H) ppm; ^{13}C NMR: δ 38.1, 123.7(2C), 128.5(2C), 130.2, 145.8 ppm.MS : m/z 157(M^{+}).

3-Nitro-dibenzothiophene (20a)

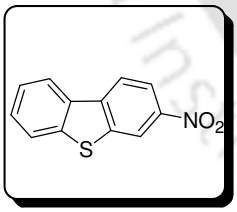

Yellow Solid;

IR(KBr): 743(vs), 1050(w), **1338(s)**,1437(s), **1514(m)** cm^{-1} ; ^{1}H NMR: δ 7.48-7.54 (m, 4H), 7.58-7.79(m, 4H), 7.97(s, 2H); ^{13}C NMR: δ 121.8, 123.4, 127.4, 129.0, 130.4, 131.2, 132.4, 134.5, 136.6, 136.9, 143.2, 154.9.

Dibenzothiophene-5-oxide (20b)

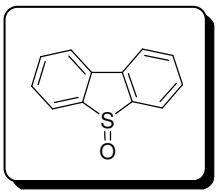

Light yellow solid; (m.p. 198 ^{0}C)

IR (KBr): 557(s), 754(vs), **1025(vs)**, 1067(s) 1443(m) cm^{-1}; ^{1}H NMR: δ 7.48(t, *J*= 7.6 Hz, 2H), 7.58(t, *J*= 7.6 Hz, 2H), 7.79(d, *J*= 8.0 Hz, 2H) , 7.97(d, *J*= 8.0 Hz, 2H); ^{13}C NMR: δ 121.8(2C), 127.4 (2C), 129.4 (2C), 132.4 (2C), 136.9(2C), 144.9(2C).

3-Nitro-pyridine (21a)

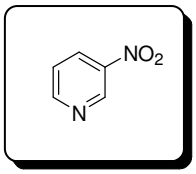

Yellow Liquid;

IR(neat): 1022(w), **1345(s)**, **1530(s)**, 1596(m) cm^{-1}; ^{1}H NMR: δ 7.86(t, *J*=8.0 Hz, 1H), 8.51(d, *J*=8.4 Hz, 1H), 8.71(d, *J=4.*8 Hz, 1H) 9.73(s, 1H) ppm; ^{13}C NMR: δ 124.6, 130.3, 143.2, 144.8, 155.1 ppm; MS: m/z 124(M^{+}).

Pyridine-N-oxide (21b)

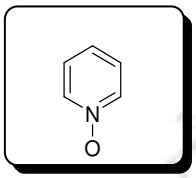

Colorless liquid;

IR(neat): 1077(m), **1276(s)**, 1457(s), 1729(s) cm^{-1}; ^{1}H NMR : δ 7.39(t, *J*=4.8 Hz, 2H), 7.57(d, *J*=4.8 Hz, 2H), 8.46(t, *J*=4.8 Hz, 1H) ppm; ^{13}C NMR: δ 123.6(2C), 135.4, 149.6(2C) ppm.

3-Benzenesulfinyl-propionitrile (22)

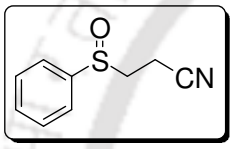

Viscous light yellow liquid;

IR (neat): 543(m) **1044(s)**, 2362(m) cm^{-1}; ^{1}H NMR: δ 2.81(t, *J*= 8.4 Hz, 2H), 3.17-3.26(m, 2H), 7.53-7.73(m, 5H) ppm; ^{13}C NMR: 15.7, 49.6, 117.5, 123.4(2C), 129.4(2C), 130.7, 145.9 ppm.

Hexanesulfinyl-benzene (23)

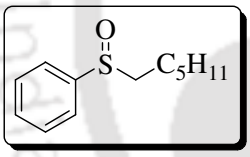

White solid;

IR (KBr): 693(s) 749(s) **1041(vs)**, 1089(s), 1444(s) cm^{-1}; ^{1}H NMR: δ 0.86(t, *J* = 6.4 Hz, 3H), 1.25-1.47(m, 6H), 1.56-1.77(m, 2H), 2.74-2.87(m, 2H), 7.47-7.52(m, 3H), 7.60-7.62(m, 2H) ppm; ^{13}C NMR: δ 14.2, 23.4, 27.3, 29.5, 32.7, 123.4(2C), 129.7(2C), 130.6, 146.6 ppm.

2-Propenesulfinyl-benzene (24)

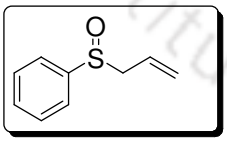

Viscous liquid;

IR (neat): 758(s), 927(s), **1040(s)**, 1096(s), **1440(s)** cm^{-1}; ^{1}H NMR: δ 3.48-3.60(m, 2H), 5.18 (d, *J* = 16.8 Hz, lH), 5.33 (d, 1H, *J* = 10.8 Hz, 1H), 5.58-5.68(m, lH), 7.48-7.53(m, 3H), 7.55-7.58(m, 2H) ppm; ^{13}C NMR: δ 57.6, 115.9, 123.5(2C), 129.6(2C), 130.9, 132.7, 146.1 ppm.

Benzylsulfinyl-benzene (25)

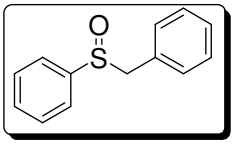

White Solid; (m.p. 126 ^{0}C)

IR (neat): 765(s), **1035(s)**, cm^{-1}; ^{1}H NMR: δ 3.99(d, *J* = 12.4Hz, 1H), 4.11(d, *J* = 12.4Hz, 1H), 6.97(d, 2H), 7.19-7.28(m, 3H), 7.34-7.44(m, 5H) ppm; ^{13}C NMR: δ 63.8, 124.5(2C), 128.3, 128.5(2C), 128.9(2C), 129.2, 130.4(2C), 131.2, 142.7 ppm.

Octadecylsulfinyl-benzene (26) 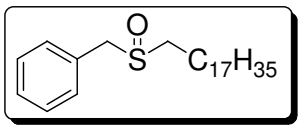	**White solid;** (m.p. 99^{0}C) IR (neat): 696(m) **1015(s)**, **1024(s)**, 2848(vs), 2917(vs) cm^{-1}; ^{1}H NMR: δ 1.20(s, 33H), 1.60-1.74(m, 2H) 2.53(t, *J*=7.6 Hz, 2H) 5.18(d, *J* = 16.8Hz, 1H), 5.31(d, *J* = 10.8Hz, 1H), 7.26-7.37(m, 5H) ppm; ^{13}C NMR: δ 14.3, 22.6, 22.8, 29.0, 29.3, 29.5, 29.5, 29.7, 29.7(3C), 29.8(5C), 32.12, 51.1, 58.4, 128.4, 129.1, 130.1(3C) ppm.
3-Benzenesulfinyl-propionamide (27) 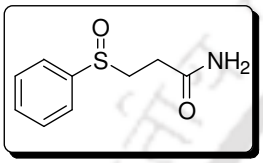	**White Solid;** IR (KBr): 690(m), **1040(s)**, 1416(s), 1685(s), 3310(s) cm^{-1}; ^{1}H NMR: δ 2.45-2.53(m, 1H), 2.74-2.81 (m, 1H), 2.91-2.98(m, 1H), 3.23-3.30(m, 1H), 5.61(s, 1H), 6.33(s, 1H), 7.44-7.62(m, 5H) ppm; ^{13}C NMR: δ 33.7, 49.8, 123.5(2C), 129.6(2C), 130.9, 146.1, 177.2 ppm.
3-Benzenesulfinyl-methyl propionate(28) 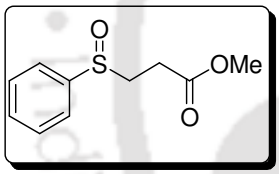	**White Solid;** IR(KBr): 783(s) **1050(vs)**, 1467(m), **1680(vs)** cm^{-1}; ^{1}H NMR: δ 2.51-2.59(m, 1H), 2.79-2.86(m, 1H), 2.87-2.99(m, 1H), 3.20-3.28(m, 1H), 3.65(s, 3H), 7.506-7.55(m, 3H), 7.59-7.63(d, 2H) ppm; ^{13}C NMR: δ 50.4, 30.7, 49.5, 123.9(2C), 129.0(2C), 130.5, 146.1, 172.0 ppm.
3-Benzenesulfinyl-butyraldehyde (29) 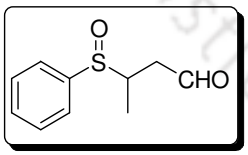	**Light yellow liquid;** IR(neat): 758(m), **1067(s)**, 1365(m), **1675(vs)** cm^{-1}; ^{1}H NMR: δ 1.17(d, *J*=6.8 Hz, 3H), 2.51-2.59(m, 1H), 3.05-3.11(dd, *J*=14.8, 3.6 Hz, 1H), 3.57-3.62(m, 1H), 7.49(t, *J*=8.0 Hz, 2H), 7.59(t, *J*=8.0 Hz, 1H), 7.78(d, *J*=7.2 Hz, 2H), 9.65(s, 1H) ppm; ^{13}C NMR: δ 21.3, 37.7, 50.2, 127.8(2C), 129.2(2C), 133.1(2C), 200.7 ppm; MS: m/z 198(M$^+$).
2-Phenylmethanesulfinyl-ethanol (30) 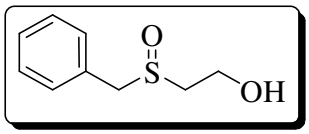	**Viscous yellow liquid;** IR (neat): 615(m), 749(m) **1025(s)**, 1445(m) cm^{-1}; ^{1}H NMR : δ 2.72-2.78(m, 2H), 2.80-2.87(m, 2H), 3.78(s, 1H), 4.10(s, 2H), 7.29-7.31(m, 2H), 7.34-7.38(m, 3H); ^{13}C NMR: δ 53.3, 55.2, 58.0, 128.6(2C), 129.1(2C), 130.0, 130.5 ppm; MS: m/z 168 (M$^+$).

2-Phenylmethanesulfinyl-benzothiazole (31)

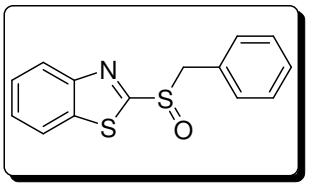

Brownish solid; (m.p. 121 ^{0}C)

IR(KBr): 697(s), 758(s), **1048(vs)**, 1313(m),1467(m) cm^{-1}; ^{1}H NMR: δ 4.31 (d, *J* = 13.2 Hz, 1.5H) , 4.50 (d, *J* = 13.2 Hz, 1.5H), 7.17(d, *J*=7.2 Hz, 2H), 7.24-7.31(m, 3H), 7.48(t, *J*=4.8 Hz,1H), 7.57(t, *J*=4.8 Hz,1H), 7.93(d, *J*=8.0 Hz,1H), 8.01(d, *J*=8.0 Hz,1H) ppm; ^{13}C NMR: δ 62.9, 122.4, 124.1, 126.3, 127.1, 128.9(3C), 130.6(3C), 136.2, 153.9, 177.1 ppm.

Butanesulfinyl-butane (32)

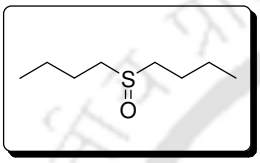

Colorless liquid;

IR (KBr): **1021(vs)**, 1463(s), 2960(vs) cm^{-1}; ^{1}H NMR (400 MHz $CDCl_3$): δ 0.92(t, 6H), 1.39-1.49(m, 4H), 1.66-1.80 (m, 4H), 2.55-2.67(m, 4H) ppm; ^{13}C NMR (100MHz, $CDCl_3$): 14.2(2C), 22.3(2C), 30.1(2C), 52.3(2C) ppm.

DMSO(33)

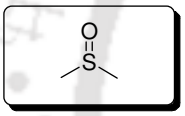

Colorless liquid;

IR (neat): 709(w), 935(s), **1019(s)**, 1407(s), 16489(s) cm^{-1}; ^{1}H NMR : δ 2.98(s, 6H) ppm; MS: m/z 78 (M^+).

Glycosyl sulfoxide* (34)

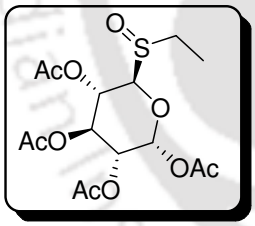

Light yellow solid;

IR (KBr): 721(m), **1038(s)**, 1226(s), 1748(vs) cm^{-1}; ^{1}H NMR: δ 1.36(t, *J*=6.0 Hz, 3H), 1.99-2.05(m, 12H), 3.05-3.17(m, 2H), 3.80(d, *J*=6.4 Hz, 1H), 4.21(m, 1H), 4.45(d, *J*=10.0 Hz, 1H), 5.08(t, *J*=9.2 Hz, 1H), 5.28(t, *J*=9.6 Hz, 1H), 5.45(t, *J*=9.6 Hz, 1H) ppm; ^{13}C NMR: 14.9, 20.6, 24.2, 62.2, 68.3, 69.8, 73.9, 75.8, 76.9, 77.2, 77.5, 83.5, 169.5(2C), 170.3, 170.8 ppm.

4-ethyldibenzothiophene-5-oxide (35)

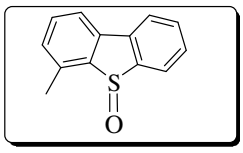

White Solid;

IR (KBr): 654(w), **1028(s)**, 1356(m), 2987(s) cm^{-1}; ^{1}H NMR : δ 4.32 (d, *J* = 12.8 Hz, 1.5H) , 4.50 (d, *J* = 13.2 Hz, 1.5H), 7.15(d, *J*=6.8 Hz, 3H) 7.24-7.27 (m, 3H), 7.46 (t, *J*=6.4 Hz, 1H), 7.56 (t, *J*=6.4 Hz, 1H), 7.92 (d, *J*=8.0 Hz, 1H), 8.08 (d, *J*=8.0 Hz, 1H) ppm; ^{13}C NMR: δ 13.7, 124.5(2C), 127.3(4C), 128.1(2C), 129.3(2C), 137.2, 138.7 ppm.

Spectra of some selected compounds

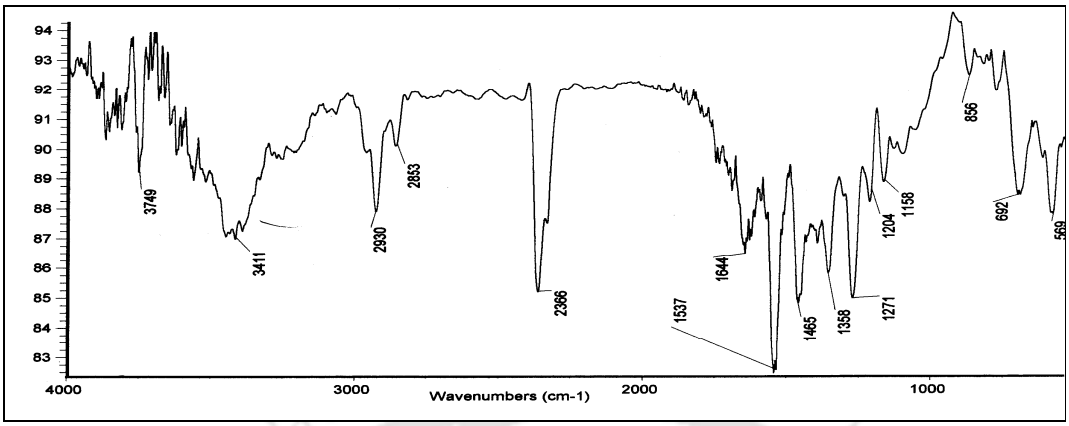

(a)

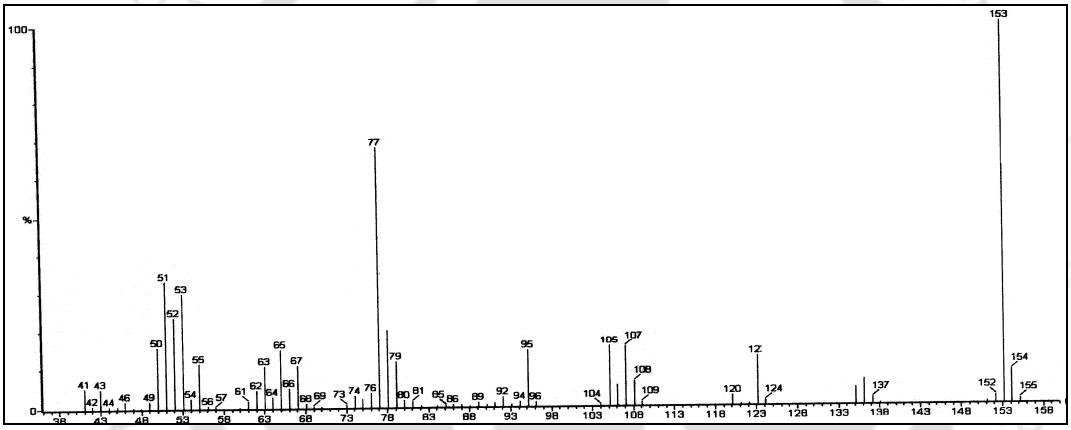

(b)

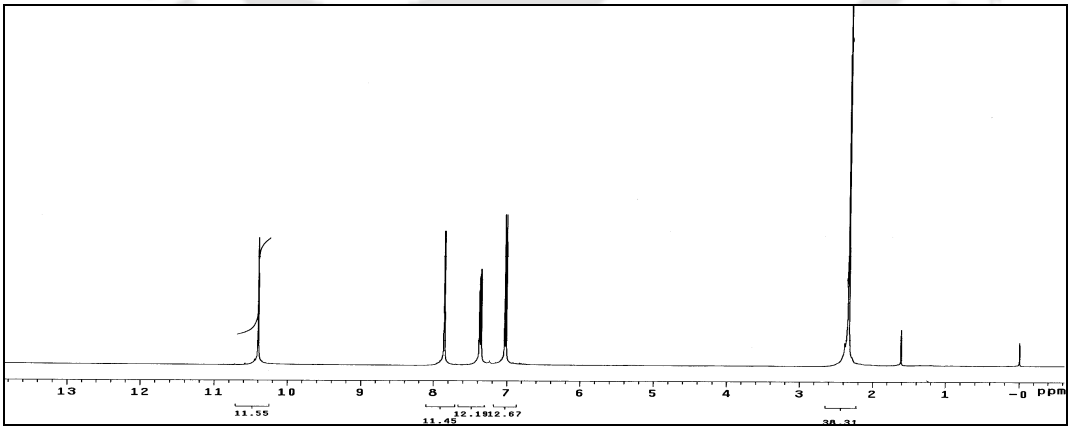

(c)

Figures 5.S1 (a) FTIR spectrum, (b) GCMS profile and (c) ^{1}H NMR spectrum of **p-cresol**

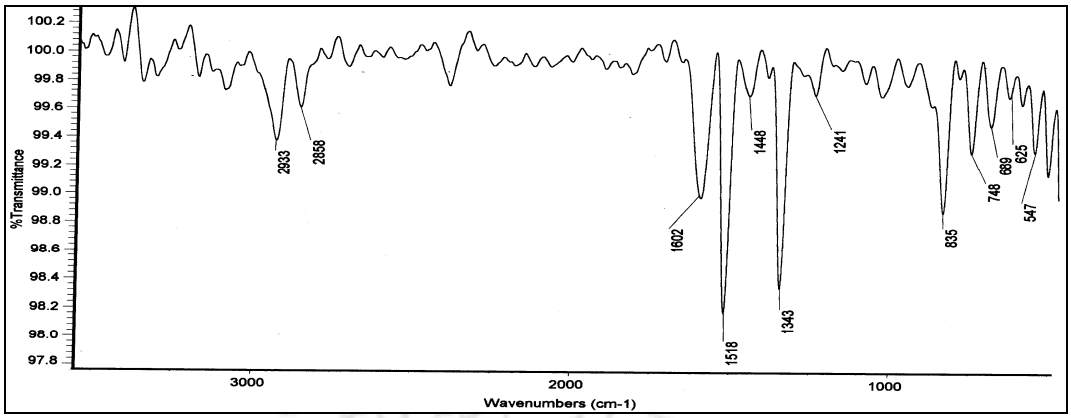

(a)

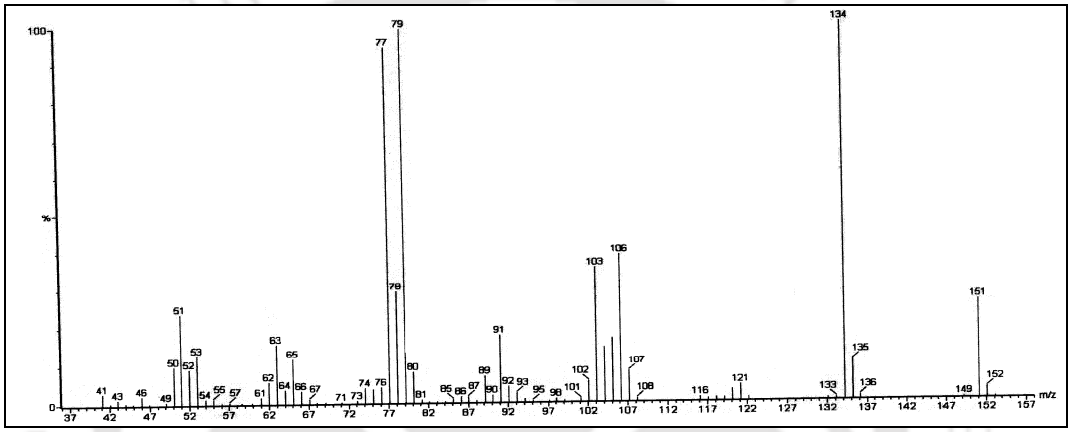

(b)

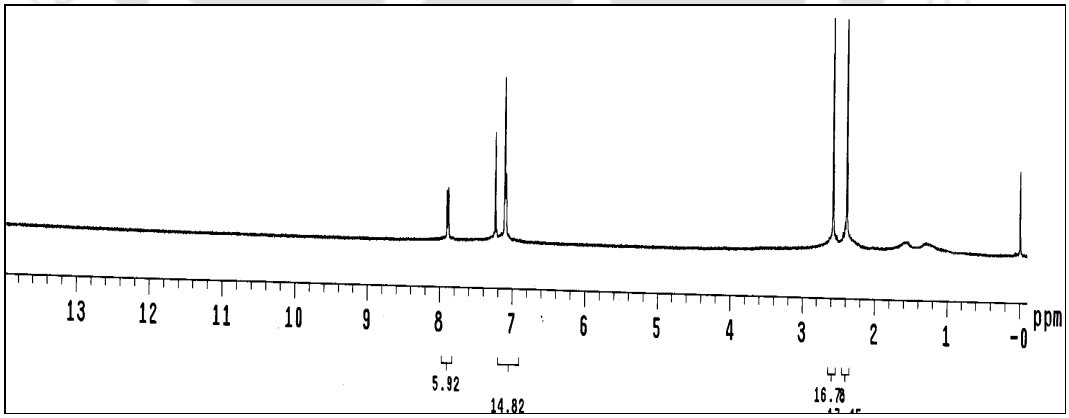

(c)

Figures 5.S2 (a) FTIR spectrum, (b) GCMS profile and (c) ^{1}H NMR spectrum of ***m*-xylene**

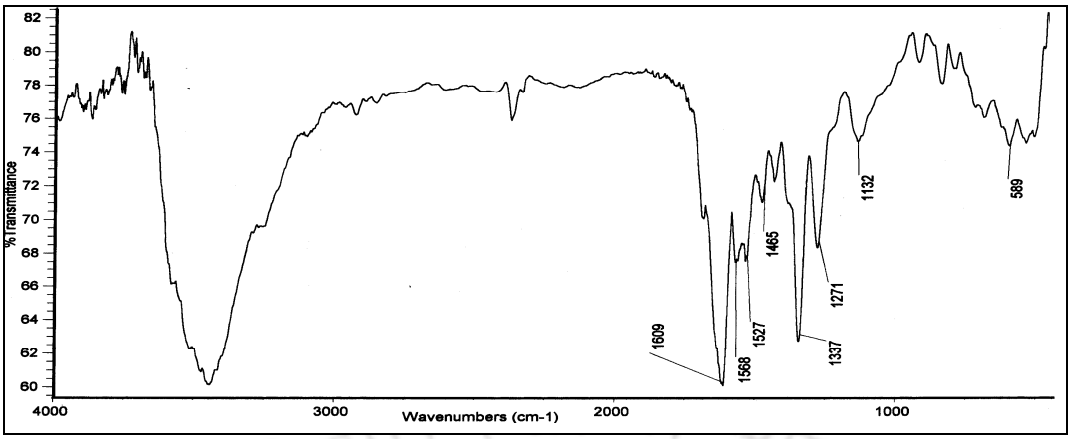

(a)

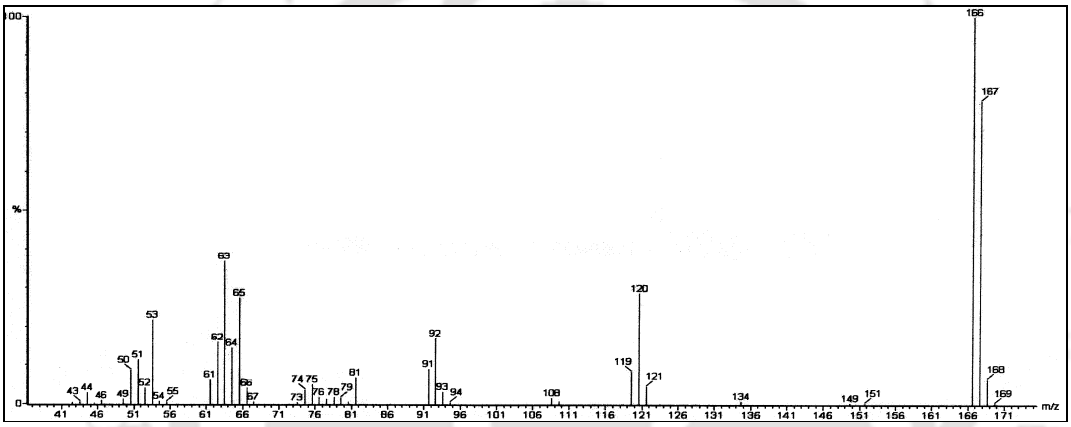

(b)

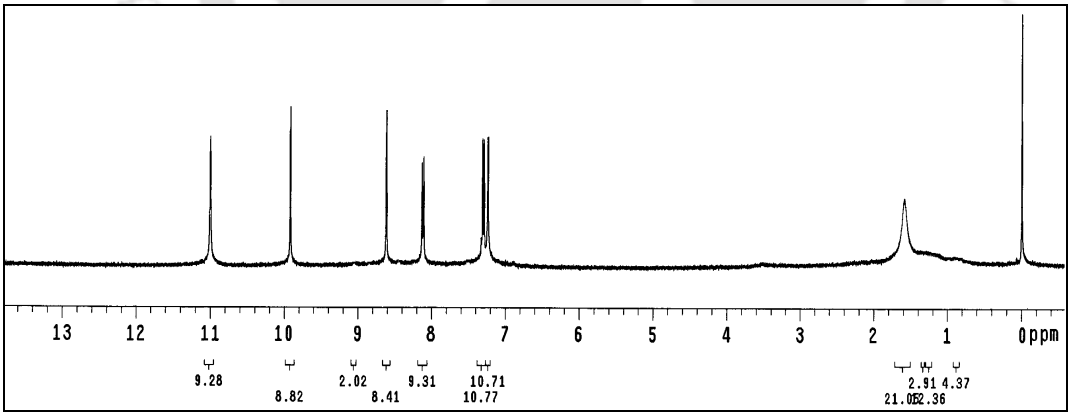

(c)

Figures 5.S3 (a) FTIR spectrum, (b) GCMS profile and (c) ^{1}H NMR spectrum of **4-hydroxy benzaldehyde.**

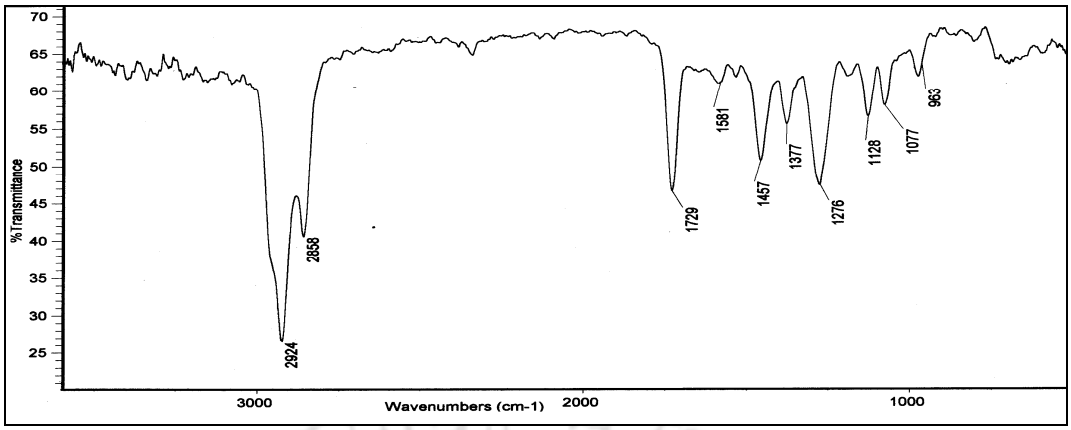

(a)

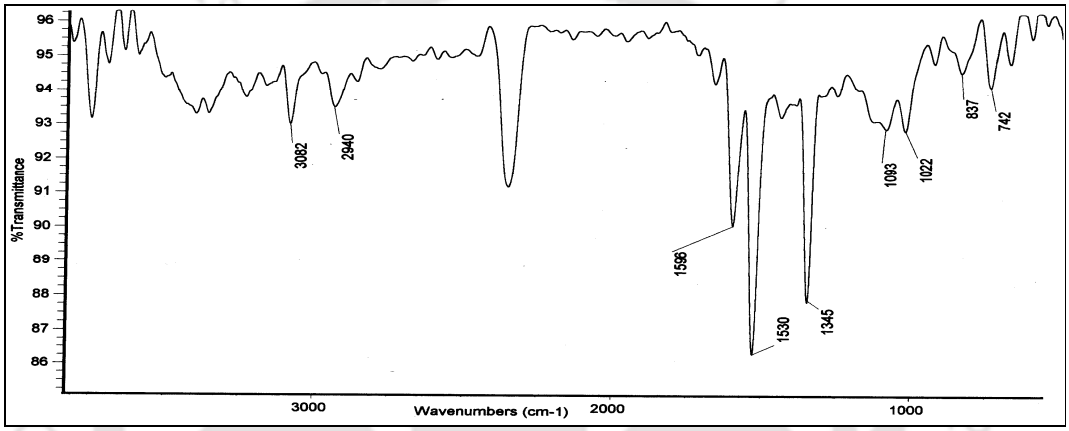

(b)

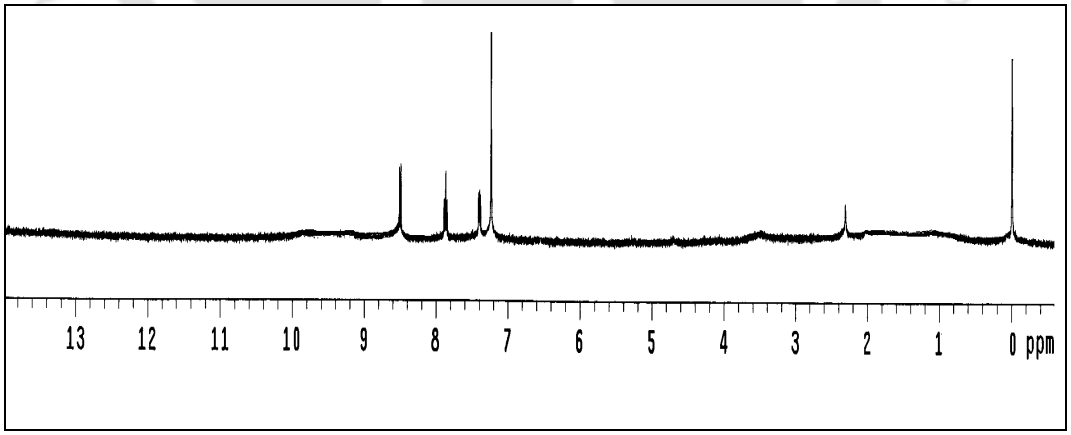

(c)

Figures 5.S4 (a) FTIR spectrum of **pyridine n-oxide**, (b) FTIR spectrum of **3-nitropyridine** and (c) ^{1}H NMR spectrum of **3- nitopyridine**

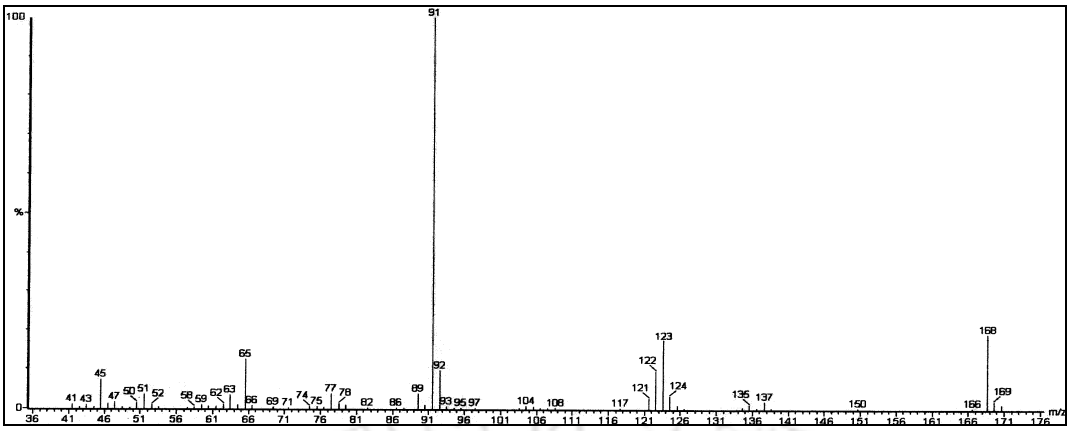

(a)

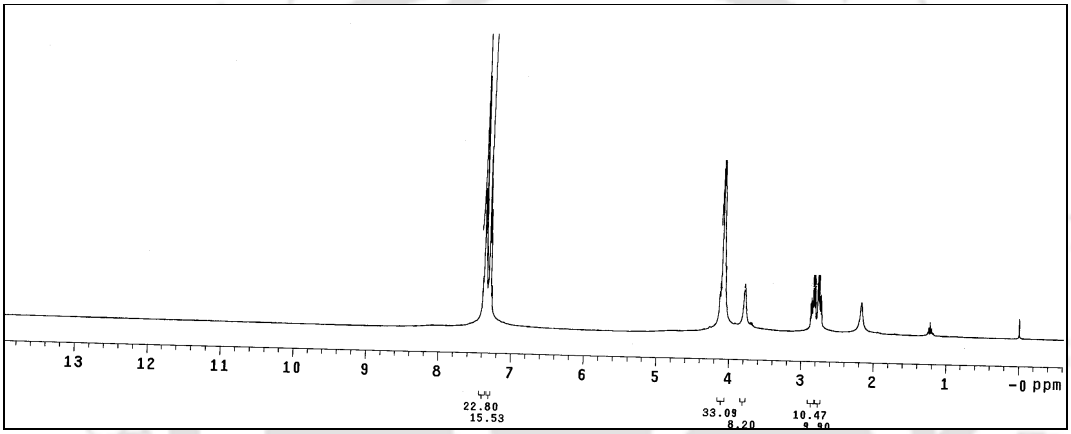

(b)

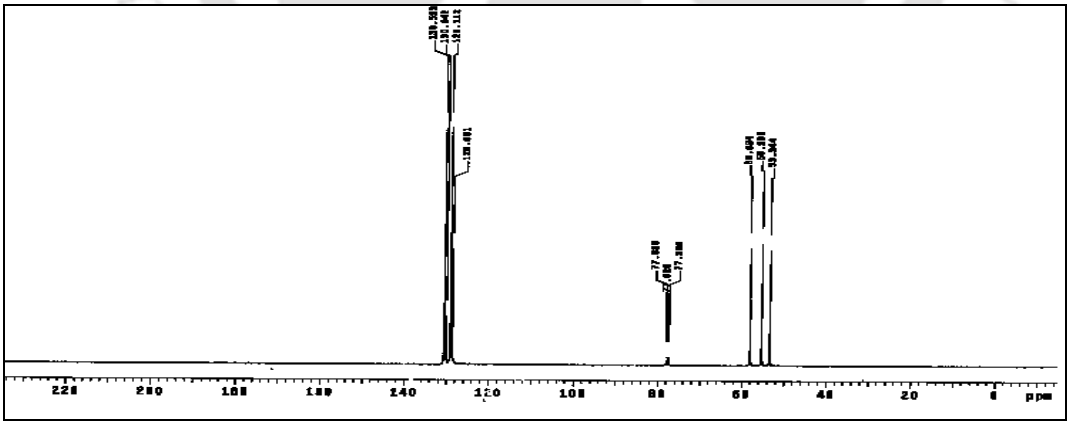

(c)

Figures 5.S5 (a) GCMS profile, (b) ^{1}H NMR spectrum and (c) ^{13}C NMR spectrum of **2-Phenylmethanesulfinyl-ethanol (30)**

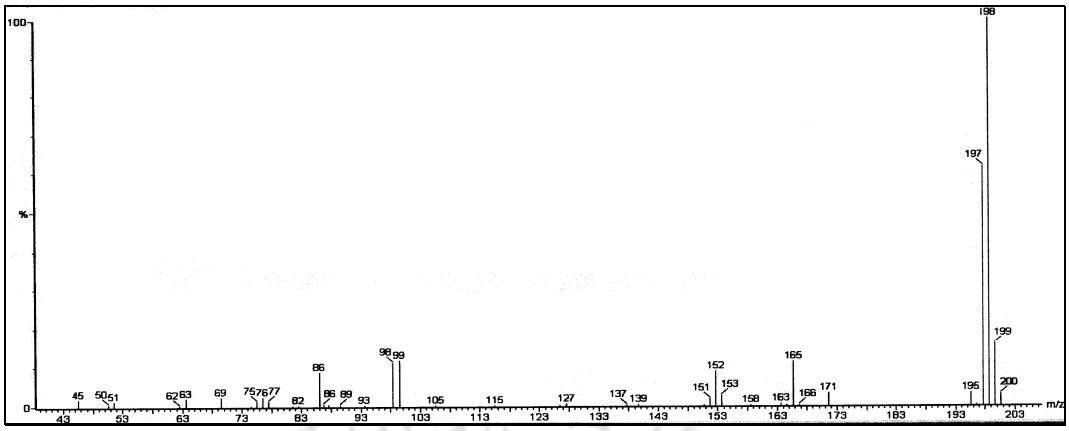

(a)

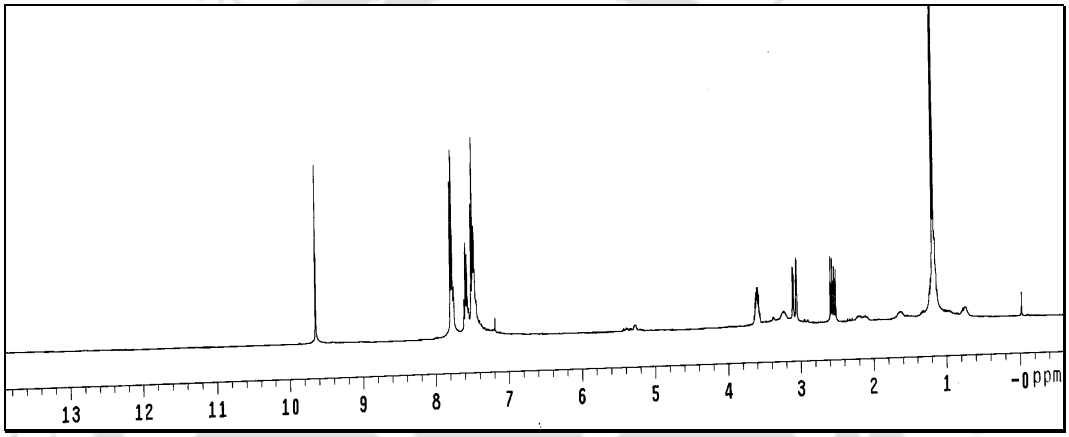

(b)

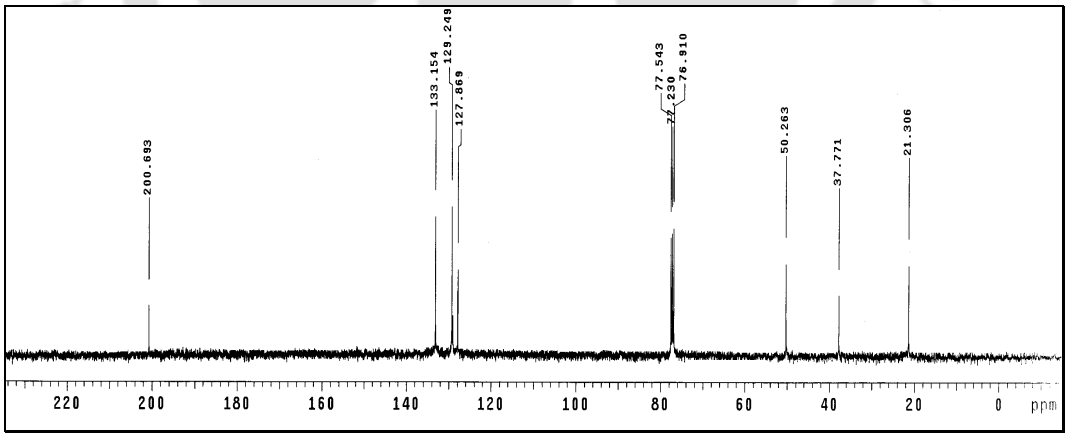

(c)

Figures 5.S6 (a) GCMS profile, (b) ^{1}H NMR spectrum and (c) ^{13}C NMR spectrum of **3-Benzenesulfinyl-butyraldehyde (29)**

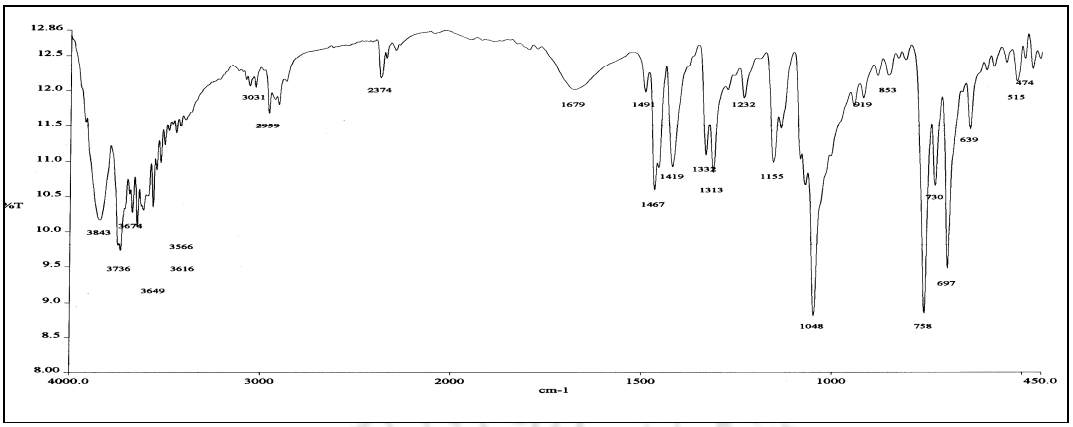

(a)

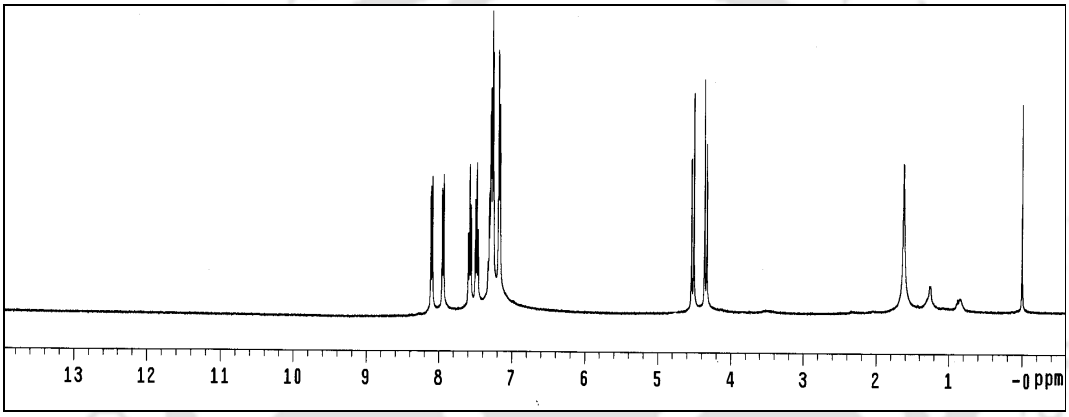

(b)

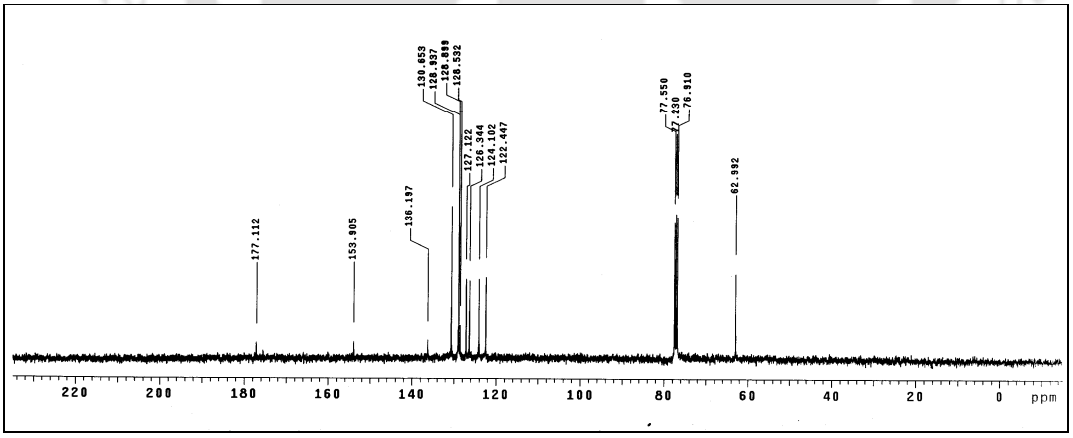

(c)

Figures 5.S7 (a) FTIR spectrum, (b) ^{1}H NMR spectrum and (c) ^{13}C NMR spectrum of **2- Phenylmethanesulfinyl-benzothiazole (31)**

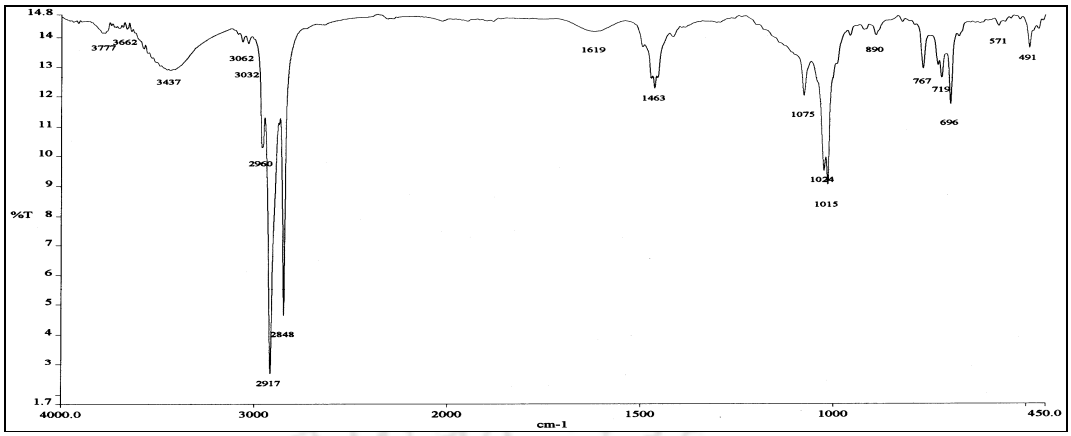

(a)

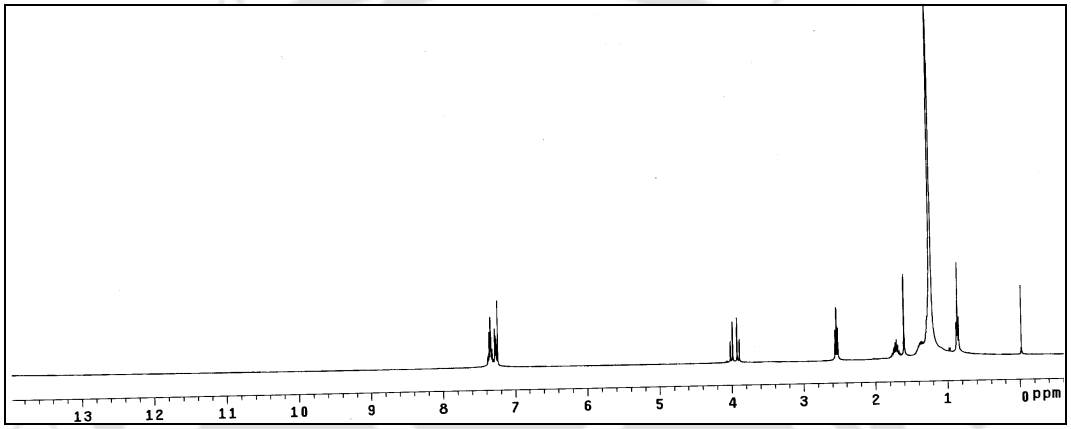

(b)

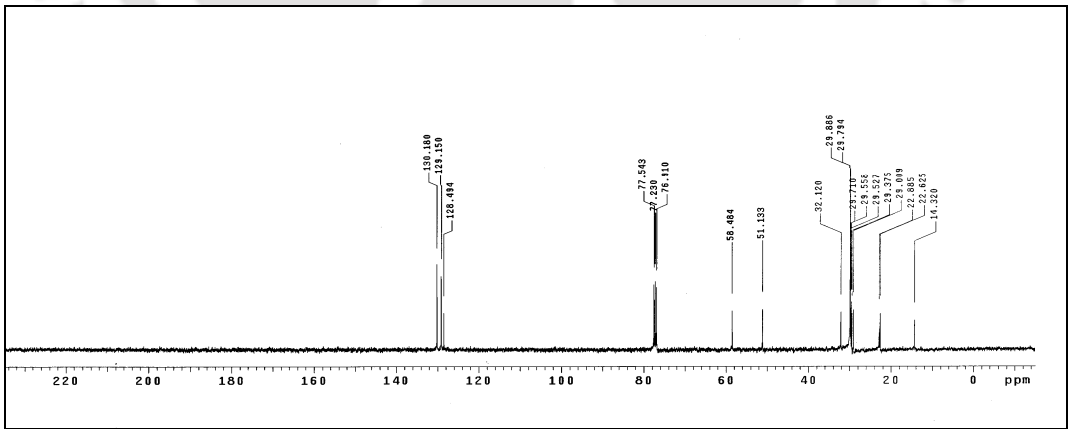

(c)

Figures 5.S8 (a) FTIR spectrum, (b) ^{1}H NMR spectrum and (c) ^{13}C NMR spectrum of **Octadecylsulfinyl-benzene (26)**

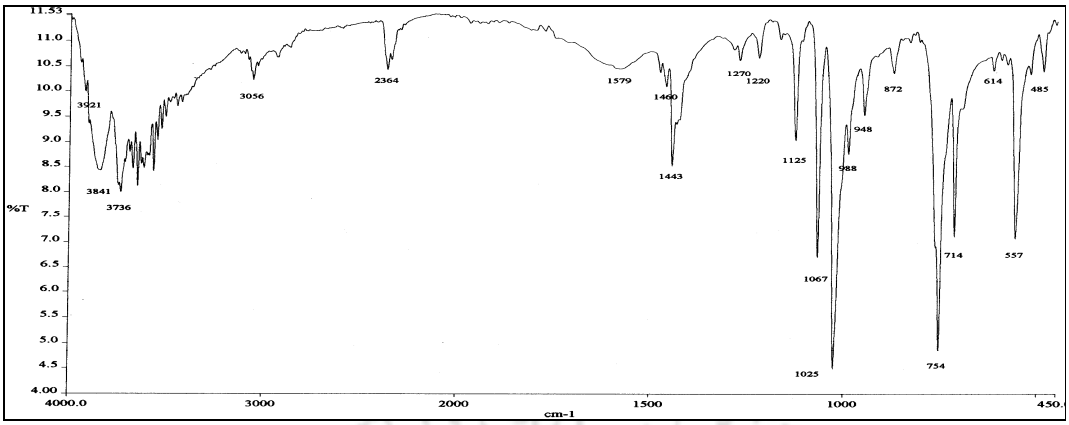

(a)

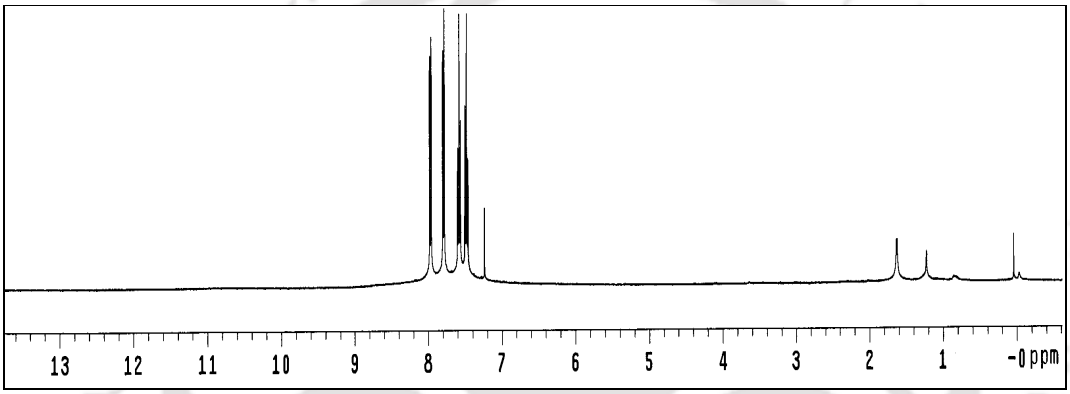

(b)

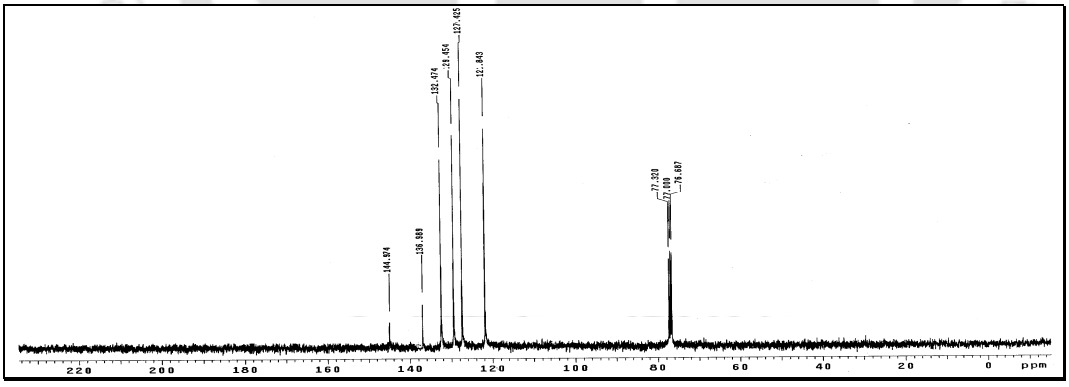

(c)

Figures 5.S9 (a) FTIR spectrum, (b) ^{1}H NMR spectrum and (c) ^{13}C NMR spectrum of **Dibenzothiophene 5-oxide (20b)**

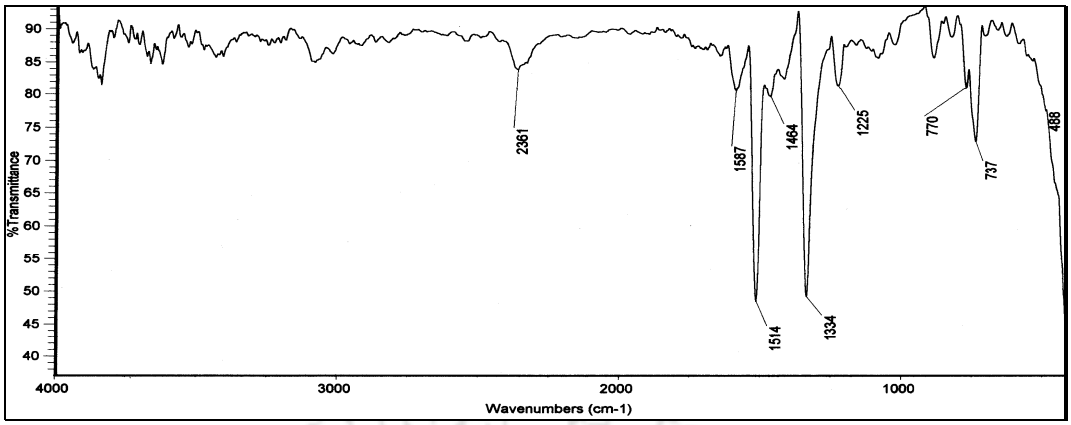

(a)

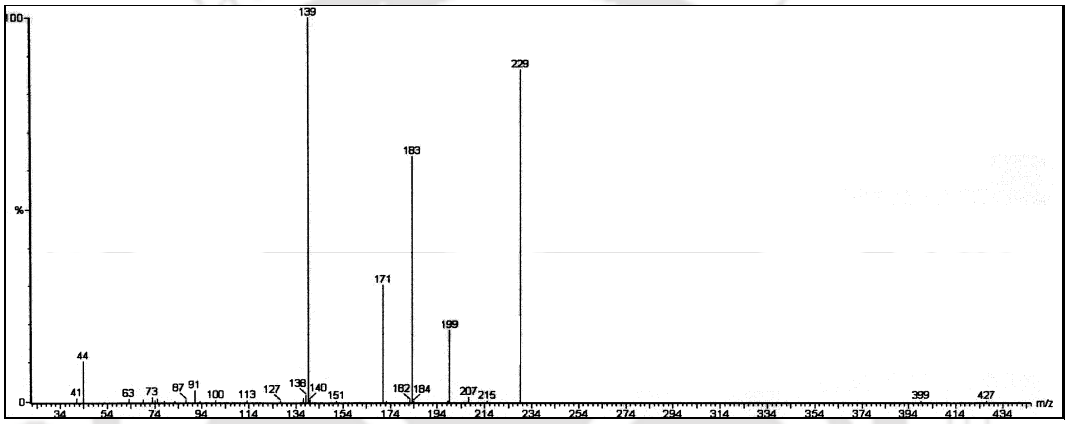

(b)

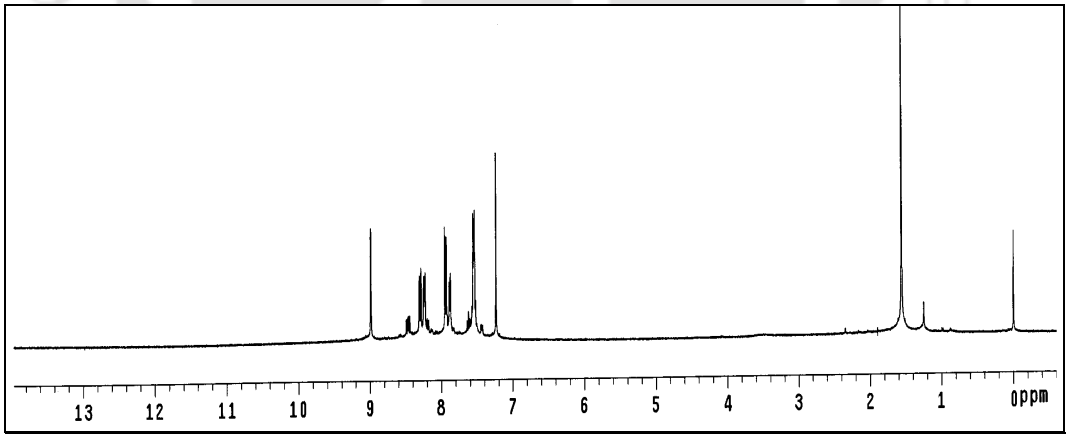

(c)

Figures 5.S10 (a) FTIR spectrum, (b) GCMS profile and (c) ^{1}H NMR spectrum of **3-Nitro-dibenzothiophene (20a)**

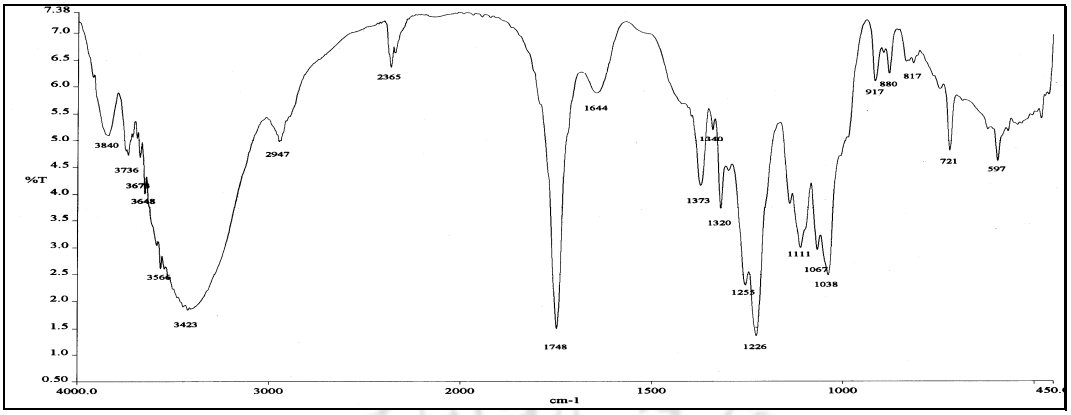

(a)

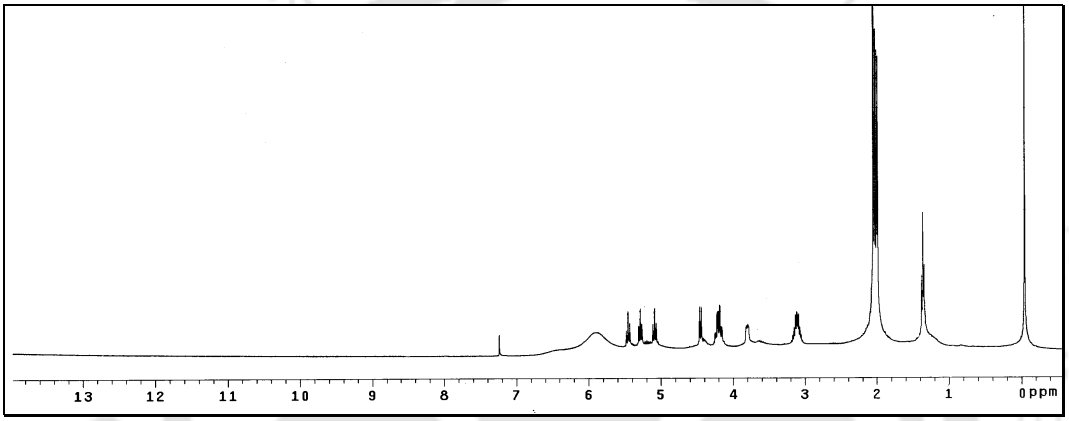

(b)

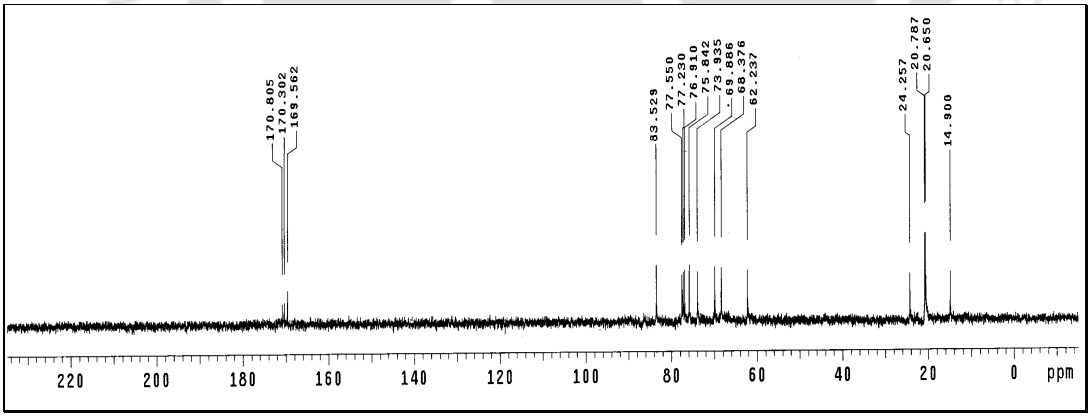

(c)

Figures 5.S11 (a) FTIR spectrum, (b) ^{1}H NMR spectrum and (c) ^{13}C NMR spectrum of **Glycosyl sulfoxide (34)**

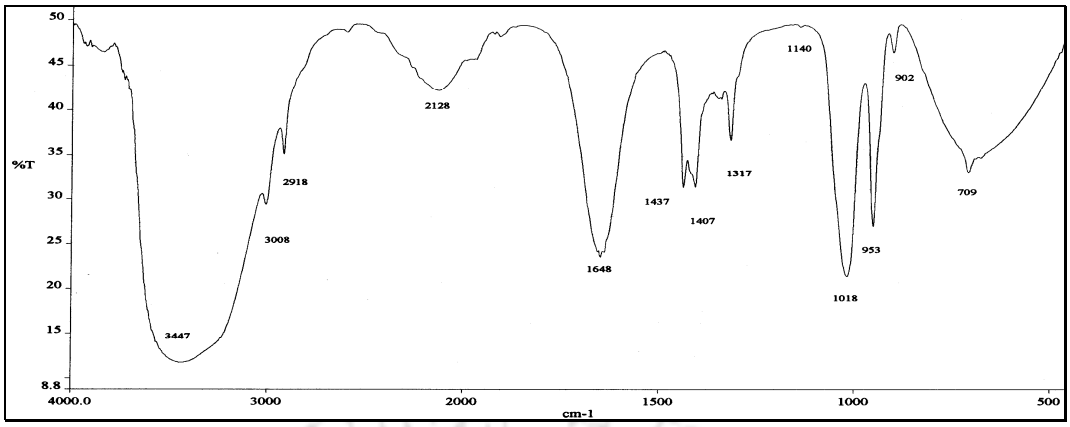

(a)

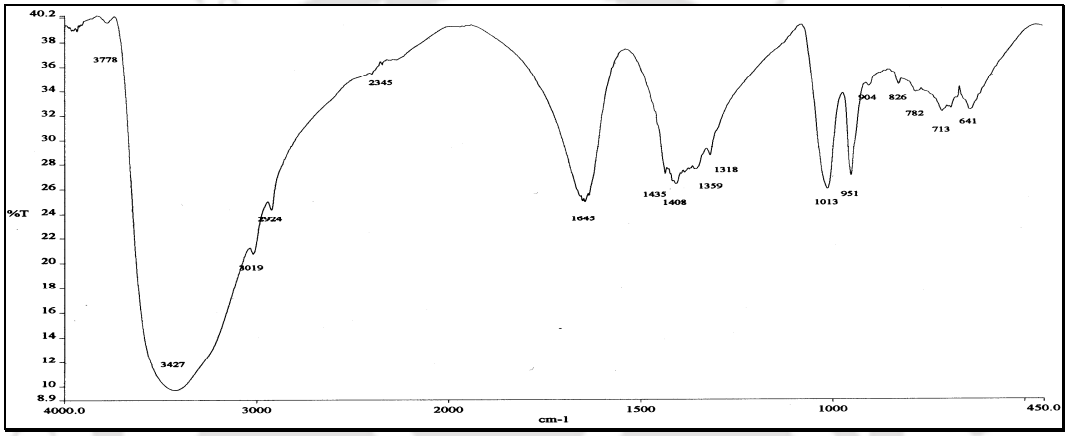

(b)

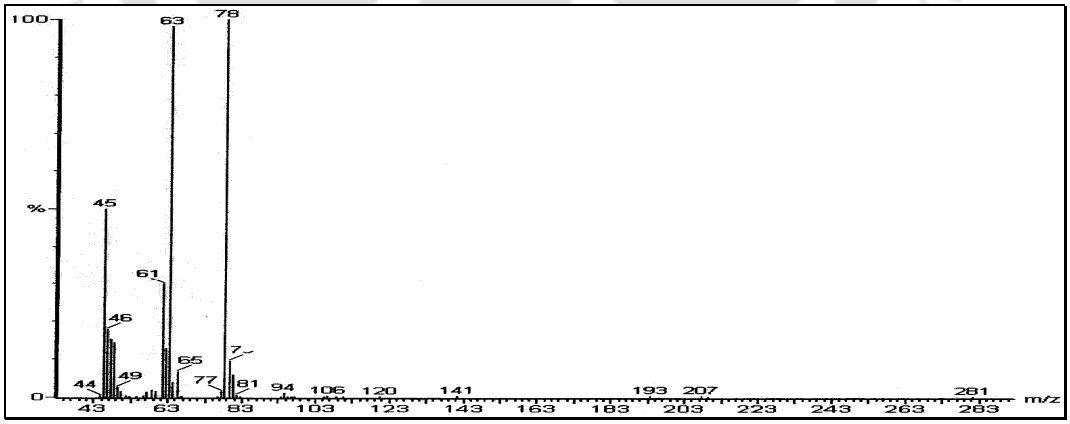

(c)

Figures 5.S12 (a) FTIR spectrum of standard **DMSO**, (b) FTIR spectrum of **DMSO** obtained from reaction and (c) GCMS profile of **DMSO**.

List of Publications

- *European Journal of Organic Chemistry,* ***2007***, 374-378, Borax as an Efficient metal-free catalyst for Hetero-Micheal Reactions in an Aqueous Medium, Sahid Hussain, **Saitanya K Bharadwaj**, Mihir K Chaudhuri and Harajyoti Kalita.
- *Catalysis Communication,* ***2008,*** 9, 919-923, $Al(H_2PO_4)_3$: An efficient catalyst for nitration of organic compounds with nitric acid, **Saitanya K Bharadwaj**, Sahid Hussain, Manoranjan Kar and Mihir K Chaudhuri.
- *Applied Catalysis A: General,* ***2008,*** 243, 62-67, Acid Phosphate impregnated Titania Catalyzed Nitration of Aromatic Compounds with Nitric Acid, **Saitanya K Bharadwaj**, Sahid Hussain, Manoranjan Kar and Mihir K Chaudhuri.
- *Catalysis Letter,* ***2008,*** 124, 100–104, $Al(H_2PO_4)_3$: An Efficient and Effective Solid Acid Catalyst for Transesterification of *b*-keto Esters Under Solvent Free Condition, Papori Goswami and **Saitanya Kumar Bharadwaj**.
- *Tetrahedron Letters,* ***2009,*** 50, 3767, Chemoselective Sulfoxidation by H_2O_2 or HNO_3 using a Phosphate Impregnated Titania, **Saitanya K Bharadwaj**, Sasanda N Sharma, Sahid Hussain, and Mihir K Chaudhuri.
- *European Journal of Organic Chemistry,* ***2009,*** 3319-3322, Borax Catalyzed and pH Controlled Selective Oxidation of Organic Sulfides by H_2O_2: An Environmentally Clean Protocol, Sahid Hussain, **Saitanya K Bharadwaj**, Ravindra Pandey and Mihir K Chaudhuri.
- ***Indian patent, Filed for, 2009*** **(1011/KOL/2008 dated 29/07/09),** Catalytic process for Extraction of Bromide from Sea Water, Mihir K Chaudhuri, **Saitanya K Bharadwaj**, Neraaj Chandrol and Sahid Hussain.

To be communicated

- New vanadium Drug for Diabetes, *(Indian patent).*
- Synthesis, Investigation of Reactivity and DFT studies of newer peroxovanadates with rare μ-η^1: η^2-O_2.
- Exploitation of interaction of ternary system Vanadium-H_2O_2-Citric acid at physiological pH 7.2.
- A Novel process of direct Bromination of phenol with Sea Water.
- Effect of Fluorine in reactivity of Peroxovanadates(V).